Enzymatic cascade reactions toward amino- and oxyfunctionalized fine and bulk chemicals

Mai, 2020

Dissertation

zur Erlangung des Doktorgrades der Naturwissenschaften

Dr. rer. nat.

vorgelegt der Fakultät für Chemie

der Universität Bielefeld

von

Jana Löwe, M. Sc

geboren in Bremerhaven am 8.6.1991

Enzymatische Kaskadenreaktionen zur Synthese von amino- und oxyfunktionalisierten Fein- und Bulkchemikalien

Mai, 2020

Dissertation

zur Erlangung des Doktorgrades der Naturwissenschaften

Dr. rer. nat.

vorgelegt der Fakultät für Chemie

der Universität Bielefeld

von

Jana Löwe, M. Sc

geboren in Bremerhaven am 8.6.1991

1. Gutachter: Prof. Dr. Harald Gröger,
Industrielle Organische Chemie und Biotechnologie
Fakultät für Chemie, Universität Bielefeld
2. Gutachter: Prof. Dr. Karl-Josef Dietz,
Biochemie und Physiologie der Pflanzen
Fakultät für Biologie, Universität Bielefeld

Die vorliegende Arbeit wurde am Lehrstuhl für Industrielle Organische Chemie und Biotechnologie an der Universität Bielefeld unter Leitung von Prof. Dr. Harald Gröger angefertigt. Ein Teil der Promotion fand unter Leitung von Prof. Dr. Yasuhisa Asano, Arbeitsgruppenleiter des Enzyme Chemistry Laboratory an der Toyama Prefectural University, Biotechnology Research Center, in Japan vom 18.04.2018 bis 16.05.2018 statt (DAAD Projekt 57345566, Cyanid-freie enantioselektive Synthese von Nitrilen mit Enzymen im Förderprogramm, Programm Projektbezogener Personenaustausch Japan 2017). Die Arbeit wurde durch das Stipendium aus dem SFB-Vorhaben Biokatalyse/Projektsäule Oxyfunktionalisierung zum Thema Organische Chemie mit Designerzellen sowie von der Firma Windmöller GmbH finanziert. Die Dissertation wurde selbstständig verfasst und hat in der gegenwärtigen oder einer anderen Fassung noch nicht einer anderen Fakultät oder Hochschule vorgelegen.

Jana Löwe

Parts of this work have already been published, submitted for publication or were presented at conferences:

Publications

D. Maynard, S. M. Müller, M. Hahmeier, **J. Löwe**, I. Feussner, H. Gröger, A. Viehhauser, K. –J. Dietz. One-pot synthesis of bioactive cyclopentenones from linolenic acid and docosahexaenoic acid, *Bioorg. Med. Chem* **2018**, *26*, 1356-1364.

J. Löwe. A. A. Ingram, H. Gröger, Enantioselective synthesis of amines *via* reductive amination with a dehydrogenase mutant from *Exigobacterium sibiricum*: Substrate scope, co-solvent tolerance and biocatalyst immobilization, *Bioorg. Med. Chem* **2018**, *7*, 1387-1392.

J. Löwe, A. Siewert, A. –C. Scholpp, L. Wobbe, H. Gröger, Replacing co-substrates by carbon dioxide, water and light: an alternative perspective towards biocatalytic production of bulk chemicals exemplified for aliphatic amines, *Sci. Rep* **2018**, *8*, 10436-10443.

J. Löwe, O. Blifernez-Klassen, T. Baier, L. Wobbe, O. Kruse, H. Gröger, Type II flavoprotein monoxygenases PsFMO-A from a bacterium *Pimelobacter sp.* Bb-B catalyzes enantioselective Baeyer-Villiger oxidations with a relaxed cofactor specificity, *J. Biotechnol.* **2019**, *294*, 81-87.

F. Uthoff, **J. Löwe**, C. Harms, K. Donsbach, H. Gröger, Total Synthesis of Ozanimod Based on a Biocatalytic Key Step, *J. Org Chem* **2019**, *8*, 4856-4866.

J. Löwe, H. Gröger, Fatty Acid Hydratases: Versatile Catalysts to Access Hydroxy Fatty Acids in Efficient Syntheses of Industrial Interest, *Catalysts* **2020**, *10*, 237-249.

J. Löwe, K.-J. Dietz, H. Gröger, From a biosynthetic pathway toward a biocatalytic process and chemocatalytic modifications: Three-step enzymatic cascade to the plant metabolite 12-OPDA and metathesis-derived products, *Adv. Sci.* 2020, doi: 10.1002/advs.201902973.

Patents

J. Löwe, F. Uthoff, C. Harms, K. Donsbach, H. Gröger, 2018, Enantioselective Biocatalytic Preparation of 4-Cyano-Substituted 1-Aminoindane and Ozanimod, EP 18167058.9, 06.06.2018.

Poster Presentations

J. Löwe, H. Gröger, Substrate Scope of the Synthesis of chiral aryl-substituted amines using an amines dehydrogenase, 07/2017, Budapest, Biotrans Conference.

J. Löwe, H. Gröger, Oxidative processes towards 12-OPDA as a precursor of jasmonic acid, 03/2017 Aachen, SusChemSys 2.0.

J. Löwe, H. Gröger, Lutz Wobbe, Replacing co-substrates by carbon dioxide, water and light: a novel perspective towards bulky amines, 04/2018, Bielefeld, 8th Int. CeBiTecResearch Conference, Bielefeld. – Poster price awarded

J. Löwe, H. Gröger, Oxidative processes towards 12-OPDA as a precursor of jasmonic acid, 07/2018, New England, Biocatalysis Gordon Research Conference

J. Löwe, H. Gröger, Oxidative processes towards 12-OPDA as a precursor of jasmonic acid, 03/2019, Karlsruhe, 10th Workshop on Fats and Oils as Renewable Feedstocks for the Chemical Industry.

J. Löwe, K. –J. Dietz, H. Gröger, Enzymatic cascade towards the plant metabolite 12-OPDA and metathesis-derived compound library design, 12/2019, Bielefeld, Multi-Step Syntheses in Biology and Chemistry-An International Young Investigator Conference.

Oral Presentations

J. Löwe, H. Gröger, Biocatalytic Production of Amines via an Amine Dehydrogenase: from Substrate Scope Studies to Process Concepts, 09/2017 Bad Sassendorf, 4th CeBiTec Retreat.

J. Löwe, H. Gröger, Oxidative processes towards 12-OPDA as a precursor of jasmonic acid, 03/2018, Aachen, SusChemSys 2.0.

J. Löwe, K. –J. Dietz, H. Gröger, Enzymatic cascade towards the plant metabolite 12-OPDA and metathesis-derived compound library design, 12/2019, Bielefeld, Multi-Step Syntheses in Biology and Chemistry-An International Young Investigator Conference.

“Wohin führt das alles? Was wird aus uns? Das waren unsere jungen Fragen und es gab darauf junge Antworten. Es führt zueinander. Wir werden wir selbst.“

— Patti Smith, Just Kids

„Hin und wieder hat das Schicksal Ähnlichkeit mit einem örtlichen Sandsturm, der unablässig die Richtung wechselt. Sobald du deine Laufrichtung änderst, um ihm auszuweichen, ändert auch der Sturm seine Richtung, um dir zu folgen. Wieder änderst du die Richtung. Und wieder schlägt der Sturm den gleichen Weg ein. Dies wiederholt sich Mal für Mal, und es ist, als tanztest du in der Dämmerung einen wilden Tanz mit dem Totengott. Dieser Sturm ist jedoch kein beziehungsloses Etwas, das irgendwoher aus der Ferne heraufzieht. Eigentlich bist der Sandsturm du selbst. [...] Und auch wenn der Sandsturm vorüber ist, wirst du kaum begreifen können, wie du ihn durchquert und überlebt hast. Du wirst auch nicht sicher sein, ob er wirklich vorüber ist. Nur eins ist sicher. Derjenige, der aus dem Sandsturm kommt, ist nicht mehr Derjenige, der durch ihn hindurchgegangen ist.“

— Haruki Murakami, Kafka am Strand

Danksagung

Zuallererst möchte ich meinem Doktorvater Prof. Dr. Harald Gröger danken. Vielen Dank für die jetzt schon seit sechs Jahren andauernde Förderung meiner wissenschaftlichen Arbeiten und für die Aufrechterhaltung meiner Begeisterung im Themengebiet Biokatalyse. Herzlichen Dank für die Freiheit in der Bearbeitung der vielen faszinierenden Projekte, die Einbindung in so viele Kooperationen, für jede Herausforderung und das Vertrauen.

Herrn Prof. Dr. Karl-Josef Dietz danke ich nicht nur für die freundliche Übernahme des Zweitgutachtens, sondern auch für die harmonische und erfolgreiche Zusammenarbeit in dem SFB-1318: Halogenierung und Oxyfunktionalisierung durch Enzymkatalyse.

Für die Finanzierung dieser Arbeit danke ich der Windmöller GmbH sowie dem Deutschen Akademischen Austauschdienst (DAAD) im Rahmen des geförderten Projektes (DAAD Projekt 57345566, Cyanid-freie enantioselektive Synthese von Nitrilen mit Enzymen im Förderprogramm, Programm Projektbezogener Personenaustausch Japan 2017). Außerdem danke ich dem DAAD für die Förderung meiner Teilnahme an der Biocatalysis Gordon Research Conference 2018 im Rahmen des Kongressreiseprogramms. In Zusammenhang mit der Forschungsreise nach Japan danke ich Prof. Dr. Yasuhisa Asano, dem Arbeitsgruppenleiter des Enzyme Chemistry Laboratory, Toyama Prefectural University, Biotechnology Research Center von der Toyama Prefectural University. Vielen Dank für die fürsorgliche Aufnahme sowohl in das Land als auch in die Arbeitsgruppe sowie für die Erweiterung meines Horizonts im Bereich der Biotechnologie. Außerdem danke ich der ganzen Arbeitsgruppe des Enzyme Chemistry Laboratory, besonders Aem Nuyler für die tolle Zeit und die sonntäglichen Reisen quer durch die Präfektur Toyama.

Des Weiteren danke ich dem interdisziplinären Netzwerk SusChemSys 2.0 für die Aufnahme in das Programm, die vielen Meetings, Exkursionen zu Industriepartnern und Soft-Skill-Workshops.

Darüber hinaus möchte ich meinen vielen Kooperationspartnern danken. Zuallererst danke ich der Pharmazell GmbH, insbesondere Dr. Kai Donsbach für die Zusammenarbeit auf dem Projekt zur Synthese von Ozanimod. Außerdem danke ich der Firma Windmöller GmbH, speziell Guido Horst, Dr. Thomas Hohberg, Georg Kruse und Ulrich Windmöller, für die Einbindung in ein spannendes Projekt und die tolle Zusammenarbeit. Außerdem danke ich den *in-house* Kooperationspartnern, allen voran Prof. Dr. Karl-Josef Dietz und Daniel Maynard für die tolle Zusammenarbeit an dem 12-OPDA-Projekt. Darüber hinaus danke ich Dr. Lutz Wobbe und Prof. Dr. Olaf Kruse für die gelungene Kooperation. Ich danke allen, dass sie mir tiefe Einblicke in die Physiologie der Pflanzen verschafft haben.

Besonders möchte ich mich bei der Analytik-Abteilung für die Messung der NMR-und MS-Proben bedanken, hier sind vor allen Dingen Dr. Andreas Mix, Peter Mester, Marco Wißbrock, sowie Dr. Jens Sproß, Heinz-Werner Patruck und Sandra Heitkamp zu nennen. Darüber hinaus danke ich dem Chemikalienlager um Heike Kosellek. Für das Korrekturlesen dieser Arbeit danke ich Anke Hummel, Hilmi Yavuzer, Michael Stricker, Karla Wagner, Jannis Nonnhoff, Hannah Bork, Niklas Adebar, Alessa Hinzmann, Lukas Schober, Alina Nastke, Franziska Kühn, Carmen Plass, Daniel Maynard und Dr. Nadine Zumbrägel.

Eine große Unterstützung waren Ingo Kröger, Karla Wagner, Waldemar Meiser, Michael Stricker, Nathalie Nottmeier und Natalie Gutsch, die im Rahmen ihrer Ausbildung oder eines Forschungspraktikums einen großen Teil zu dieser Arbeit beigetragen haben. In ihren Bachelorarbeiten haben Ramona Paulus, Tatjana Pietrowski, Viktoria Pflug und Aaron Ingram Teilprojekte bearbeitet und waren somit auch eine große Hilfe. Danke euch allen für euer Mitwirken.

Ein ganz besonderer Dank geht natürlich an die frühere OC1 und jetzige IOCB. Allen voran mit Thomas Geisler, der immer für ein funktionstüchtiges Labor gesorgt hat. In diesem Zusammenhang danke ich ebenfalls Anika Hegemann, einerseits für die Zusammenarbeit auf zahlreichen Projekten und die Unterstützung meiner Forschung, andererseits danke ich für die zahlreichen Fußballspiele mit Nacht-und-Nebel-Aktionen und die Unterstützung in jeder Lebenslage. Außerdem danke ich Angelika Bendick für ihre ständige Unterstützung bei bürokratischen Aufgaben sowie vielen organisatorischen Dingen. Dr. Anke Hummel danke ich für die Beantwortung zahlreicher Fragen zu biotechnologischen und mikrobiologischen Arbeiten sowie für die stetige Aufrechterhaltung meiner Begeisterung für die Biokatalyse. Außerdem danke ich Melissa Kracht für die Pflege des S1- Bereichs.

Ich danke der „alten OC1“, hier zu nennen Dr. Severin Wedde, dem „Girls-Lab“ Dr. Ji Eun Choi, Keiko Oike, Dr. Florian Uthoff und Dr. Yasunobu Yamashita. Darüber hinaus danke ich Dr. Matthias Pieper, Dr. Philipp Rommelmann und Dr. Tobias Betke, vielen Dank auch für die Freundschaft über die Promotion hinaus.

Aus der „alten OC1“ möchte ich mich ganz besonders bei Dr. Nadine Zumbrägel bedanken. Vielen Dank für die schöne Zeit im Labor und für die Zeit während und nach den Konferenzen, wir waren in jeder Lebenslage ein fantastisches Team. Außerdem danke ich für die innige Freundschaft, der der Abschluss der Promotion keinen Abbruch getan hat.

Darüber hinaus danke ich der „neuen OC1“ - oder jetzt IOCB - für die tolle Zeit, eine effektive Zusammenarbeit und eine tolle Arbeitsatmosphäre. Doch auch über die Arbeit hinaus danke ich euch für das Basketballspielen, die Spieleabende, Arbeitsgruppenausflüge, Theater- und anschließende Weinmarktbesuche, Campus-Festivals und Feiern. Ich diesem Zusammenhang danke ich Hilmi Yavuzer und Michael Stricker, nicht nur für die innigen Gespräche über Biochemie, sondern auch für eure Freundschaft.

Ich danke Franziska Kühn für ihr Organisationstalent und die gemeinsamen Mittagessen. Vielen Dank an Alessa Hinzmann für die gemeinsamen zahlreichen Aktivitäten im SusChemSys-Cluster und die vielen schönen Basketballabende. Ich danke außerdem Alina Naskte und Niklas Adebar für ein kurzes, aber ergebnisreiches Kooperationsthema und für eine immer lustige und arbeitsreiche Atmosphäre im Büro. Lukas Schober danke ich für ein immer offenes Ohr für komplexe chemische Zusammenhänge, aber auch für private Themen, sowie für die Erheiterung im Kaffeeraum in den Pausen. Ganz besonders möchte ich hier Jannis Nonnhoff erwähnen, der mit mir für die zweite Hälfte meiner Promotion ein tolles Laborteam gebildet hat.

Darüber hinaus danke ich den neuen IOCB-Mitgliedern, hier zu nennen Tim Guntelmann, Luisa Koch, Laura Bernhard, Alina Guntermann und Karla Wagner. Vor allem danke ich Hannah Bork für eine dynamische und enthusiastische Zusammenarbeit auf dem gemeinsamen Kooperationsthema.

Außerdem danke ich meinen „Handball-Mädels“, ganz besonders Ameli und Inga, sowie Marcel, ihr seid der Beweis dafür, dass Freundschaft über alles hinausgeht. Ich bin froh, dass ihr da seid. Außerdem danke ich den „Bündern“ Addi, Babsi, Richard, Matti, Michi und Raffi für ihre Freundschaft. Ganz besonders danke ich Timo, ohne dich wäre ich jetzt nicht da, wo ich jetzt bin. Danke für alles.

Mein ganz besonderer Dank geht an Carmen Plass, nicht nur als tolle Laborkollegin, die immer ein offenes Ohr für mich hatte und mich auch an langen Labortagen immer unterstützt hat, sondern auch als tolerante und selbstlose Partnerin immer für mich da ist. Together we are what we can't be alone. – Dropkick Murphys

Der größte Dank gilt meiner Familie. Ihr seid die verrücktesten und liebenswertesten Menschen, die ich kenne. Ganz besonders danke ich meinen Eltern Karina und Roland für ihre bedingungs- und grenzenlose Liebe und Unterstützung egal in welcher Lebenslage. Ich bin froh, dass ihr mir immer einen Ort gegeben habt, an den ich jederzeit zurückkommen kann. Außerdem danke ich meinem Bruder Josh. Du bist nicht nur ein toller Bruder, sondern auch ein guter Freund und ein großes Vorbild, durch deine Stärke konnte ich so manchen Weg gehen. Darüber hinaus danke ich meinen Großeltern, ganz besonders meinem Opa Wolfgang, deine aufmunternden Worte waren mehr wert, als du dir vorstellen kannst.

Contents

1 Abstract

The present work involves three cascade reactions catalyzed by enzymes. The first cascade involved the synthesis of aryl-substituted chiral amines using an amine dehydrogenase, a mutant of a leucine dehydrogenase originated from *Exiguobacterium sibiricum* (EsLeuDH-DM). In this regard, acetophenone was investigated as the most promising aryl-substituted substrate. In this context, 1-phenylethylamine could be produced with a concentration of 50 mM. Besides, aliphatic amines and primary amines were synthesized using EsLeuDH-DM in combination with the cofactor regeneration system based on a formate dehydrogenase and formate. The formate was secreted by the algae *Chlamydomonas reinhardtii*. The algae was provided by Wobbe from the working group Algae Biotechnology & Bioenergy, Bielefeld University. The combination of the algae-based cofactor recycling system and EsLeuDH-DM lead to hexylamine, cyclohexylamine, butan-2-amine and butylamine with conversions of >99%. Furthermore, a new flavine monooxygenase (FMO) from *Pseudomonas sp.* provided by the workgroup Algae Biotechnology & Bioenergy, Bielefeld University, of Kruse was successfully combined with the new cofactor regeneration system. The second topic dealt with the synthesis of polyols. This part of the presented work was processed in cooperation with the industrial partner Windmöller GmbH. These polyols were produced in a cascade reaction based on a fatty acid hydratase and a lipase. In a preparative synthesis 10-hydroxystearic acid was produced using the fatty acid hydratase from *Stenotrophomonas nitritireducens* (Sn-Ohy). Afterward, the 10-hydroxystearic acid was effectively esterified with 1,6-hexanediol in a high gram-scale reaction (7.8 g, 20%). Additionally, the Sn-Ohy has been successfully immobilized and used in a scale-up experiment with 400 g L^{-1}. In this regard, 10-hydroxystearic acid was isolated with a yield of 59%. The third cascade reaction towards leads to 12-OPDA, a precursor of the plant-derived hormone jasmonic acid. This topic was prepared in cooperation with the workgroup of Dietz Plant Biochemistry & Physiology, Bielefeld University. For the effective synthesis of 12-OPDA the commercially available lipoxygenase from *Glycine max* was coupled with the recombinant allene oxide synthase (AOS) and allene oxide cyclase (AOC2) from *Arabidopsis thaliana*. The AOS and AOC2 were successfully used as a whole cell catalyst, where both enzymes were included. In this context, 12-OPDA (1 g L^{-1}) could be synthesized with a 90:10 ratio of the desired product to the side product and a yield of 28%. With an extraction optimization the yield of 12-OPDA could be raised to 61%. Additionally, it was possible to synthesize the 12-OPDA in segmented flow with 99% conversion, compared to 34% in the batch process. Furthermore, it was possible to show an enhancement in isolation with the segmented flow process (61%) compared to the batch process (36%). Finally, four 12-OPDA derivatives were synthesized using olefin cross-metathesis with high conversions and moderate yields.

2 Introduction

Biocatalysis is one of the main catalysis methods, besides organocatalysis and metal catalysis being used for chemical reactions. Biocatalysis describes the use of a living system or enzymes to catalyze chemical reactions.[1] In the last decades, the use of biocatalysis in chemical industry is more and more rising. The applications range from pharmaceuticals, food- and beverage, cosmetics, fine chemicals, flavors, fragrances industries[2] or waste treatment.[3]

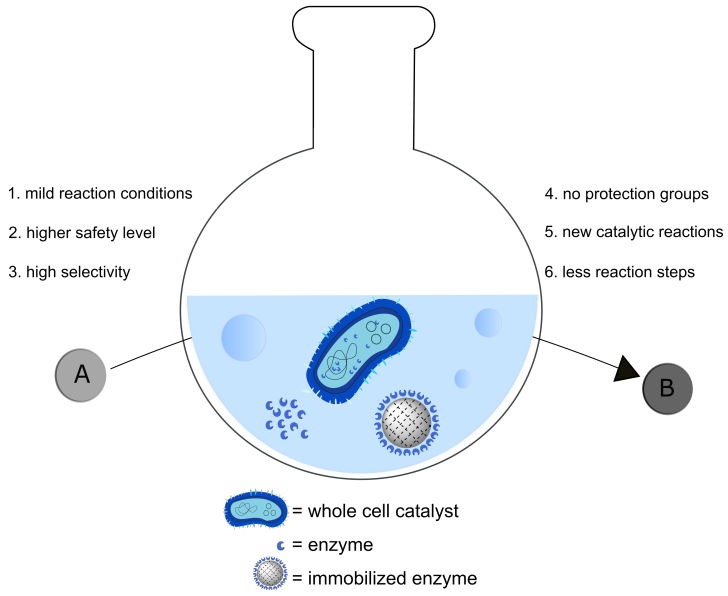

Figure 1: Biocatalysis: Conversion of substrate A to product B using biocatalyst as whole cells, free enzymes or immobilized enzymes.[3–6]

Biocatalysis has ecological and economic advantages compared to other catalytic methods. Due to milder reaction conditions, the energy consumption decreases. Further advantages are high specificity, reactions without protection groups,[3] more safety,[4] less synthetic steps[5] and new catalytic reactions (Figure 2).[6] Overall, there are three possibilities to find new catalytic activities of enzymes. These options are searching for new microorganisms in nature, protein engineering or library screening. Searching for enzymes in nature has the advantage to find new enzymes in special habitats con-

cerning the environmental conditions. In detail, it is possible to search in interesting environments, in which specific products can be isolated or to find microorganisms living in extreme habitats were, for example, the temperature is high or low, the pH or salt concentration is extraordinary.[7] These microorganisms contain enzymes, which can act e.g. at high temperatures and are therefore interesting for different applications. By isolating these microorganisms or their genomes gene bank or strain-collections can be generated which can be used for high-throughput screening.[8] The other possibility to create novel enzymatic activities are protein engineering, which is used to modify amino acid sequences of enzymes by rational design or directed evolution (Figure 2).[9] In rational design amino acids are selectively exchanged.[9] Examples for rational design are error-prone polymerase chain reactions,[10] saturation mutagenesis, random mutagenesis[11] at defined positions. A combination of both methods is called semi-rational design, like CAST (combinatorial active-site saturation test).[8,12] New enzymes are sought or generated to improve properties such as pH tolerance, solvent stability or enantioselectivity. Especially enantioselectivity plays an important role. Enantiomers can have the same physical properties, but interact differently, for example, with proteins in the human or animal body or have a different odor and taste. The synthesis of chiral molecules can be done in an asymmetric fashion or by the means of resolving a racemate.[13] Some enzymes are so selective that they are already widely used in the pharmaceutical industry.[3]

2.1 The four waves of biocatalysis

Bornscheuer *et al.* described the development of biocatalysis by using the metaphor of waves. They clustered the history of biocatalysis into four waves up to now, which is why the current time can be assigned to the fourth wave of biocatalysis.[6,14] In the first wave whole living cells were used to synthesize enantiomerically pure compounds like (*R*)-mandelonitrile from benzaldehyde (Figure 2).[15]

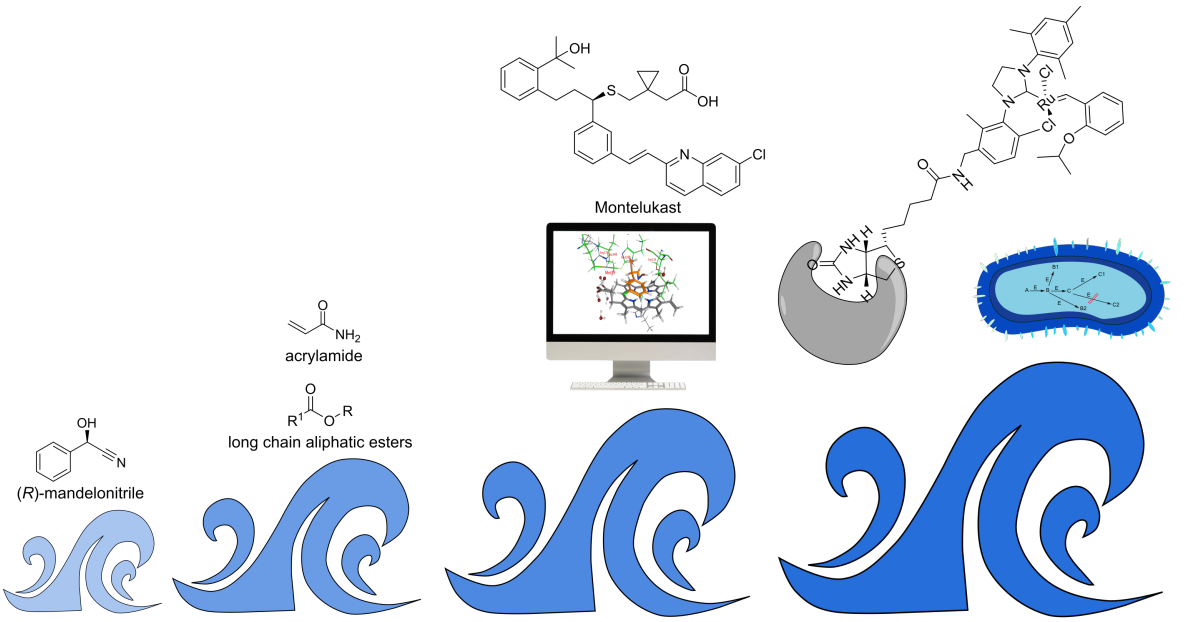

Figure 2: The four waves of biocatalysis.

During this wave, the lack in stability and the limited access towards biocatalyst were the major problems.

Therefore, screening and immobilization of the enzymes were major points, which were successfully addressed.[14]

The second wave in the 1980s and 1990s of biocatalysis dealt with the problems of the first wave and expand the enzyme database, as well as the implementation of genetic modification of enzymes. Some selected examples are the use of hydroxynitrile-lyase for the synthesis of cyanohydrins from aldehydes and ketones,[16] the nitrile-hydratase-catalyzed hydration of acrylonitrile to acrylamide[17] or the lipase- catalyzed esterification of decyl oleate, cetyl ricinoleate, myristyl myristate and decyl cocoate (Figure 2).[18]

The third wave of biocatalysis was set in motion by the work of Stemmer[19] and Arnold[20] in the mid and late 1990s. Arnold received the Nobel Prize in chemistry in 2018 for directed evolution. They developed molecular biological methods that quickly and comprehensively evolve enzymes. Followed by the use of DNA shuffling[19] and

error-prone polymerase chain reaction[10] in combination with high-throughput screening,[8] gene synthesis, sequence analysis and computer-based modeling. To that time, chemical industry mostly focused on hydrolases, ketoreductases, co-factor regeneration and protein stability in organic solvent. Furthermore, they focused on the switch from glucose to glycerol because its cheaper, as it accumulates as waste product.[21] Additionally, biocatalytic synthesis of Montelukast[22] and Sitagliptin[23] developed by *Merck* as important drugs against allergies and diabetics have to be mentioned as achievements of the third wave. Montelukast can now be made accessible *via* the decisive step of using an engineered ketoreductase[22] (Figure 2), as well as Sitagliptin by the means of a transaminase.[23] Another example is the synthesis of branched-chain alcohols for the use of biofuels from amino acid metabolism, created through a metabolic engineered *Escherichia coli*.[24]

The fourth present wave of biocatalysis includes the discovery of novel enzymes or enzyme functions.[6,14] This includes enzymes with promiscuous activities developed by mutagenesis or other enzyme modifications, such as artificial metalloenzymes generated by Ward that catalyze metathesis reactions[25–27] (Figure 2) or even the generation of a *de novo* metalloprotein from short peptides.[28] Furthermore, multi enzymes catalyzed processes were implemented, including a range of enzymes, which convert over several steps hand in hand a substrate into a complex product.[29]

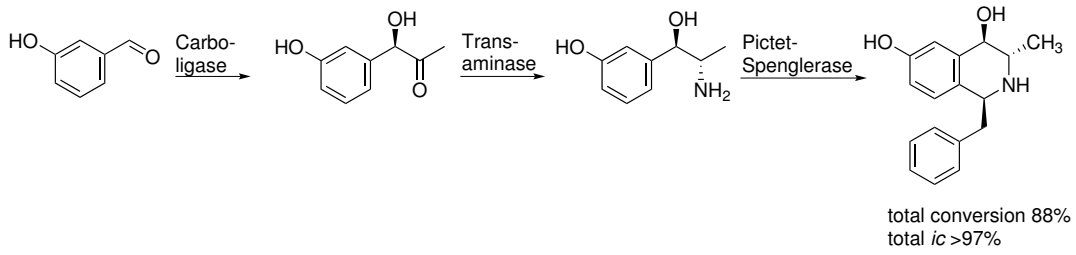

Scheme 1: Enzymatic 3-step cascade to an isoquinoline derivative using an acetohydroxy acid synthase I from *Escherichia coli* (EcAHAS-I), transaminase from *Chromobacterium violaceum* (Cv2025) and norcoclaurine synthase variant from *Thalictrum flavum* (ΔTfNCS-A79I). *Ic* is defined as isomeric content.[29]

One example is shown in the figure below, where a complex tetrahydroisoquinoline is prepared starting from an aldehyde in three enzymatic steps with a impressive overall conversion of 88% (Scheme 1): Furthermore, immobilization engineering[30] is a part of the fourth wave of biocatalysis, as well as microreactor[31] technology, biocatalytic flow reactions and the organization of sequencing of enzyme superfamilies.[32] Additionally, metabolic engineering is a major part. Two selected examples are the long-chain alkene biosynthesis in *Micrococcus luteus*[33] or the polyketide biosynthesis in *Escherichia coli* (Figure 2).[34]

3 Motivation and goal

The use of biocatalysis is of great importance in many aspects. It is not only of great interest in the academic world but also in chemical industry.[14] Special attention should be paid to cascade reactions, where enzymes work hand in hand to synthesize a desired product.[29] Cascade reactions are widely represented. In this context, enzymes can be interlocked with each other in a cascade reaction or an additional enzyme can be used as an auxiliary for a reaction sequence, which is also a cascade reaction. This work consists of three separate parts, which all contain cascade reactions. The three parts consist of enzyme-catalyzed production of firstly amines, secondly hydration of fatty acids and thirdly the synthesis of a hormone precursor. The first part includes the synthesis of amines, which is performed by using an amine dehydrogenase (Scheme 3).

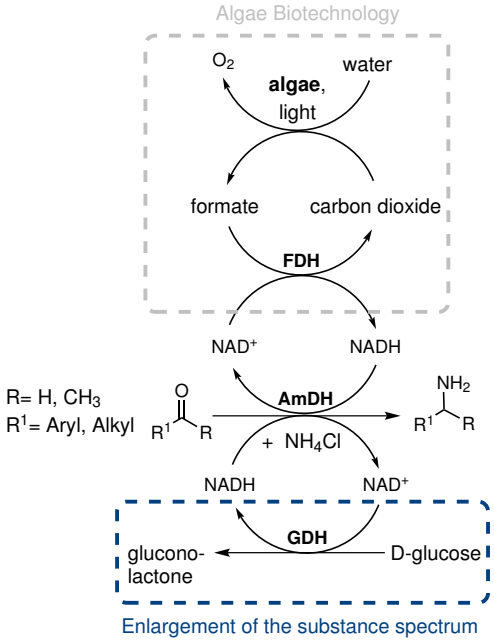

Scheme 2: Content of amine dehydrogenase-catalyzed reactions- In grey, algae production of formate as cosolvent for successful regeneration of cofactor. In blue, cofactor recycling by the means of glucose dehydrogenase and D-glucose for the screening of a range aryl-substituted ketones.

With this amine dehydrogenase, aryl-substituted amines with the cofactor regeneration system based on D-glucose and glucose dehydrogenase, should be implemented.

Furthermore, the amine dehydrogenase should be combined with algae biotechnology as a alternative, green cofactor recycling using CO_2 as a cofactor. The second topic is the synthesis of hydroxy fatty acids and their esterification (Scheme 3), to synthesize different polyols. These polyols should be later converted by the cooperation partner Windmöller GmbH to specific polyurethanes.

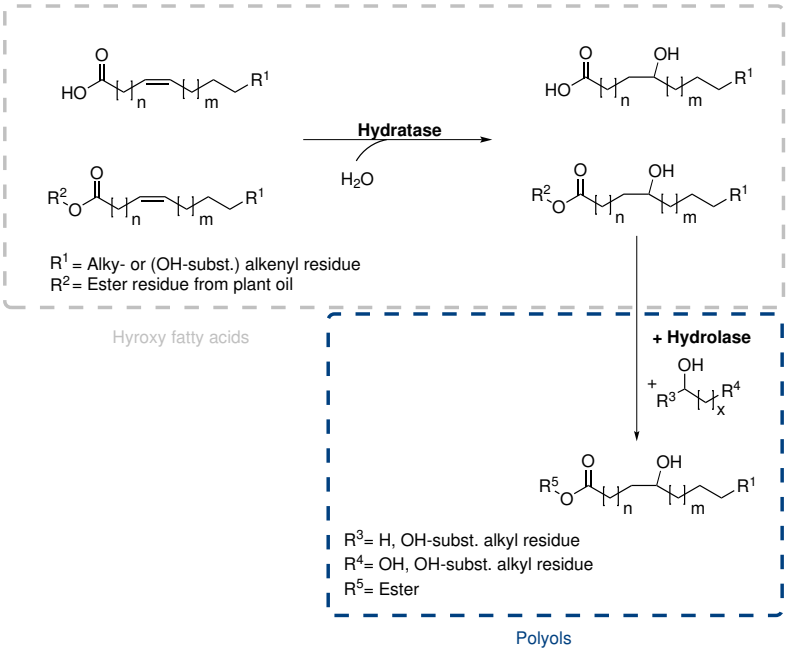

Scheme 3: Content of fatty acid hydratase-catalyzed reactions- In grey the hydratisation of fatty acids, esters and oils by the mean of fatty acid hydratases are shown. In blue the conversion of the hydrated fatty acids, esters and oils with polyols to complex ester for the production of polyurethanes are shown.

This cascade consists of a fatty acid hydratase, catalyzing the hydration of fatty acids, which was later combined with a lipase for esterification of the hydroxy fatty acids with different polyols. The third topic includes the synthesis of 12-oxo-phytodienoic acid (**1**, 12-OPDA) (Scheme 4), the first active intermediate in the jasmonate biosynthesis. The motivation of this cascade was to synthesize 12-OPDA (**1**) enzymatically on a large scale with high purity for later experiments with plant metabolism, which will be performed by the working group of Dietz, Biochemistry & Physiology of Plants, Bielefeld University.

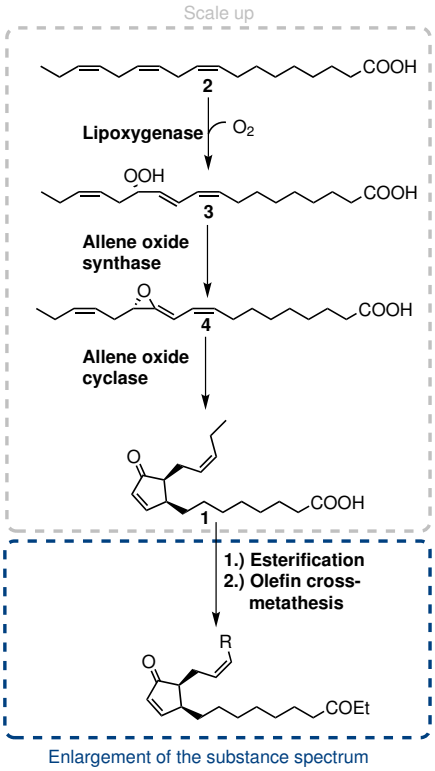

Scheme 4: Content of **12-OPDA (1) synthesis**- In grey, three step enzymatic cascade reaction with lipoxygenase (13-LOX), allene oxide synthase (AOS) and cyclase (AOC2). In blue further conversion of 12-OPDA (**1**) starting with esterification, followed by olefin cross-metathesis.

Thereby the aim is the usage of a three enzyme cascade consisting of a lipoxygenase catalyzing α-linolenic acid ((**2**), LA) to (9*Z*,11*E*,13*S*,15*Z*)-13-hydroperoxyoctadeca-9,11,15-trienoic acid (**3**, 13-HPOT), an allene oxide synthase, which converts the 13-HPOT (**3**) to (9*Z*,15*Z*,13*S*)-12,13-epoxyoctadeca-9,11,15-trienoate (**4**, 12, 13-EOT) and an allene oxide cyclase to produce 12-OPDA (**1**). In this context, the individual synthetic steps should be optimized and adjusted to each other. In addition, various 12-OPDA (**1**) derivatives were synthesized using olefin metathesis to test its activity towards plant metabolism.

4 Amine dehydrogenase-catalyzed reactions

4.1 Current state of science

4.1.1 Importance of amines

Amines are important building blocks in fine and bulk chemicals, as well as in pharmaceuticals.[35] The synthetic routes are very diverse and differ in whether primary, secondary, tertiary or chiral amines should be preserved.

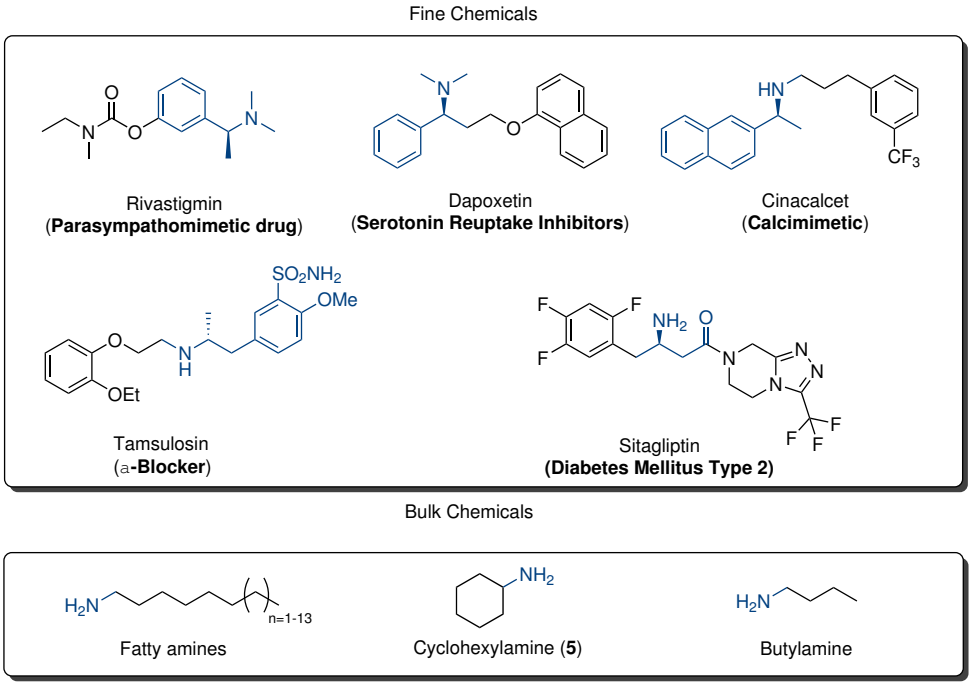

Figure 3: Important chemicals including amines.[35–38]

In Figure 3, there are some pharmaceuticals which contain chiral amines as functional groups, as well. Obviously, not only the amine functionality is a central moiety, but also the chirality plays an important role. Enantiomerically pure amines are a whispered functional moiety in nearly 50% of all pharmaceuticals,[39] they have been widely used as auxiliaries, resolving agents or agrochemicals.[35]

Aliphatic amines like cyclohexylamine (**5**) are synthesized by the means of the corresponding ketone or aldehyde and ammonia over nickel catalysts at 20 MPa and 150–200 °C with hydrogen over a fixed-bed catalyst. Fatty amines are produced by hydrogenation of fatty nitriles at 80–140 °C and 1–4 MPa over nickel or cobalt catalysts (Scheme 5).[38]

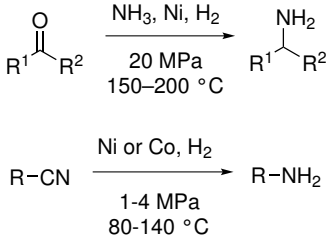

Scheme 5: Chemical Synthesis towards aliphatic and fatty amines.[38]

Other common procedures to obtain amines are the Gabriel-Synthesis or Leuckart Wallach reaction.

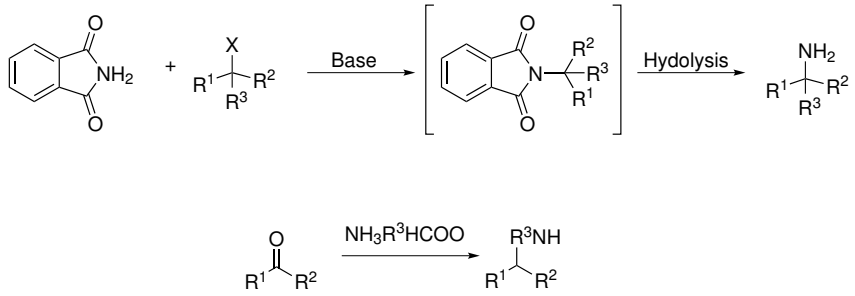

Scheme 6: Gabriel synthesis and Leukart Wallach reaction towards amines.[38]

The Gabriel synthesis is based on phthalimid, which reacts under basic conditions with an alkylhalegonids, after hydrolysis, the amine is formed (Scheme 6).[40]
The Leukart Wallach reaction starts with a ketone and reacts with ammonium formate under high temperatures towards the amines.[41] A classical chemical method for the synthesis of chiral amines is the crystallization with chiral carboxylic acids (Scheme 7).[42]

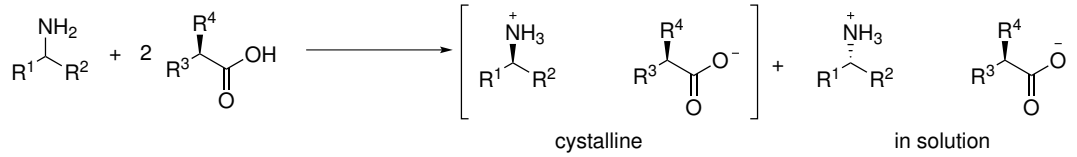

Scheme 7: Racemate resolution through fractional crystallization of racemic amines salts and enantiomerically pure carboxylic acids.[43]

Another method is the asymmetric reductions of C=N-double bonds of imines or oximes with chiral reagents or alkylations using internal chiral auxiliaries (Scheme 8).[44]

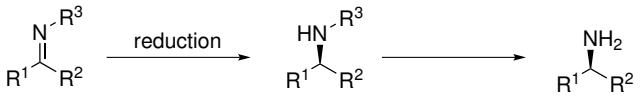

Scheme 8: Reduction of C=N double bond for the enantioselective synthesis of amines.[43]

The diastereoselective hydrogenation of SCHIFF bases starting from a ketone using (*R*)-phenylethylamine ((*R*)-**6**) is a method to produce chiral secondary amines.

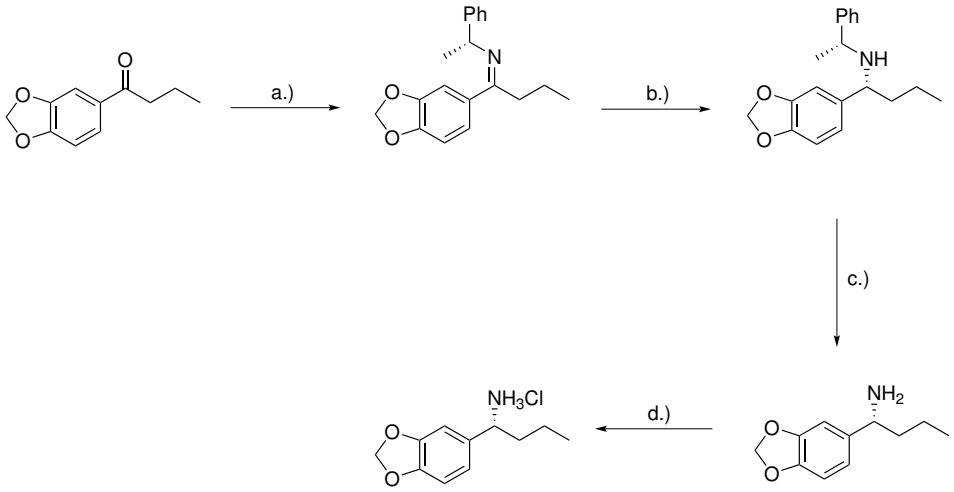

Scheme 9: Diastereoselective hydrogenation of a SCHIFF base. a) $TiCl_4$ (0.55 eq.), (*R*)-PEA (1.2 eq.), Et_3N (2 eq.), toluene. b) Ra-Ni, H_2, toluene-EtOH, c) 10% Pd/C (10 wt%), H_2, AcOH, toluene-EtOH. d.) HCl in *i*-PrOH-toluene; *i*-PrOH-*n*-heptane.[45]

This reaction starts with the formation of an imine with chiral benzylamine, followed by reduction using RANEY-Nickel.

Afterward, a cleavage and salt formation follows (Scheme 9). All in all, there are only a few possibilities for the synthesis of chiral amines, therefore a biosynthetic approach is a promising alternative to obtain enantiomerically pure amines.

4.1.2 Enzymes for chiral amine synthesis

The preparation of enantiomerically pure amines can be realized by using enzymes.[46] Particularly suitable biocatalysts are lipases, amine oxidases amine dehydrogenases, transaminases, imine reductases and amine oxidases (Figure 4).[35]

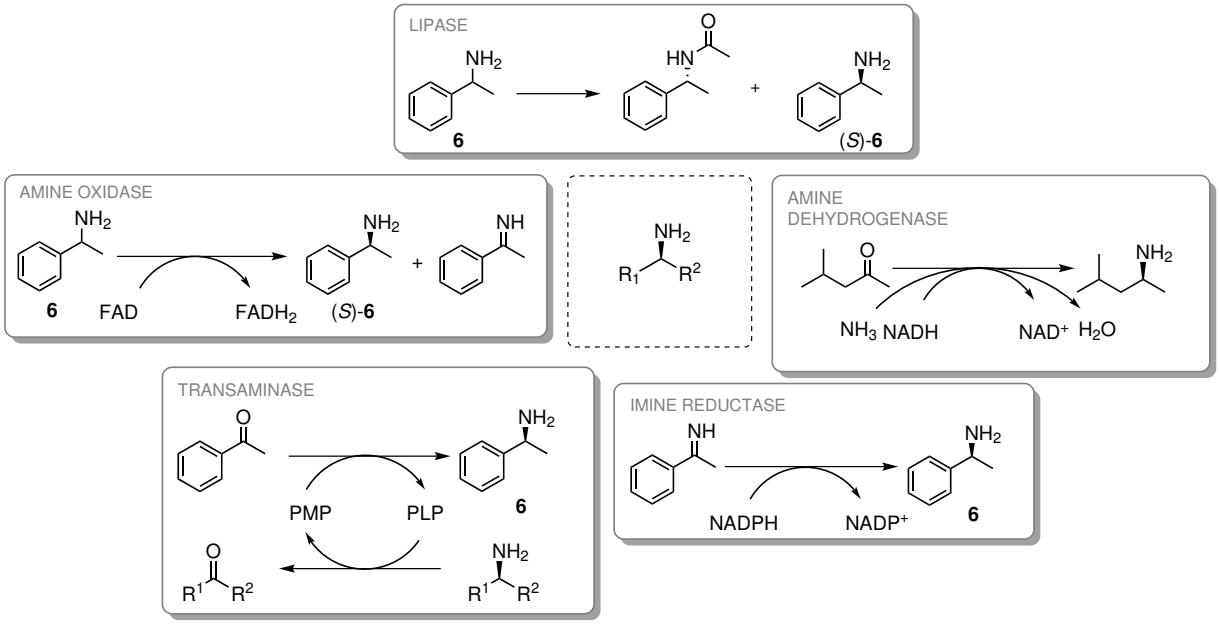

Figure 4: Enzymes for the production of chiral amines.

Lipases are enzymes from the class of hydrolases, which catalyzes the hydrolysis of long-chain glycerides and fatty acids.[47] Hydrolases catalyze the reaction *via* a catalytic triad, which usually contains the amino acids serine, aspartic acid or glutamic acid and histidine[48] in their active sites, whereby the nucleophilic serine is located in a conserved pentapeptide sequence GXSXG.[49]

Scheme 10 shows the mechanism of the catalytic triad located in the active site of hydrolases.

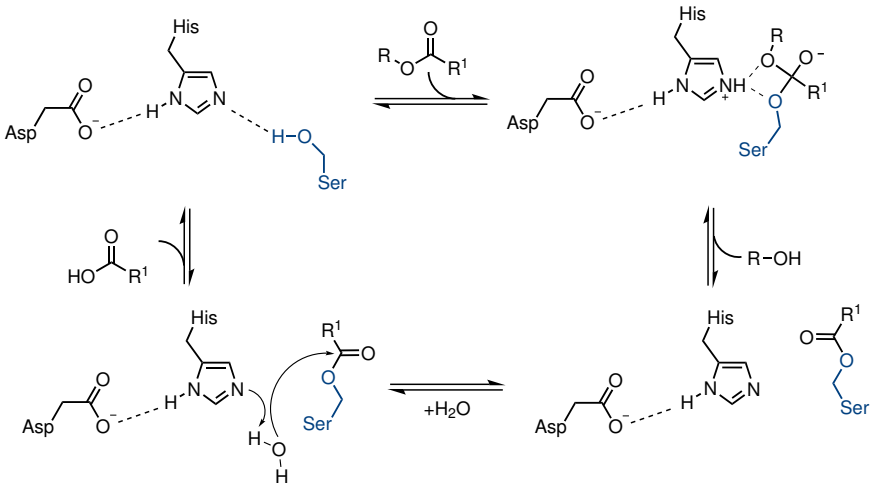

Scheme 10: Catalytic triade consisting of serine, aspartic acid and histidine.

In the first step aspartic acid forms a hydrogen bond with the nitrogen of the histidine, while the other nitrogen of the histidine forms a hydrogen bond with the hydroxy-group of the serine, which leads to a polarization and therefore to an increase in the nucleophilicity of the oxygen atom. This enables the oxygen of the serine to attack the carbon of the acyl donor, resulting in an acyl-enzyme intermediate. The tetrahedral intermediate is stabilized by hydrogen bonds and a so-called oxyanion hole is formed.[50] The reaction ends with the release of the product.

Another interesting feature of lipases is the activation over a water-lipid interface. The active site is shielded by a helical oligopeptide (lid). When the lipase interacts with the hydrophobic interface, the lid opens, the active pocket is exposed and the substrate can be bound.[50–52]

Industrial applications of lipases vary over oleo-chemicals, detergents, polymers, food processing, pharmaceutical, waste, cosmetics and biodiesel.[53] A famous example for the usage of lipases in chemical industry is a kinetic resolution of racemic amines established by BASF (Scheme 11).[43,54,55]

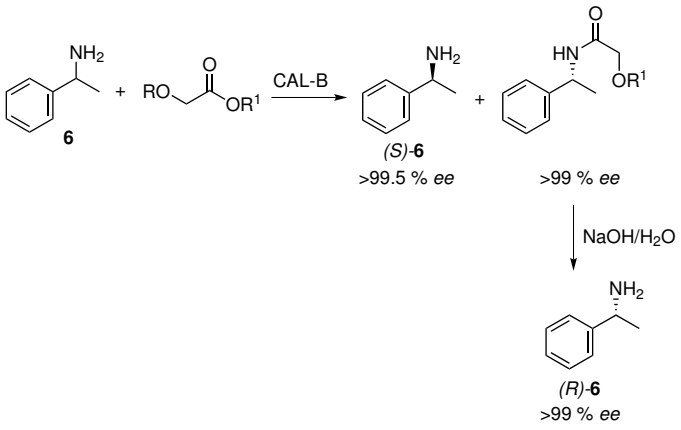

Scheme 11: Kinetic resolution of 1-phenylethylamine (**6**), implemented by BASF.[56]

Amine oxidases are another enzyme-class used for the synthesis of chiral amines. They belong to the enzyme family of oxidoreductases that catalyze the oxidative hydrolysis of primary amines to aldehydes, they can be subdivided into copper-dependent and flavine-dependent enzymes. The most known amine oxidases are monoamine oxidases (MAO).[57] The catalytic cycle of an MAO is shown in figure 16, the hydrolysis forms the aldehyde or ketone and ammonia is released. It is completed by the regeneration of the FAD cofactor *via* conversion of oxygen to hydrogen peroxide (Figure 12).[58]

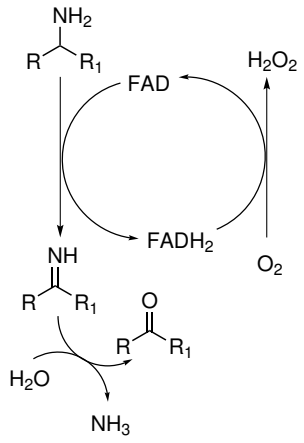

Scheme 12: MAO-catalyzed reaction.[57]

Another example for the biocatalytic synthesis of amines are imine reductases (IRED).[59]

Imine reductases are NADPH-dependent oxidoreductases, which catalyze the asymmetric reduction of imines to their corresponding amines.[59,60] In 2010 the first imine reductase an (*R*)-IRED and (*S*)-IRED from *Streptomyces sp.* GF3587 and *Streptomyces sp.* GF3546 was described by Mitsukura *et al.* (Scheme 13)[61]

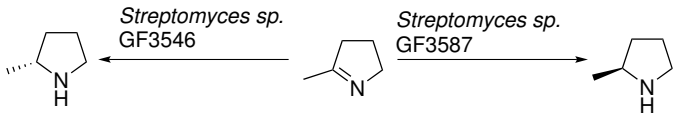

Scheme 13: Reduction of 2-methyl-1-pyrroline by *Streptomyces sp.* strains.[59]

In 2015 Hussain *et al.* published an article with a range of cyclic imines that were reduced towards cyclic amines.[62] In the same year Wetzl *et al.* showed a huge range of new imine reductases out of a variety of strains.[63] Further investigations were done with 1-methyl-3,4-dihydroisoquinoline as a model substrate.[60,64] In 2018 Zumbrägel *et al.* published the reduction of cyclic sulfur-containing imines.[65] Furthermore, a reductive aminase was described, which describes one subgroup of imine reductases. These enzymes catalyze the formation of the imine followed by reduction (Scheme 14).[66]

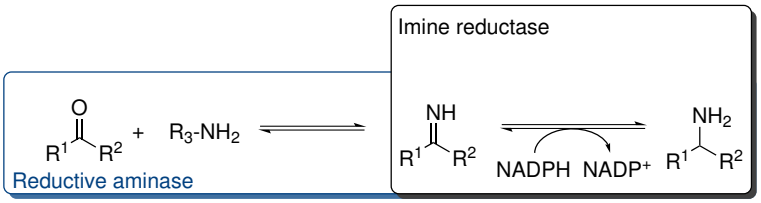

Scheme 14: Reactions catalyzed by imine reductase and reductive aminase.[66]

Another biocatalytic approach towards chiral amines is the use of transaminases.[67] Transaminases either catalyze the a kinetic racemate cleavage or an asymmetric amination of prochiral ketones.[68] ω-Transaminases are pyridoxal-5'-phosphate-dependent and catalyze the deamination of a primary amine while simultaneously aminating a ketone or an aldehyde.[69]

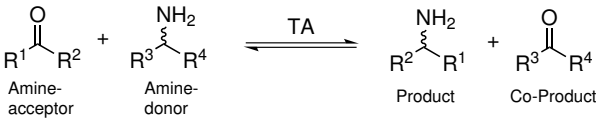

Scheme 15: Reaction scheme of transaminases.[69]

In Scheme 15, the reaction for transaminases is shown. The amine acceptor, amine donor, product and co-product are in equilibrium with each other.[70] As amine donor L-alanine or isopropylamine can be used, whereas the most common amine donor is L-alanine, which is converted to pyruvate in the transamination reaction. To drive this reaction towards the product side, the by-product has to be further converted. Therefore, pyruvate is converted utilizing a lactate dehydrogenase towards lactate.[71] Another method is the use of isopropylamine, which is converted to acetone and can be removed from the reaction mixture by evaporation to shift the equilibrium to the product side.[72] One famous example of the industrial use of transaminases is the biocatalytic approach towards the antidiabetic drug Sitagliptin (Scheme 16). The chemical synthesis based on the asymmetric hydration of an enamine, which is formed by the addition of ammonium acetate. The hydration takes place at high pressure *via* rhodium-based chiral catalysis. The rhodium has to be removed from the product after the reaction. As a result, transaminases have been considered as an alternative. Towards this end, the (*R*)-selective transaminase ATA-117, a homolog of an enzyme from *Arthrobacter sp.* was engineered using several cycles of site saturation mutagenesis to convert the keto-function towards the amine in one step with the desired selectivity.[23]

4.1.3 Amine dehydrogrogenase

In addition amine dehydrogenases (AmDH) can be used for the production of chiral amines. Amino acid dehydrogenases catalyze the oxidative deamination of the amino acid and the reductive amination of the corresponding α-keto acid.[73]

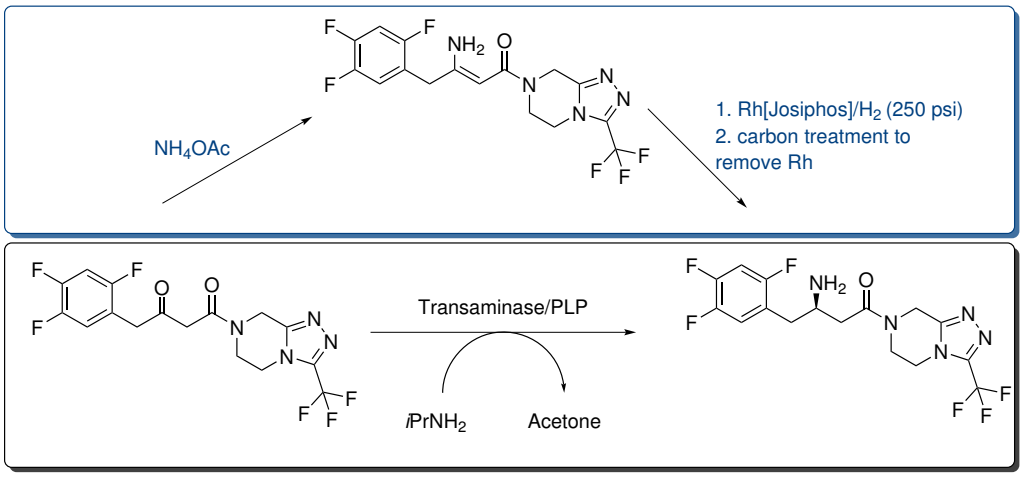

Scheme 16: Chemical and enzymatic synthesis of Sitagliptin.[23]

The first naturally occurring amine dehydrogenase was described in 1968.[74] In 2000 Itoh *et al.* isolated an NAD^+/NADH-dependent amino alcohol dehydrogenases from *Streptomyces virginiae* IFO 12827, catalyzing the reversible dehydrogenation of serinol, but it showed only low enantioselectivities.[75] A quinohemoprotein-containing amine dehydrogenase was published in 2003 from Sun *et al.* with a strict substrate specificity.[76] Due to the lack of catalytic activity and selectivity Abrahamson *et al.* used *structure-based Combinatorial Active-site Saturation Test* (CAST)[77] to generate an amine dehydrogenase from an amino acid dehydrogenase. During this CAST application amino acids in or adjacent to the active pocket were selected and grouped to perform subsequent saturation mutagenesis.[78]

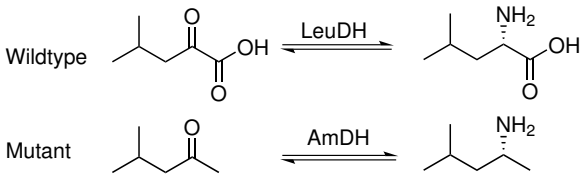

Scheme 17: Amino acid dehydrogenase reaction *vs* amine dehydrogenase reaction.[78]

The starting point for the creation of an AmDH was the use of an leucine dehydrogenase from *Bacillus stereothermophilus* as an initial protein scaffold (Scheme 17).

For the determination of substrate–binding pocket interactions, the holo crystal structure of the phenylalanine dehydrogenase (PheDH) from *Rhodococcus sp.* M4 was used. The K67 and N263 of the phenylalanine dehydrogenase (PheDH) from *Rhodococcus sp.* M4 are directly interacting with the carboxylic residue of the amino acid. With these results in hand several rounds of CAST were performed. Therefore, the leucine dehydrogenase from *Bacillus stereothermophilus* could successfully be changed into an amine dehydrogenase including the mutations K68S/E114V/N261L/V291C.[78] In 2013 Abrahamson *et al.* used this method again to produce an AmDH from a phenylalanine dehydrogenase out of *Bacillus badius* which was the first example for the conversion of benzylic ketones, such as *p*-fluorophenylacetone.[79] One year later Bommarius *et al.* created a chimeric enzyme based on the structure of the phenylalanine dehydrogenase from *Rhodococcus sp.* M4 and a leucine dehydrogenase from *Bacillus sphaericus* with an increase in activity and thermal stability.[80] This study was expanded by applying this enzyme to a biphasic aqueous-organic system.[81] Additionally, in 2015 Xu et al. described the application of the two-site mutation (K77S/N270L) towards a leucine dehydrogenase from *Exigobacterium sibiricum* (EsLeuDH-DM). With this enzyme in hand, they tested a range of short-chain secondary aliphatic ketones and alkyl cyclic ketones as substrates.[82] Chen *et al.* adapted the method for a phenylalanine dehydrogenase (PheDH) from *Rhodococcus sp.* M4.[83] In the same year Mutti *et al.* published a redox neutral cascade, combining an alcohol dehydrogenase from three different strains with an amine dehydrogenase from *Bacillus sp.* to convert a variety of aromatic and aliphatic alcohols (Scheme 18).[84]

In 2017 two other cofactor recycling systems were implemented to regenerate NADH. One the one hand a formate dehydrogenase (FDH)[85] was used and the other hand a NADH Oxidase, which were both coexpressed in a whole cell biocatalyst.[86]

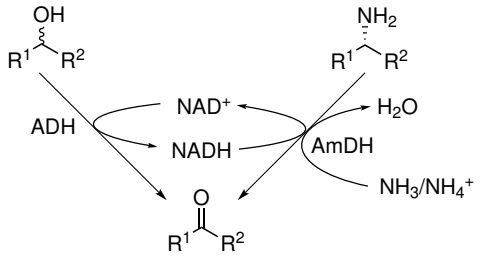

Scheme 18: Tandem reaction for the hydrogen-borrowing amination of alcohols.[84]

In the following years, a significant range of successful immobilization procedures were shown like immobilization on magnetic nanoparticles,[87] hybrid titania nanoparticles,[88] on EutM-SpyCatcher,[89] porosity glass Fe(III) ion affinity beads,[90] a hydrophobic support and a support for covalent binding[91] or EziG carriers.[92]

4.1.4 Immobilization of enzymes

Enzyme immobilization is a versatile tool to optimize the catalyst conditions.[93] The most advantages of immobilization are the stability, reusability,[94] and better separation.[95] The known procedures for enzyme immobilization are binding to a carrier, the entrapment or the cross-linking of enzymes (Figure 6).[96]

The immobilization on a carrier can be done *via* adsorption or covalent bonding, e.g. non-specific physical adsorption, like VAN DER WAALS forces, hydrogen bonds, and hydrophilic interactions (Figure 6). Furthermore, bio-specific adsorption is another possibility[97] or immobilized metals,[98] ionic interactions or hydrophobic interactions.[99] In addition, the carrier can consist of different materials. One possible support is an organic polymer, like resins, natural polymers such as cellulose or inorganic polymers like silica. There are also smart polymers known like magnetic particles.[96] Another way for the immobilization of enzymes is the entrapment in a polymeric mesh such as agar, polyacrylamide gel or calcium alginate.

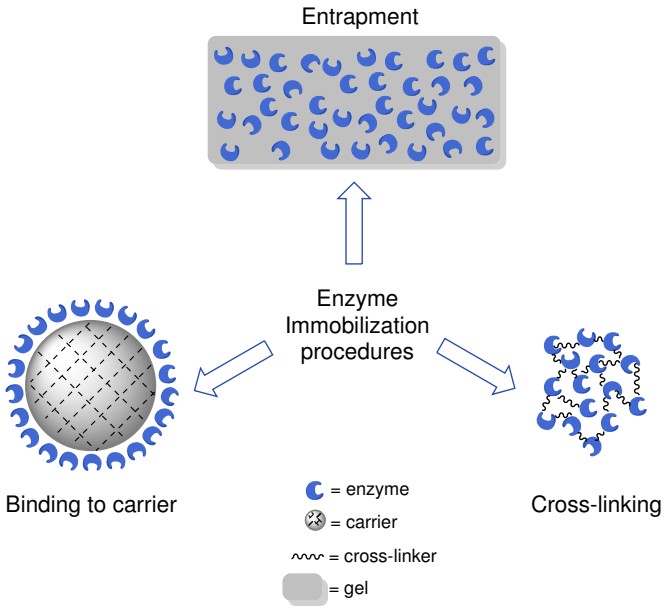

Figure 5: Different methods for immobilizing enzymes.[96]

The entrapment is done during the polymerization reaction and/or cross-linking reaction in the presence of the enzyme of interest.[100] The third possibility for enzyme immobilization is the cross-linking. Towards this end, bonds between individual enzyme aggregates or crystals are produced by a mediating reagent such as glutaralaldehyde (CLEAs/CLECs).

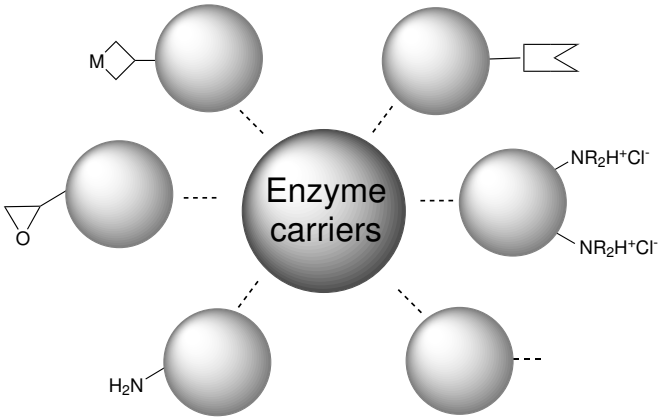

Figure 6: Different methods for immobilizing enzymes.

CLEAs are prepared by mixing salts, water miscible organic solvents or non-ionic polymers, to aqueous protein solutions which leads to their precipitation and therefore to aggregation.[96] The immobilization of enzymes also plays an important role in industrial applications. In the following only a few examples are listed utilizing immobilized enzymes e.g. lipases, which are covalently immobilized for the chiral resolution of alcohols and amines or for the production of biodiesel from triglycerides or the transesterification of food oils.

Scheme 19: Hydrolysis of benzylpenicillin by the means of Penicillin G acylase.

Another example is the use of glucose isomerase for the production of high fructose from corn syrup[101] or the production of acrylamide *via* nitrile hydratase. A very famous example is the antibiotic modification by the means of Penicillin G acylase (Scheme 19).[102]

4.1.5 Combination of amine dehydrogenase and algae biotechnology

4.1.6 *Chlamydomonas reinhardtii*

Photoautotrophic microbes can be divided into prokaryotic (Cyanobacteria) and eukaryotic (Microalgae). Microalgae are unicellular photosynthetic organisms, that are ubiquitous present in freshwater and marine environments.[103] Because of their ability to produce energy and feedstock products, e.g. biodiesel or hydrogen,[104] they are very interesting for the production of bulk products, such as fuels.[105,106]

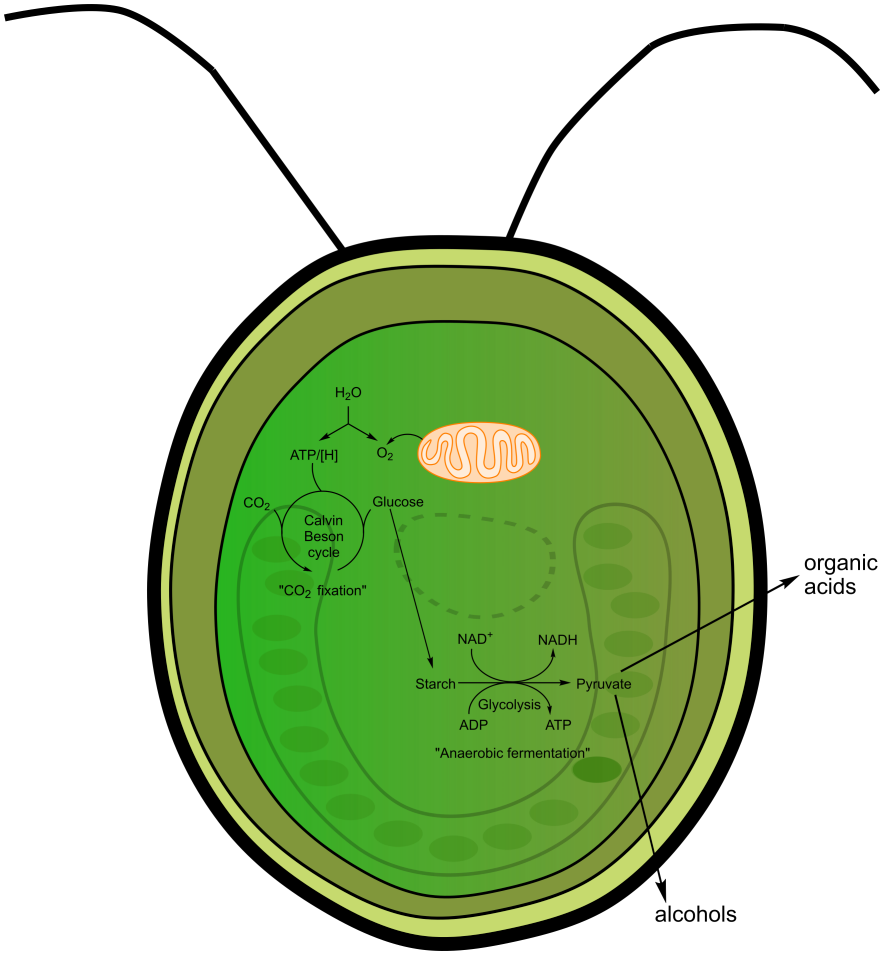

Figure 7: "Light reaction" and "anaerobic fermentation" reaction of *Chlamydomonas reinhardtii*.[103,107]

One of those microalgae is the green algae *Chlamydomonas reinhardtii* (Scheme 7), which contains multiple mitochondria, two anterior flagella and a chloroplast which contains the complex photosynthetic apparatus.[108] The difference to other plants is that every cell of the green algae *Chlamydomonas reinhardtii* is a viable organism and is doing photosynthesis.[103] The light reaction starts with the light-induced oxidation of water in photosystem II and ends after several redox reactions in the production of energy (ATP) and reducing equivalents NADPH. ATP and NADPH are consumed by the Calvin-Benson cycle to produce carbohydrates from CO_2.[103,107] These carbohydrates are metabolized in the anaerobic fermentation during glycolysis under consumption of NAD^+ and $NADP^+$ to pyruvate. The pyruvate is further metabolized in several fermentation circles (Figure 7). The produced substrates in these circles are secreted to the outer medium; examples for these substrates are formate, lactate, malate, acetate, succinate and alcohols like ethanol and glycerol.[109]

4.2 Motivation and goal for amine dehydrogenase-catalyzed reactions

As already described in detail in the current state of science many results have been achieved in the field of amine dehydrogenases. In this work, the amine dehydrogenase EsLeuDH-DM, a double mutant (K77S/N270L)[82] of a leucine dehydrogenase from *Exiguobactertium sibiricum*, was used.[110] So far, the EsLeuDH-DM was applied in a redox-neutral cascade. Chen *et al.* start from alcohols, which are converted with an alcohol dehydrogenase to the corresponding ketone. These ketones (aliphatic ketones, cyclic ketones, and acetophenone (**7a**)) were further converted using EsLeuDH-DM.[82] The aim of this first major topic is the use of the amine dehydrogenases EsLeuDH-DM for the production of aryl-substituted and primary amines. The topic is divided into two parts: The first part will deal with the substrate expansion of the amine dehydrogenase in combination with the cofactor recycling system of glucose dehydrogenase (GDH) from *Bacillus subtilis*[111,112] and D-glucose (Scheme 20). In this context, aryl-substituted ketones shall be investigated, as they serve as key building blocks for pharmaceuticals.[35] The K_M-value and possible cosolvents are to be determined with the best substrate. Subsequently, the EsLeuDH-DM has to be immobilized for better reusability.

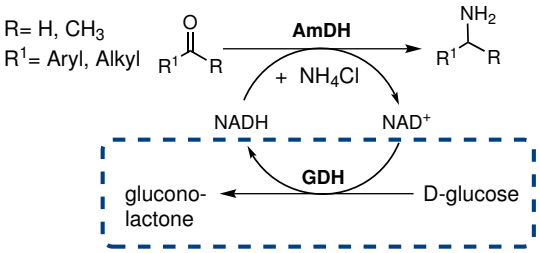

Scheme 20: Concept for amine dehydrogenase- Cofactor recycling by the means of glucose dehydrogenase (GDH) and D-glucose for the screening of a range aryl-substituted ketones using the amine dehydrogenase EsLeuDH-DM (AmDH) from *Exiguobactericum sibiricum*.

The second major part of this chapter deals with the conversion of aldehydes to amines in combination with the cofactor regeneration based on algae biotechnology.

Cofactor recycling plays a important issue in biocatalysis because many processes are catalyzed by enzymes that require a cofactor. Cofactor regeneration systems have the advantage that the cofactor does not have to be added in stoichiometric quantities. This, in turn, has high costs as a consequence. Nevertheless, for cofactor recycling the cosubstrate has to be present in a stoichiometric amount or in excess. Examples for cofactor recycling systems are D-glucose and glucose dehydrogenase, glucose-6-phosphate and glucose-6-phosphate dehydrogenase, formate and formate dehydrogenase or isopropanol and alcohol dehydrogenase, therefore waste products such as isopropanol or gluconolactone are generated.[113] Nowadays some interesting ways for cofactor recycling are mentioned such as the use of the light-gathering photosystem in cyanobacteria, which is able to regenerate the nicotinamide cofactor NADPH.[113,114] In cooperation with Wobbe, who established an algae which forms up to 3 mM formate, a new cofactorregeneration system was designed. This system is based on the *in situ*-cofactor recycling using the photoautotrophic microorganism *Chlamydomonas reinhardtii*.[115]

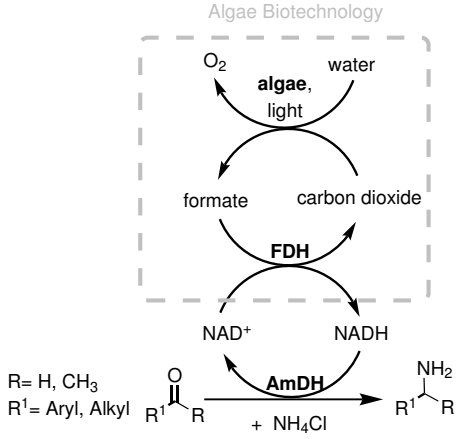

Scheme 21: Concept amine dehydrogenase in combination with algae biotechnology- Algae production of formate, using as cosolvent, for successful regeneration of cofactor for the combination with amine dehydrogenase.

The algae provides the formate, by *in situ*-formation from carbon dioxide, water and light. This system was combined with the formate dehydrogenase from *Candida boidinii* (cbFDH)[116] (Scheme 21). Therefore, experiments with the algae supernatant and reactions during algae fermentation were performed with aldehydes as substrates. The resulting primary amines are widely used as corrosion inhibitors, agrochemicals or pharmaceuticals,[38] therefore the access to such products *via* enzymatic processes is very attractive.

4.3 Results and discussion of amine dehydrogenase-catalyzed reactions

4.3.1 Spectrophotometrical activity tests with EsLeuDH-DM and aryl-substituted ketones

As already described in detail in the current state of science, in 2012 Abrahamson *et al.* implemented the methodology for the production of an amine dehydrogease from an amino acid dehydrogenase.[78] While amino acid dehydrogenases form hydrogen bonds to the carboxyl group of the amino acid to stabilize the interaction between the substrate and the enzyme, the mutant variant can enter non-polar interactions with the substrate. Chen *et al.* constructed an amine dehydrogenase by mutation of two amino acids from a leucine dehydrogenase from *Exiguobacterium sibiricum* (EsLeuDH-DM).[82] This double mutation was reproduced in previous studies[117] and examined concerning kinetics and substrate scope. In respect thereof, the K_M-value of the best substrate was evaluated, biotransformations were performed and the substrate loading was increased.

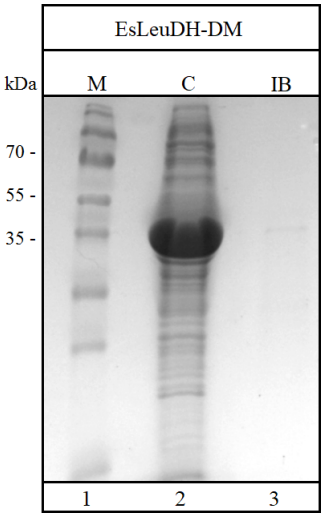

Figure 8: SDS-PAGE of overexpressed EsLeuDH-DM, induced at an OD_{600} of 0.5. Stained with Coomassie Brilliant Blue R-250. **lane 1**: marker (*ThermoScientific* PageRuler Stained Protein Ladder) , **lane 2**: crude extract, **lane 3**: inclusion bodies.

First of all, the expression of EsLeuDH-DM was further optimized by adding IPTG at OD_{600} of 0.5. The successful expression was monitored using SDS-PAGE (Figure 8).[117] In literature the activity for acetophenone (**7a**) was mentioned with 0.09 U mg^{-1} at an expression temperature of 25 °C and induction at OD_{600} between 0.6-0.8.[82] In previous studies from the author of this thesis an activity of 0.07 U mg^{-1} at a expression temperature of 20 °C and induction at OD_{600} 0.7 was found.[117]

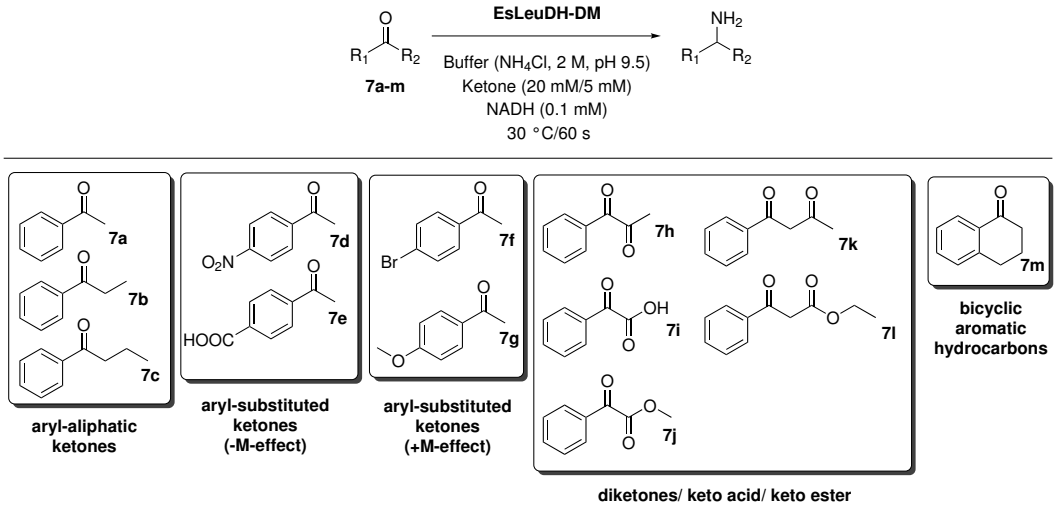

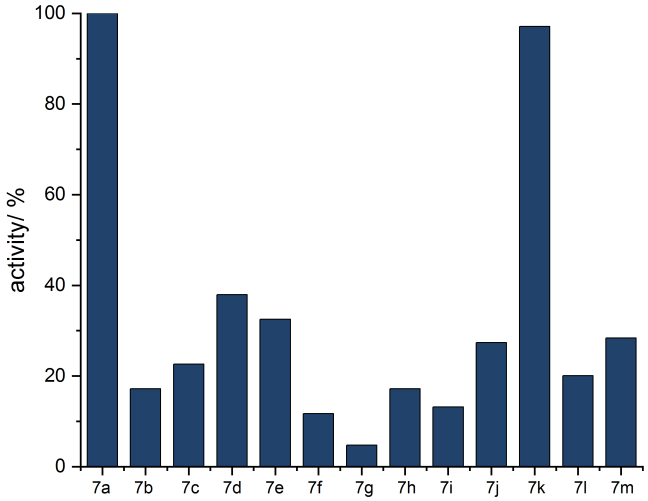

Figure 9: Substrate scope for EsLeuDH-DM investigated *via* photometric activity.

In this work an activity of 0.14 U mg^{-1} for acetophenone (**7a**) could be reached after induction at OD_{600} 0.5 and an expression temperature of 20 °C. Thus, the activity could be raised in this thesis by expression optimization. Further, the substrate scope of EsLeuDH-DM was examined with the optimized enzyme in hand. First, the substrate scope was investigated *via* a spectrophotometric activity assay. Therefore, a variety of aryl-substituted ketones with different substituents were investigated (Figure 4.3.1). The best activity was observed with acetophenone (**7a**), also benzoylacetone (**7k**) shows comparable results. Furthermore, EsLeuDH-DM shows a higher activity towards aryl-substituted ketones with a negative mesomeric effect **7d-e**, compared to aryl-substituted ketones with a positive mesomeric effect **7f-g**. Also diketones **7h-l** were accepted as substrates for EsLeuDH-DM, as well as bicyclic ketones **7m** (Figure 9).

4.3.2 Determination of K_M-value for acetophenone (7a)

After investigation of the substrate scope, the enzyme was purified using Ni^{2+}-NTA column chromatography (Figure 10).

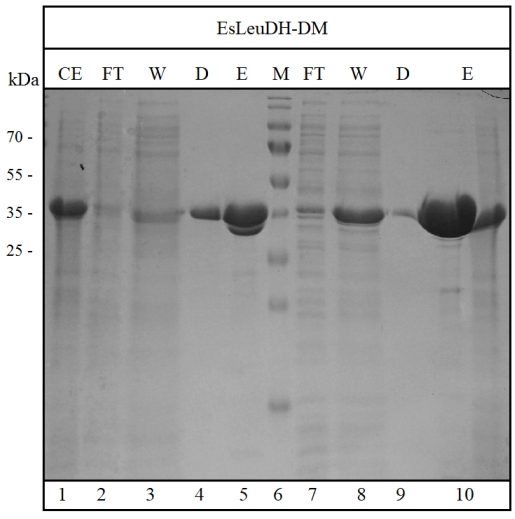

Figure 10: SDS-PAGE from purified EsLeuDH-DM. Stained with Coomassie Brilliant Blue R-250. **lane 1-5** shows desalting with 20 mM NaPi-Buffer, **lane 7-10** shows desalting with 100 mM NaPi-Buffer, **lane 1**: crude extract, **lane 2**: flow through, **lane 3**: wash, **lane 4**: desalting, **lane 5**: elution, **lane 6**: marker (*ThermoScientific* PageRuler Stained Protein Ladder), **lane 7**: flow through, **lane 8**: wash, **lane 9**: desalting, **lane 10**: elution.

By using higher salt-concentration during desalting, the protein concentration could be raised to the double amount. Despite precipitation in both buffers on ice an active enzyme with high purity could be isolated. After purification K_M-value was measured. To determine the MICHAELIS-MENTEN constant (K_M) for the reductive amination of acetophenone (**7a**), the activities of the purified enzyme were first determined using spectrophotometric activity assay at different substrate concentrations. The consumption of NADH was determined at 340 nm and a reaction temperature of 30 °C. By plotting the activities against the substrate concentration, followed by a non-linear fit of the curve, the K_M-value can be determined. For acetophenone (**7a**) a high K_M-value of 26.3 mM was evaluated. The high K_M-value indicates a low affinity of the enzyme to the substrate.

However, the course of the curve for acetophenone (**7a**) does not indicate substrate inhibition at these substrate concentrations.

4.3.3 Kinetic studies for the biotransformations with EsLeuDH-DM and GDH

With acetophenone (**7a**), as the most promising aryl-substituted substrate for the amine dehydrogenase EsLeuDH-DM biotransformations were performed. Therefore, the cofactor recycling system consisting of glucose dehydrogenase (GDH) and D-glucose as a cosubstrate for *in situ* cofactor regeneration was used. The substrate concentration was varied from 20 mM to 100 mM. Because of the high K_M-value for EsLeuDH-DM, high substrate concentrations have to be used. From a synthetic perspective, however, this is not a disadvantage, as high substrate loads were used.

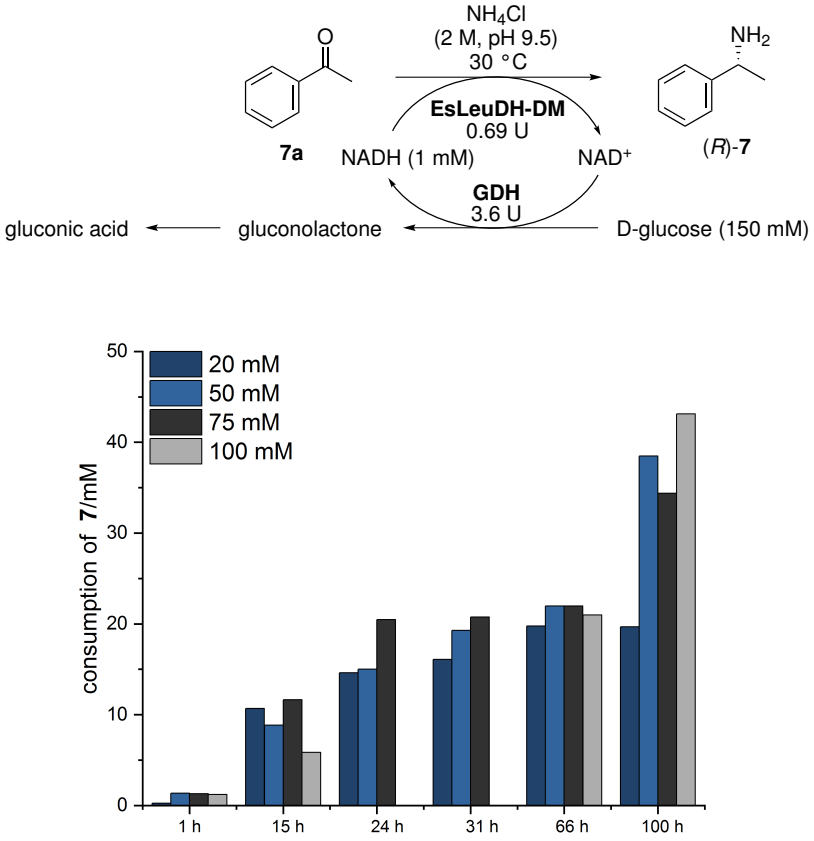

Figure 11: Biotransformations of acetophenone (**7a**) using EsLeuDH-DM with substrate concentrations from 20 mM to 100 mM.

The Michaelis-Menten constant corresponds to the substrate concentration at which the reaction rate is half of v_{max}. Therefore, the substrate concentration has to be at least 52.6 mM to achieve maximum reaction velocity. The initial reaction rate is faster at higher substrate concentration, which can be rationalized by the K_M-value. Despite an extended reaction time of 100 h, it was not possible to reach a higher product formation than 43% (Figure 11). For achieving higher product amounts, a dosing experiment was performed.

Within 75 h acetophenone (**7a**) (100 mM) was added at a rate of 13 ng min^{-1} to the reaction mixture. After 66 h, a conversion of 50% could be reached. Whereas in the batch process only 21% conversion after 66 h could be achieved (Figure 12).

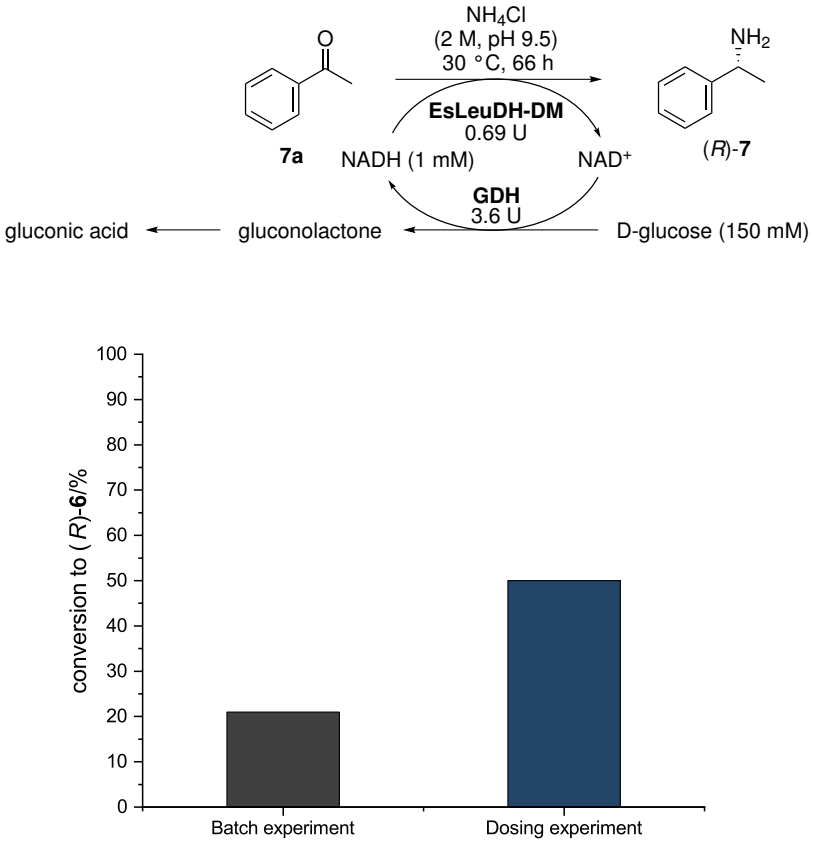

Figure 12: Biotransformations of acetophenone (**7a**) using EsLeuDH-DM with substrate concentrations of 100 mM in batch process and in a dosing experiment.

This results probably indicates deactivation of the enzyme, which can be suppressed by dosing the substrate **7a** to the reaction mixture. Substrate inhibition can be excluded based on the results of the K_M-value determination.

4.3.4 Stability tests for EsLeuDH-DM at different substrate concentrations of 7a

The stability of EsLeuDH-DM was investigated at different substrate concentrations (20, 50, 100 mM) (Figure 13). The activity was investigated after incubation of the enzyme with the substrate **7a** at fixed times. Afterward, the decrease in NADH was monitored photometrically at 340 nm for 60 seconds.

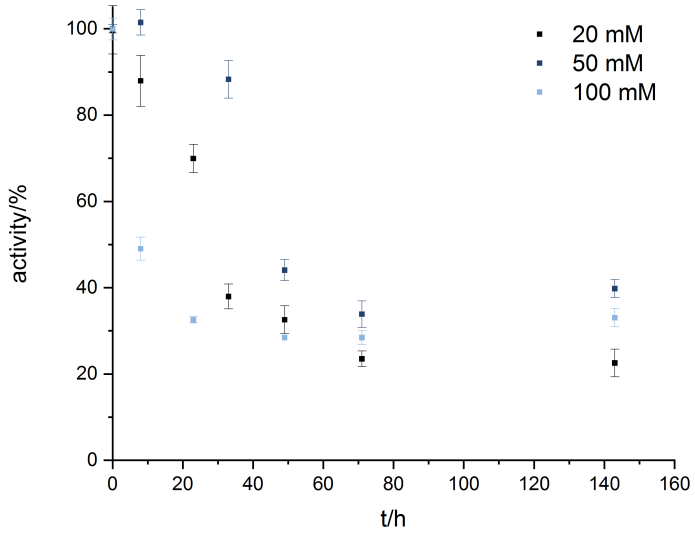

Figure 13: Stability of EsLeuDH-DM at different acetophenone (**7a**) concentrations.

There is a decrease in the activity of the enzyme after about 30 h, this could also be an explanation for the slow conversion after 30 h reaction time. This development can be observed for all substrate concentrations. After 30 h, the activity saturates at about 30% of the initial activity. This, in turn, underlines the assumption of deactivation of the enzyme. Table 1 shows the half-life of the enzyme at different substrate concentrations.

Table 1: Determination of the half-life of EsLeuDH-DM at different substrate concetrations.

Conc./mM	Half-life of enzyme/h
20	30
50	47
100	8

These results show that the dosing experiment probably has a positive influence on the half-life of the enzyme, because there is always a lower substrate **7a** concentration in the reaction solution, compared to the direct addition of 100 mM substrate. Therefore, the enzyme is not deactivated as quickly.

Consequently, the EsLeuDH-DM can convert more substrate in the dosing experiment in the same reaction time. Furthermore, the stability of the cofactor was examined in 2 M NH_4Cl buffer, pH 9.5 with at 30 °C. The results are shown in the following chart:

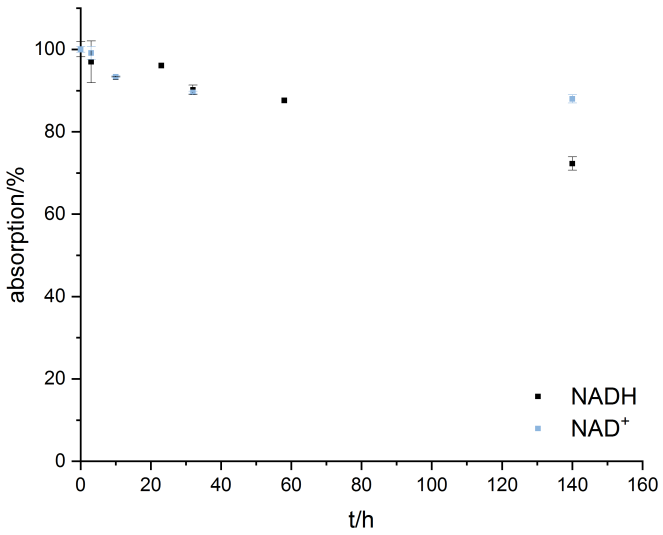

Figure 14: Stability of NADH and NAD^+ in NH_4Cl buffer (pH 9.5, 2 M).

Table 2: Evaluation of salt concentration in combination of EsLeuDH-DM.

Cofactor	Half-life of enzyme/h
NADH	200
NAD^+	-

The cofactor is stable even at high salt concentrations and basic pH (Table 2, Figure 14). This in turn shows that the instability of the cofactor does not play a role in this reaction set-up.

4.3.5 Cosolvent-screening for EsLeuDH-DM

To increase the solubility of the substrate **7a**, different water-miscible cosolvents were screened. In this context, initial and long term stability of the enzyme EsLeuDH-DM

towards these cosolvents were tested. Such a solvent system would then enable the use of higher substrate concentration under homogeneous conditions, as well as the option to operate at the maximum reaction rate (v_{max}). Therefore, a selection of four water-soluble cosolvents has been examined with volumetric percentages of up to 30% (v/v). Hence, ethanol, isopropanol, methanol and dimethyl sulfoxide (DMSO) were tested. EtOH, MeOH and isopropanol show poor long term stability for EsLeuDH-DM (the results are shown in the experimental section). The best results were achieved with DMSO (Figure 15).

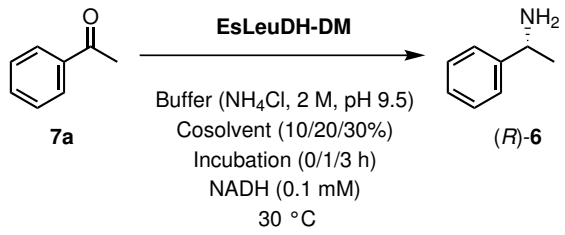

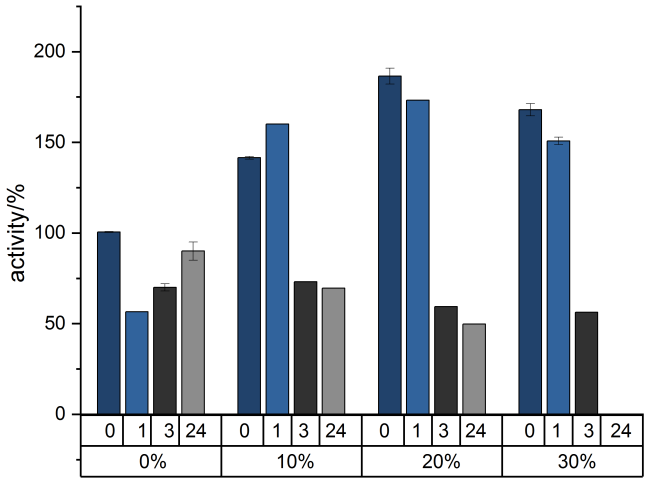

Figure 15: Photometric activity assay with acetophenone (**7a**) and DMSO as cosolvent.

These results show that DMSO, compared to EtOH, MeOH and isopropanol, is the best cosolvent in concentrations up to 20 vol% (*v/v*) (Figure 15). Furthermore, the relative activity was increased, and the long-time stability is comparable to the results without cosolvent. The increase in activity in the presence of DMSO could be related to the partial unfolding of the enzyme[118] and therefore, result in a better entrance of the substrate **7a** into the active site. The utilization of 20 vol% DMSO (*v/v*) will allow higher dissolved substrate **7a** concentrations in the aqueous phase and lead to scale-up possibilities for preparative biotransformation.

4.3.6 Immobilization of EsLeuDH-DM and preparative reaction with immobilized EsLeuDH-DM

As already mentioned in the current state of science a comprehensive selection of immobilization strategies for the fixation of enzymes are known.

Ingram successfully established a methodology for the immobilization of EsLeuDH-DM in his bachelor thesis under the supervision of the author of this thesis.[119] Ingram utilized two commercially available, a hydrophobic carrier from *Lewatit*® VP OC 1600 and a carrier for covalent binding from *Sigma Aldrich* Immobead IB-150P. The epoxy carrier carries epoxy residues, while the hydrophobic carrier forms non-polar, hydrophobic bonds. Before immobilization both carriers were washed with buffer, the hydrophobic carrier was washed with 50 mM KPi buffer and the covalent carrier was washed with 500 mM KPi buffer. The immobilization was carried out over-night, afterward, the mass ratio of protein and carrier, yield, loading, and efficiency were examined using photometric Bradford assay.

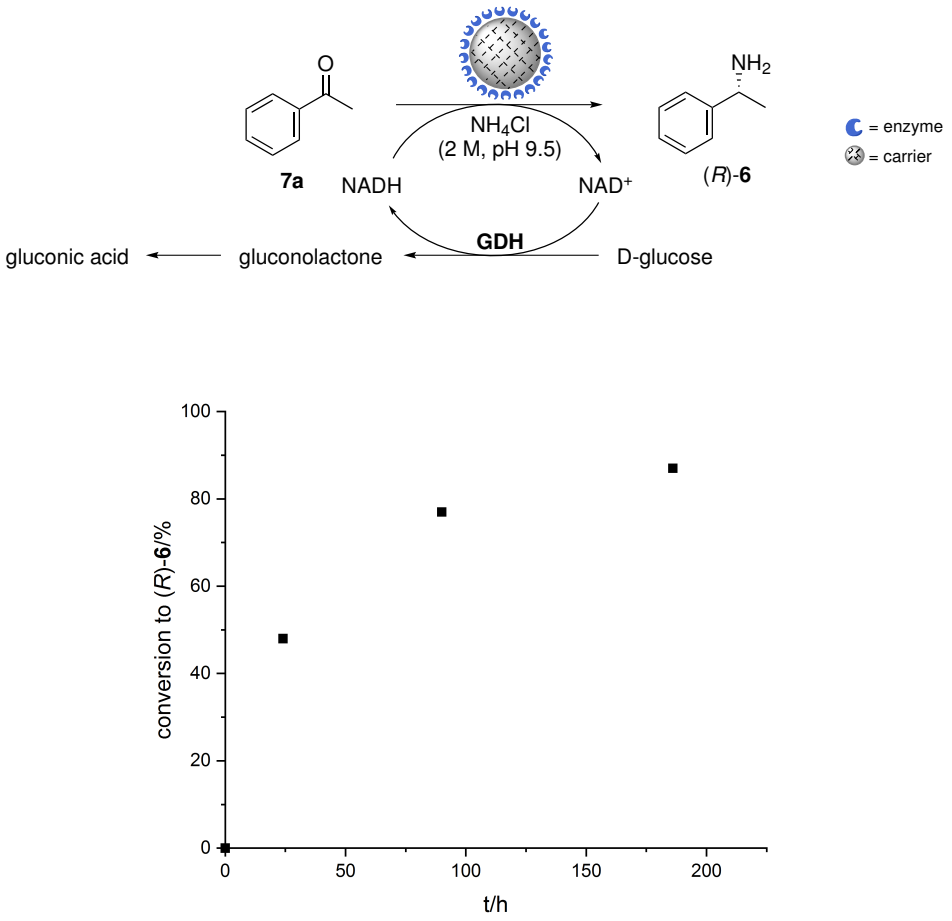

Figure 16: Conversion of acetophenone (**7a**) with immobilized EsLeuDH-DM.[119]

The covalent carrier had an immobilization yield of 48% with 11.8 mg g^{-1} protein on the solid support. The hydrophobic carrier showed an immobilization yield of 54% and 63.2 mg g^{-1} protein bound on the support. Both enzyme carriers showed no leaching. Because of the enormous loading, the hydrophobic carrier was used for a preparative reaction. After 100 h reaction time conversion of 78% was achieved (Figure 16).[119] In the experiment using non-immobilized enzymes 77% conversion was reached applying the same amount of enzyme. These results make the process competitive with the non-immobilized enzyme reaction, especially with regard to the possibility for recycling of the enzyme and better separation of the product. For all experiments a *ee*-value of >99% could be achieved.

The results on the expansion of the substrate scope, further characterization and successful immobilization of the amine dehydrogenase EsLeuDH-DM were published in the journal Bioorganic and Medicinal Chemistry: J. Löwe, A. A. Ingram, H. Gröger, Enantioselective synthesis of amines *via* reductive amination with a dehydrogenase mutant from *Exigobacterium sibiricum*: Substrate scope, co-solvent tolerance and biocatalyst immobilization, *Bioorg. Med. Chem.* **2018**, *7*, 1387-1392.

4.4 Microalgal photosynthesis for the biocatalytic production of bulk chemicals in combination with amine dehydrogenase

In this chapter, the use of microalgal photosynthesis in combination with amine dehydrogenase was used to produce bulk amines. Besides D-glucose and glucose dehydrogenase for cofactor recycling, which was used for amine dehydrogenase and aryl-substituted amine production, there is the possibility to use formate and formate dehydrogenase for cofactor recycling (Scheme 22).

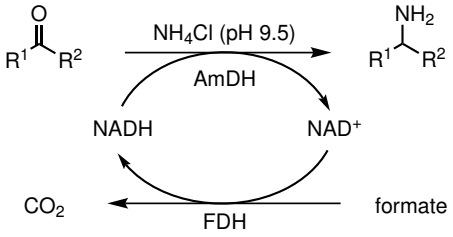

Scheme 22: Reaction of AmDH with cofactor recycling system consisting of formate dehydrogenase (FDH) and formate.

As already mentioned, *Chlamydomonas reinhardtii* secrets alcohols and organic acids, like formate into the outer media after dark fermentation process.

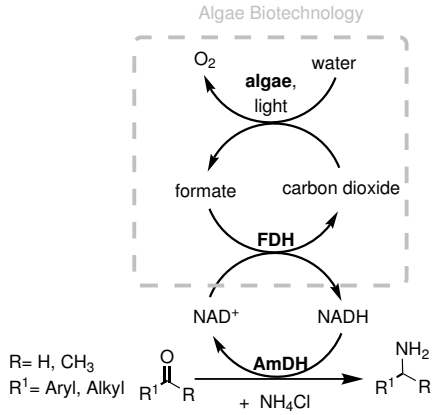

Scheme 23: Reaction of AmDH with cofactor recycling system consisting of formate dehydrogenase (FDH) and formate from algal supernantant.

This formate can be used for *in situ* cofactor regeneration, to produce bulk amines in combination with amine dehydrogenase (Scheme 23).

4.4.1 Spectrophotometrical activity assay for EsLeuDH-DM and aldehydes

In this context, first a range of aldehydes were tested *via* spectrophotometric assay to examine the compatibility of these kind of substrates towards EsLeuDH-DM.

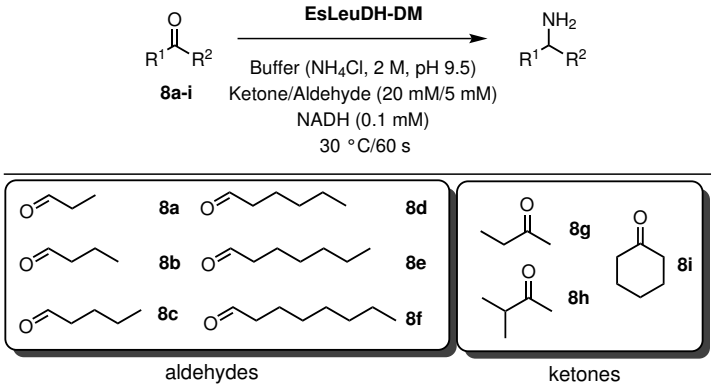

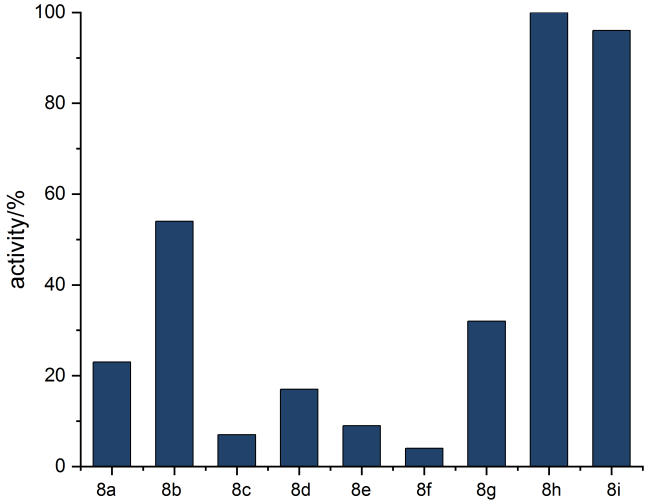

Figure 17: Activities of EsLeuDH-DM for aldehydes **8a-f** and ketones **8g-i** investigated *via* spectrophotometric assay.

Figure 17 shows the activity of EsLeuDH-DM towards short-chain **8a-c**, long-chain aliphatic aldehydes **8d-f** and short-chain ketones **8g-h**, as well as for cyclohexanone (**8i**).

For the amine dehydrogenase EsLeuDH-DM, it was the first time that such a range of aliphatic ketones was investigated. The best activity towards isopropyl methyl ketone (**8h**) was set to 100% with 2.15 $U \cdot mg^{-1}$. Cyclohexanone (**8i**, 2.06 $U \cdot mg^{-1}$) and 2-butanone (**8g**, 0.69 $U \cdot mg^{-1}$) show the most promising results. In literature, an activity of 0.14 $U \cdot mg^{-1}$ for 2-butanone (**8g**) and 0.87 $U \cdot mg^{-1}$ for cyclohexanone (**8i**), was reported.[82] Activity decreases significantly with a chain length of four carbon atoms to five carbon atoms. This phenomenon can probably be explained by the natural substrate leucine. The leucine dehydrogenase, the origin of the mutant EsLeuDH-DM, has leucine as a natural substrate, which contains four carbon atoms. This could be a reason for the strong decrease of the activity with the extension of the carbon chain. Because of the high activity towards cyclohexanone (**8i**), the kinetic data were investigated. Therefore, purified EsLeuDH-DM was used. For the determination of the MICHAELIS-MENTEN constant (K_M), the reductive amination of cyclohexanone (**8i**), was determined using spectrophotometric activity assay at different substrate concentrations. The consumption of NADH was followed at 340 nm and a reaction temperature of 30 °C. By plotting the activities against the substrate concentration and a non-linear fit of the curve the K_M-value, K_i-value, and v_{max}-value can be determined.

Table 3: Results for the kinetics of EsLeuDH-DM towards cyclohexanone (**8i**).

K_M/mM	K_i/mM	v_{max}/mol · min^{-1}
1.70	128	0.94

The determination shows a low K_M-value of 1.70 mM, which indicated a quite high affinity for the substrate. The K_i-value is particularly high, as a result, substrate inhibition will only play a role at very high concentrations (Table 3).

For achieving the maximal velocity of the reaction, 3.4 mM of the substrate **8i** has to be used for further biotransformations, with EsLeuDH-DM and cyclohexanone (**8i**).

4.4.2 Kinetics for EsLeuDH-DM and hexanal (8d)

To investigate the compatibility of EsLeuDH-DM with aldehydes in biotransformations, the amine dehydrogenase was used with the implemented GDH and D-glucose cofactor recycling system (Figure 18).

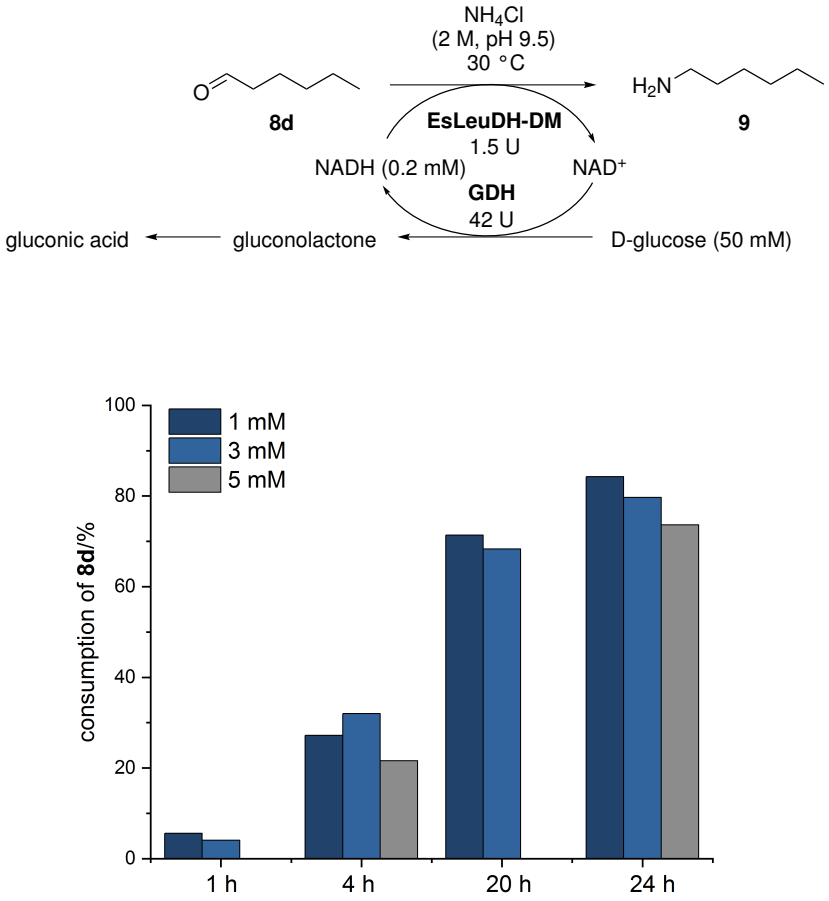

Figure 18: Biotransformation of hexanal (**8d**) with EsLeuDH-DM.

Therefore, a reaction from hexanal (**8d**) towards hexylamine (**9**) with 1, 3, or 5 mM for up to 24 h were performed in a 1 mL scale.

After 24 h a conversion of about 80% for each concentration was reached. These initial results show the applicability of amine dehydrogenase EsLeuDH-DM with aldehydes in biotransformations (Figure 18). With these results in hand, the enzymatic reductive amination with the amine dehydrogenase (EsLeuDH-DM) and formate dehydrogenase (commercially available cbFDH from *Candida boidinii* (*Sigma Aldrich* F8649, lyophilized powder)) with formate, was estimated. For the *in situ* cofactor recycling system, the photoautotrophic microorganism *Chlamydomonas reinhardtii* was established. The algae provides the formate for the process, which is *in situ* formed from carbon dioxide, water, and light.

4.4.3 Evaluation of optimal salt concentration during biotransformations with EsLeuDH-DM and algae fermentation

For the compatibility of amine dehydrogenase-catalyzed amine formation and algae biotechnology, two approaches were investigated: first experiments using the algae supernatant and second, experiments using the formate, which is produced *in-situ* during algae fermentation.

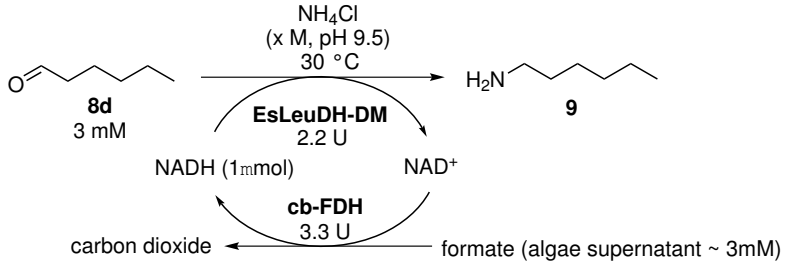

Table 4: Impact of different salt concentrations on the activity of EsLeuDH-DM in combination with algae biotechnology.

Salt concentration/mM	conv./%
248	65
122	>99
50	>99
25	>99

For the biotransformations some selected aldehydes and ketones as substrates were chosen. In cooperation with WOBBE, from the workgroup Algae Biotechnology & Bioenergy, Bielefeld University, a cofactor regeneration system was created. WOBBE established an alga, which forms up to 3 mM formate. The first investigation was the evaluation of the optimal salt concentration (NH_4Cl) for the reaction of the aldehydes and ketones with the algae *C. reinhardtii*. Therefore, a reaction with hexanal (**8d**) and algae was performed. A higher salt-concentration leads to a smaller amount of product, probably because the high salt concentration can damage the algae (Table 4).

This phenomenon can also be seen in the reaction mixtures with different salt concentrations (Figure 19). The chlorophyll is probably leaching out of the cell, as a consequence, the reactions mixture gets brighter (from left high salt concentration, to right less salt concentration, Figure 19). Therefore, further reactions were performed with 100 mM salt concentration.

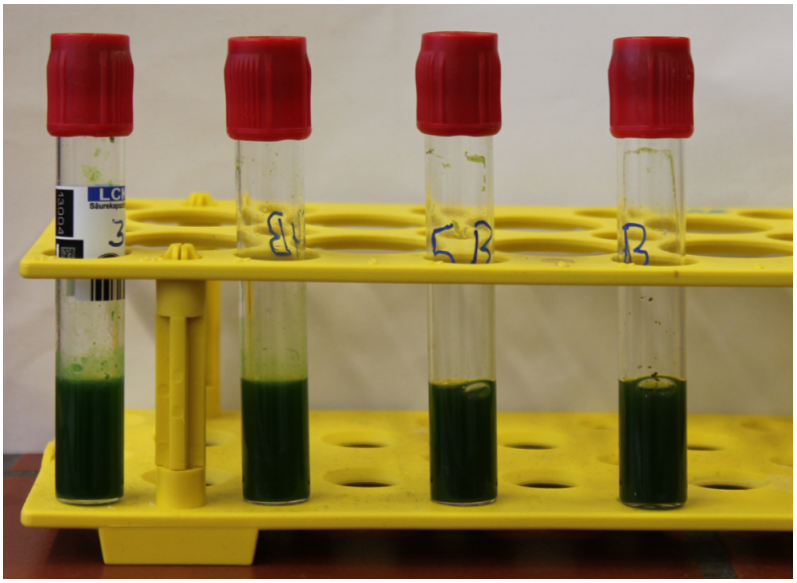

Figure 19: Biotransformation of EsLeuDH-DM with hexanal (**8d**) during algae fermentation with different salt concentrations - 238 mM, 122 mM, 50 mM, 25 mM - from left high salt concentration, to right less salt concentration.

4.4.4 Biotransformations with EsLeuDH-DM and algae supernatant

First, experiments were performed with algae supernatant (secreted supernatant after fermentation of the algae) with hexanal (**8d**), octanal (**8f**), and cyclohexanone (**8i**). The reaction was performed at 30 °C for 40 h .

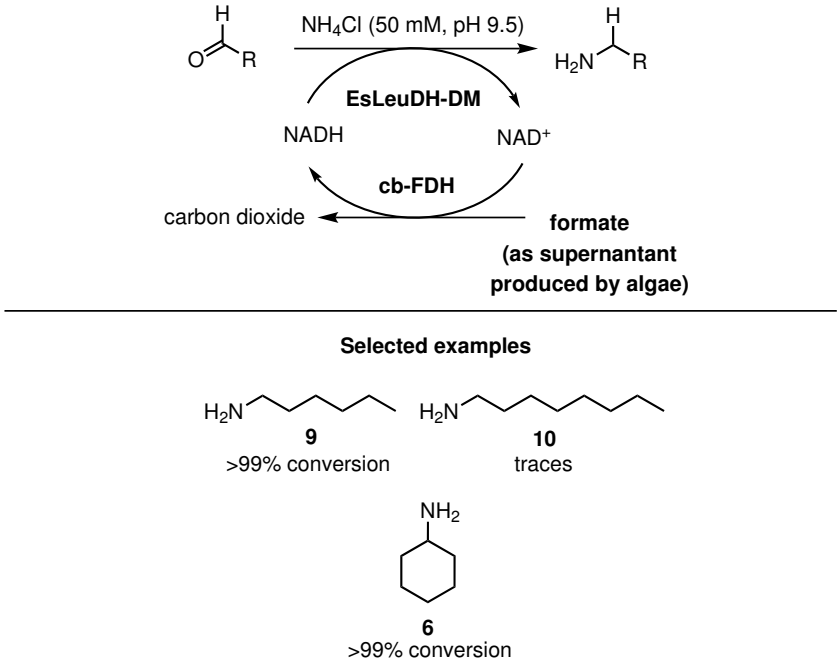

Scheme 24: Biotransformation of carbonyl compounds with EsLeuDH-DM with formate from algae supernatant.

The results for the biotransformations correspond to the results of the activity assay. Cyclohexylamine (**5**) and hexylamine (**9**) were synthesized with >99% conversion. Octylamine was only synthesized with trace amounts. This low conversion can be explained by the low specific activity of the amine dehydrogenase for long-chain aliphatic aldehydes, in combination with its very low solubility (Scheme 24).

4.4.5 Biotransformations with EsLeuDH-DM during algae fermentation

Finally, the amine formation was performed during algae fermentation.

Therefore, butanone (**8g**), butanal (**8b**), hexanal (**8d**), and cyclohexanone (**8i**) were chosen as substrates. The reaction was performed at 30 °C for 40 h with photoautrophically grown *C. reinhardtii* cells (1 mL cell suspension in HSM medium; 10^8 cells).

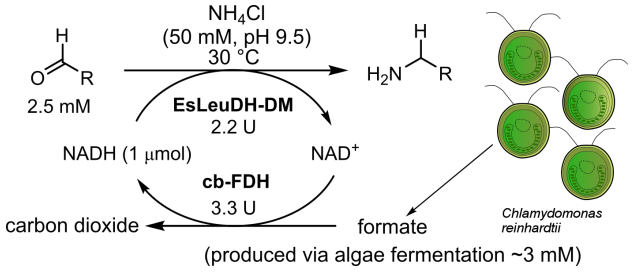

Table 5: Biotransformation of aldehydes with EsLeuDH-DM during algae fermentation.

Substrate	consumption/%
Butanone (**8g**)	>99
Butanal (**8b**)	>99
Hexanal (**8d**)	>99
Cyclohexanone (**8i**)	>99

For all reactions full conversion towards the desired amines was achieved (Table 5). These results are comparable to those using supernatant obtained after algae fermentation. Thus, the *in-situ* produced formate can also be used for the synthesis of amines.

These results on the combination of amine dehydrogenase and algae biotechnology were published in the journal Scientific Reports: J. Löwe, A. Siewert, A.–C. Scholpp, L. Wobbe, H. Gröger, Replacing co-substrates by carbon dioxide, water and light: an alternative perspective towards biocatalytic production of bulk chemicals exemplified for aliphatic amines, *Sci. Rep* **2018**, *8*, 10436-10443.

4.5 Summary and outlook amine dehydrogenase-catalyzed reactions

Within this chapter, it was possible to extend the substrate scope of the amine dehydrogenase EsLeuDH-DM with regards to, aryl-substituted amines, aldehydes, and a variety of cyclic and aliphatic ketones. Furthermore, the EsLeuDH-DM was characterized in terms of kinetics and stability towards acetophenone (**7**) and an optimal water-miscible cosolvent. Additionally, the amine dehydrogenase could be successfully immobilized.[119] This system can now be used for future experiments. An interesting issue, which has still to be investigated, is the combination of the cosolvent with the immobilized enzyme, as well as the recyclability of the immobilized enzyme.

In addition, it was possible to combine the amine dehydrogenase with the algae biotechnology. The formate formed by the algae can be used as a secret. Furthermore, it is possible to synthesize primary amines during fermentation. For the best of our knowledge, it was the first time to use algae fermentation process for *in-situ* cofactor regeneration. This, in turn, provides a platform for an alternative, inexpensive cofactor regeneration system. This is especially important concerning the costs in a chemical process that can be caused by the co-substrate. These costs are often a knock out criterion in bulk chemical production. In this process it was possible to generate an organic cosubstrate from only formal CO_2, water and light. Which, in turn, could make this process in the future applicable for the production of bulk chemicals. In this context, it would be interesting to increase the concentration of formate, which currently lies at 3 mM, to be able to apply the synthesis of aliphatic amines in the bulk range.

5 Combination of flavine-dependent monooxygenases and algae biotechnology

5.1 Current state of science

In 1899 Baeyer and Villiger published the formation of an ester from a ketone or a lactone from a cyclic ketone by using peroxides or peroxy acids (Scheme 25) which is now named after both chemists.

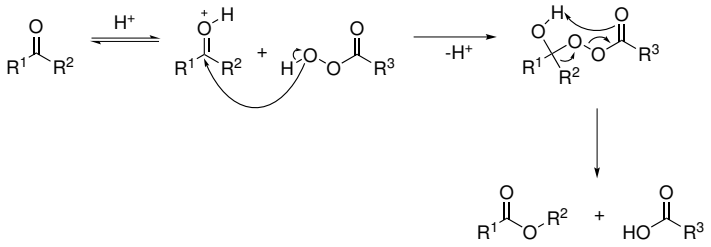

Scheme 25: Baeyer-Villiger reaction.[120]

The electrophilicity of the caboxylic carbon-atom is initially increased by protonation of the carbonyl oxygen or a Lewis acid. The peracid acts as a nucleophile and attacks the carbocation and the so-called Criegee intermediate is produced. The elimination of the carboxylic acid leads to an electron sextet on oxygen and this causes a migration of the substituent, this reaction proceeds concerted. The ester is formed by deprotonation.[120]

5.1.1 Flavine-dependent monooxygenases

Flavine-dependent monooxygenases (FMO) which catalyzes oxidation reaction, contains a FAD as a prosthetic group and NADPH as a cofactor.[121] During their catalytic activity monooxygenases induce a splitting of O_2, transfer one oxygen into a substrate and reduce the other oxygen to H_2O.[122] FMOs can be divided into six classes (A, B, C, D, E, F), class A and B are single component monooxygenases, bearing a tightly bound FAD and are dependent to NAD(P)H.

Class C, D, E and F FMOs are two-component monooxygenases. Class C uses reduced FMN and D, E and F FAD for oxygen activation.[123] Class B FMOs are further subservient into four classes: NMOs which catalyze N-hydroxylations, Type I Baeyer-Villiger monooxygenases (BVMO), Type I FMOs and Type II FMOs, which are also NADH-dependent.[124] The FAD plays a significant role in the catalytic activity of FMOs, on this occasion all monooxygenases have a flavine C(4a)hydroperoxide intermediate which is formed.[122,123]

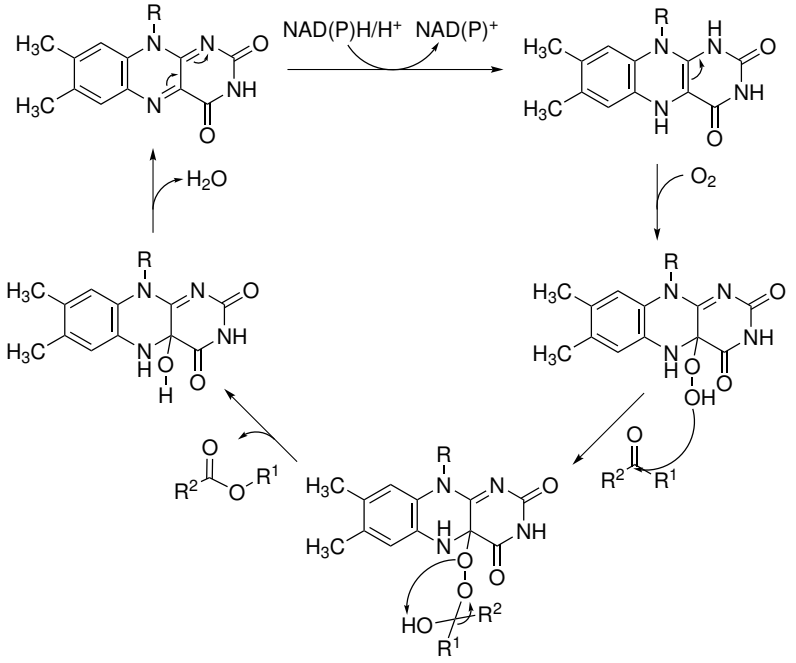

Scheme 26: FAD catalysis cycle.

The first step of the catalytic cycle is the reduction of FAD *via* NAD(P)H, followed by an oxidation to produce the 4a-hydroperoxyflavine. Sheng *et al.* showed that the C4a-flavine oxygen adduct can exist in two states. The first intermediate is a flavine C4a-peroxide, this intermediate becomes protonated to form the flavine C4a-hydroperoxide. These two states can interconvert. On this occasion, the peroxide nucleophilic attacks the carbonyl compound and forms a tetrahedral intermediate. After rearrangement, the product is released, and the 4a-hydroxyflavine is formed again (Scheme 26).[125]

The most famous monooxygenase is the cyclohexanone monooxygenase CHMO from *Acinetobacter sp.* NCIMB 9871. In *Acinetobacter sp.* NCIMB 9871, CHMO metabolizes cyclohexanone (**8i**) towards ϵ-caprolactone, in a reaction cascade starting from cyclohexanol towards the final product adipate.[126] This discovery opened the door for the use of monooxygenases in biocatalysis. One example is the conversion of bicyclo[2.2.1]heptane-2-ol towards the corresponding lactone. This process is combined with an alcohol dehydrogenase (ADH) and shows the advantage of recycling of $NADP^+$ in a closed-loop system (Scheme 27).[127]

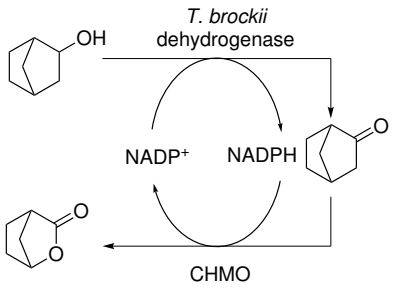

Scheme 27: Coupling of ADH with a CHMO.[127]

Another example is the biocatalytic route towards ϵ-caprolactone. The starting material for this reaction is cyclohexanol, which is first oxidized towards the corresponding ketone, and afterward further oxidized to ϵ-caprolactone (Scheme 28).[128–130]

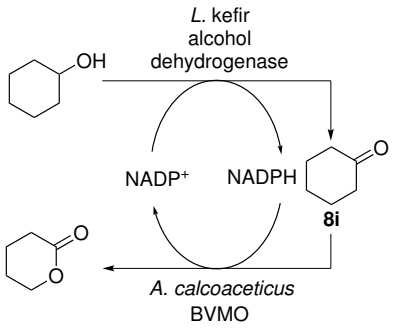

Scheme 28: Coupling of ADH with a BVMO.[128–130]

The product can be applied as a monomer for a huge range of industrial relevant polymers.[128]

5.2 Flavine monooxygenase-catalyzed reactions

The major issue of this topic is the combination of algae biotechnology with flavine monooxygenases (FMO).[131] As already mentioned in the motivation, cofactor recycling is a necessary issue but it also leads to waste products. To avoid these side products and produce the co-substrate (in this case formate) *in-situ* the elegant cofactor recycling system based on algae biotechnology was also used for flavine monooxygenase-catalyzed reactions (Scheme 29). The FMOs were provided by the workgroup of Kruse from the workgroup Algae Biotechnology & Bioenergy Research Group, Bielefeld University. They could show that these FMOs isolated from *Pimelobacter* sp. Bb-B lives together in a complex microbial consortium with *Botryococcus braunii*, a colony-forming green microalga. The new FMOs have to be combined with the modified photoautotrophic microorganism *Chlamydomonas reinhardtii*[115] established by Wobbe, Algae Biotechnology & Bioenergy Research Group, Bielefeld University. The modified *Chlamydomonas reinhardtii* forms up-to 3 mM formate, which is further used in combination with the formate dehydrogenase (cbFDH)[116] to recycle the cofactor for the reaction.

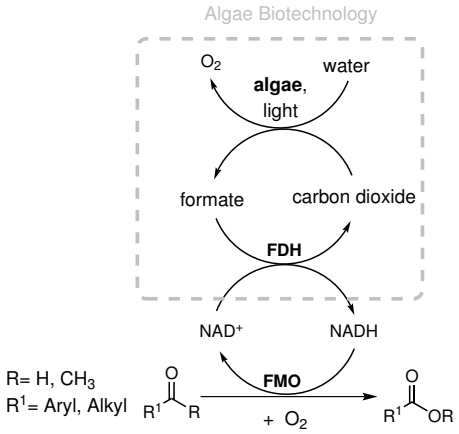

Scheme 29: Content of formate dehydrogenase in combination with algae biotechnology- Algae production of formate using as cosolvent for successful regeneration of cofactor in combination with new FMOs from *Pimelobacter* sp. Bb-B.

Before combining the working cofactor regeneration system with the new and promising FMOs, the enzymes had to be characterized in terms of substrate scope and activity.

The most suitable substrate is then used for the established system.

5.3 Microalgal photosynthesis for the biocatalytic production of cyclic esters in combination with flavine monooxygenases

5.3.1 Spectrophotometrical activity tests for flavine monooxygenases

In cooperation with Wobbe and Kruse from the Algae Biotechnology & Bioenergy Research Group, Bielefeld University, three new type-II FMOs (*Pimelobacter* sp. 1534, *Pimelobacter* sp. 3122 and *Pimelobacter* sp. 5301) has to be characterized regarding substrate scope. Afterward, the type-II FMOs were combined with the established *in situ*-cofactor recycling methodology from algae using the photoautotrophic microorganism *Chlamydomonas reinhardtii*. The algae provids the formate, which is formed from carbon dioxide, water and light. The formate is afterwards combined with a formate dehydrogenase. First, an activity assay was done with several ketones. Therefore, three type-II FMO's from *Pimelobacter* sp. 1534 (*Ps*FMO-A), *Pimelobacter* sp. 3150 (*Ps*FMO-B) and *Pimelobacter sp.* 5351 (*Ps*FMO-C) being investigated, in terms of activity. The substrates contain a range of different ketones, aliphatic (**11d**), aryl-substituted (**11a, 11e, 5**) and cycloalkanones (**11b-c, 8i, 11h**). The highest activity for the most substrates showed the *Ps*FMO-A, especially for camphor (**11g**) and bicyclo[3.2.0]hept-2-en-6-one (**11f**) with about 0.06 U mg^{-1} (Figure 20). These results are under accordance with literature.[124,132] In this context, the kinetic constants towards bicyclo[3.2.0]hept-2-en-6-one (**11f**), were investigated. For the K_M-value 1.86 mM and for the k_{cat}-value 1.51 s^{-1}, was validated, which was a very promising starting point to perform biotransformations with bicyclo[3.2.0]hept-2-en-6-one (**11f**), as well as with cyclohexanone (**8i**).

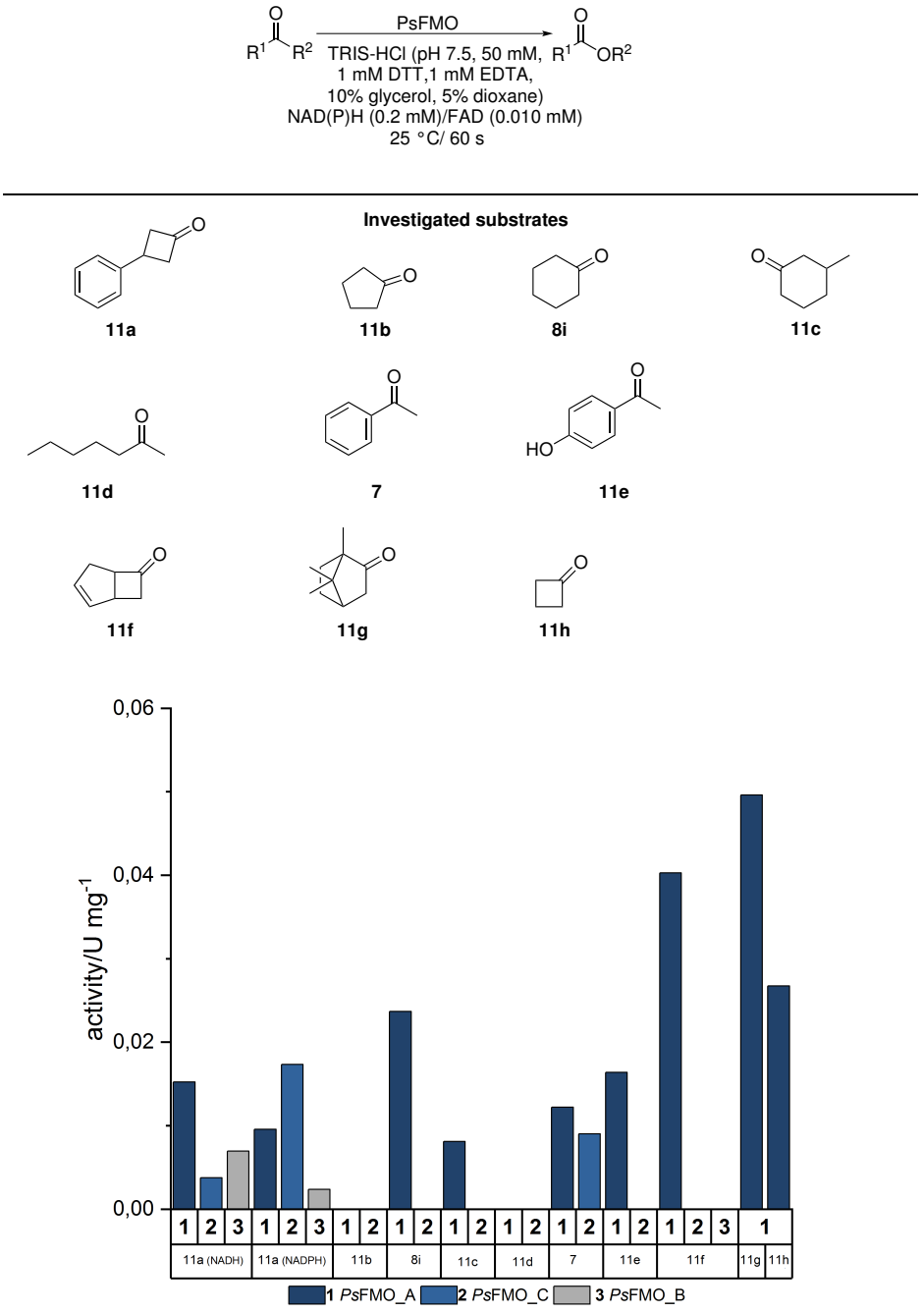

Figure 20: Substrate scope of PsFMO-A-C studied through spectrophotometric assays. All activity tests were performed with NADH unless otherwise specified.

5.3.2 Biotransformations with flavine monooxygenases and GDH

In the first reaction, glucose dehydrogenase and glucose were used for cofactor recycling (**Reaction 1**). With this established system, the use of the enzyme in a biotransformation reaction, was tested. In the biotransformation with bicyclo[3.2.0]hept-2-en-6-one (**11f**), using FMOs, four possible products can be formed formed, the so-called normal lactone (N) (oxygen is inserted next to the tertiary carbon) or the abnormal lactone (ABN) (oxygen is inserted opposed to the secondary carbon). For both substrates, it is possible to form (1*S*,5*R*) or (1*R*,5*S*) enantiomers (Scheme 30).

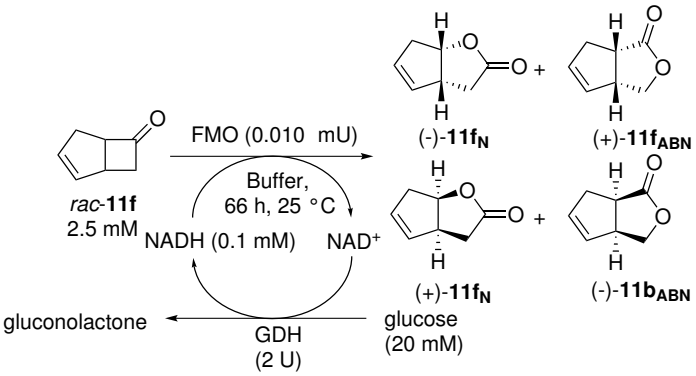

Scheme 30: Biotransformation using PsFMO-A with bicyclo[3.2.0]hept-2-en-6-one (**11f**) and GDH (glucose dehydrogenase) as a cofactor regeneration system.

Under these reaction conditions no conversion was detected for cyclohexanone (**8i**) These results are in accordance with literature.[132] For bicyclo[3.2.0]hept-2-en-6-one (**11f**) a conversion of 89% (*Ps*FMO-A) was detected, whereas for the *Ps*FMO-B and *Ps*FMO-C no conversion could be determined.

5.3.3 Biotransformations with flavine monooxygenases and FDH

With these results in hand the reaction with bicyclo[3.2.0]hept-2-en-6-one (**11f**) and the *Ps*FMO-A was investigated with the commercially available cbFDH (*Sigma Aldrich* F8649, lyophilized powder, 5.0-15.0 units/mg protein) from *Candida boidinii*. First, commercially available formate was used and afterward, the secreted formate, based on the algae metabolism (Scheme 31).

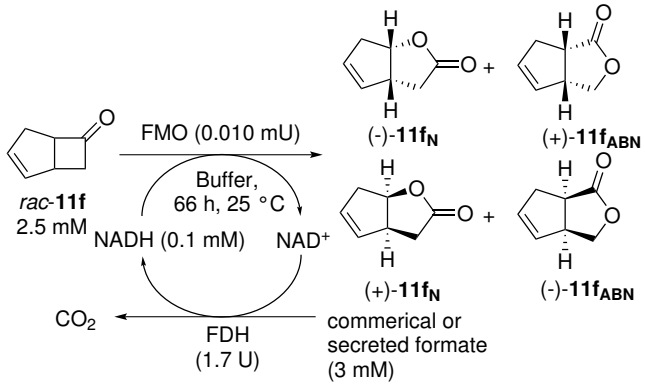

Scheme 31: Biotransformation using PsFMO-A with bicyclo[3.2.0]hept-2-en-6-one (**11f**) and FDH (formate dehydrogenase) as a cofactor recycling system.

For the commercially available formate, 85% consumption of the starting material **11f** was remarked (**Reaction 2**). For the formate from the algae supernatant, even a conversion of 94% (**Reaction 3**) was observed. These results underline again, the applicability of this methodology for cofactor recycling.

Table 6: Regiodivergent oxidation of racemic bicyclo[3.2.0]hept-2-en-6-one (**11f**).

Reaction	Consumption/% (N/ABN)	ee_N/% ee_{ABN}/%
1	89	99 (1*R*,5*S*)
	1.5:3	30 (1*R*,5*S*)
2	85	99 (1*R*,5*S*)
	1.5:3.5	34 (1*R*,5*S*)
3	94	99 (1*R*,5*S*)
	2:3	57 (1*R*,5*S*)

An overview of the *ee*-values and the ratio between "abnormal" (ABN) and "normal" (N) lactone are shown in the Table 6. In all reactions (1-3) the "abnormal" ketone is preferentially formed, whereas the *ee*-value for the "normal" lactone is always with a value of <99% (Table 6).

The results on the combination of new flavine monooxygenases and algae biotechnology were published in the journal Journal of Biotechnology: J. Löwe, O. Blifernez-Klassen, T. Baier, L. Wobbe, O. Kruse, H. Gröger, Type II flavoprotein monooxygenases PsFMO-A from a bacterium *Pimelobacter sp.* Bb-B catalyzes enantioselective Baeyer-Villiger oxidations with a relaxed cofactor specificity, *J. Biotechnol.* **2019**, *294*, 81-87.

5.4 Outlook flavine monooxygenase-catalyzed reactions

The formate from algae could be used for cofactor recycling and successfully combined with flavine monooxygenase. At this stage, the substrate spectrum of the enzymes is very limited. One possibility to increase the substrate spectrum is the use of mutagenesis. In this context, it would be interesting to be able to convert cyclohexanone to synthesize ϵ-caprolactone, a bulk chemical that is of great importance. The advantage of the present system is that it does not require the use of an expensive cosubstrate. The cosubstrate is generated *in-situ* using algae biotechnology. Formate is produced from formal CO_2, water, and light and thus represents a cost-effective alternative. Besides, it would be a benefit to increase the concentration of the formate. A higher formate concentration enables the application of algae biotechnology in bulk chemistry.

6 Hydration of C=C double bonds by the means of fatty acid hydratases

6.1 Current state of science

6.1.1 Water addition to C=C double bonds

Alcohols are widely used in chemical products, such as agrochemicals, food additives, fragrances, and pharmaceuticals,[133] as well as for biofuels.[134] Chemically, the production of alcohols is considered by a ring-opening of an epoxide using a GRIGNARD reagent or a LEWIS acid.[135] The addition of water to none-activated double bonds is a more challenging endeavor.[136] Nevertheless, this is a useful tool for the production of alcohols, mainly because water is a cheap and easily accessible reactant. In summary, there are two possibilities to functionalize C=C double bonds with water. First, there is the electrophilic addition of water to an isolated C=C double bond, which follows the MARKOWNIKOW rule or the addition to a polarized, electron-deficient double bonds, which proceeds in a MICHAEL-type reaction (Scheme 32). Two disadvantages have to be mentioned in the addition of water to C=C double bonds. On the one hand, it is an equilibrium reaction and on the other hand, water is a poor nucleophile.[137]

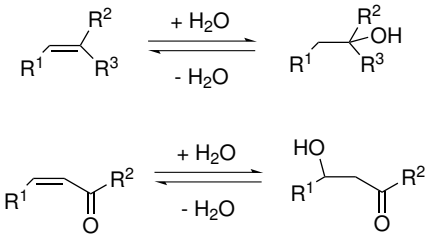

Scheme 32: General reaction scheme for water addition to C=C double bonds.

Examples for the chemical, acid-catalyzed water addition to C=C double bonds is the hydration of propene using sulfonated polystyrene ion-exchangers or tungsten oxide catalyst using high pressure.[137]

The MICHAEL addition of water to electron-deficient double bond, is for example possible, by the use of amino acids, like lysine.[138]

More capable catalysts for the use of water as a nucleophile to hydroxylate double bonds are enzymes. In the case of hydratases, which can catalyze the reaction, they fix the electrophile and nucleophile in their active site. This due to a stabilized transition state whole the reaction proceeds .[139] The nucleophilic addition of water to C=C double bonds are catalyzed by so called hydratases or hydro-lyases, these enzymes either catalyzes the hydroxylation of isolated C=C double bonds or the nucleophilic addition to an α,β unsaturated carbonyl compound. In this context, they are able to activate the water by the means of a metal ion or without any cofactor.[137] Examples for metal-ion containing hydratases are class I fumarases, which catalyzes the nucleophilic addition to an α,β-unsaturated carbonyl compound.[140] Class I fumarases contain an iron-sulfur cluster, which mimics a LEWIS acid and therefore activates the water molecule. Class II fumarases are cofactor independent enzymes, catalyzing the addition of water using a two acid–base α-amino acid residues.[141] In contrast to the chemical route, in which only the *anti*-product or no selectivity is observed, enzyme-catalyzed addition or elimination of water can also proceed in a *syn*-position.[142]

Most hydratases have a narrow substrate spectrum, like kievitone hydratases, which catalyzes the detoxification of kievitone by converting it to a tertiary alcohol[143] or linalool dehydratase-isomerase, which converts myrcene towards linalool.[144] Another example is the carotenoid-1,2-hydratase, having acyclic carotenes as natural substrates.[145] All these enzymes belong to the family of enzymes adding water to isolated C=C-bonds. As already mentioned, there is an additional enzyme class, which catalyzes the reversible MICHAEL addition of water to α,β-unsaturated acids, like fumaric acid (fumerase)[140] or to unsaturated thioesters like hydroxycinnamoyl-CoA hydratase lyase.[146] Furthermore, the addition to α,β-unsaturated ketones is possible, by the means of MICHAEL

hydratase.[147] Another enzyme class with several fields of application, which catalyzes the addition of water to none-activated C=C double bonds, can be found in fatty acid hydratases, this topic is discussed in more detail in the following chapter.

6.2 Fatty acid hydratases

Hydroxy fatty acids are of major interest for industrial applications, mainly used as starting materials for polymers[148] or cyclic lactones,[149] fragrances and antibiotics[150] as well as for plasticizers,[151] surfactants,[152] lubricants[153] and detergent formulations.[154] Chemically, the access to hydroxy fatty acids is particularly challenging due to the great variability in the length of the carbon chain and the degree of saturation. However, some synthesis for specific hydroxy fatty acids are known. For instance a C=C double bond can be unspecifically hydroxylated by epoxide formation and subsequent ring opening.[155] A selected example is the multi-stage synthesis of (*S*)-9-hydroxy fatty acids. This synthesis is composed of two key steps: the asymmetric terminal epoxide formation from protected α,ω-diols and the subsequent ring-opening by Grignard reaction, followed by deprotection reactions and a Jones oxidation (Scheme 33).[156]

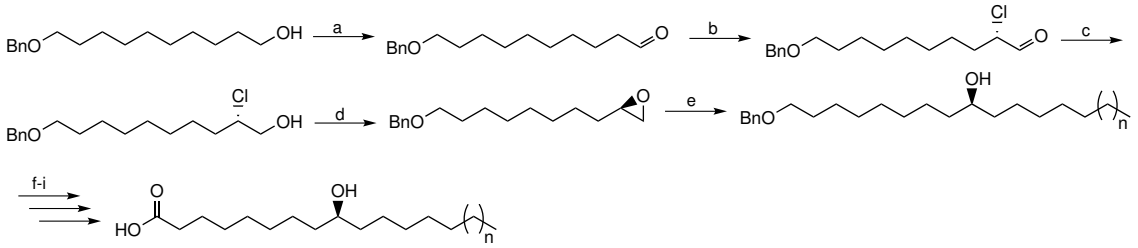

Scheme 33: Synthesis of (*S*)-9-hydroxy fatty acids. (a) PCC, CH_2Cl_2; (b) (2*R*,5*S*)-2-(*tert*-butyl)-3,5-dimethylimidazolidin-4-one trifluoroacetate (20 %), 2,3,4,5,6,6-hexachlorocyclohexa-2,4-dien-1-one, THF (c) $NaBH_4$, EtOH; KOH, EtOH, H_2O; (d) $C_6H_{13}MgBr$ or $C_8H_{17}MgBr$, CuI, dryTHF; (e) $CH_3(CH_2)_{14}COCl$ or $CH_3(CH_2)_{16}COCl$, CH_2Cl_2; (f) AcCl, pyridine, CH_2Cl_2;(g)H_2, Pd/C, EtOH; (h) Jones reagent, acetone; (i) LiOH, THF/H_2O.[156]

Other possibilities to functionalize fatty acids are reflected in enzymes like 12-hydroxylases, cytochrome P450 monooxygenases, lipoxygenases,[157] and peroxygenases (Scheme 34).[158]

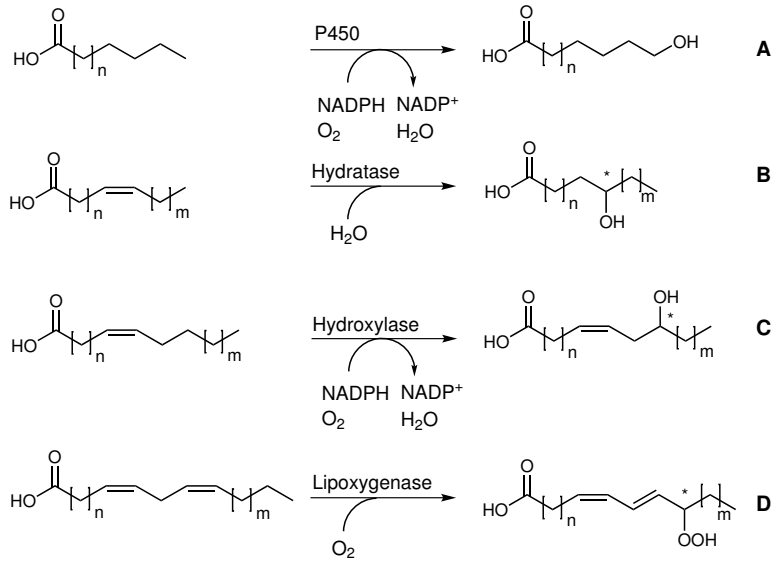

Scheme 34: Oxyfunctionalization of fatty acids. (**A**) Hydroxylation of terminal position through P450 monooxygenase (**B**) Fatty-acid hydratases catalyzed addition of water to a double bonds (**C**) Hydroxylases catalyzed formation of hydroxy fatty acid (**D**) Hydroxyperoxide formation through lipoxygenases.[157,159]

Fatty acid hydratases (FAH) catalyze the addition of water towards inactivated, isolated C=C double bonds of fatty acids. This enzyme class was firstly described by Wallen *et al.* in 1962.[160] Until now, the physiological effect is not clear, probably the functionalization leads to detoxification of compounds. The similarity of FAHs lies in a conserved *N*-terminal nucleotide binding motif (GXGXXG$X_2$1E/D), where the flavin adenine dinucleotide (FAD) is none-covalently bound.[161] The FAD redox-state does not change during the reaction and is therefore not involved in the reaction itself, but probably it has a stabilizing effect on the substrate in the active site. Furthermore, the FAD could serve for the correct assembly of amino acids in the active site.[161] The first crystal structure of a fatty acid hydratase was the linoleate hydratase (Lhy) from *Lactobacillus acidophilus*, determined by Volkov *et al* without any cofactor bound.[162] In 2015 the first crystal structure with FAD bound was published and a proposed mechanism postulated, which is shown below:[161] The reaction mechanism starts with an induced partial positive charge at the double bond, which leads to protonation of the tyrosine, while the FAD stabilizes the positive charge.

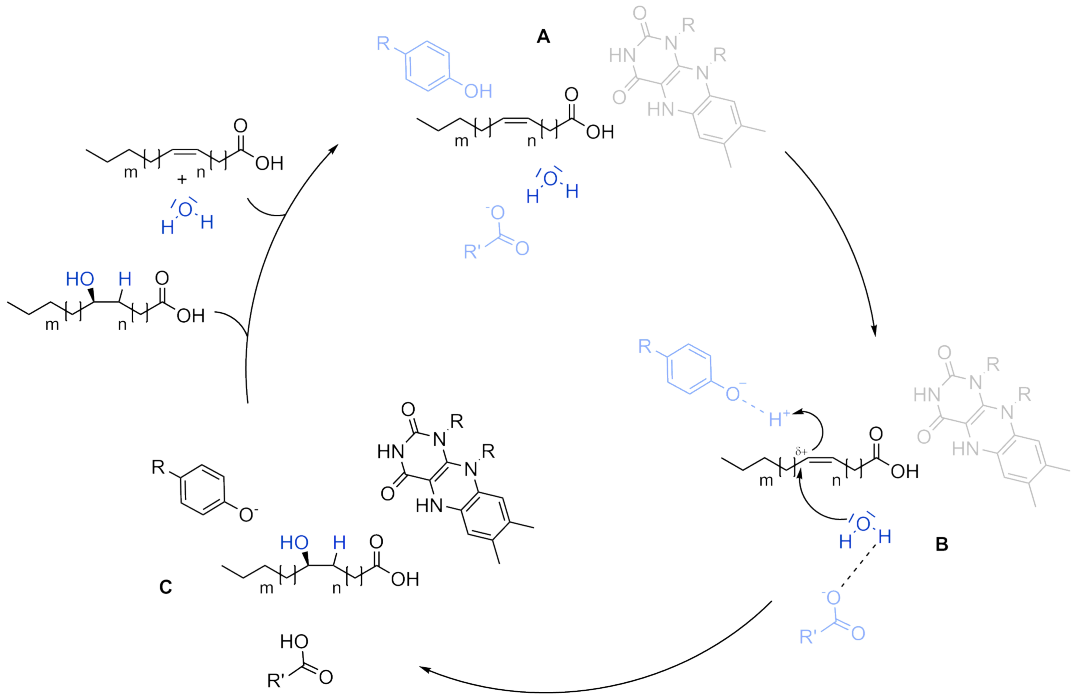

Scheme 35: Proposed reaction mechanism OA from *Elizabethkingia meningoseptica*. **A** Starting from a tyrosine, glutamate and FAD surrounding the substrate. **B** Nucleophilic attack of a water molecule to the partial positive double bond. **C** Release of the product and protonated glutamate.[161]

Furthermore, there are two amino acids N218 and F227 at the *C*-terminus of an α-helix, which additionally stabilizes this positive charge. The water can attack the double bond, while the glutamate gets protonated, and the hydroxy funcionalzed fatty acid, mostly the (*R*)-enantiomers, is formed (Scheme 35).[161] For the addition of water, the C=C double bond has to be in *cis*-conformation, furthermore, a free carboxylate is necessary.[163] Moreover, a chain length of at least 11 carbon atoms is required,[164] as well as a distance of seven carbon atoms between the carboxylic moiety and the hydrated double bond.[163] Most enzymes were tested for the conversion of C18 fatty acids. Also some examples with C11 to C16,[164] as well as C20 to C22 were known.[165] In this regard, the most enzymes catalyze the hydroxylation of the *cis*-9 double bond, only a few adding water to the *cis*-12 double bond.[166,158] In the end of the 80ies until the end of the 90ies a range of strains were tested according to the activity of adding water to fatty acid double bonds.[167–169,170]

The identification and purification of the isolated enzyme was reported at the beginning of 2000. In 2009 the first oleate hydratase (Ohy) from *Elizabethkingia meningoseptica* (Em-Ohy) was isolated and characterized.[171] In the following a collection of oleate and linoleate hydratases were described, like *Stenotrophomonas maltophilia*[172] oleate hydratase, *Lysinibacillus fusiformis* oleate hydratase,[173] *Lactobacillus plantarum* (Cla-Ohy) linoleic acid hydratase[174] or the *Lactobacillus acidophilus* linoleic acid hydratse, which is involved in the selective oxyfunctionalization of mono- and di-hydroxy fatty acids,[158] *Stenotrophomonas nitritireducens* oleate hydratase (Sn-Ohy)[175] and many more. These enzymes were widely used to produce hydroxy fatty acids on a large scale. One of the first application was the usage of *C. tropicalis* 3-hydroxy-Δ-9-*cis*-1,18-octadecenedioic acid, which produces 19.4 g L^{-1} hydroxy-substituted fatty acid.[169] The application of fatty acid hydratases towards the production of high amounts of hydroxy fatty acids have caused a sensation again from the 2010s onwards. In this context, there are some working groups, which have a strong influence on these processes. One is the working group around Oh from Konkuk University in Korea, who published a huge range of applications. Selected examples are the use of *Stenotrophomonas maltophilia* oleate hydratase for the production of 49 g L^{-1} 10-hydroxystearic acid (**12**)[176] or the production of the hydroxylated linoleic acid with a linoleate 13-hydratase in recombinant whole cells from *Lactobacillus acidophilus*, which produces 79 g L^{-1}.[177] Much research work on this field was also done by the Ogawa group at Kyoto University. One example they published was the *Lactobacillus plantarum* linoleic acid hydratase, which was overexpressed in *E.coli* and used for the conversion of 280 g L^{-1} linoleic acid into (*S*)-10-hydroxy-*cis*-12-octadecenoic acid (**14**) with an enantiomeric excess (*ee*) of >99%.[178]

6.3 Motivation and goal for fatty acid hydratase-catalyzed reactions

This project includes two parts, the enzymatic synthesis of tailor-made hydroxy-substituted fatty acids, esters or oils and the production of a polyol-library, realized by the means of esterification of hydroxy-substituted fatty acids with polyols. The first issue is the development of an efficient synthesis process for tailor-made hydroxy-substituted fatty acid esters using fatty acid hydratases (Scheme 36). To this end, existing technology will be evaluated and suitable product samples will be produced, which will then be tested by the project partner WINDMÖLLER GmbH for the production of polyurethane. The starting point of this cooperation is a Korean patent. In this patent the direct use of the vegetable oil instead of the free fatty acid as substrates for hydroxy-substituted fatty acid esters are reported.[179]

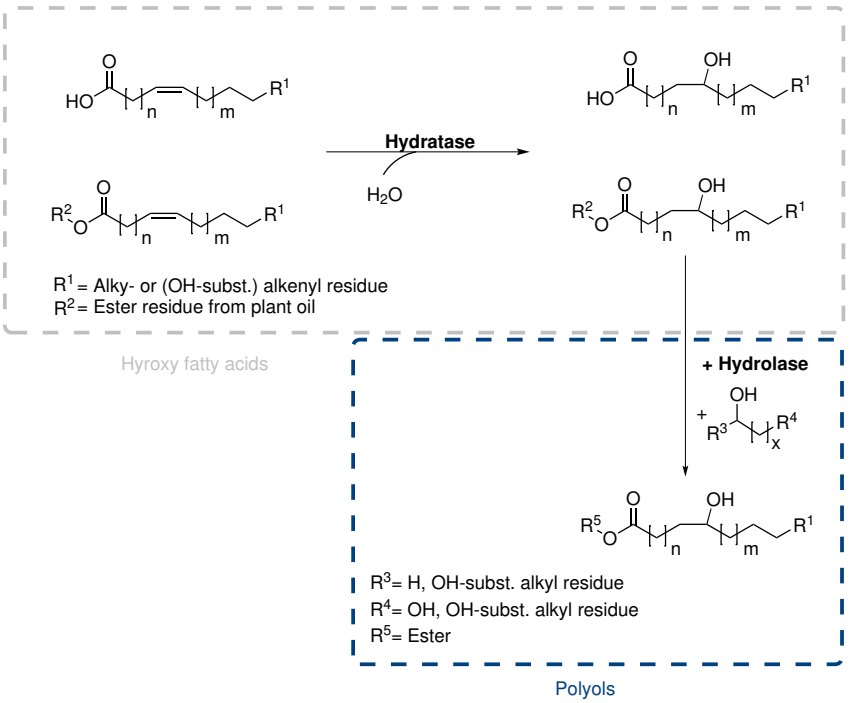

Scheme 36: Content of fatty acid hydratase-catalyzed reactions- In grey, hydration of fatty acids esters and oils by the mean of fatty acid hydratases. In blue, conversion of the hydrated fatty acids esters and oils with polyols to complex ester for the production of polyurethanes.

Initially, the approach is to express selected fatty acid hydratases and reproduce reactions based on literature data. Subsequently, the fatty acid hydratases (FAHs) will be used in a substrate screening, concerning the conversion of fatty acids and the direct conversion of vegetable oil. The main focus is the process development on synthesis processes with high substrate concentrations using a separable and recyclable biocatalyst. The second part, in turn, deals with the subsequent esterification of the hydroxy-substituted fatty acids with different alcohols to build up a polyol-library. These polyols will be used for the synthesis of specified polyurethanes by the cooperation partner Windmöller GmbH. The advantage of this approach lies in the composition of the polyols. The different hydroxy fatty acids can be combined with different polyol-linkers. This, in turn, generates a large platform, which provides access to various polyurethanes.

6.4 Results and discussion for fatty acid hydratase-catalyzed reactions

The aim of this project is the efficient and environmentally friendly approach towards tailor-made hydroxy-substituted fatty acid ester using fatty acid hydratases. The first step and also a major task for this project was to search through literature-based data, to find suitable biocatalysts (hydratases) for the synthesis of hydroxy fatty acids. Therefore, monounsaturated and diunsaturated fatty acid hydratases and also dihydroxylating fatty acid hydratases were chosen. Five genes were selected after literature research, encoding for fatty acid hydratases. These hydratases were used in recombinant *E.coli* strains for overexpression. These enzymes were chosen, because of hydroxylation pattern, as well as the applicability in large scale.[164,171,174,175] The Cla-Lhy from *Lactobacillus plantarum*, in this work named as Lp-Lhy, is as linoleic acid hydratase, which is mostly hydroxylating C18-double unsaturated fatty acids.[174] The bacterial strain *Lactobacillus acidophilus* contains two fatty acid hydratases the La-Ohy (oleate hydratase), as well as the La-Lhy (linoleate hydratase). These enzymes show activity towards C18-C22 fatty acids,[174] additionally the linoleate hydratase (La-Lhy) is also active in terms of dihydroxylation.[165] The fatty acid hydratase from *Elizabethkingia meningoseptica* Em-Ohy is probably the most frequently mentioned and studied fatty acid hydratase in literature,[161,171,180,181] showing activity against fatty acids from C11 to C18.[164] Last but not least the oleate hydratase from *Stenotrophomonas nitritireducens* was chosen, converting C18 fatty acids to its corresponding hydroxylated product.[175]

6.4.1 Overexpression of fatty acid hydratases

The first issue was to investigate the overexpression in *E.coli*, starting with overexpression in auto induction (AI) media. The results are shown in the SDS-PAGE below:

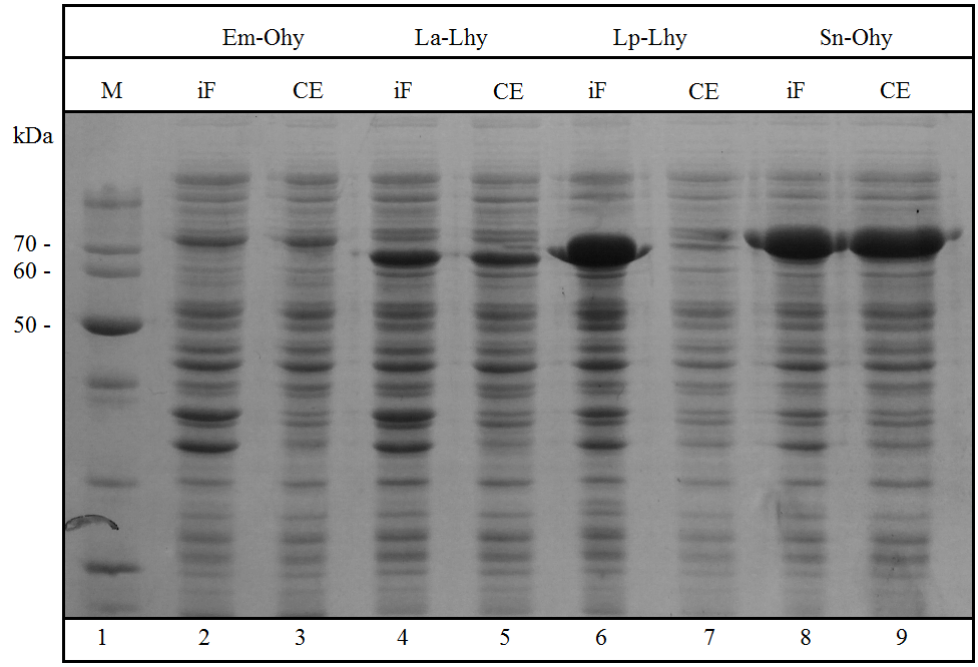

Figure 21: SDS-PAGE of overexpressed fatty acid hydratases, induced at OD_{600} of 0.6 to 0.8. Stained with Coomassie Brilliant Blue R-250. **lane 1**: marker (Thermo Scientific PageRuler Stained Protein Ladder), **lane 2**: insoluble fraction Em-Ohy, **lane 3**: crude extract Em-Ohy, **lane 4**: insoluble fraction La-Lhy, **lane 5**: crude extract La-Lhy, **lane 6**: insoluble fraction Lp-Lhy, **lane 7**: crude extract Lp-Lhy, **lane 8**: insoluble fraction Sn-Ohy, **lane 9**: crude extract Sn-Ohy.

In this SDS-PAGE no La-Ohy is shown. The overexpression of La-Ohy was investigated before, with unsatisfying results. Therefore, the La-Ohy was not investigated in further experiments. The Em-Ohy has a molecular weight of 73.5 kDa,[164] a light overexpression of this enzyme could be seen in the SDS-PAGE, even in the soluble fraction. The La-Lhy (68.0 kDa[174]) shows a slightly higher overexpression, and is also in the soluble fraction. The overexpression of the Lp-Lhy with a molecular weight of 66.4 kDa[174] is very strong, however, all of the expressed enzyme is in the insoluble fraction. In contrast, the Sn-Ohy (73.0 kDa[175]) is also strongly overexpressed, but is soluble (Figure 21).

6.4.2 Analytics of hydroxy-substituted fatty acids

The conversion for all reactions was analyzed *via* ^{1}H NMR-spectroscopy.

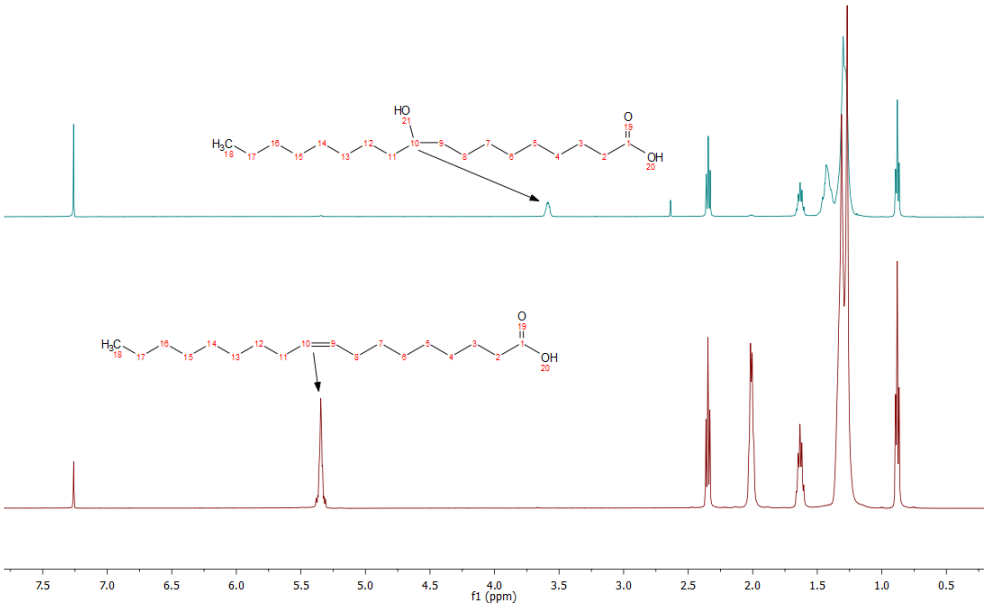

Figure 22: ^{1}H NMR-Spectrum of 10-hydroxystearic acid (**12**) (top) and oleic acid (**15**) (below) in comparison.

For the determination of the product formation protons of the substrate **15** and the product **12** were related to each other. In this context, the two protons of the double bond of oleic acid (**15**) at 5.34 ppm and the proton (3.59 ppm) located at the hydroxy-functionalized carbon-atom of 10-hydroxy stearic acid (**12**) (Figure 7) were used.

6.4.3 Analytical scale experiments with fatty acid hydratases

With these results in hand literature-based biotransformations were reproduced, to evaluate the activity of the fatty acid hydratases. Therefore the following compositions, according to literature, were chosen.[164,174,175]

All enzymes show activity (Table 7). Another idea was to use directly the oil for the hydroxylation to skip the esterification step with polyols.

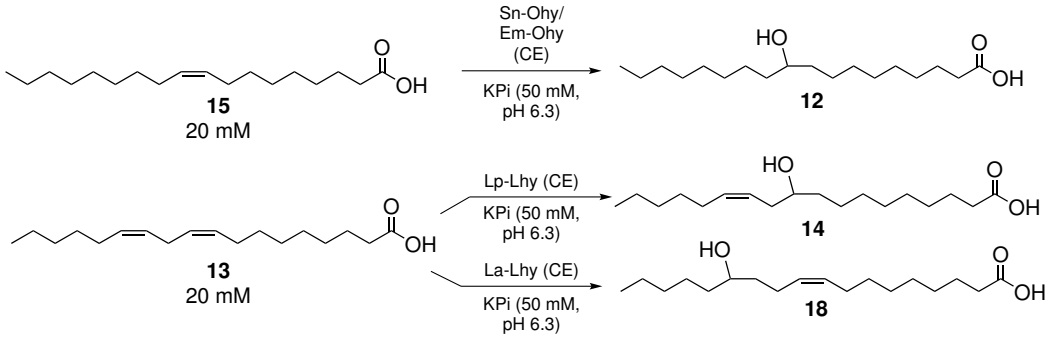

Table 7: Composition of fatty acid hydratase reactions in analytical scale for fatty acids hydration.

Hydratase	Substrate	Form.[a]	NADH	FAD	Conv/%
Lp-Lhy	Linoleic acid (**13**)	WC[b]	25 mmol L^{-1}	0.1 mmol L^{-1}	83
Sn-Ohy	Oleic acid (**15**)	CE[c]	-	-	>99
Em-Ohy	Oleic acid (**15**)	CE[c]	-	-	>99
La-Lhy	Linoleic acid (**13**)	CE[c]	-	-	79

[a] Formulation, [a] Whole cells (WC), [b] Crude extract (CE)

In this context, the esters were synthesized, to exclude that the ester functionality is not the problem for the FAHs. The fatty acids were esterified in toluene with molecular sieve by the means of methanol and hydrochloric acid at 110 °C for 1.5 h. After work-up the esters could be isolated with a yield between 70% and 82%. The following reactions with the esters were performed according to the previous reactions performed for the acids. The La-Ohy was not used further, because no conversion was detected for the fatty acids. The results and the composition of the reactions with the fatty acid esters are shown in Table 8.

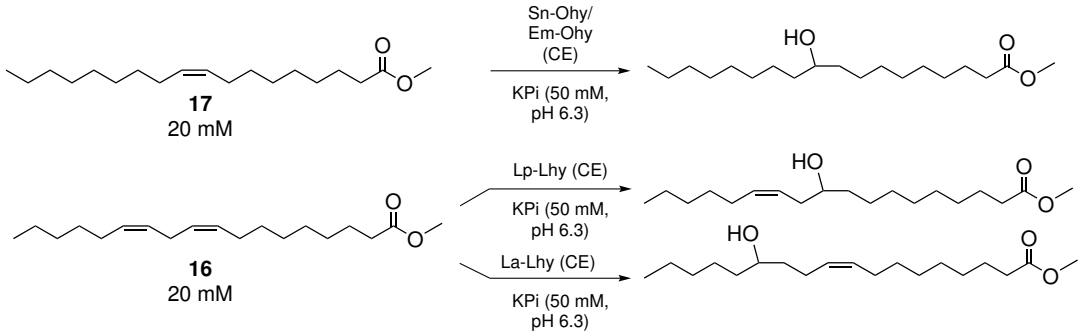

Table 8: Composition of fatty acid hydratase reactions in analytical scale for fatty acid esters hydration.

Hydratase	Substrate	Form.[a]	NADH	FAD	Conv/%
Lp-Lhy	Methyl linoleate (**16**)	WC[b]	25 mmol L^{-1}	0.1 mmol L^{-1}	0
Sn-Ohy	Methyl oleate (**17**)	CE[c]	-	-	0
Em-Ohy	Methyl oleate (**17**)	CE[c]	-	-	0
La-Lhy	Methl linoleate (**16**)	CE[c]	-	-	0

[a]Formulation, [b] Whole cells (WC), [c] Crude extract (CE)

In contrast to the acids, no conversion to the hydroxylated fatty acid esters could be determined (Table 8). This result was to be expected, since the fatty acid hydratases need a free carboxylate for the fixation of the substrate in the active pocket.[163] Nevertheless, sunflower oil was used as a substrate, with no positive results as well.

6.4.4 Kinetics for Em-Ohy and Sn-Ohy with oleic acid (15)

To get a deeper insight into the enzyme activity kinetics with the oleate hydratases (Em-Sny and Sn-Ohy) in isopropanol (5%, *v/v*) were performed. The linoleate hydratases were not further investigated. Tthere is a dramatic decrease in activity of Sn-Ohy after 60 min (Figure 23). The Em-Ohy shows a promising kinetic curve and completion of the reaction after 250 min (Figure 23). This phenomenon of activity-loss could possibly explain by the FAD-dependence of these enzymes.

In literature, it was shown that there was a losing activity and after treatment with FAD, the activity could be recovered fully.[161]

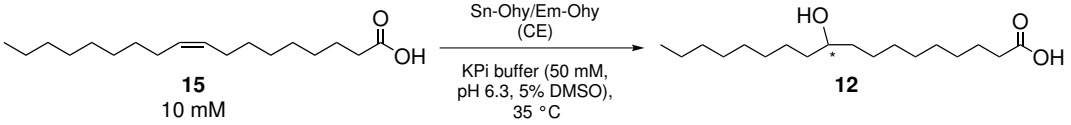

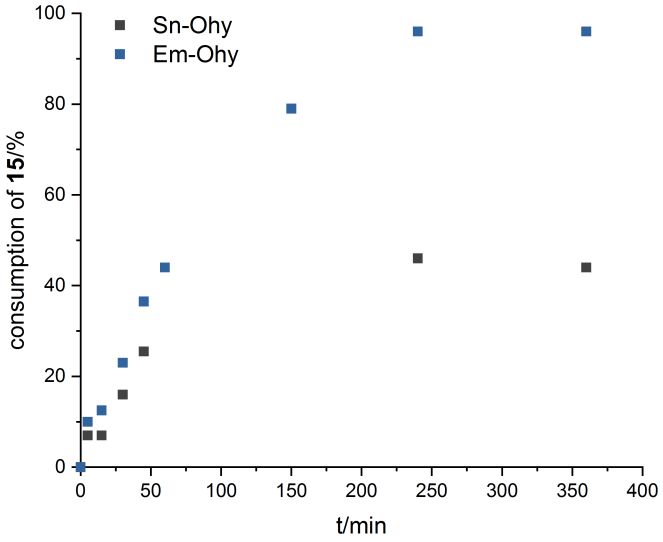

Figure 23: Reaction curve for Sn-Ohy and Em-Ohy for the hydration of **15**.

Another reason for the deactivation of the enzyme could be the content of isopropanol (5%, *v/v*) in the reaction mixture.

6.4.5 Cosolvent screening for Em-Ohy and Sn-Ohy

In the following study, an alternative cosolvent for Em-Ohy and Sn-Ohy was examined. Promising cosolvents, which were investigated are DMSO, isopropanol and as non-miscible cosolvents MTBE and cyclohexane. Furthermore, FAD and NADH were tested to investigate the impact of the cosolvent according long-term stability. These results show that DMSO is the best suitable cosolvent for both enzymes.

The addition of FAD during the reaction has no real impact on the enzymes. Not water-miscible cosolvents show a negative impact on the stabilization of the enzyme, because no, or hardly any conversion was detected (Figure 24).

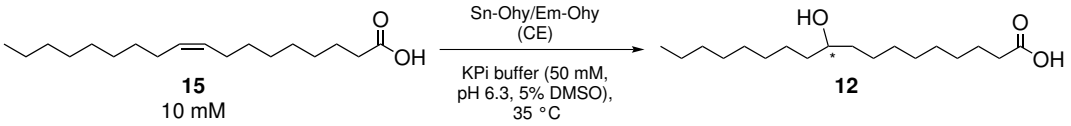

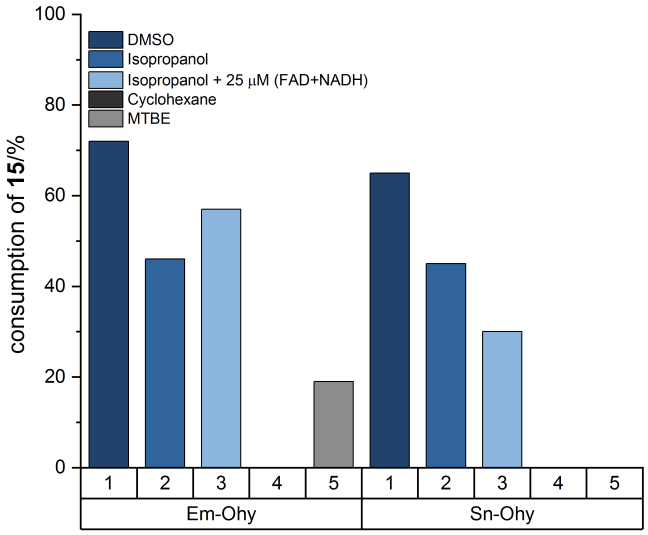

Figure 24: Cosolvent screening and influence of FAD for Sn-Ohy and Em-Ohy after 60 min incubation time.

6.4.6 Analytic scale reactions with Em-Ohy and Sn-Ohy with polyunsaturated fatty acids

With DSMO, as a suitable cosolvent in hand, biotransformation with polyunsaturated fatty acids were investigated using Em-Ohy and Sn-Ohy. Therefore, linoleic acid (**13**) and linolenic acid (**2**) were examined. The conversion of both enzymes stops after a certain consumption of substrate (Figure 25).

For the Em-Ohy the reaction stops after 2 mM hydroxy substituted linoleic acid (**14**) and 3 mM hydroxy substituted linolenic acid were formend. The Sn-Ohy could not convert more substrate than 8 mM hydroxy substituted linoleic acid (**14**) and 8 mM hydroxy substituted linolenic acid.

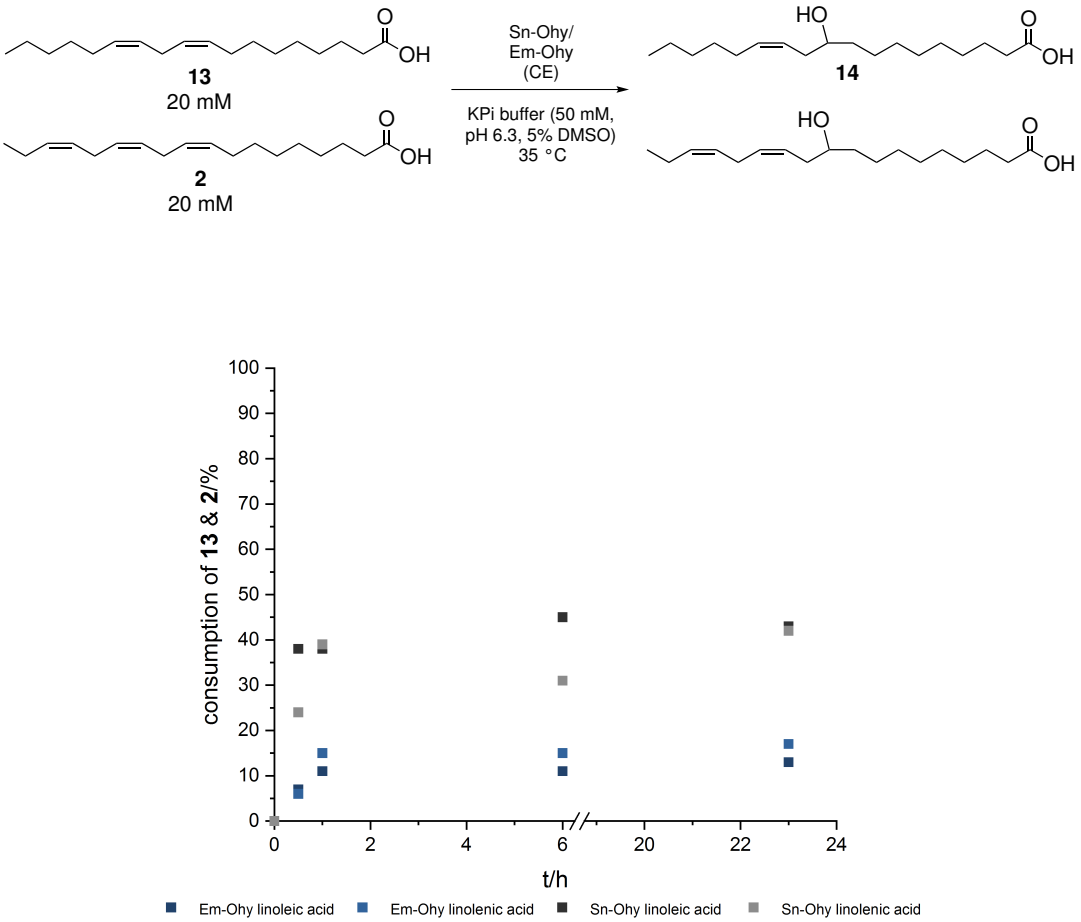

Figure 25: Kinetics for Sn-Ohy and Em-Ohy in terms of linoleic acid (**13**) and linolenic acid (**2**).

These results could indicate product inhibition or deactivation (Figure 25). This phenomenon could probably only be determined for the polyunsaturated fatty acids, because these are partly soluble in water as hydroxylated species, whether the hydroxylated oleic acid (**15**) is a solid and not water-soluble anymore. As a consequence these substrates will not be further investigated for these enzymes.

6.4.7 Stability tests for Em-Ohy and Sn-Ohy crude extract

In the following the stability under process conditions, and the storage of Em-Ohy and Sn-Ohy crude extract in KPi buffer were investigated. In this context, the enzyme was incubated in KPi-buffer (50 mM, pH 6.3) at 35 °C (see incubation times in (Figure 26)). Afterward, oleic acid (**15**) in DMSO was added to the reaction mixture. After one hour, the crude product was isolated and analyzed using ^{1}H NMR-spectroscopy (Figure 26).

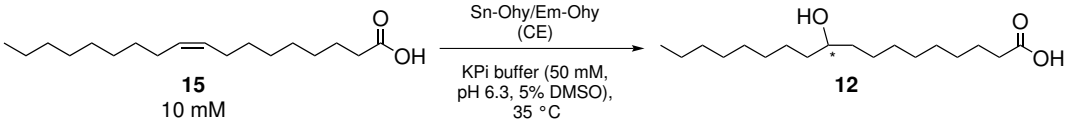

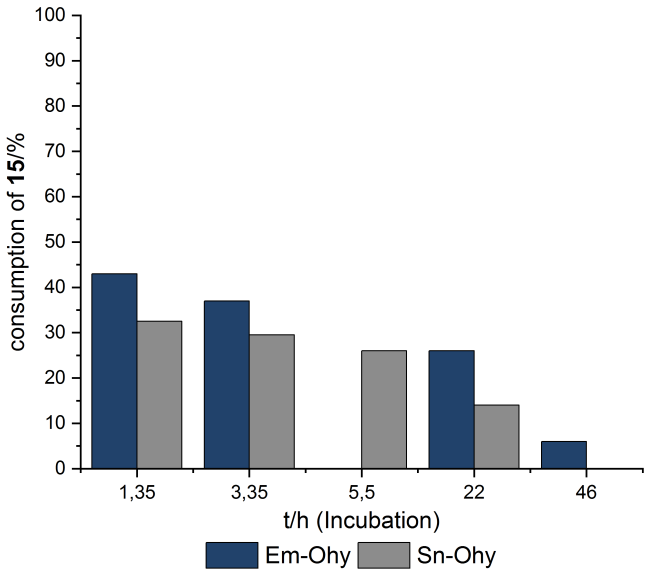

Figure 26: Stability of Sn-Ohy and Em-Ohy crude extract in KPi buffer (50 mM, pH 6.3) at 35 °C.

The diagram shows decreased activity for Em-Ohy and Sn-Ohy (Figure 26). Under these conditions, the Em-Ohy is stable for over 46 h. The Sn-Ohy is stable between 22 h and 46 h.

In addition, the storage stability for the enzymes was tested. Therefore, the crude extract of the enzyme was stored for 22 h at different temperatures.

Subsequently, oleic acid (**15**) in DMSO was added to the reaction mixture. After one hour, the crude product was isolated and analyzed using ^{1}H NMR-spectroscopy (Figure 26). Figure 27 shows no significant changes in the activity at different storage temperatures.

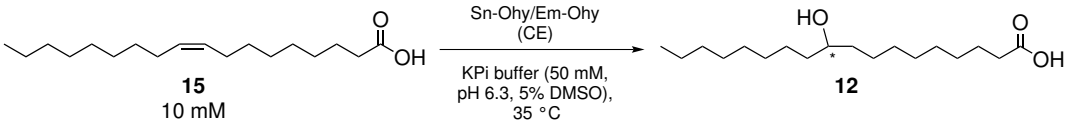

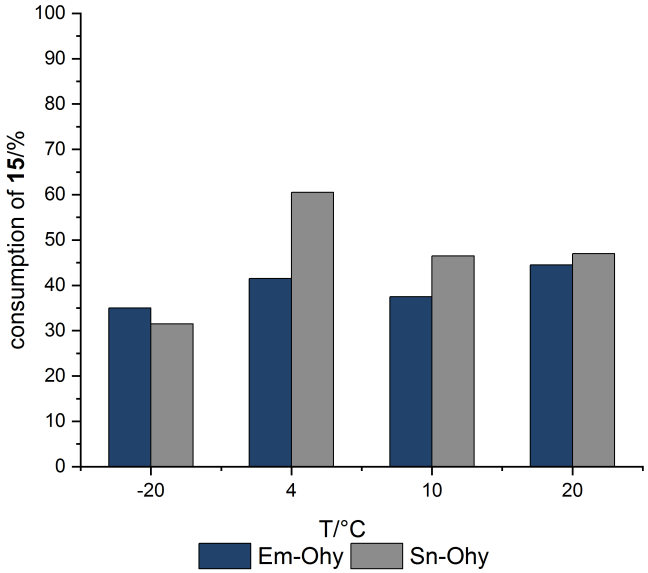

Figure 27: Stability tests for Em-Ohy and Sn-Ohy at different storage temperatures.

6.4.8 Parameter tests for Em-Ohy- and Sn-Ohy-catalyzed hydration

Because of the previous results, additional reaction conditions were evaluated for the improvement of the oleate hydratase stability. Therefore, citrate buffer[175] was used, the addition of NADH and FAD in combination were investigated,[161] as well as whole cells, to improve the stability of the enzymes. Furthermore, glucose was added to the reaction solution, which was also recommended for better reaction conditions.[182]

For the parameter screening, each enzyme was incubated for 24 h and 35 °C, afterward, the reaction was started.

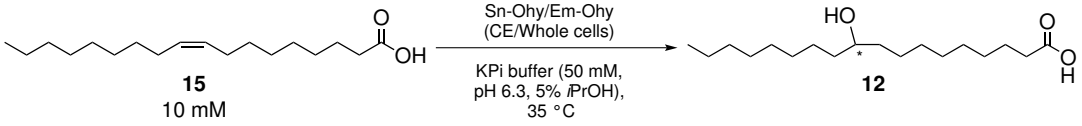

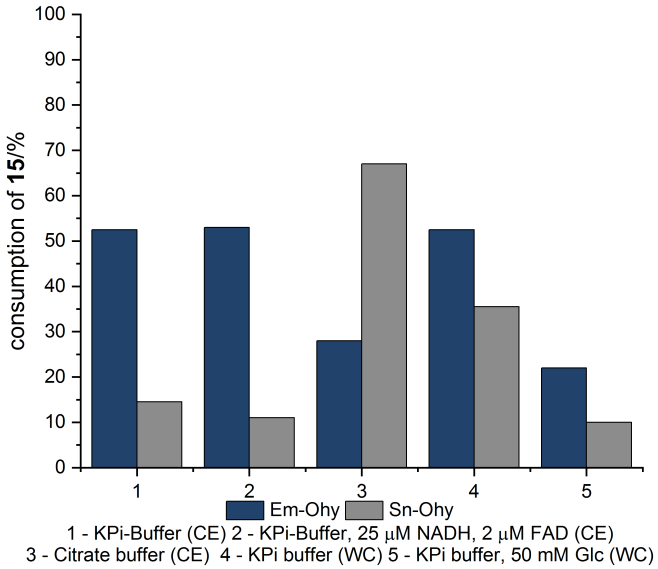

Figure 28: Parameter screening with the influence of KPi buffer, citrate buffer, crude extract (CE), whole cells (WC), FAD and glucose (Glc).

For the Em-Ohy, no significant improvement of stability was determined. The Sn-Ohy shows improved stability in citrate buffer and with whole cells. The addition of FAD, as well as glucose, shows no, or even a negative impact on stability. All in all, the activity and the stability of Sn-Ohy could be improved by especially chancing the buffer.

For the Em-Ohy no effective improvement could be achieved (Figure 28). As a consequence only the Sn-Ohy was used for further improvement and scale-up experiments. First, two additional parameters were investigated. On the one hand, the influence of NaCl, which was reported as a positive impact on fatty acid hydratases-catalyzed reactions was examined.[174]

On the other hand, the influence of the oleic acid (**15**) purity was evaluated.

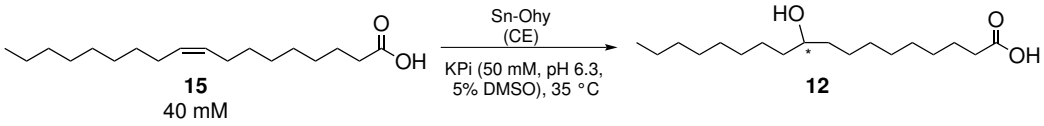

15
40 mM

12

Table 9: Evaluation of NaCl influence and purity of oleic acid (**15**) on Sn-Ohy activity.

Reaction-Nr.	Additive	Purity	Conv/%
1	Without NaCl	99% purity oleic acid (**15**)	48
2	With NaCl	99% purity oleic acid (**15**)	52
3	Without NaCl	90% purity oleic acid (**15**)	26
4	Without NaCl	99% purity oleic acid (**15**)	25

The results in Table 9 shows no significant change in the activity with or without NaCl, whereupon all following experiments are performed without NaCl. It was shown that a lower oleic acid (**15**) purity does not have an inhibiting effect on the Sn-Ohy. Due to the costs of raw material, the less pure oleic acid (**15**) can also be used, especially for the up-scaling experiments.

6.4.9 Lab scale-up experiments for Em-Ohy- and Sn-Ohy-catalyzed hydration

The starting point for scale-up experiments at elevated lab-scale was the application of the optimized process using 4 mmol and 40 mmol substrate concentration, as well as whole cells and crude extract. The whole cells showed more promising results in the previous experiments. Until now, the whole cells were not combined with citrate buffer. From previous data, a reaction time of 24 or 48 hours was chosen.

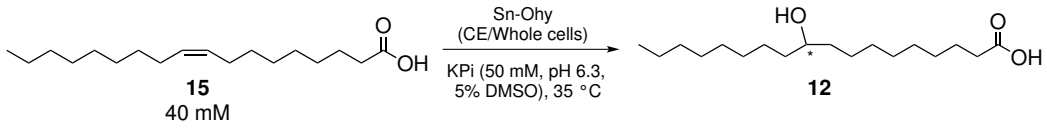

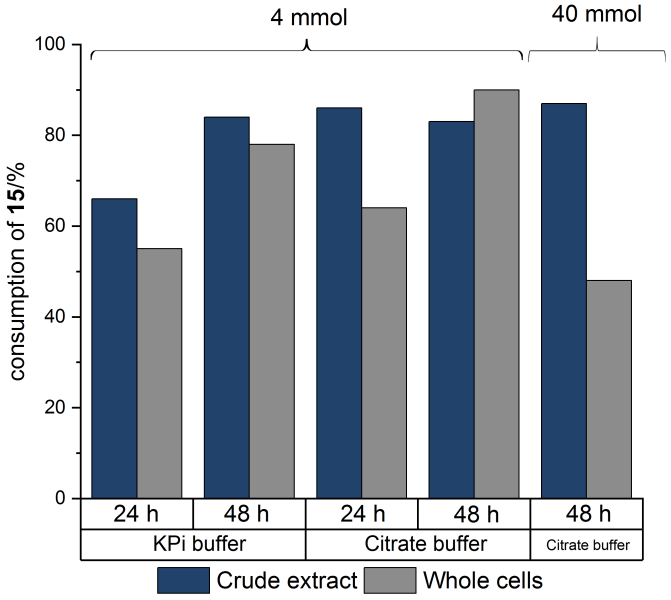

Figure 29: Elevated lab-scale experiment for Sn-Ohy with 4 and 40 mmol and oleic acid (**15**).

Furthermore, citrate buffer and KPi buffer were compared. The scale-up experiments at elevated lab-scale show high consumption of the fatty acid **15** already after 24 h in KPi buffer, as well as in citrate buffer. The consumption in citrate buffer with crude extract is higher (86%) compared to the consumption of oleic acid (**15**) in KPi-buffer (66%). After 48 h, the consumption in both buffers is nearly identical. The increase from 4 mmol to 40 mmol substrate concentration in citrate buffer with crude extract was successful (Figure 29). With whole cells, however, the experiment at elevated lab-scale (40 mmol) in citrate buffer shows less consumption of the fatty acid **15**, compared to the reaction with the crude extract. The result of lower consumption with whole cells is probably due to emulsion formation of the product **12** with the whole cells. As a consequence, the isolation of the product **12** is probably more difficult.

6.4.10 Reactions with immobilized Sn-Ohy

Another significant investigation was the immobilization of the Sn-Ohy, due to the fact of a potential application in chemical industry. Therefore, stability and recyclability were important subject matters, which can be easily handled by the means of immobilization.[183] The initial experiments were done by PIETROWSKI in her bachelor thesis. First, she was able to optimize the expression of Sn-Ohy. In her work, PIETROWSKI was able to find a support for the Sn-Ohy which can be recycled. After digestion of the cells, the crude extract was successfully immobilized on the hydrophobic carrier *Lewatit*® VP OC 1600. No leaching could be observed for the immobilized enzyme, which also could be recycled, in small scale.[184] These results were used as a starting point for further immobilization optimization. The first issue was the loading of the carrier, as well as the immobilization rate and time. The general immobilization procedure starts with washing of the carrier material with KPi buffer (50 mM, pH 7.5). Afterward, the carrier was suspended in the enzyme solution in KPi buffer (50 M, pH 6.3). First, the ratio between enzyme and carrier (*w/w*) was varied from 1:4 to 1:20. The immobilizations were performed at 20 °C for 18 h and 80 rpm. Second, the immobilization rate and time were increased to 24 h and 180 rpm. After incubation, the supernatant was removed with a pipette and the carrier was washed once with KPi buffer (10 mM, pH 7.5). The protein concentration of the crude extract and supernatant were validated *via* BRADFORD assay, according to GOP11. The immobilization loading was calculated according to equation 3.

The immobilization reactions were performed with the same Sn-Ohy crude extract on different days. Reaction 1-4, 5-6 and 7-8 were performed at the same day (Table 10).

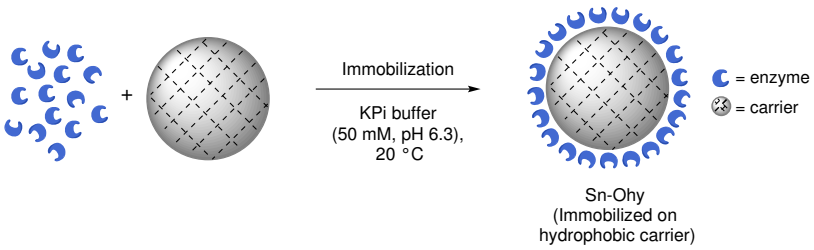

Table 10: Investigated of the immobilization parameters of Sn-Ohy crude extract on *Lewatit*® VP OC 1600 carrier.

Reation-Nr.	Ratio enzyme:carrier	Immob.[a] time/h	Immob.[a] rate/rpm	Loading/%
1	1:4	18	80	55
2	1:9	18	80	53
3	1:15	18	80	72
4	1:20	18	80	67
5	1:9	24	80	72
6	1:15	24	80	70
7	1:9	18	80	85
8	1:9	18	180	80

[a] Immobilization

The results vary from about 50 to 85% loading yield. In principle, it cannot be concluded that the highest possible loading of the carrier is the best option because high loadings can lead to diffusion problems. Accordingly, it is important to achieve the optimum loading with high diffusion of the substrate through the pores of the support.

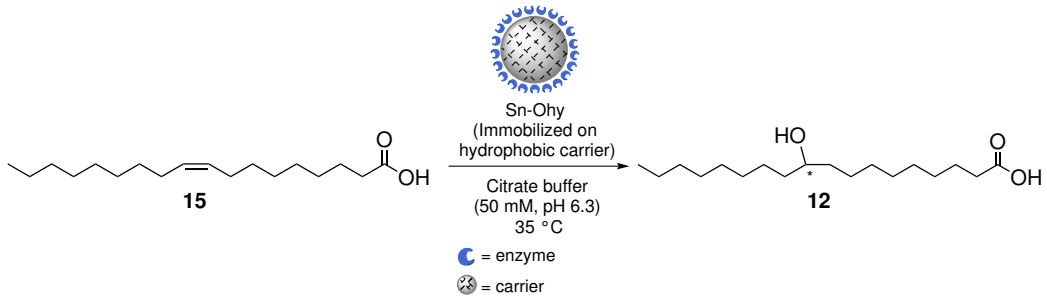

Table 11: Reactions with immobilized Sn-Ohy crude extract on *Lewatit*® VP OC 1600 carrier.

Reation-Nr.	Ratio enzyme:carrier	Immob.[a] time/h	Immob.[a] rate/rpm	Conv.[b]/%
1	1:4	18	80	40
2	1:9	18	80	53
3	1:15	18	80	64
4	1:20	18	80	-
5	1:9	24	80	63
6	1:15	24	80	35
7	1:9	18	80	85
8	1:9	18	180	80

[a] Immobilization, [b] Conversion

Nevertheless, the best immobilization conditions show 1:9 carrier at 80 rpm for 18 h incubation (Table 10). With these results in hand biotransformations were performed.

The best conversions were achieved in reaction 7 and 8 (Table 11). In reaction 7, a 1:9 enzyme/carrier ratio and an immobilization rate of 80 rpm was used. In reaction 8, appear to be a ratio of 1:9 enzyme/carrier and an immobilization rate at 180 rpm (Table 11).

6.5 Lab scale-up reactions with immobilized Sn-Ohy

To verify the applicability of the immobilized Sn-Ohy in large scale, scale-up experiments at elevated lab-scale were performed with the best immobilization procedure (1:9 enzyme/carrier, 80 rpm) and optimized reaction conditions. Therefore, the Sn-Ohy crude extract was immobilized on hydrophobic carrier, according to GOP 17.

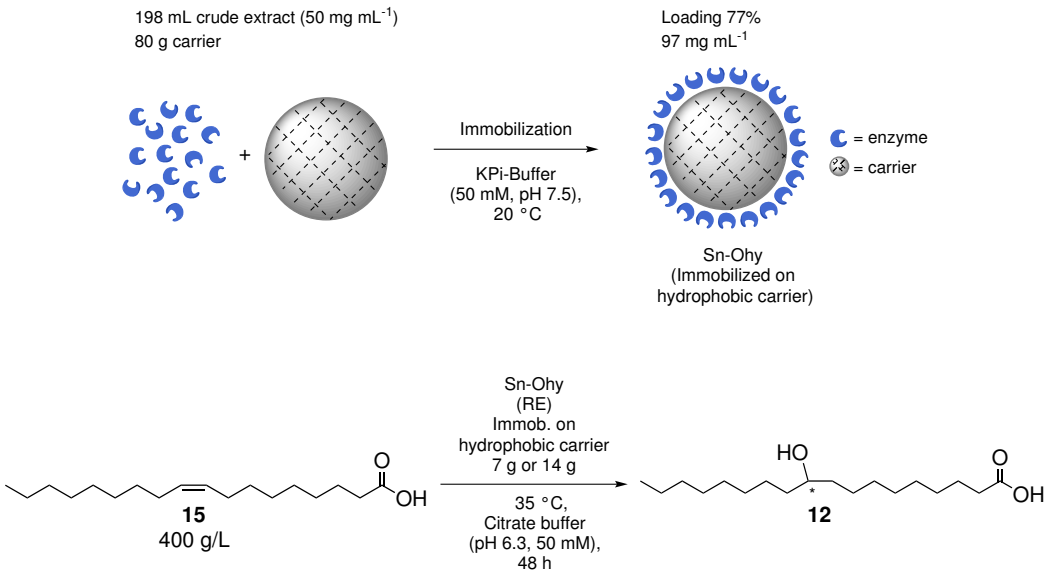

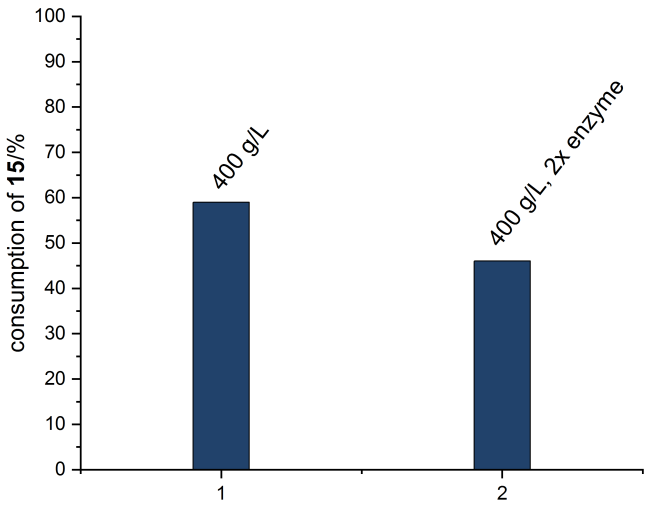

Figure 30: Elevated lab-scale experiment with immobilized Sn-Ohy.

The immobilization was performed by Hannah Bork.[185] The reaction of 400 g oleic acid (**15**) per L buffer shows conversion to **12** of about 60%, after 48 h, which refers to a theoretical yield of approximately 250 g 10-hydroxystearic acid (**12**) (Figure 30).

By duplication of the enzyme amount, the conversion is even less, probably because of diffusion problems of the fatty acid **15** in the carrier pores.

Until now, 250 g L^{-1} 10-hydroxystearic acid (**12**) represents an outstanding result, compared to the literature.[172,173,176,186]

Therefore, these results show a good starting point for further optimization and raise the questions, how can conversions be increased and how can the product be isolated without loss and without substrate contamination (Figure 30).

6.5.1 *SpinChem*® reactor reactions with immobilized Sn-Ohy

For the recycling and the separation of the carrier from the product, a reaction with a *SpinChem*® reactor was implemented (Figure 31).[187] The reactor has the advantage of spatial separation of the immobilized enzyme from the reaction mixture. The reactor is temperature controlled. In the reactor a rotating cylinder is stirred using a KPG-stirrer.

Figure 31: *SpinChem*® reactor.

In this rotating cylinder a solid phase (immobilized Sn-Ohy) is fixed as a packed bed. The composition, substrate loadings and results for the reactions performed in the *SpinChem*® reactor are shown in the table below:

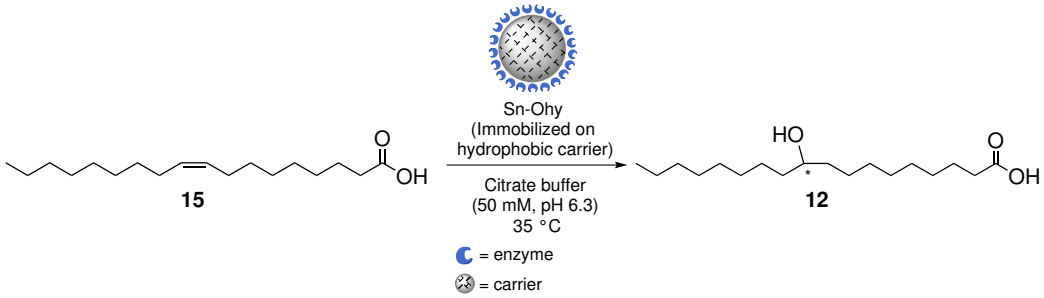

Table 12: Results of hydration reaction with hydrophobic carrier using different parameters.

Nr.	Carrier/g	Substrate/g L^{-1}	rpm	Dosing/mL min^{-1}	Glass balls	Conv./%
1	17.7	179	400	no	no	2
2	7.3	77	400	no	no	7
3	7.0	89	400	0.007	no	<1
4	4.0	89	850	0.0035	yes	42

The first *SpinChem*® reactor test was performed with loading of 17.9 g (179 g L^{-1}, 64 mmol) carrier, a stirring rate of 400 rpm, a reaction time of 48 h. With these reaction conditions only <5% conversion could be achieved. The reason for this low conversion is probably the emulsification of the oleic acid (**15**) with the carrier (Figure 32). Therefore, the amount of immobilized enzyme and substrate were first reduced and to prevent the formation of an emulsion.

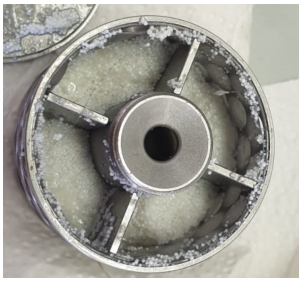

Figure 32: Formation of emulsion of the carrier with oleic acid (**15**) in the *SpinChem*® reactor rotating cylinder.

In this reaction (77 g L^{-1}), a conversion of about 10% could be observed, the oleic acid (**15**) was emulsified with the carrier, too. As a consequence, the substrate was added over 24 h, which resulted in emulsification of carrier and oleic acid (**15**), as well. To prevent this emulsification, the stirring rate and the dosing time were increased and glass balls were placed in the spiked reactor. Due to their polarity, they could prevent emulsion. Furthermore, the carrier-amount was reduced. With these reactions conditions, a conversion of about 42% could be achieved (Table 12). In the following experiments, Hannah Bork will further optimize the reaction.

6.5.2 Modification of hydroxy fatty acids

Hydroxy fatty acids as an isolated product are an interesting substance class.,[148–154] In addition, they can be further esterified with various polyols (Scheme 37) in order to generate novel hydroxy fatty acid esters with adjusted OH-number.

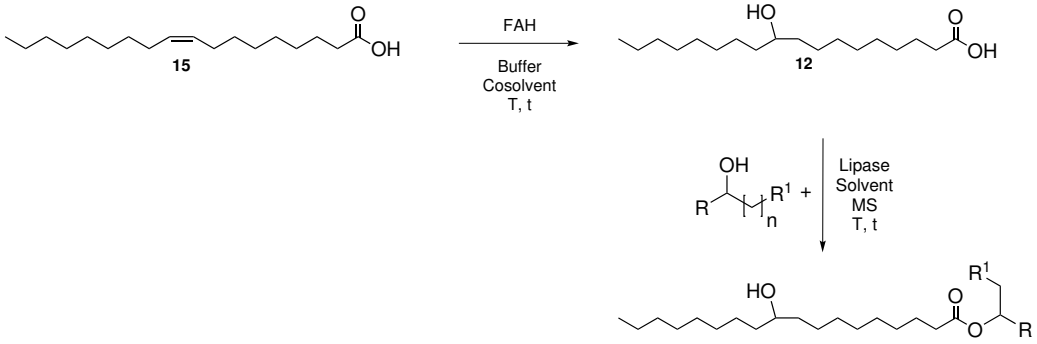

Scheme 37: Two-step enzymatic synthesis towards the hydroxy-substituted diol **21**.

These polyols can be further converted with isocyanates to polyurethanes. For the establishment of polyol production as material for polyurethanes, the model reaction oleic acid (**15**) converted to 10-hydroxystearic acid (**12**) was investigated. The 10-hydroxystearic acid (**12**) was esterified with 1,6-hexanediol (**20**) towards the polyol.

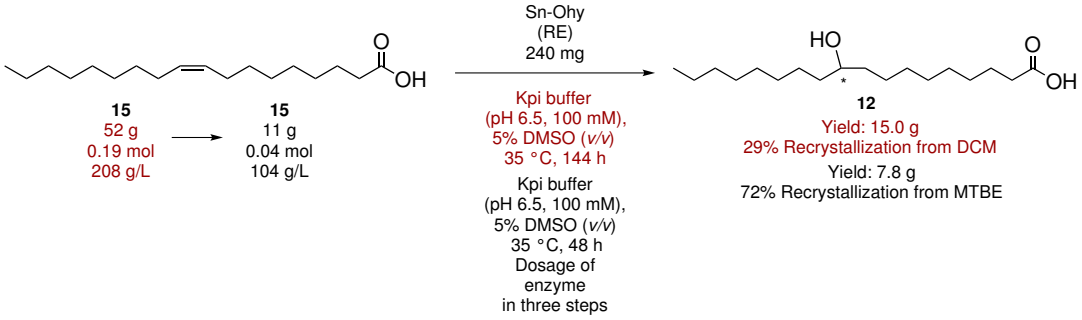

Scheme 38: First step of the enzymatic synthesis towards the hydroxy-substituted diol **21** with and without the dosing of the substrate **15**.

The first reaction was done in a simple batch set-up for 6 days, with oleic acid (**15**) (52 g, 0.19 mol) and Sn-Ohy crude extract in KPi buffer (pH 6.3, 100 mM, 5% DMSO *v/v*) with an overall yield of 15 g (no conversion was evaluated). The crude product was purified *via* recrystallization from dichloromethane (Scheme 38). The hydration was further optimized by dosing the enzyme to the reaction solution. Furthermore, MTBE was used for recrystallization, instead of DCM. Therefore, the reaction was started by adding 80 mg Sn-Ohy crude enzyme. After 7 h, and after 14 h reaction time, 80 mg Sn-Ohy crude enzyme were added. After a total reaction time of 48 h, the reaction was quenched, and 7.8 g 10-hydroxystearic acid (**12**) was isolated after recrystallization from MTBE with a yield of 72% and a purity of 97% (Scheme 38). The second step was performed in a *SpinChem*® reactor at 35 °C. Therefore, CAL-B and molecular sieve were used and a solvent mixture of MTBE and *n*-hexane. Hexane-1,6-diol (**20**) was used with 0.5 eq. The reaction was performed for 14 h.

The problem of the purification was the separation of the hexane-1,6-diol (**20**) from the product **21**. Therefore a lot of washing and column chromatography steps were necessary to gain high purity. Afterward, 7 g of the desired product **21** with a purity of 97% could be isolated (Scheme 39). To evaluate whether the hydroxy fatty acid can also be esterified with other alcohols, a series of solid and liquid diol, and triols were tested.

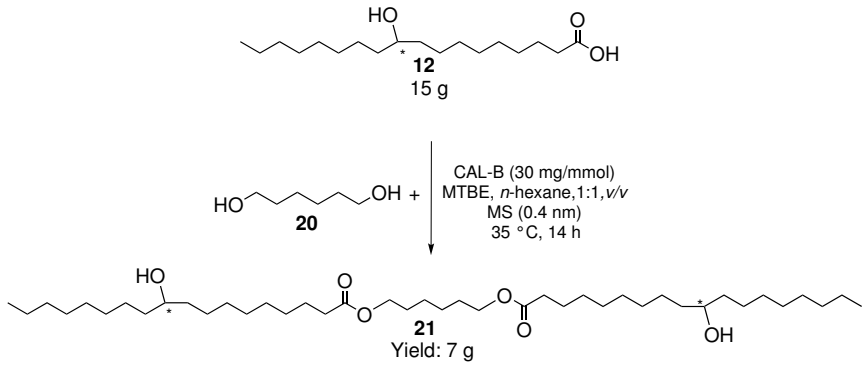

Scheme 39: Second step of the enzymatic synthesis towards the hydroxy-substituted diol **21**.

Additional solvents (MTBE, toluene, diethyl ether, and 2-methyl-THF) were also tested to ensure better solubility of the hydroxy fatty acid. For this purpose, the product was dissolved in the solvent and heated to 60 °C. Toluene proved to be a promising solvent (optical determination). Afterward, reactions with CAL-B in toluene and molecular sieve at 60 °C for 14 h were done (Scheme 40). All monomers, dimers and trimers were successfully identified *via* mass spectra analysis. Until now, no conversion and yield were determined.

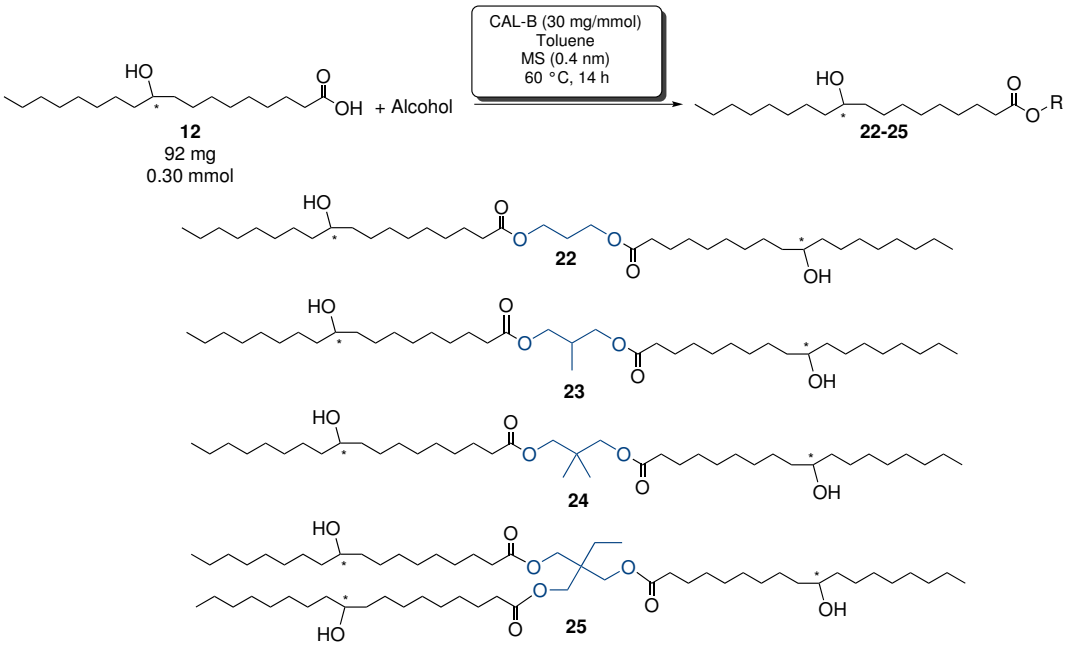

Scheme 40: Esterification of 10-hydroxystearic acid (**12**) with different alcohols.

In this context, it was also evaluated whether the self-condensation product is formed. For this purpose the 10-hydroxystearic acid (**12**) was esterified with CAL-B in toluene and molecular sieve at 60 °C for 5 h, both with and without diol. The esterification with the diol could be detected by ^{1}H NMR-spectroscopy. The self-condensation product could be excluded with ^{1}H NMR-spectroscopy, as well as with mass spectrometry. Thus, no self-condensation could be observed, using this reaction conditions.

6.5.3 Hydrolysis of sunflower oil

Another starting point for the synthesis of polyols is the usage of the oils, as a cheap and bio-based raw material.[188] Since the oils are no substrates for the fatty acid hydratases, they would first have to be hydrolyzed. One idea of the WINDMÖLLER project was the use of vegetable oil for the synthesis of polyols. Therefore, the hydrolysis of sunflower oil was tested with different literature known lipases.[175,186,189–191]

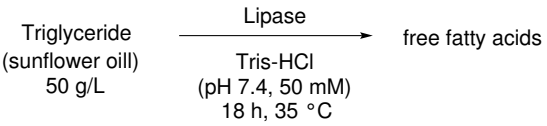

Table 13: Conversions of lipase-catalyzed hydrolysis of triglycerides.

Reaction-Nr.	Lipase	Conv/%
1	CAL-B	8
2	CAL-A	85
3	*C. rugosa*	>99
4	*B. cepacia*	88

C. rugosa lipase shows the highest conversion with >99% after 18 h (Table 41). Furthermore, the reaction time could also be reduced towards 3 h, also in citrate buffer (pH 6.3, 50 mM). These results offer the possibility for the combination of the lipase with the FAH. Afterward, the hydrolysis and the hydration were combined, which shows successful conversion (Scheme 41), which could not exactly been determined because of overlapped signals in the ^{1}H-NMR-spectrum.

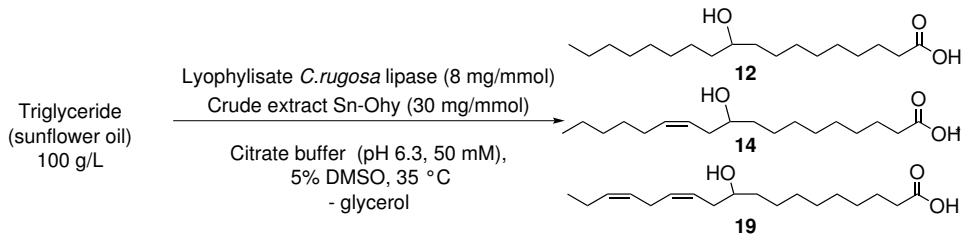

Scheme 41: Conversions of lipase-catalyzed hydrolysis of triglycerides, followed by hydration *via* Sn-Ohy.

6.6 Summary and outlook for fatty acid hydratase-catalyzed reactions

For the production of hydroxy-fatty acids, four enzymes were selected (La-Lhy, Lp-Lhy, Sn-Ohy, Em-Ohy). The selection was based on the amounts of substrate that the enzymes can convert according to the literature and on the high variability of the products.[165,171,174,175] All enzymes could be successfully expressed.[184]

To test the enzymes in terms of activity, reactions were performed under literature-known conditions.[165,171,174,175] The fatty acids could be successfully converted. Additionally, the esters and the oils could not be converted with the FAHs, since the FAHs require free carboxylates to bind the substrate in the active pocket.[163]

The most promising enzyme is the oleate hydratase from *Stenotrophomonas nitritireducens*. It could be shown that citrate buffer (pH 6.3, 50 mM), 35 °C and the enzyme formulation as crude extract are the optimal reaction conditions for Sn-Ohy. DMSO can be used as cosolvent, but the enzyme is also active without addition of cosolvent. The Sn-Ohy crude extract was successfully immobilized on the hydrophobic carrier *Lewatit*® VP OC 1600. No leaching could be observed for the enzyme and the immobilized Sn-Ohy could also be recycled.[184] Due to these promising results, the immobilization of Sn-Ohy was further investigated.

It was shown that the Sn-Ohy can be immobilized on the *Lewatit*® VP OC 1600 carrier with a 1:9 enzyme/carrier (*w/w*) ratio at 20 °C, 80 - 160 rpm for 18 h. Furthermore, it was possible to convert oleic acid (**15**) in a large scale reactions in a flask, as well as in the *SpinChem*® reactor with high loadings and up to 250 g L^{-1} isolated 10-hydroxystearic acid (**12**). Additionally, this process provides a good basis for further research. According to the current state of research, only a few processes for the production of 10-hydroxystearic acid (**12**) are known, but none on such a large scale. In literature, processes with product amounts of 30-50 g L^{-1} for the production of 10-hydroxystearic acid (**12**) are published.[172,173,176,186] Only Ogawa achieved comparable conversions with 280 g L^{-1} towards (*S*)-10-hydroxy-*cis*-12-octadecenoic acid (**14**).[178] In summary, it can be concluded that the intention of developing a separable and active biocatalyst for the synthesis of hydroxy fatty acids was successful. Furthermore, it was shown that by this method, it is possible to produce hydrated fatty acids on a large scale.

For further optimization of 10-hydroxystearic acid (**12**) production, two challenges have to be addressed in the future, one the one hand, the isolation of the product, and on the other hand, the recycling of the enzyme. First studies of Hannah Bork in her master thesis shows recyclability.[185] The isolation of the product has to optimized. Therefore immobilized enzyme and product has to be separated from each other.

Nevertheless, 10-hydroxystearic acid (**12**) is a solid product, therefore one approach would be to find a polyol containing 10-hydroxystearic acid (**12**), which is liquid. Another possibility to produce liquid hydroxy fatty acid would be an enzyme, which converts poly-unsaturated fatty acids, like linoleate hydratases.[177,178]

In the second topic, the esterification of hydroxy fatty acids with polyols using CAL-B was examined. In this regard, a large scale example with hexane-1,6-diol (**20**) was performed.

Furthermore, three diols and one triol were used for the esterification with **12**.

Thus, the purpose of the production of polyols from hydrated fatty acids could also be achieved. In this regard, further optimization has to be performed. Furthermore, it would be interesting to expand the polyol-library and find new polyols for the synthesis of polyurethanes with new properties.

7 Biocatalytic access towards 12-oxo phytodienoic acid 12-OPDA (1)

7.1 Current state of science

7.1.1 (-)-Jasmonic acid (26)

Plant hormones are responsible for a variety of functions in plants, like growth and development,[192] defense against fungi, oomycetes, bacteria, viruses, and nematodes,[193] or the protection from abiotic stress, such as temperature extremes, heavy metal toxicity or high-light intensity.[194] One famous example for plant hormones are (-)-jasmonic acid (**26**, (-)-JA) and its derivatives. They can activate genes encoding for pathogen and insect resistance, as well as genes for vegetative storage proteins. Jasmonate (**26**) consists of two stereogenic centers at C3 and C7 position (Figure 33) and is therefore represented in four isomers. The (+)- and (-)-jasmonic acid **26** can be found in the more stable *trans* configuration. The *cis* configuration is prone to epimerization *via* a keto-enol tautomerization involving C6 and C7.[195]

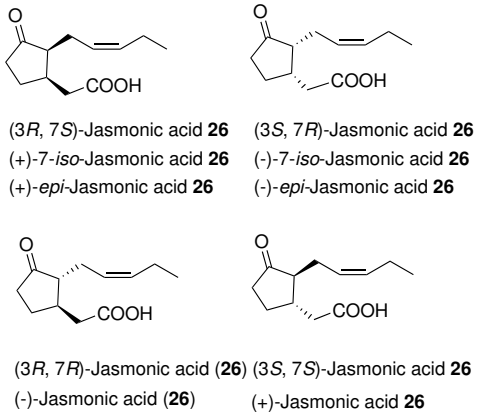

Figure 33: Jasmonic acid **26** isomers.

The synthesis of (-)-jasmonic acid (**26**) starts with the liberation of linolenic acid (**2**) from phospholipids or glycerolipids in the chloroplast membrane of the plant by the means of acyl hydroxylases.

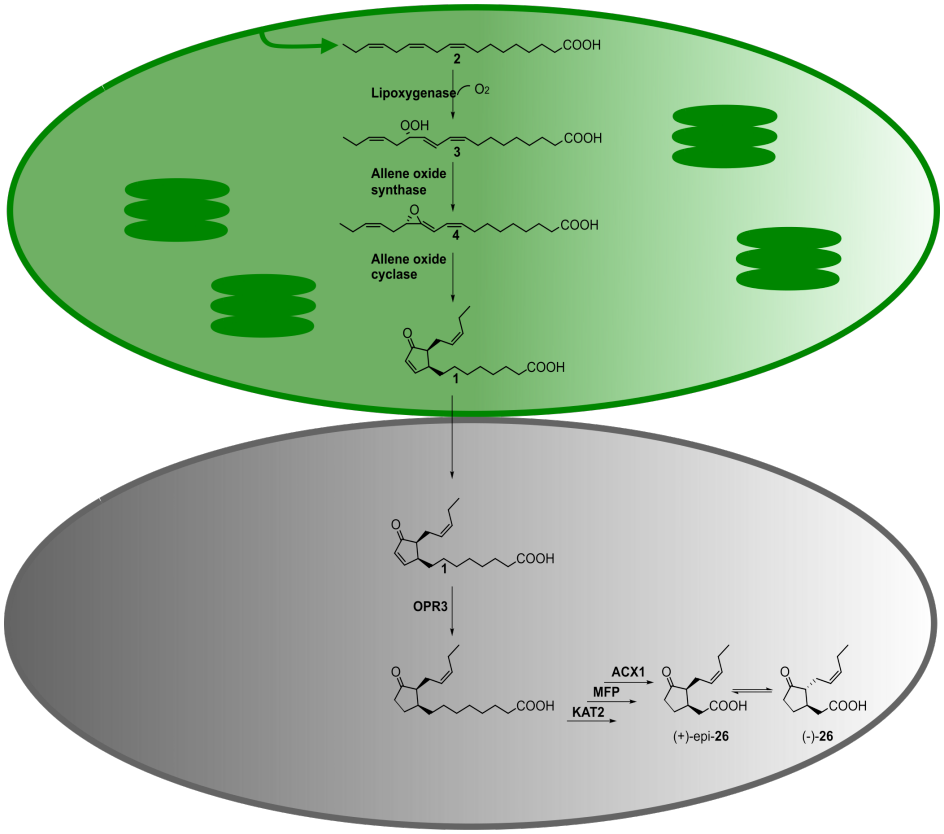

Figure 34: Synthesis of (-)-jasmonic acid (**26**) in plants. LA **2** hydroperoxidation of 13-HPOT (**3**) by 13-LOX, conversion by AOS to 12,13-EOT (**4**), cyclization to 12-OPDA (**1**) by AOC. Transport to peroxisome and reduction by OPR3 ene reductase, followed by a β-oxidation and a isomerization to active (+)-or(-)-JA **26**.

Linolenic acid (**2**) is converted *via* a 13-lipoxygenase (13-LOX) toward the 13-hydroperoxy-9,11,15-octadecatrienoic acid (**3**, 13-HPOT). 13-HPOT (**3**), in turn, is converted by the means of an allene oxide synthase (AOS) towards the instable (13*S*)-12,13-epoxy-octadecatrienoic acid (**4**, 12,13-EOT), which is easily decomposed towards the racemic 12-OPDA (**1**), as well as to the α-and γ-ketone. The active allene oxide cyclase catalyzes the cyclization of **4** into the active intermediate 12-oxo phytodienoic acid ((+)-12-OPDA (**1**)).[196] 12-OPDA (**1**) is then exported through the chloroplast outer membrane protein JASSY.[197]

JASSY recognizes 12-OPDA probably *via* its steroid acute (START) domain, a domain that can be found in various plant and human lipid binding proteins. This domain is responsible for recognizing of hydrophobic molecules (12-OPDA (**1**)). The import into the peroxisome takes place through an ATP-dependent ABC transport (CTS) or an ion trapping mechanism.[197,198]

In the peroxisome 12-OPDA (**1**) is reduced by means of a OPDA reductase (OPR3), followed by three cycles of β-oxidation towards (+)-7-*iso*-JA (**26**), which is afterwards isomerized towards (-)-JA (**26**) (Figure 34).[199] (-)-Jasmonic acids (**26**) are not only relevant as plant hormones, they are also used in the perfume industry as methyl jasmonic acid or *Hedione*[200] as ingredients (Figure 35). These lipid derived molecules are therefore of broad interest and despite their relevance in understanding of plants responses to external influences, they play a major role in our daily lives.

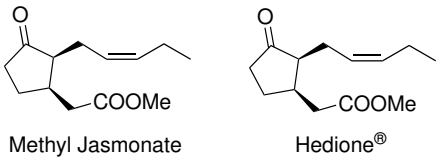

Figure 35: Methyl jasmonate and *Hedione*, ingredients of perfumes.[200]

7.2 12-Oxo Phytodienoic Acid (1)

In 1978 Zimmerman and Feng firstly described the synthesis of 12-OPDA (**1**) by incubation of linolenic acid (**2**) with an extract of flaxseed acetone powder.[201] About nine years later the same authors examined the physiological role of 12-OPDA (**1**) in connection with wound healing.[202] The biosynthesis is initiated by reactive oxygen species (ROS), leaf wounding, or hypersensitive response.[203] 12-OPDA (**1**) consists of a cyclopentenone ring, substituted with an aliphatic acid chain in C3 position and an alkene-chain in C2 position (Scheme 42). The synthesis of 12-ODPA (**1**) is synthesis explained in the chapter before.

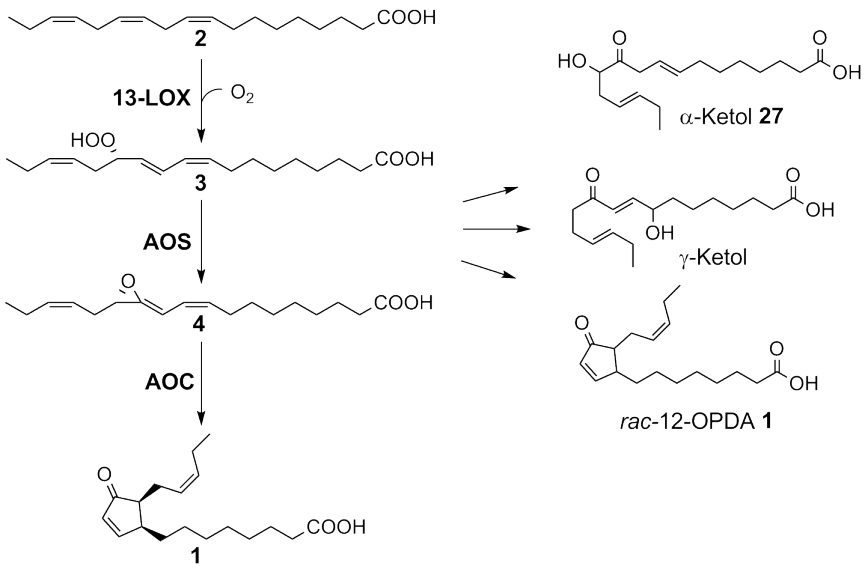

Scheme 42: Synthesis of 12-OPDA (**1**) in plants. LA **2** hydroperoxidation of 13-HPOT (**3**) by 13-LOX, conversion by AOS to 12,13-EOT (**4**), cyclization to 12-OPDA (**1**) by AOC. Decomposition of 12,13-EOT (**4**) in α-ketol **27**, γ-ketol **27** and *rac*-12-OPDA (**1**).

The structure of 12-OPDA (**1**) shows great similarity to prostaglandins (Scheme 43). These are produced in mammilian cells from arachidonic acid, which is hydrolysed from the plasmamembrane by phospholipases. They are further converted by the prostaglandin G7H synthase or the cyclooxygenase (COX) and are produced in increased amounts during inflammatory responses.[204] Not only (-)-jasmonic acid (**26**) is responsible for gene regulation in plants, 12-OPDA (**1**) can also switch on regulating genes.[205] One example is the binding of 12-OPDA (**1**) to cyclophilin 20-3 (Cyp 20-3). Cyclophilin 20-3 is a bifuntional enzyme in the chloroplast, on the one hand it shows peptidylprolylisomerase and on the other hand reductase activity. After binding of 12-OPDA (**1**) to Cyp 20-3, it forms a complex with serine acetyltransferase 1 (SAT1), which afterwards forms a heterooligomeric complex with O-acetylserine(thiol)lyase B to a cystein synthase complex (CSC). This complex, however, induces the production of cysteine, which, in turn, increases the cellular reduction potential and is responsible for the expression of 12-OPDA (**1**)-responsive genes.[206]

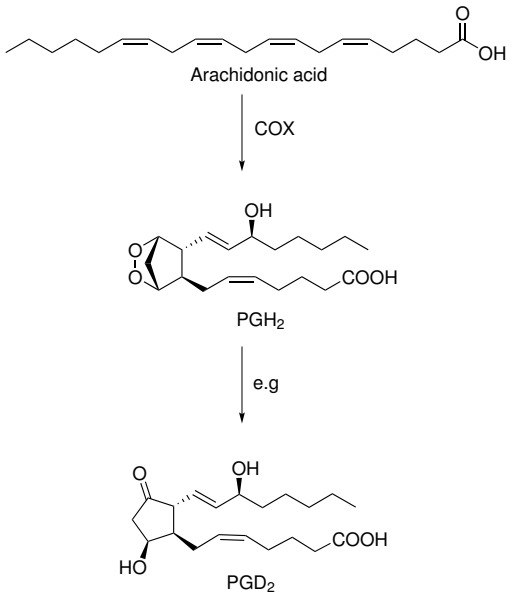

Scheme 43: Synthesis of prostaglandins, starting with arachidonic acid and conversion with cyclooxygenase.[204]

This is just one of the many examples, in which 12-OPDA (**1**) is involved in plant defense mechanisms. Access to this interesting hormone precursor is, on the one hand, chemically, starting from a norbornene derivative, followed by a diastereoselective insertion of side chain and a retro-DIELS-ALDER reaction (Scheme 44).[207]

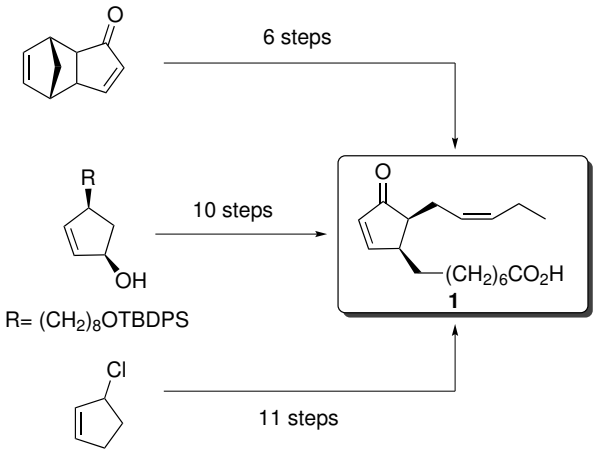

Scheme 44: Synthesis of 12-OPDA (**1**) starting from the norbornene derivative,[207] a cyclopent-2-enol enantiomer[208,209] or a prochiral cyclopenten-2-yl chloride.[210]

NONAKA *et al.* start from a cyclopent-2-enol enantiomer and after 10 synthetic steps they obtained the desired product (Scheme 44).[208,209]

A third possibility was established by Ernst *et al.*, using prochiral cyclopenten-2-yl chloride (Scheme 44).[210] Another possibility is the enymatic approach towards 12-OPDA (**1**). Here an unsaturated fatty acid instead of a cyclopentenone derivative is used as starting material. The first enzymatical approach was described by Zimmermann and Feng in 1978. In this approach flaxeed extract and LA **2** were used.[201] In 1996 Laudert *et al.* used a combination of soybean lipoxygenase, *Arabidopsis thaliana* AOS and *Solanum tuberosum* AOC for the synthesis 12-OPDA (**1**).[211] They described the coupling of AOS and AOC to a solid matrix, followed by the synthesis of 12-OPDA (**1**) with 13-HPOT (**3**) derived from LA (**2**). In 2007 Zerbe *et al.* use on Ni^{+2}-NTA immobilized AOS and AOC2, combined with 13-HPOT (**3**) synthesized from LA **2** with soybean LOX.[212] Kajiwara *et al.* use a flaxeed extract, coupled with an allene oxide cyclase to obtain 12-OPDA (**1**).[213] A very extravagant route was established from Le *et al.*, using covalently immobilized soybean lipoxygenase, recombinant rice allene oxide synthase-1 and rice allene oxide cyclase.[214] Maynard *et al.* combined commerical available soybean lipoxygenase or LOX6 from *Arabidopsis thaliana* with recombined AOS and AOC2 also from *Arabidopsis thaliana* as crude lysats.[215]

7.2.1 13-Lipoxygenase

The first enzyme in the 12-OPDA (**1**) cascade is the 13-LOX. In general, lipoxygenases are none-heme iron-containing dioxygenases. For their activity they need a 1-cis,4-cis-pentadiene system.

The mechanism of lipoxygenases is divided into four steps (Scheme 36). The first step is the hydrogen abstraction from the bisallylic methylene, the electron is transferred to the ferric-iron, which reduces the Fe^{3+} to Fe^{2+} and a radical species appears.

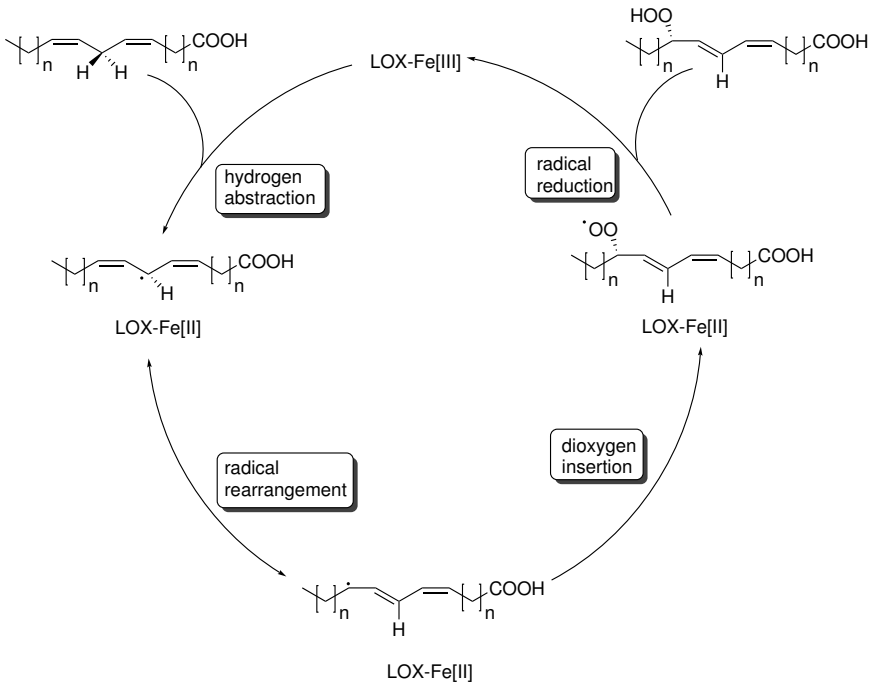

Scheme 45: Step I: Hydogen abstraction and reduction of the iron. Step II: Radical rearrangement to the methylene- or carboxylate end. Step III: Dioxygenen insertion. Step IV: Radical reduction by means of the iron, which is reoxidized and the product is released.

Afterwards the radical is rearranged (step II), either to the methylene end, as shown in Scheme 36, or to the carboxylate end. In the third step the oxygen is inserted. In the following fourth step, the radical is reduced by the electron from the divalent iron ion, whereby the iron is oxidized to its initial state.[216] The comparison of several LOX catalysis reactions from plants reveal that only the hydrogen in C11 position is removed, because of the rearrangement mechanism the C9 or C13 hydroperoxide can be produced. The position (C9 or C13) is determined by the means of the substrate orientation.[217]

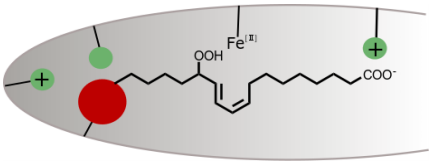

Figure 36: Space related orientation of linolenic acid (**2**) in the active site of LOX.[217]

For 13-LOX linolenic acid (**2**) is forced with its methylene group first in the active pocket- and as for the 9-LOX it is *vice versa*.

This access into the active site is, in turn, determined by the size of the active site residing amino acids (Figure 36).[217]

7.2.2 Allene oxide sythase

Allene oxide synthases (AOS) are members of the cytochrome P450 subfamily,[218] which containing heme as a cofactor.[219] Because of their ability to use a peroxycosubstrate, there is no need for the reducing agent NADPH.[220]

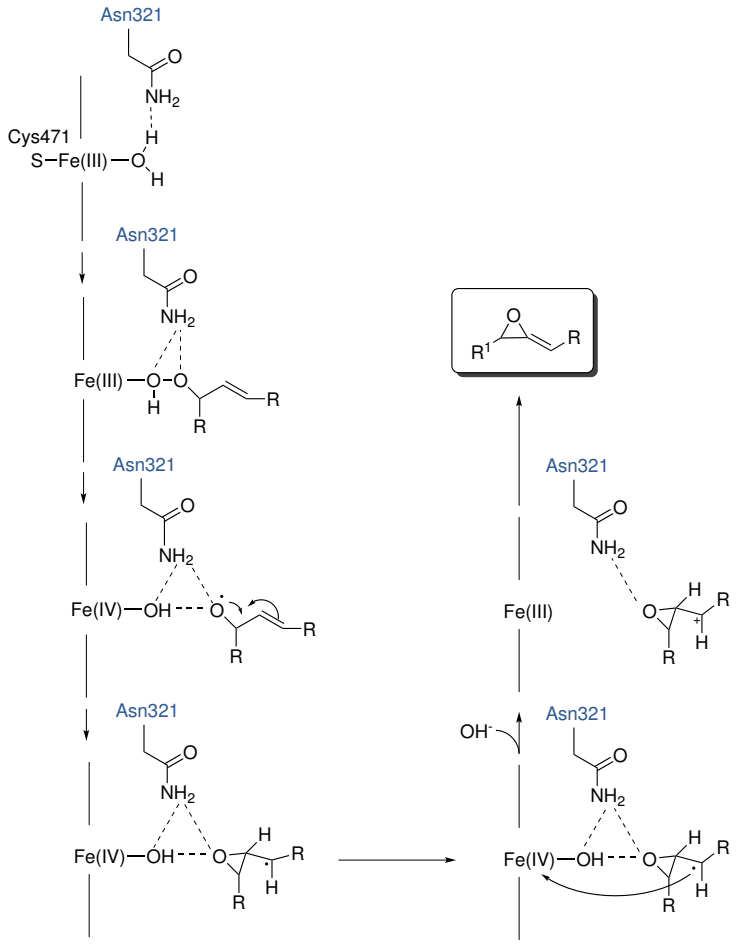

Scheme 46: Mechanism of AOS. Step I: Binding of the substrate in the active site. Step II:O-O-homolysis and O-radical formation. Step III: Formation of an epoxide and relocation of the radical. Step IV: Oxidation of the carbon-radical. Step V: β-Elimination and allene oxide formation[221]

Until now, the characterization is a difficult undertaking, since AOS is a membrane-associated protein and is therefore difficult to isolate.[218] Mechanistically, the allene oxide synthases show an impressive work, starting with the coordination of the hydroperoxide oxygene of the substrate with the ferric heme iron and the carboxamide (hydrogen-bond) of the asparagine. The iron was previously coordinated by two water molecules. After a O-O-homolysis an O-radical is formed and the iron is oxidized to Fe(IV).[221] As a result, the bonds are rearranged and an epoxid is formed, the radical is relocated to the adjacent carbon-atom. In the following the carbon-radical is oxidized by the means of the S-Fe(IV)-OH, which is also enabled by phenylalanine which stabilize the carbocation. After a β-elimination of a proton, the allene oxide is released (Scheme 46).[221]

7.2.3 Allene oxide cyclase

Allene oxide cyclase is a dimeric enzyme, which catalyzes the stereospecific cyclization of unstable allene oxides.[222] In *Arabidopsis thaliana* four active isoenzymes exist, which are active as homo or heteromers.[223] The reaction of an allene oxide synthase starts with the binding of the allene epoxide in the active pocket, whereas the Glu23 introduces a negative charge, which leads to delocalization of the double bond, which, in turn, has a ring opening of the epoxy moiety as a result.[224,225]

The oxyanion is stabilized by a water molecule. Five surrounding amino acids form a polar region to stabilize the water molecule. Afterwards a *cis-trans* isomerization takes place and a nonplanar ring-like pentadienyl carbocation is formed. This carbocation is stabilized by means of a phenylalanine and a cysteine. The *cis-trans* isomerization of C10-C11 is followed by a C8-C9 isomerization. The spontaneous cyclization of the epoxide, in turn, proceeds by an dipolar ring closure (Scheme 47).[224,225]

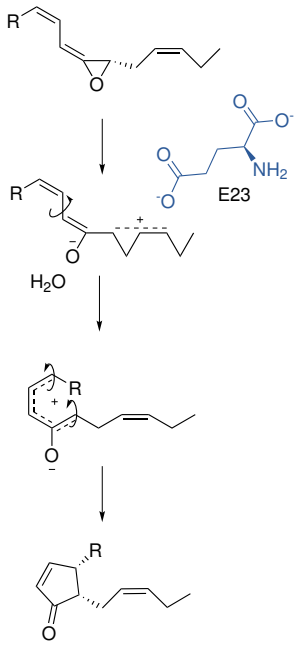

Scheme 47: Mechanism of AOC: Step I: Binding of the allene epoxide in the active pocket, Step II: Delocalization of the double bond and ring opening of the epoxy moiety. Step III: *Cis-trans* isomerization Step IV: conrotary pericyclic ring closure[224,225]

7.3 Metathesis

Olefin metathesis has a long history, starting with a few coincidences. In year 1957, Ziegler discovered during the oligomerization of ethylene that instead of oligomer chains, 1-butene was formed, which was later explained by nickel impurities.[226] A similar discovery was made by Eleutrio from Dupont, when he saw cyclopentene split with a tungsten catalyst, instead of the expected polymerization.[227] The term olefin metathesis was coined in 1967 by *Goodyear Tire and Rubber Company*, who published the reaction of 2-pentene with a homogeneous tungsten-based catalyst.[228] The mechanism was finally elucidated by Chavin, who postulated the formation of a metalcarbene, followed by a metal-cyclobutane intermediate and a newly forming olefin (Scheme 48).[229]

The first isolated carbene-metal complex was isolated by Fischer, the now called "Fischer-Carbene" is directly bound to a strong π-acceptor.[230]

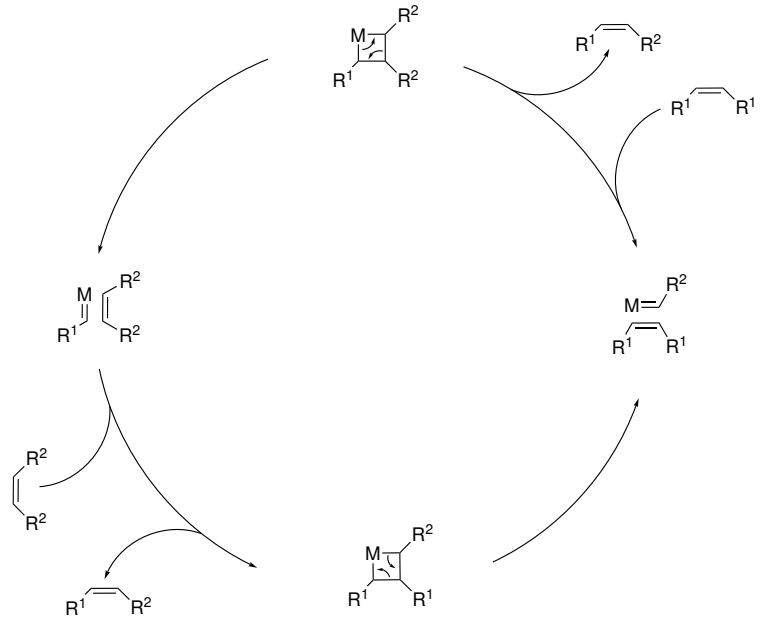

Scheme 48: Catalytic cycles of the metathesis reaction. Metathesis starts with a metal-carbene complex, which forms a metal-cyclobutane complex with another alkene and plays a central role in the catalysis cycle. From the metal-cyclobutane complex, the elimination of the statistically distributed olefin proceeds.

The first carbene-metallcomplex which was suitable for olefin metathesis was synthesized by Schrock, a tantalum-complex with *tert*-butoxidligands.[231] In consequence, Schrock changed the metal from tantalum to tungsten and molybdenum. The disadvantage of the tungsten and molybdenum complexes, however, is their costly production, which is due to their sensitivity to oxygen and moisture.[232] Grubbs on the other hand discovered that ruthenium (II) complexes showed high activity in olefin metathesis, and in the following years developed a number of active catalysts,[233–243] which are both more oxygen and water resistant.[244] In 1995, the first generation catalyst-generation was introduced, with two tricyclohexylphosphine ligands (Figure 37).

To increase the activity of the catalyst, one of the phosphine ligands was replaced by an *N*-heterocyclic carbene. The carbene as a strong-π donor increases the reactivity and is more stable, compared to the phosphine ligand.[244] These catalysts of the second generation were published in 1999 (Figure 37).

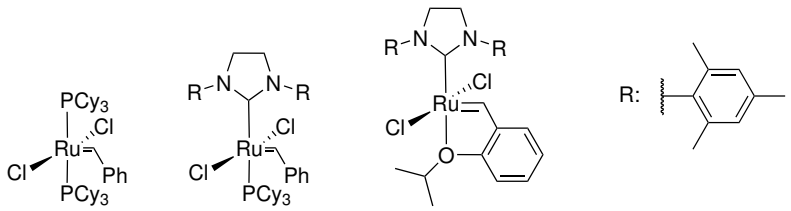

Figure 37: GRUBBS-catalysts of the first and second generation and GRUBBS-HOVEYDA catalyst of the second generation.

In 2000 HOVEYDA introduced GRUBBS-HOVEYDA catalysts (Figure 37), which have an *ortho*-propyl ether function on the benzylidene ligand which coordinates to ruthenium instead of the phoshpin-ligand. Due to this ligand change, the activity is lowered compared to the catalyst published before, but the catalyst gets more stable, since no phosphine ligands are present.[245]

The sterically very demanding residues at the nitrogen of the carben act stereoretentively, so *Z*-olefins are obtained from *Z*-olefins again.[246] GRUBBS, SCHROCK and CHAUVIN received the NOBEL prize in 2005 for their findings and research in the field of olefin metathesis. Synthetic applications of cross-metathesis with naturally occurring fatty acids have already been successfully performed. For example, the fatty acids found in soybeans, including α-linolenic acid (**2**), have been successfully metabolized with ethene, propene, butene and octene,[247] and even the metathesis of large molecules such as triolein with 2-butene has been performed with over 90% conversion.[248]

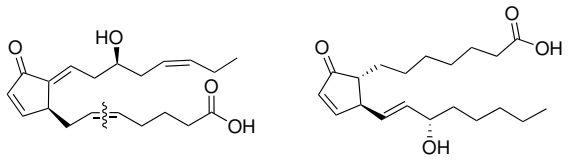

Figure 38: Structural formula of Δ12-PGJ$_3$ with indicated double bond formed by cross metathesis and the prostaglandin A$_1$

Furthermore, stereoretentive metatheses have been used for the synthesis of prostaglandins, such as Δ12-prostaglandin J_3 , which have structural similarities to 12-OPDA (**1**), such as the cyclopentenone ring, two aliphatic side chains in α- and β-position to carbonyl carbon, as in the successfully synthesized or naturally occurring prostaglandin A_1.[245] Also derivatives of (-)-jasmonic acid (**26**) were reported, produced by the means of olefin-cross-metathesis (Figure 38).[249]

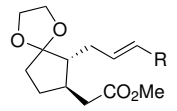

R= CH_2CO_2Me, CH_2OAc,
CH_2CH_2OH, CN, CH_2iPr

Figure 39: Jasmonic acid derivatives, synthesized by the means of olefin metathesis[249]

7.4 Motivation and goal for the biocatalytic access towards 12-OPDA (1)

A comparison of the chemical and enzymatic access to 12-OPDA (**1**) reveals a much more complex process for the chemical routes. The chemical synthesis of 12-OPDA (**1**) typically starts with a cyclopentenone-or norbornene derivative followed by a multi-step synthesis.[207,209,210] The biocatalytic approach in nature whereas starts with an unsaturated fatty acid, followed by a three-step enzymatic synthesis.[195] Using the enzymatic cascade as a starting point for the synthesis of 12-OPDA (**1**) only a few mg of the product can be isolated until now.[212–214,250] Due to the pharmacological and agricultural relevance of 12-OPDA (**1**),[215] it is very motivating to understand the natural synthesis of **1**, and consequently to perform its enzymatic synthesis on a gram scale.

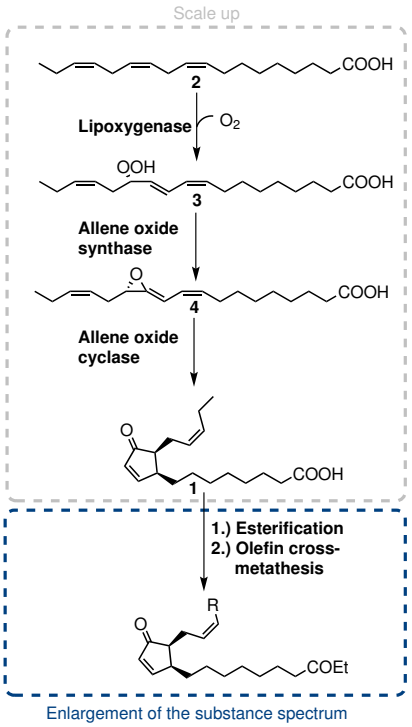

Scheme 49: Content of 12-OPDA (1) synthesis- In grey three step enzymatic cascade reaction with lipoxygenase, allene oxide synthase and cyclase. In blue further conversion of 12-OPDA (**1**) starting with esterification, followed by olefin cross-metathesis.

Moreover, it is of great interest to have the product in a higher scale and purity in a simple reaction set-up. For this purpose the enzymes have to be characterized, and the individual steps must be understood. This set-up will later be applied in segmented flow to optimize reproducibility, on the one hand and reaction control on the other. This project was investigated in cooperation with Adebar and Nastke from Industrial Organic Chemistry and Biotechnology, Bielefeld University. Another intention of this topic is the creation of a library of 12-OPDA (**1**) derivatives. Therefore, the strategy of alkene-cross metathesis (CM) was used, as a mild and manageable reaction, which was already used for (-)-jasmonic acid (**26**)[249] and prostaglandin derivatization.[245] For this reason, this method was used to expand the 12-OPDA (**1**) molecule-class and generate a new, diverse library. In this context, a variety of olefines shall be screened, as well as the best solvent, temperature, and catalyst for the CM.

7.5 Results and discussion for the biocatalytic access towards 12-OPDA (1)

7.5.1 Characterization and optimization of 13-LOX-catalyzed reaction

The synthesis of 12-OPDA (**1**) in higher scale and purity is a milestone for further development of 12-OPDA (**1**) activity in plants, like gene expression or interaction with molecules. Since the cascade consists of three steps, each step has to be validated in detail. The first aim was the reproduction of literature-based data, starting with the first step of 13-HPOT (**3**) synthesis (Scheme 50).

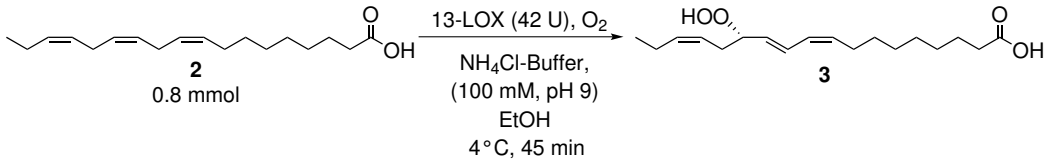

Scheme 50: Synthesis of 13-HPOT (**3**), starting from linolenic acid (**2**), using 13-LOX from soybean as catalyst.

The first issue was a spectrophotometric assay to confirm the activity of 13-LOX and evaluate the best reaction conditions. Therefore, linolenic acid (**2**) was diluted in degassed ethanol and then dissolved in ammonium chloride buffer (100 mM, pH 9). Commercially available lipoxygenase from *Glycine max* (*Sigma Aldrich* L7395, Type I-B, lyophilized powder) was used, and the reaction was carried out at 4 °C. Reaction was controlled *via* TLC (Cyclohexane/EtOAc/AcOH, 3:1:0.1, *v/v*) and stopped after 30 min, a yield of 20% was isolated. This quite low yield, as well as the high loading of the enzyme, was the starting point for the optimization of the reaction. First, an activity test was performed to investigate the best reaction conditions for the 13-LOX. Therefore, an activity assay by the means of a spectrophotometric assay was done. In this regard buffer, buffer concentration and pH, temperature, and ethanol amount were investigated.

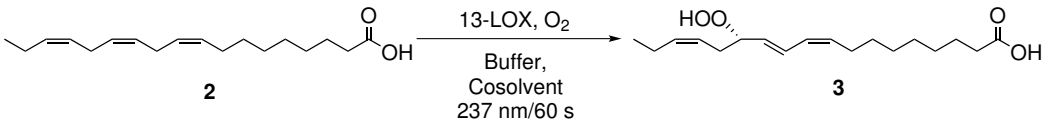

2 **3**

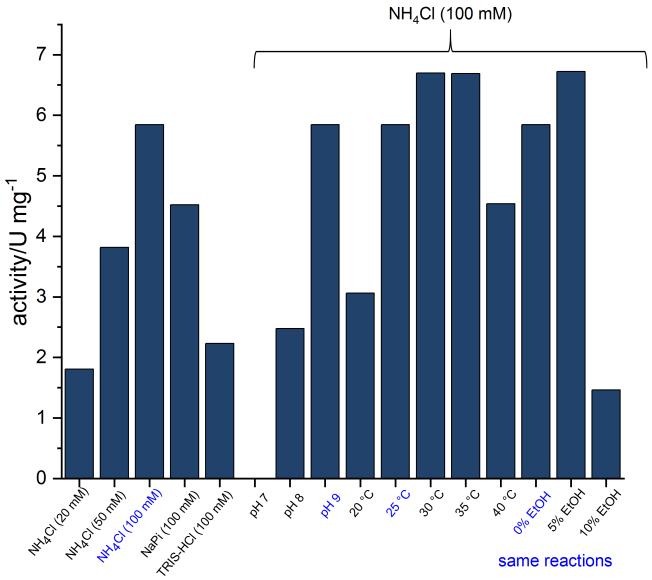

Figure 40: Activity assay for 13-LOX, by monitoring the formation of 13-HPOT (**3**) under different conditions for 1 min and 234 nm.

The best results were made with NH_4Cl, 100 mM buffer concentration, pH 9, 30 to 35 °C and 5% ethanol (Figure 40). Interestingly, the conversion with higher buffer concentration is higher, possibly because the pH value is lowered by the acid, or by stabilizing effects of the salts. At a basic pH it is guaranteed that the linolenic acid (**2**) is deprotonated, as shown in Figure 40 The fixation of the fatty acid is probably better, because of the positive charge in the active pocket. The protonation of the acid (at acidic pH) could worsen the fixation of the substrate in the active pocket.

The addition of ethanol also shows a positive effect, so the improved solubility of the linolenic acid (**2**) might be a reason for the increased activity. Additionally, the fatty acid esters were evaluated as possible substrates so that these can possibly better pass through the membrane while using whole cell catalysts.

Therefore, the methyl (**28**)- and ethyl ester (**29**) were synthesized with methanol or ethanol, in toluene, with hydrochloric acid at 4 °C. The methyl ester was obtained with a yield of 98% and the ethyl ester with a yield of 58%. In the next step, the commercially available lipoxygenase from *glycine max* was tested with linolenic acid (**2**), methyl- (**28**) or ethyl ester (**29**). The esters were used as a substrate, assuming that this improves the membrane permeability and/or the workup. Therefore, an activity assay using a spectrophotometric assay was done which shows low activity (Figure 41). These results underline that the basic pH value has a positive effect towards the activity of the 13-LOX, probably because of ionic interactions of its carboxylate with positively charged arginine in the active site of 13-LOX.[217] This would also explain the poor activity of 13-LOX towards the esters.

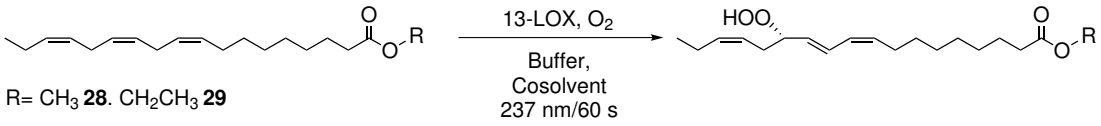

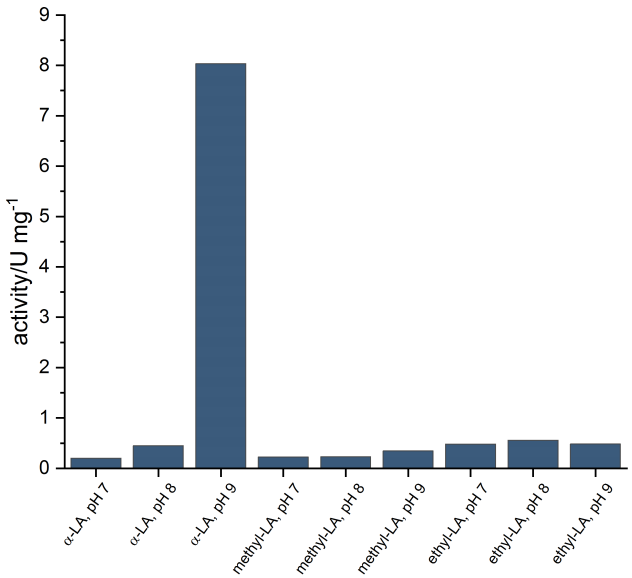

Figure 41: Activity assay for 13-LOX, by monitoring the formation of 13-HPOT (**3**) esters under different conditions for 1 min and 234 nm.

13-HPOT (**3**) is the first intermediate in 12-OPDA (**1**)-synthesis, to comprehend the stability and the behavior of this hydroperoxide, the biocatalytic approach towards 13-HPOT (**3**) with 13-LOX was investigated. The activity assay was a good starting point for getting a deeper insight into the catalytic activity of the commercially available 13-LOX. Nevertheless, the most important factor is probably the oxygen input into the system, this parameter, as well as reaction time could not be investigated *via* spectrophotometric assay. While no additional oxygen was reported in the literature, this was one of the points worthy to investigate.[212,213]

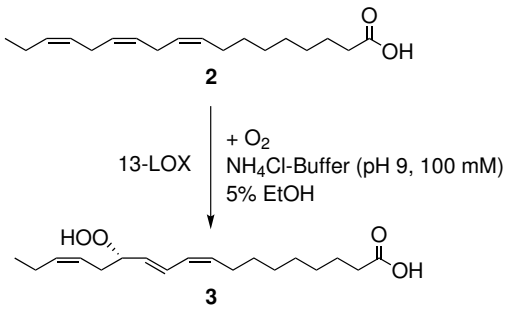

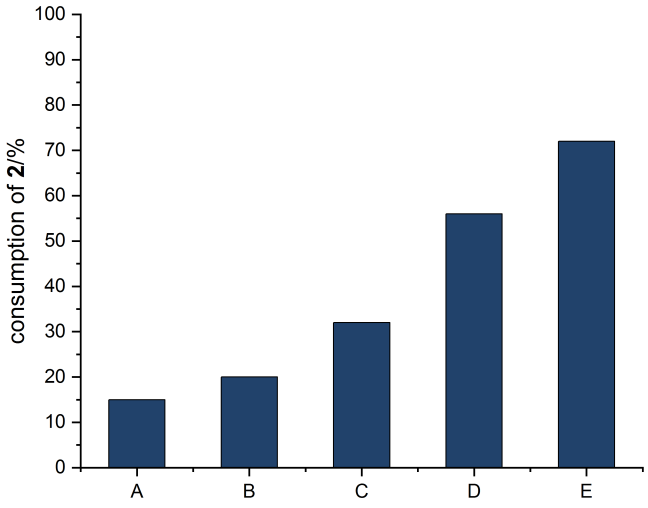

Figure 42: Synthesis of 13-HPOT (**3**) with 13-LOX, influence of oxygen concentration and temperature on the consumption of **2**.

Therefore, a reaction was performed in a simplified reaction set-up with oxygen in ammonium chloride buffer. Contrarily to the results of the activity assay, where higher temperatures show higher activities, the start temperature was set to 4 °C degrees, assuming an unstable product. Reaction A was done in an open flask, B and C with oxygen saturation, during the reaction, using an oxygen balloon. Reaction D and E were performed with oxygen saturation before and during the reaction. The reaction yield is higher with oxygen saturation of the reaction system, therefore reaction time can be reduced. The reduction of the reaction time has the consequence of less side-product **27** (shown by ^{1}H NMR spectroscopy), and thus more product **1** can be isolated. Also the reaction temperature plays an important role (reaction A to D were done at 4 °C, E at 25 °C), with an increased temperature, the activity gets higher. This can be seen in the direct comparison of reaction D, where 56% conversion could be detected, with reaction E (72% conversion).

The only difference between reaction D and E is the increased reaction temperature (4 °C to 25 °C) (Figure 42). In summary, the best reaction conditions for commercially available lipoxygenase from *Glycine max* is room temperature, the addition of 5% ethanol, NH_4Cl buffer, 100 mM buffer concentration, pH 9 and oxygen saturation of the system.

7.5.2 Characterization and optimization of AtAOS and AOC-catalyzed reaction

The starting point for the characterization was the expression of the recombinant AOS and AOC. First of all AOS and AOC2 from *Arabidopsis thaliana*, from now on called AtAOS and AtAOC2 were chosen for the reaction towards 12-OPDA (**1**). As already mentioned in the theoretical part, AOS-enzymes are mostly membrane-associated and therefore it is difficult to isolate them from the lysate.

To find the best expression conditions, an expression optimization for the enzymes AtAOS and AtAOC2 in *E. coli* BL21(DE3) and *E. coli* BL21CodonPlus(DE3)-RIL was performed. The plasmids pET24a-AtAOS and pQE30-AtAOC2 were transformed into *E. coli* BL21(DE3) and *E. coli* BL21CodonPlus(DE3)-RIL respectively. For both strains, the expression in TB medium was tested at temperatures of 37 °C, 30 °C, 25 °C. Expression in TB medium was carried out for 22 h and was induced by 0.5 mM IPTG at an OD_{600} between 0.6 and 0.8.

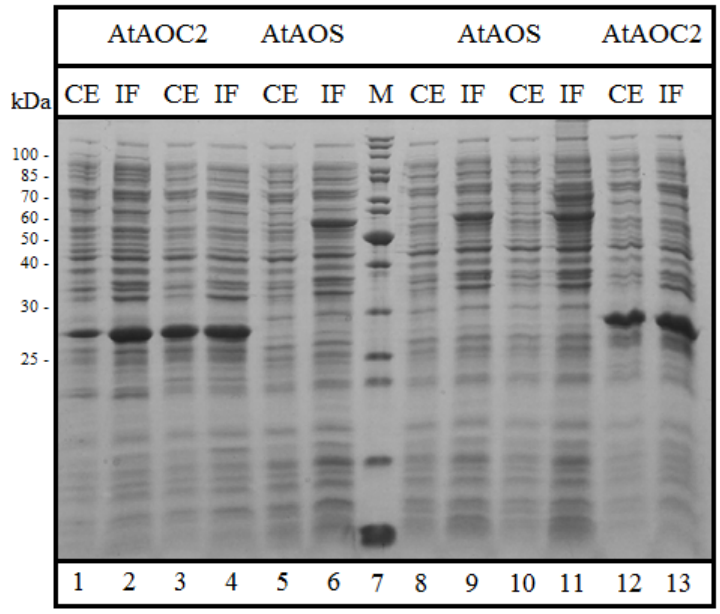

Figure 43: SDS-PAGE AtAOS and AtAOC2, expressed at different temperatures in *E. coli* BL21(DE3). Stained with Coomassie Brilliant Blue R-250, **lane 1**: crude extract expressed at 25 °C (AtAOC2), **lane 2**: insoluble fraction, expressed at 25 °C (AtAOC2), **lane 3**: crude extract, expressed at 30 °C (AtAOC2), **lane 4**: insoluble fraction, expressed at 30 °C (AtAOC2), **lane 5**: crude extract, expressed at 37 °C (AtAOS), **lane 6**: insoluble fraction expressed at 37 °C (AtAOS), **lane 7**: marker (Thermo Scientific PageRuler Unstained Protein Ladder), **lane 8**: crude extract, expressed at 25 °C (AtAOS), **lane 9**: insoluble fraction expressed at 25 °C (AtAOS), **lane 10**: crude extract expressed at 30 °C (AtAOS), **lane 11**: insoluble fraction expressed at 30 °C (AtAOS), **lane 12**: crude extract expressed at 37 °C (AtAOC2), **lane 13**: insoluble fraction expressed at 37 °C (AtAOC2).

An optimal expression temperature of 30 °C could be ensured for the AtAOS, as well as for AtAOC2 (Figure 43).

7.5.3 Purification of AtAOS and AtAOC2

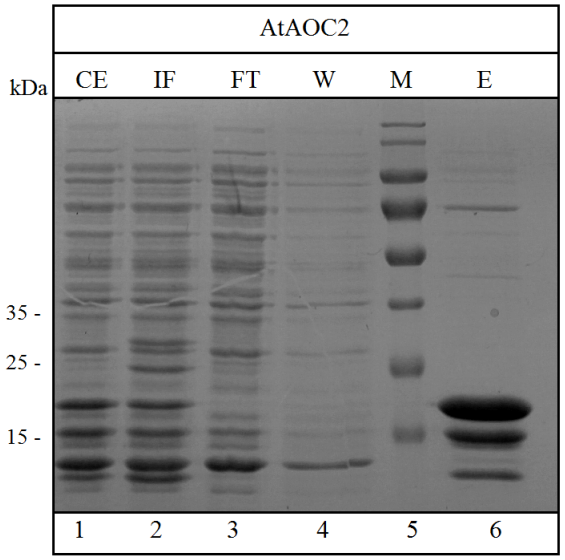

Figure 44: SDS-PAGE analysis of purified AtAOC2. Stained with Coomassie Brilliant Blue R-250. **lane 1**: crude extract, **lane 2**: insoluble fraction, **lane 3**: flow through, **lane 4**: wash, **lane 5**: marker (*ThermoScientific* PageRuler Stained Protein Ladder), **lane 6**: elution.

The purification of AtAOC2 was successfully performed using Ni^{2+}-NTA chromatography, according to GOP 13. The SDS-PAGE shows a very intense band between 25 kDa and 15 kDa (Figure 44). According to literature, AtAOC2 plus *C*-terminal His_6-tag has a molecular weight of 22 kDa.[212] Two further bands can be identified below the AtAOC2 protein. These are probably caused by proteins of the *E. coli* BL21CodonPlus(DE3)-RIL expression system. For the AtAOS no successful purification by the means of Ni^{2+}-NTA chromatography was possible. Therefore, isolation of the membrane-associated AtAOS was performed on another way to test the activity. For this purpose, *E. coli* BL21(DE3)+pET24a-AtAOS cells were digested by ultrasound and the cell lysate was centrifuged stepwise. First the cells were centrifuged (5 min, 4000x g), then the supernatant was taken and centrifuged at (20 min, 20000x g). The pellet of the last centrifugation step was resuspended in sodium phosphate buffer (50 mM, pH 7). Afterward, an SDS-PAGE of the sample was prepared. The SDS-PAGE shows that the AtAOS was successfully isolated (Figure 45).

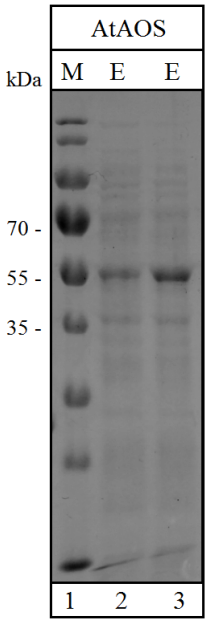

Figure 45: SDS-PAGE analysis of purified AtAOS. Stained with Coomassie Brilliant Blue R-250. **lane 1**: marker (*ThermoScientific* PageRuler Stained Protein Ladder), **lane 2**: elution (1 µg mL^{-1}), **lane 3**: elution (5 µg mL^{-1}).

The AtAOS was resuspended in sodium phosphate buffer (50 mM, pH 7) and shows a band at the level of 55 kDa which is assigned to the AtAOS.[251]

7.5.4 Activity assay with AtAOS

Since it is now possible to isolate the AtAOS enzyme, activity tests could be carried out here, as well. For the activity measurement three AtAOS-types were used: AtAOS with a *N*-terminal tag (AKKTSS) for improving protein solubility[221] without *N*-terminal tag and expression in *E. coli* ArcticExpression strain which contains chaperones for correct folding of protein.[252] The *N*-terminal tag (AKKTSS) is indispensable for the activity of the AtAOS. The best activity was shown with NaPi-Buffer at 25 °C (Figure 46).

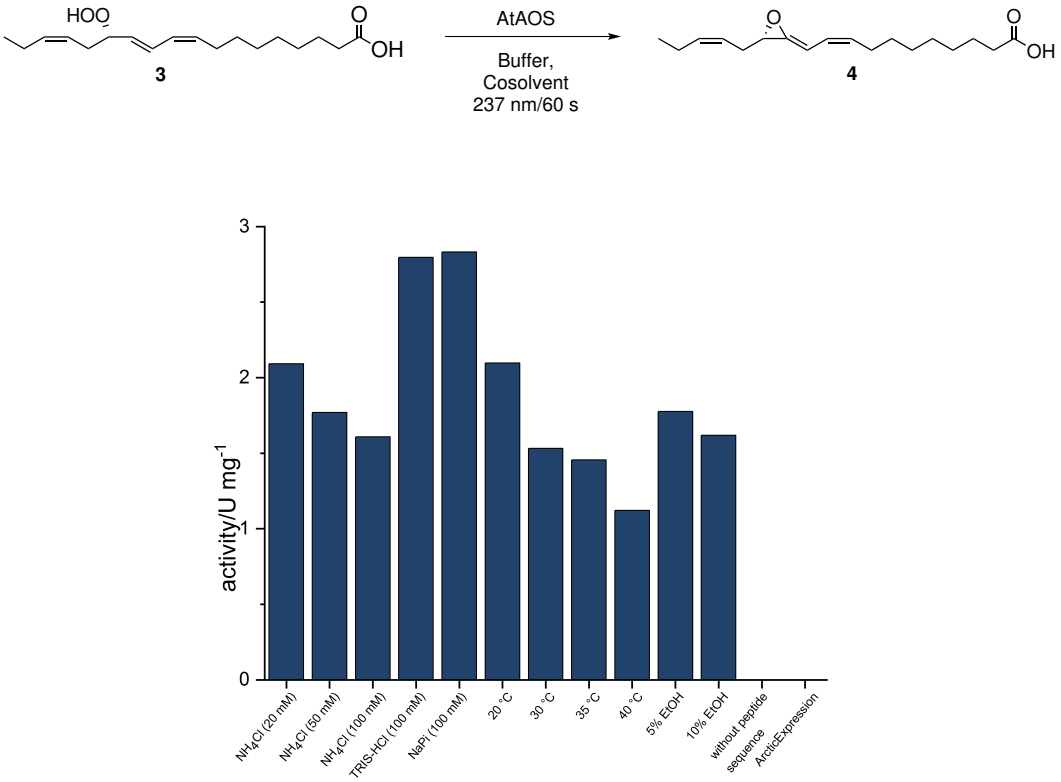

Figure 46: Activity assay for AtAOS with different parameters.

7.5.5 Preparation of an AtAOS and AtAOC2 whole cell catalyst

The enzymes AtAOS and AtAOC2 were used in a whole cell catalyst for the synthesis of 12-OPDA (**1**). The idea behind the whole cell catalyst lies in the unstable oxirane intermediate, which, by introducing both enzymes into a cell, has probably a shorter diffusion time between the two enzymes and therefore does not decompose into the undesired side-product. For this purpose the plasmids pET24a-AtAOS and pQE30-AtAOC2 were transformed into *E. coli* BL21(DE3) and *E. coli* BL21(DE3)CodonPlus-RIL. The two whole cell catalysts *E. coli* BL21(DE3)-AtAOS, AtAOC2 and *E. coli* BL21(DE3)CodonPlus-RIL-AtAOS, AtAOC2 were cultivated in expression cultures at 30 °C for 22 h.

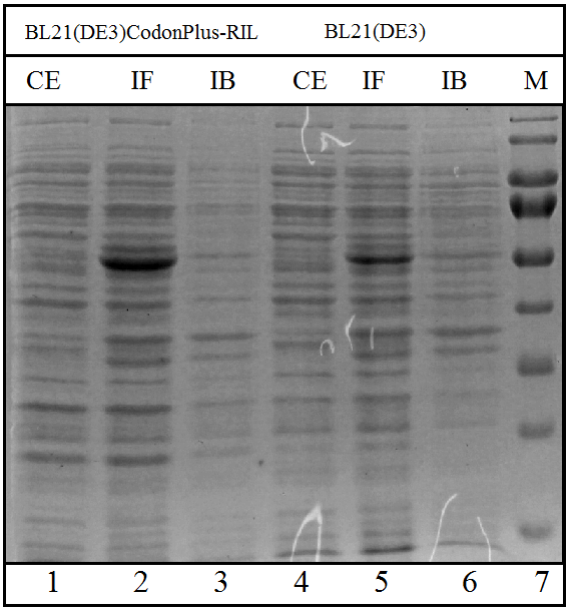

Figure 47: SDS-PAGE from pET24a-AtAOS and pQE30-AtAOC2 overexpressed in *E. coli* BL21(DE3) and *E. coli* BL21(DE3)CodonPlus-RIL. Stained with Coomassie Brilliant Blue R-250. **lane 1-3** shows overexpression in *E. coli* BL21(DE3)CodonPlus-RIL, **lane 4-6** shows overexpression in *E. coli* BL21(DE3) **lane 1**: crude extract, **lane 2**: insoluble fraction, **lane 3**: inclusion bodies, **lane 4**: crude extract, **lane 5**: insoluble fraction **lane 6**: inclusion bodies **lane 7**: marker (*ThermoScientific* PageRuler Stained Protein Ladder).

The SDS-PAGE shows a weak band between 35 kDa and 25 kDa, which is assigned to AtAOC2.[225]

In the trace "insoluble fraction", in addition to the AtAOC2 and the *E. coli* bands, another intensive band at the level of 55 kDa can be identified, which is assigned to the AtAOS (Figure 47).[218] In the inclusion body traces, only weak bands are visible in both expression systems. In general, the overexpression of AtAOS and AtAOC2 in the expression strain *E. coli* BL21(DE3)CodonPLus-RIL is significantly stronger. The SDS-PAGE (Figure 47) confirms that both proteins were overexpressed in the whole cell catalyst.

7.6 Synthesis of 12-OPDA (1)

7.6.1 ^{1}H NMR-spectroscopic analytics for the synthesis of 12-OPDA (1)

During the synthesis of 12-OPDA (**1**), the conversion, the *cis*:*trans* isomerization, and the side product formation were monitored using ^{1}H NMR spectroscopy. Therefore, specific signals were correlated.

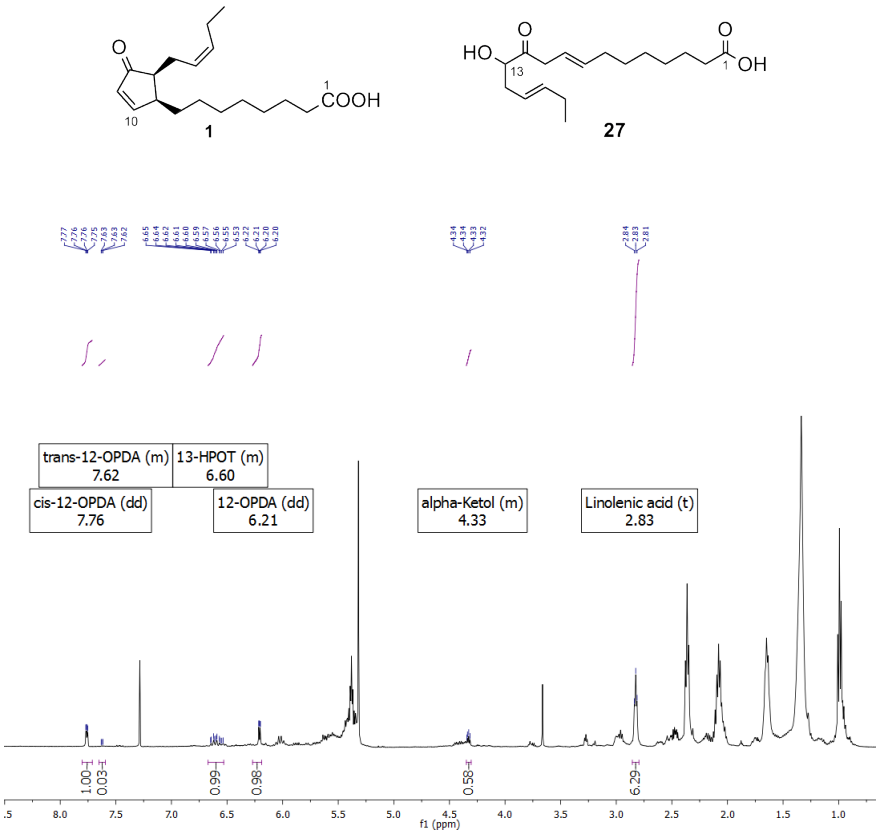

Figure 48: Example for a reaction towards 12-OPDA (**1**) shown in a ^{1}H NMR-spectrum.

In Figure 48 a ^{1}H NMR-spectrum of 12-OPDA (**1**) crude product is shown. In detail, the ^{1}H NMR-spectrum shows the side-product α-ketol **27**, *cis*-12-OPDA **1**, *trans*-12-OPDA **1**, linolenic acid (**2**), and 13-HPOT (**3**). The *cis*:*trans* ratio can be determined by comparison of the signals at 7.76 and 7.62 ppm. These signals are caused by the *cis* (7.76 ppm, (C10)*H*) or *trans* (7.62 ppm, (C10)*H*) proton.

The amount of side-product can be determined using the (C13)*H* relation with the (C10)*H* or (C11)*H* of the desired product **1**.

7.6.2 Initial experiments for the synthesis of 12-OPDA (1)

After successful production of the whole cell catalyst, the synthesis of 12-OPDA (**1**) was performed. For this purpose a reaction with α-linolenic acid (3 mM, **2**), 13-LOX (3 mg, 40 U) and whole cell catalyst (400 mg, consisting of pET24a(+)-AtAOS, pQE30-AtAtAOC2 (WCC1)) in *E. coli* BL21(DE3)CodonPlus-RIL in 100 mL ammonium chloride buffer (100 mM, pH 9, 5% ethanol) at 4 °C, was prepared.

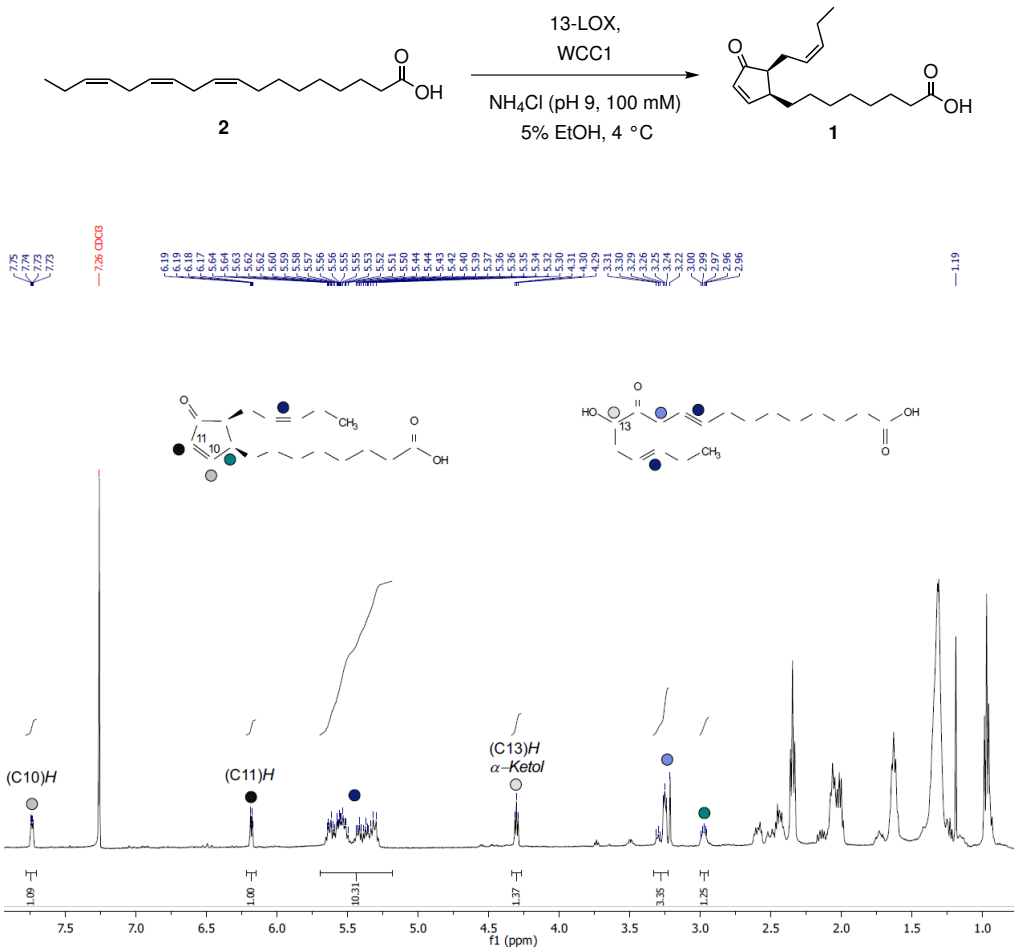

Figure 49: ^{1}H-NMR-spectrum of a 12-OPDA (**1**) and α-ketol **27** (mixture 40:60).

Contrarily to the results of the activity assay, the reaction temperature was set to 4 °C, assuming an unstable product **1**. The reaction was controlled by TLC (3/1/0.05; cyclohexane/EtOAc/AcOH, *v/v*). After 2 h no α-linolenic acid (**2**) could be detected. The reaction was stopped by adding hydrochloric acid (2 M). The reaction mixture was extracted using MTBE. The crude product was analyzed *via* ^{1}H-NMR-spectroscopy. Figure 101 shows the reaction of linolenic acid (**2**) to 12-OPDA (**1**), catalyzed by the enzymes 13-LOX, AtAOS and AtAOC2. The ^{1}H-NMR spectrum shows characteristic signals for 12-OPDA (**1**). At 7.74 ppm and 6.18 ppm two double doublets caused by the protons (C10)*H* and (C11)*H* from 12-OPDA (**1**) are represented in the spectrum. These two signals are characteristic and do not appear in any intermediate- or side-product-spectrum. However, the main side-product is represented in the ^{1}H NMR spectrum, which forms a characteristic triplet at 4.30 ppm and a multiplet at 3.24 ppm. Both signals are caused by the decomposition of 12,13-EOT (**4**) to the α-ketol **27**. The proton (C13)*H* of α-ketol **27** splits into a triplet at 4.30 ppm. The two protons at the (C11)*H* position of the α-ketol **27** forms a multiplet at 3.24 ppm. Many of the signals caused by other protons from 12-OPDA (**1**) and α-ketol **27**, overlap. Since the main side-product and 12-OPDA (**1**) show distinguishable signals in the ^{1}H NMR spectrum, the ratio can be calculated, by comparing the proton (C11)*H* of α-ketol **27** at 4.30 ppm, with the protons (C10)*H* and (C11)*H* at 7.74 ppm or 6.18 ppm from 12-OPDA (**1**). For this reaction, a ratio of 40:60 12-OPDA (**1**) to α-ketol **27** could be obtained (Figure 49).

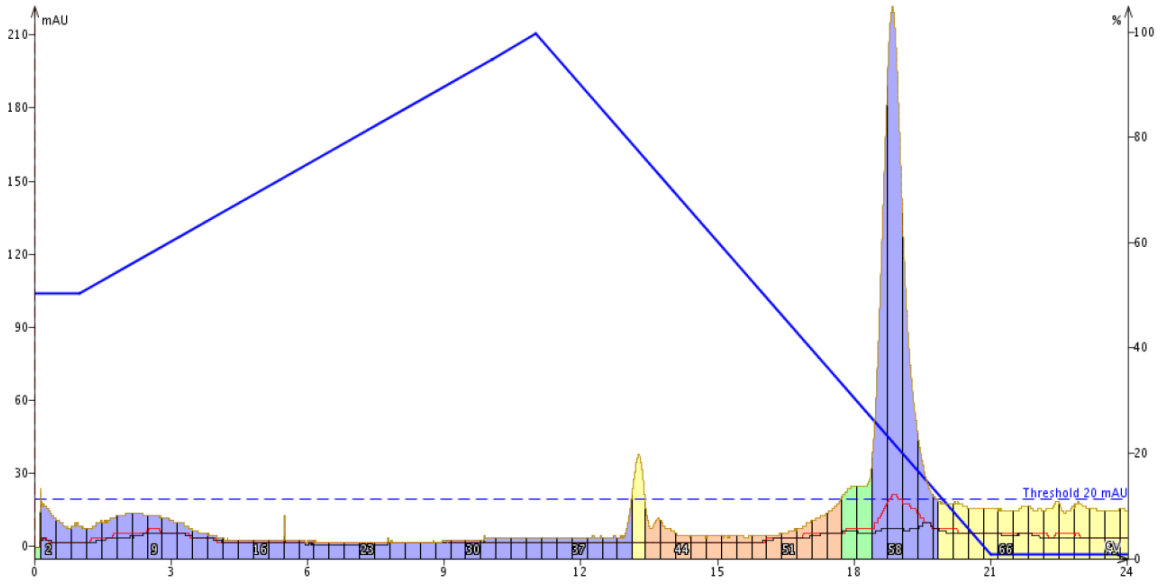

Figure 50: Chromatogramm of a 12-OPDA (**1**) and α-ketol **27** mixture, purified by Isolera One from Biotage.

By raising the amount from 400 mg to 1000 mg of whole cell catalyst, the ratio could be decreased to 95:5. These results shows that the cascade is applicable for the synthesis of 12-OPDA (**1**). Furthermore, a purification method was established, therefore a C18-column for the automated purification system Isolera One from *Biotage*® was used with acetonitrile and water with 1% acetic acid (*v*/*v*) as the mobile phase. The chromatogram shows two peaks (green and blue) with an increase in acetonitrile content of about 60%. The green peak represents the α-ketol **27** and the blue peak is 12-OPDA (**1**) (Scheme 50).

7.6.3 Synthesis of 12-OPDA (1) with a self created biocatalyst

In order to produce an own whole cell catalyst, parameters like vectors, chloroplast-target sequence and codon-optimization for *E.coli* were evaluated. It could be shown that the genes encoding for the AtAOS and AtAOC2 should be used with no codon-optimization for *E. coli*. The codon-optimization for *E. coli* leads to an improved overexpression, but no activity can be detected, this is probably caused by misfolding of the protein. Furthermore, both enzymes are only active if the chloroplast target sequence is deleted.

As a consequence, the AtAOC2 and AtAOS wild-type genes without chloroplast target sequence were acquired recombinantly (pET28a(+)-AtAOS and pET21a(+)-AOC2). The AtAOC2 was additionally recloned in pUC18 (WCC 2) and pQE30 (WCC 3). As it could be shown that the product is stable over a relatively long time, the reaction temperature was increased to room temperature, which is appropriate to the high activities of AOS and LOX obtained at temperatures above 4 °C. In addition, the WCC quantity was again reduced to 300 mg, to have a better catalyst/starting material ratio. The constructs were transformed into *E. coli* BL21(DE3) and *E. coli* BL21(DE3)CodonPlus-RIL and expressed. In a subsequent biotransformation, a one-pot synthesis was performed (Scheme 51, 52). First, a reaction with separate cells containing AtAOS and AtAOC2 (pET28a-AtAOS and pET21a-AtAOC2) (Scheme 51) and commercially available 13-LOX from *glycine max* was carried out.

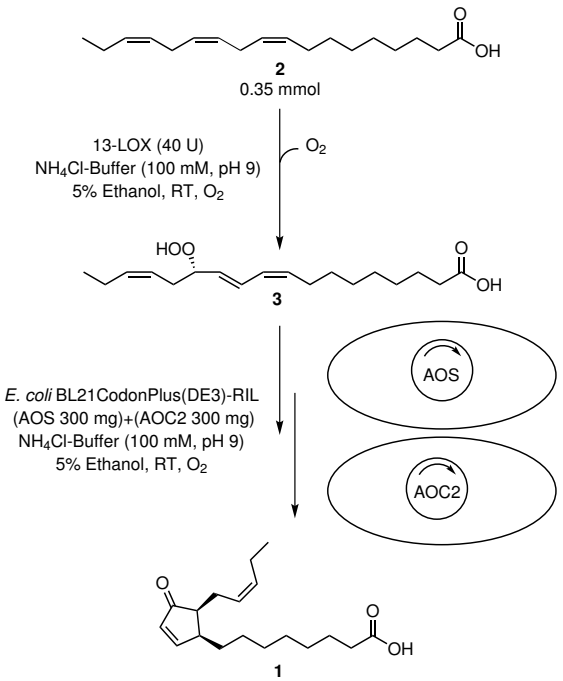

Scheme 51: Synthesis of 12-OPDA (**1**), starting from α-linolenic acid (**2**), 13-LOX and AtAOS and AOC2 in separate whole cells.

Thus, the reaction was performed at room temperature with oxygen saturation. These reaction conditions were used because of the promising results for the synthesis of 13-HPOT (**3**). An ammonium chloride buffer was chosen, with a pH of 9, according to the results of the activity assay. Furthermore, a small amount of ethanol (5%, *v/v*) was used to enhance the solubility of α-linolenic acid (**2**).

The conversion was complete with 69% product **1** and 31% of side-product **27**. In the following whole-cell catalyst, consisting of AtAOS and AtAOC2 were used (WCC 2 and WCC 3, Scheme 52).

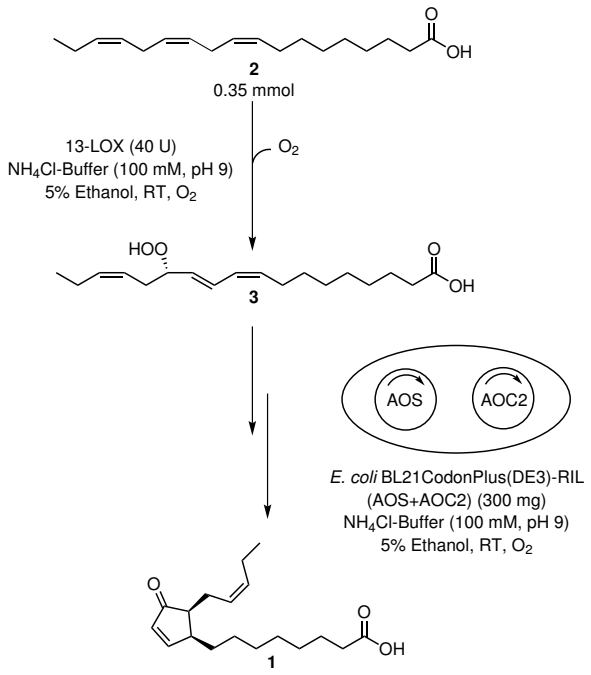

Scheme 52: Synthesis of 12-OPDA (**1**), starting with linolenic acid, 13-LOX and AtAOS and AtAOC in one whole cells.

The reactions were performed according to the set-up for the synthesis of 12-OPDA (**1**) with seperate cells. With AtAOC2 in pUC18 (WCC2) 69% product **1** and 31% side product **27** were isolated. With AtAOC2 in pQE30 (WCC 3) side-product **27** formation can be reduced to 10%.

The product **1** from the WCC 3 reaction was isolated according to GOP 25 with a yield of 28%. Additionally, a reaction without AtAOC2 was performed, leading to 23% product *rac*-**1** (proven by optical rotation (αD20: 0° (c 10, $CHCl_3$)) and 77% side-product **27**. However, this experiment shows that the AtAOC2 is active in this reaction set-up and necessary to produce enantiomerically pure 12-OPDA (**1**).

In summary, it can be concluded that there is an engraving advantage to use both plasmids of AtAOS and AtAOC2 in one cell. With this WCC in hand, a simple access to large quantities of 12-OPDA (**1**) could be created. Compared to the literature,[212,213,215] it is now possible to isolate 12-OPDA (**1**) in high purity and high yields.

It was also possible to perform an experiment at elevated lab scale with 2 $g \cdot L^{-1}$ 12-OPDA (**1**), starting from 1.64 mmol. A high selectivity of 91% was obtained, a yield of 31% and a ratio of 95:5 *cis*:*trans* was isolated. Nevertheless, only a small amount of the desired product **1** was isolated. Therefore, an extraction optimization was performed, shown in Figure 51.

For extraction optimization three approaches were examined. First, the reaction towards 12-OPDA (**1**) was performed, afterward, the reaction mixture was divided into three parts. For the first concept, the reaction mixture was centrifuged and the supernatant extracted using dichloromethane. The crude product was purified *via* column chromatography, according to GOP 25. As a result, 31% 12-OPDA (**1**) could be isolated. The second approach starts with extraction as well; the supernantant was extracted and the pellet was treated with dichloromethane and ultrasound.

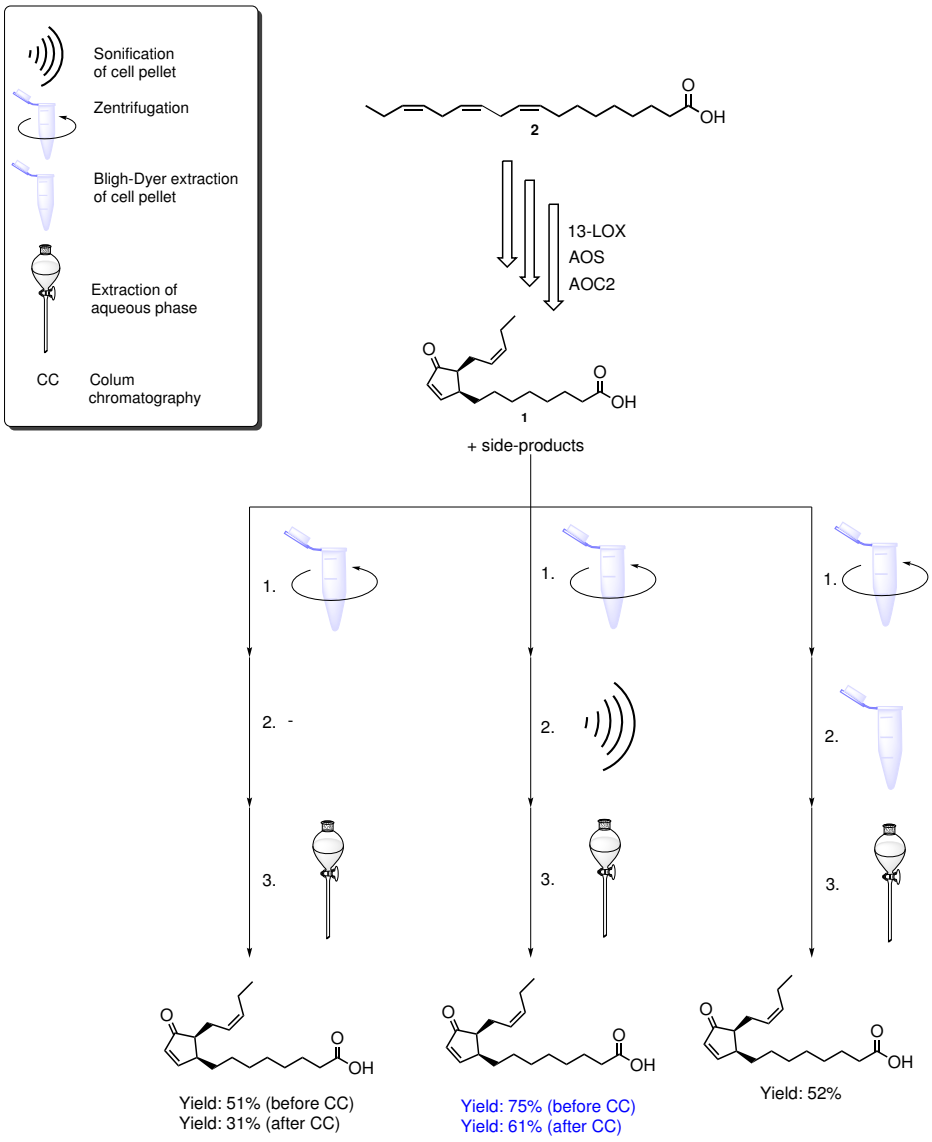

Figure 51: Synthesis of 12-OPDA (**1**), starting with linolenic acid (**2**), 13-LOX and AtAOS and AtAOC2 in one whole cells.

After column chromatography, according to GOP 25, 61% 12-OPDA (**1**) could be isolated. The enantiomeric excess is quite high because of a high optical rotation (α_D^{20}: +104° (c 10, $CHCl_3$)), which is in the same area compared to literature.[213] The third concept was a Bligh and Dyer extraction method,[253] where the pellet was dissolved in a mixture of MeOH, $CHCl_3$, H_2O, (2:1:1, *v/v*). After centrifugation (5000x g, 5 min) the chloroform phase was isolated and the solvent was removed *in vacuo*.

Since only 52% conversion was detected, no column chromatography was performed. In summary, it can be concluded that method two (ultrasound) is the most promising method and thus the yields could be increased from 31% to 61%, which means *de facto* a doubling of the yield (Figure 51). In addition, a *cis*:*trans* ratio of ≥90:≤10 for all reactions was determined.

7.6.4 Segmented flow synthesis of 12-OPDA (1)

In flow chemistry, a chemical reaction is carried out in a continuously flowing stream. The use of a continuous synthesis system has many advantages, including increased mass and temperature transfer, high reproducibility, automation, high safety, simple scalability, etc. Flow chemistry is also becoming more and more interesting for the field of biocatalysis. A lot of examples are already known in the literature.[254,255] Applications are for example the synthesis of amines *via* an immobilized transaminase from *Halomonas elongata*[256] or the production of phenylserine by using a threonine aldolase, which was immobilized covalently on Eupergit acrylic microparticles.[257] Also non-immobilized enzymes like alcohol dehydrogenase, which catalyzes hexanol oxidation, can be used.[258] In enzymatic reactions with low substrate solubility, as well as mass transfer limitations, two-phase reaction solutions shows a great advantage, as both high loads can be guaranteed and enzyme deactivation can be avoided.[259] For deactivation problems of the enzymes, segmented flow systems can be adopted.

In segmented flow the aqueous and organic phases are compartmentalized within small droplets that do not mix (Figure 52).[259]

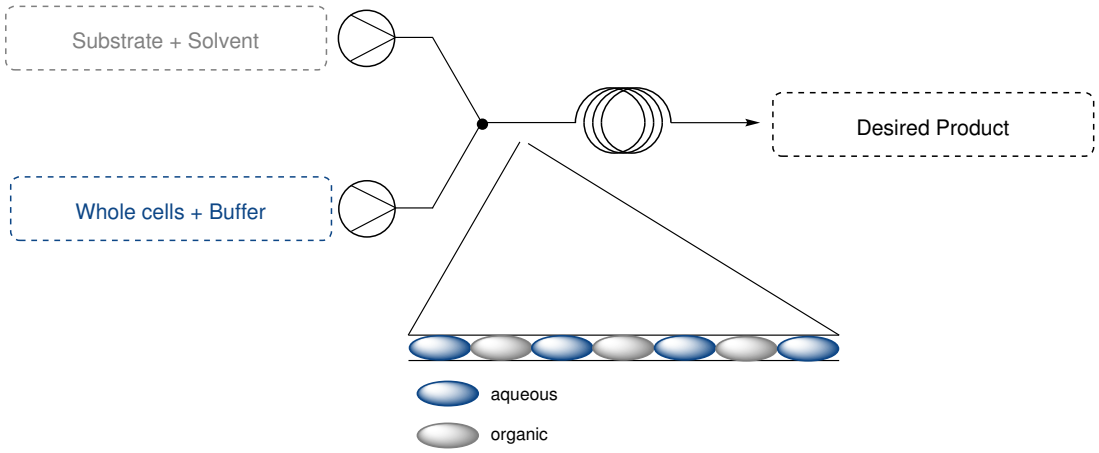

Figure 52: Schematic segmented flow set-up for a reaction of whole cells in buffer and substrate in solvent.

There are also some examples where segmented flow is used in combination with enzymes, like the 1-heptaldehyde to 1-heptanol conversion in a segmented flow capillary microreactor[31] or the conversion of acetophenone (**7a**) and triflouoracetophenone with alcohol dehydrogenases to the corresponding alcohol.[260] This reaction technology will be applied to the 12-OPDA (**1**) project. This project was investigated in cooperation with Adebar and Nastke from Industrial Organic Chemistry and Biotechnology, Bielefeld University. This application is based on the preliminary work of Adebar.[260] First, 13-HPOT (**3**) will be produced in batch, which is needed for this reaction. The reaction will be conducted in segmented flow with the whole cells containing the AtAOS and AtAOC2 in buffer with a second phase consisting of organic solvent and substrate. First, as already mentioned, the 13-HPOT (**3**) was synthesized.

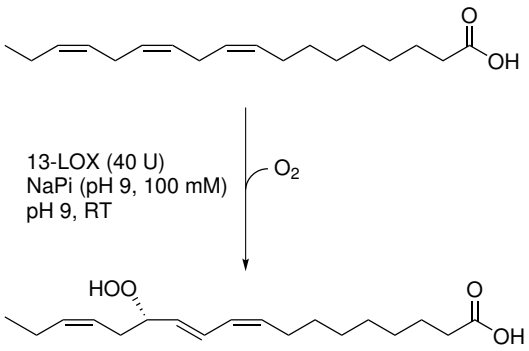

Scheme 53: Synthesis of 13-HPOT (**3**), starting with linolenic acid (**2**) and 13-LOX.

13-HPOT (**3**) could be obtained with a yield of 83% (Scheme 53). After having the starting material in hand a solvent screening for the organic phase was performed. Here two parameters were examined, on the one hand, the optimal buffer for the reaction, on the other hand, the best solvent system. These reactions were carried out in a batch reaction, in a 2 mL volume with 30 mg_{wcm} $L_{aq}{}^{-1}$ whole cells (wcm indicates wet cell mass per aqueous phase). Figure 53 shows the conversion to product **1** in investigated buffers and cosolvents in batch. The best performing buffers were sodium phosphate buffer pH 8, as well as ammonium chloride buffer pH 9. Isooctane turned out to be the most suitable solvent. Also, cyclohexane with the addition of 10% MTBE, as well as the addition of Tween 20 (1%, m/V) yielded good results.

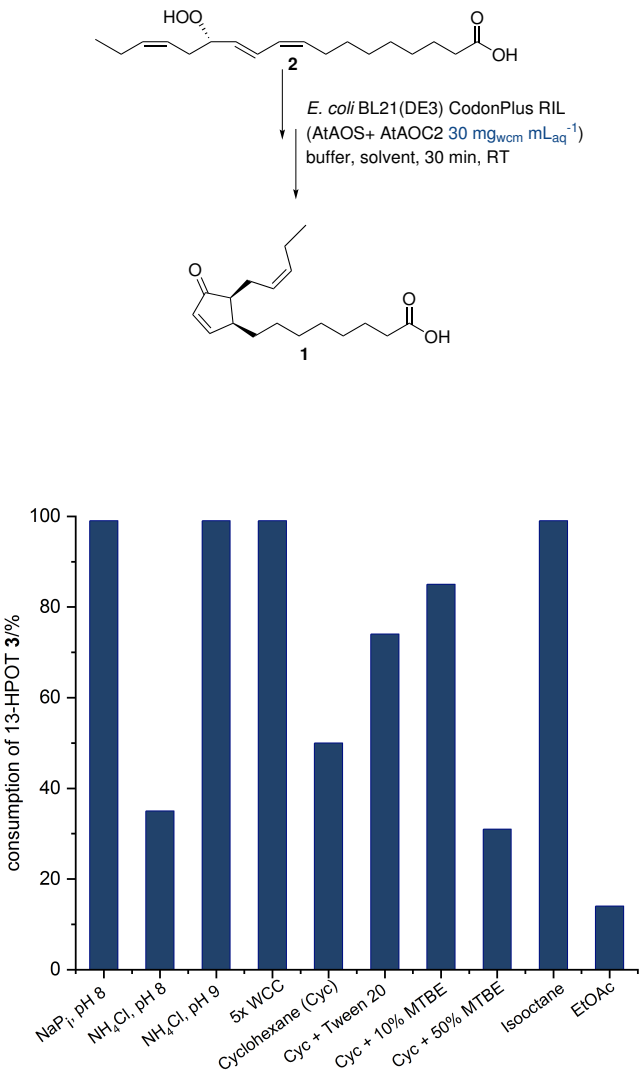

Figure 53: Synthesis of 12-OPDA (**1**) starting from 13-HPOT (**3**) (with 30 mg_{wcm} mL_{aq}^{-1} whole cells)- Cyc: Cyclohexane, Tween 20 (1%, *m/V*), 5x WCC in NaPi, pH 8.

In the next step, the amount of whole cell catalyst was reduced from 30 mg_{wcm} mL_{aq}^{-1} (wcm indicates wet cell mass) to 10 or 20 mg_{wcm} mL_{aq}^{-1}.

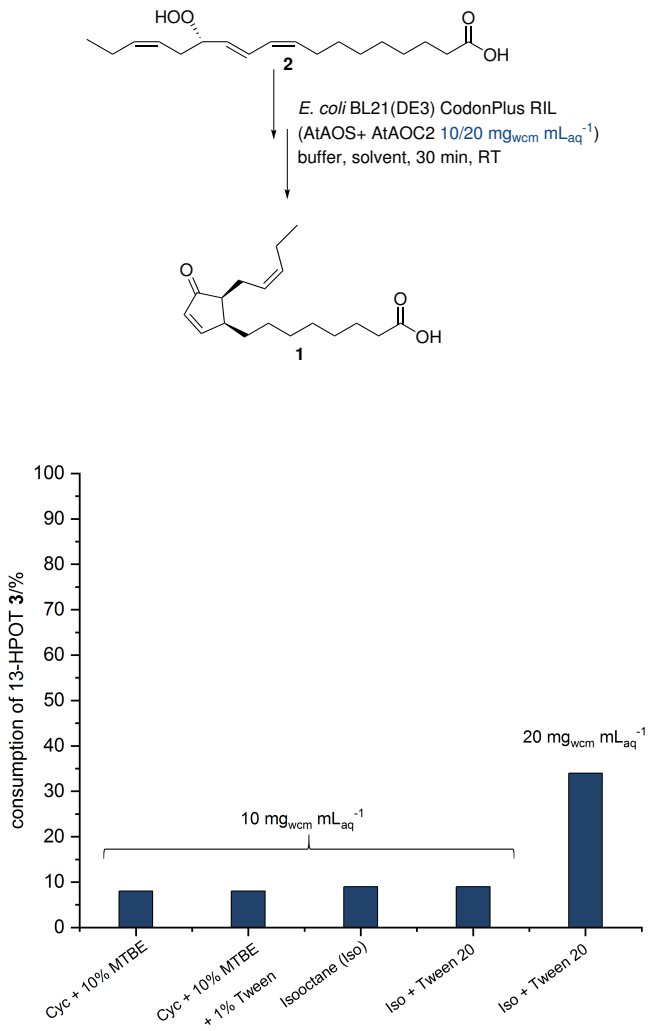

Figure 54: Synthesis of 12-OPDA (**1**) starting from 13-HPOT (**3**) (with 20 or 10 mg$_{wcm}$ mL$_{aq}$ $^{-1}$ whole cells). Cyc: Cyclohexane, Iso: Isooctane, Tween 20 (1%, m/V).

The reduction of whole cells shows a significant decrease in conversion. Addition of Tween 20 (1%, m/V) leads to no significant change in conversion in combination with isooctane as cosolvent. The best conversion for the batch reaction was 20 mg$_{wcm}$ mL$_{aq}$ $^{-1}$ whole cells with Tween 20 (1%, v/v) and isooctane with a conversion of 34% (Figure 54). For the application of 12-OPDA (**1**) synthesis in flow, the same reaction conditions were used. Additionally, the storage of the harvested cells was investigated. The cells were stored at 4 °C, and -20 °C, afterward, a reaction was performed.

For the whole cells, stored at 4 °C, an activity could be observed, at -20 °C there was no activity left. This probably indicates that the freezing process leads to the destruction of the cell membrane, and thus the organic solvent has direct contact with the enzyme, this probably leads to denaturation. The storage of the cells at 4 °C, on the other hand, could leave the cell membrane intact, so that the substrate can diffuse into the cell, but the enzyme remains stable again the organic solvent. Therefore, the cells were stored at 4 °C for further experiments. According to the optimized batch conditions, the flow reaction was performed. 13-HPOT (**3**) was dissolved in isooctane and the catalytic system (AtAOS and AtAOC2 in *E. coli* BL21CodonPlus(DE3)-RIL 20 mg_{wcm} mL_{aq} $^{-1}$) was dispensed in buffer with addition of Tween 20 (1%, m/V). These two immiscible solutions were transferred into syringes. The two streams were combined in a Y-shape mixer. After starting the reaction in a continuous stream, uniform segments were formed. These segments were led into a PFE coil reactor, where the biotransformation is performed.

Afterward, fractions (1 mL) were collected and directly quenched with hydrochloric acid (2 mM).

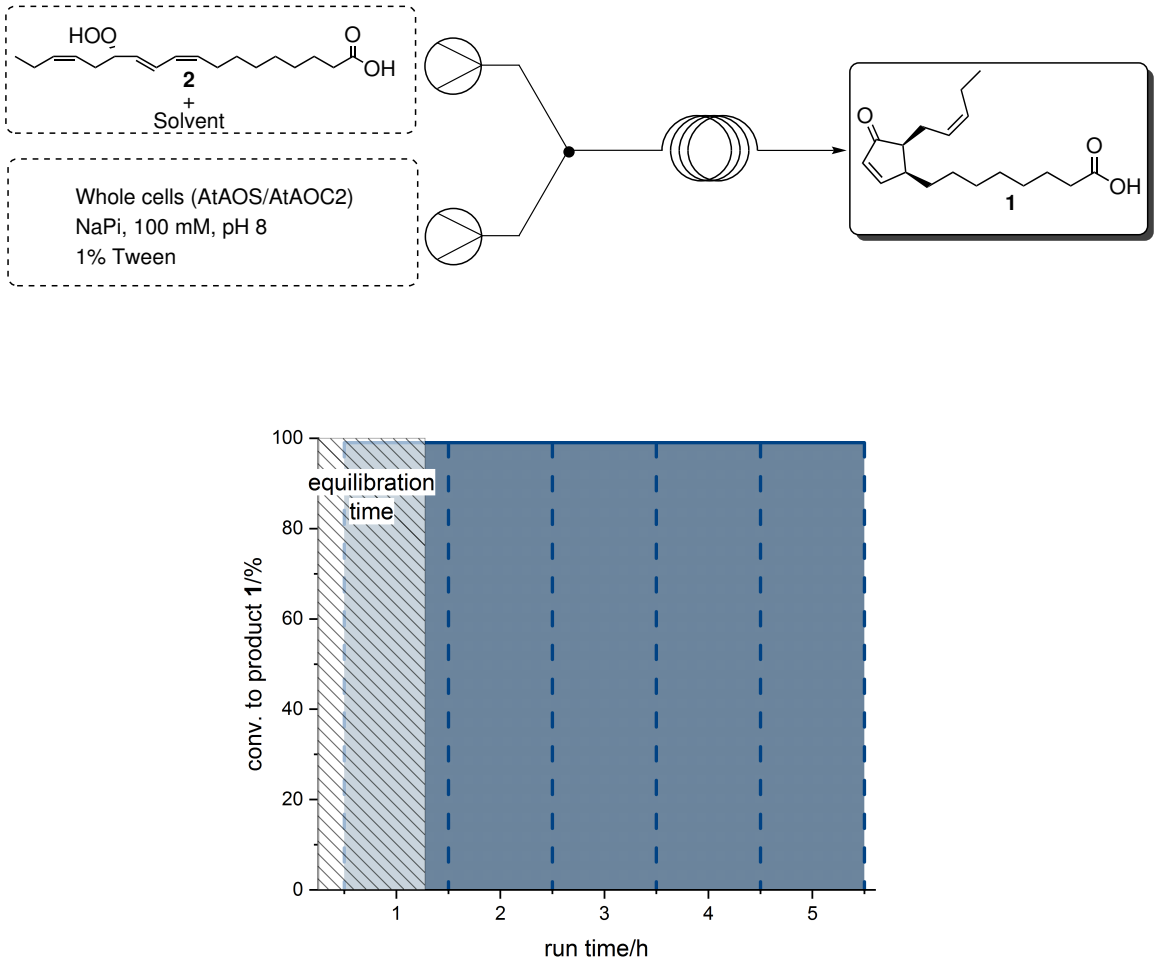

Figure 55: Synthesis of 12-OPDA (**1**) in segmented flow with 20 mg_{wcm} $mL_{aq}{}^{-1}$ whole cells in sodium phosphate buffer (pH 8, 100 mM), Tween 20 (1%, *m/V*) and isooctane with 13-HPOT (**3**). Horizontal lines show conversion for fractions collected between times indicated with dashed vertical lines. Reactor volume: 1 mL (PFE, ID: 0.5 mm), residence time: 1 h Y-mixer (ID: 1.01 mm).

For the flow experiment, a stable conversion with >99% for each fraction was detected (Figure 55). Compared to the batch experiment (34%), the conversion could be almost tripled, which again underlines the advantages of flow chemistry. The increased conversion in the flow experiment results either from the improved mass transfer[259] or from the enhanced stability of the enzyme in the segmented flow experiment.[260]

Another outstanding feature of segmented flow is the improved phase separation[260] leading to a simplified downstream process and thus higher yield. In this context, reactions with the same volumes for batch and flow were carried out. For this purpose, the organic phases of the individual fractions of the flow process were combined. The reaction mixture of the batch process had to be centrifuged because otherwise there was no phase separation (Figure 56). For the batch a yield of 36% and for the flow experiment of 65% could be realized.

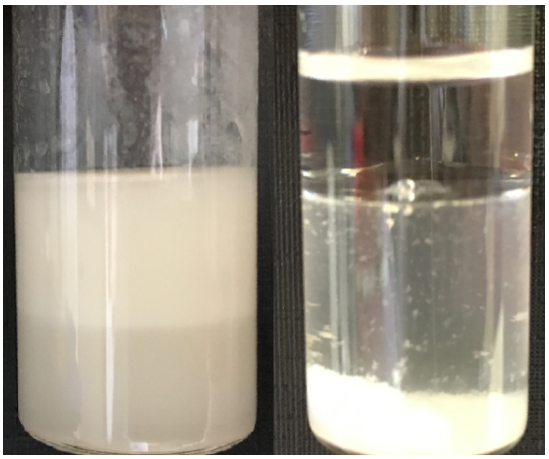

Figure 56: Synthesis of 12-OPDA (**1**) in batch (left) and flow (right).

This again shows that the segmented flow has a positive effect on the processing of a reaction with whole cells. For this reason, this setup is suitable for the synthesis of 12-OPDA (**1**). Not only the conversions could be increased, but also the isolation was optimized. Especially concerning scale-up, this setup could be advantageous because by numbering up, many reactors can be connected in series to achieve higher yields.[261]

7.6.5 Metathesis reactions with 12-OPDA (1)

12-OPDA (**1**) is a precursor of the plant hormone (-)-jasmonic acid (**26**). It is responsible for the defense against predators in plants and shows cytotoxic effects on cancer cells in humans.[203]

It is interesting to know whether and how 12-OPDA (**1**) derivatives act against plant and human cells. For this purpose, a library of derivatives of 12-OPDA (**1**) was built up by olefin-cross metathesis reactions. For the CM the HOVEYDA-GRUBBS catalyst 2nd generation was used.

This catalyst already showed the best catalytic activity towards fatty acids in the bachelor thesis of PFLUG, supervised by the author of this thesis. PFLUG investigates the olefin metathesis of unsaturated fatty acids in her bachelor thesis with different alkenes.[262] The first reaction was performed with 12-OPDA (**1**) and styrene (**30**) (3 eq.) or 4-penten-2-ol (**31**) (3 eq.) with HOVEYDA-GRUBBS catalyst 2nd generation, in toluene and room temperature from 24 to 66 h, but no conversion was detected. The reason that no conversion was detected is probably caused by deactivation of the catalyst due to the carboxylic-residue of the 12-OPDA (**1**). For this reason the acid was esterified before metathesis reaction (Scheme 54).

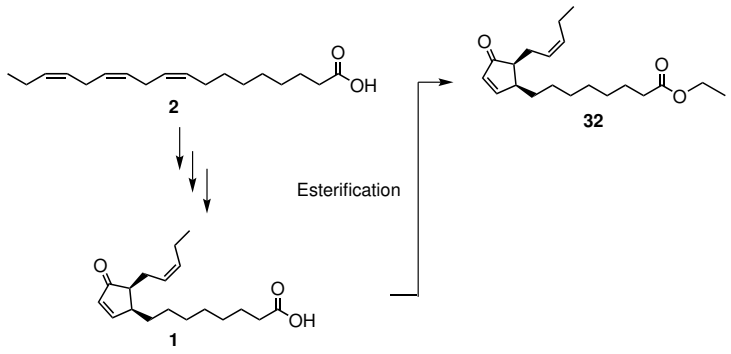

Scheme 54: Reaction cascade starting from linolenic acid (**2**) to 12-OPDA (**1**), followed by esterification.

The esterification of 12-OPDA (**1**) was carried out with methanol. *trans*-12-OPDA methyl ester is obtained as a product. The reaction was performed at different temperatures (45 °C and room temperature). The purity of the product was confirmed by ^{1}H-NMR spectroscopy. However, the product is epimerized into the biologically inactive *trans* configuration. Since this is disadvantageous for future investigations, another esterification method was initially sought.

As the epimerization is acid- and temperature-induced, chemical methods were not used. Another way of esterification is the use of enzymes, like lipases or esterases. Due to the good accessibility and handling, the lipase CAL-B from *Candida antartica* was used for the esterification with ethanol, additionally mild reaction conditions can be used here to achieve a good conversion. The mild conditions help to counteract the above mentioned epimerization. The successful synthesis of 12-OPDA-ethyl ester (**32**) was demonstrated by ^{1}H NMR spectroscopy with an excellent conversion of 99% and a yield of 92%. In the first instance, ideal reaction conditions were investigated for the metathesis reactions. All reactions were performed under inert gas and dry solvents. The analytic was performed by the means of ^{1}H NMR spectroscopy. Here, the terminal CH_3 group of the 12-OPDA (**1**) ester was used as an indicator for the conversion and put in relation to a significant signal in the product ^{1}H-NMR-spectrum. For the conversion of the bromo-derivative **34**, the (C19)*H* at 3.38 ppm and for the alkohol-derivative **39** the (C18)*H* at 5.61 ppm, was used. For the conversion of the nitril-derivative **35** the (C19)*H* was used at 3.61 ppm and for the keton-derivative **37** the (C20)*H* at 2.12 ppm.

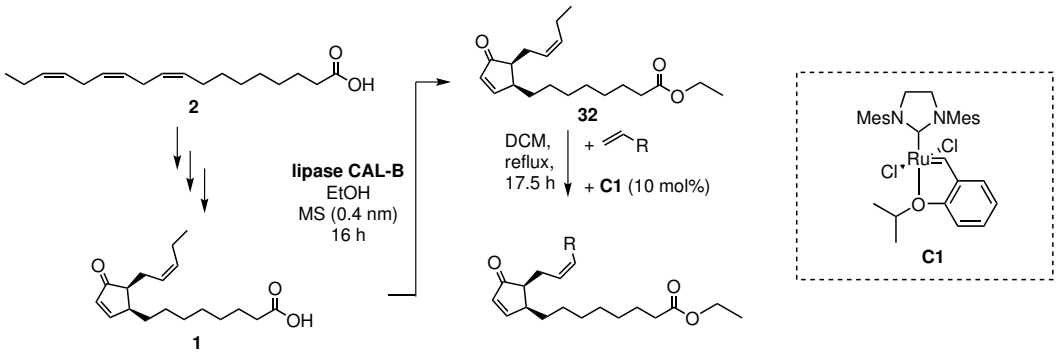

The initial reaction was performed with the 4-penten-2-ol (**31**) (3 eq.) and one equivalent of 12-OPDA-ester (**32**). To counteract the epimerization, the metathesis was first attempted at room temperature in 10 mL toluene and 1 mol% catalyst.

Table 14: Reaction cascade starting from 12-OPDA (**1**), esterification with CAL-B and metathesis reactions with different parameters.

Substrate	Eq.	Solvent	Cat./mol%	Temp/°C	Conv.%
4-Penten-2-ol (**31**)	3	Toluene (10 mL)	1	rt	10
4-Penten-2-ol (**31**)	3	Toluene (50 mL)	1	rt	1
4-Penten-2-ol (**31**)	30	-	1	rt	5
5-Bromo-1-pentene (**33**)	3	Toluene (10 mL)	1	rt	30
5-Bromo-1-pentene (**33**)	3	DCM (10 mL)	15	40	99
5-Bromo-1-pentene (**33**)	3	DCM (10 mL)	10	40	99
5-Bromo-1-pentene (**33**)	3	DCM (10 mL)	2	40	20

However, with these conditions only 10% conversion was reached after a reaction time of more than 16 h. Afterward, the amount of solvent was varied. A neat reaction with an excess of 4-penten-2-ol (**31**) was performed, as it was reported that a generally higher substrate concentration gives better results.[244] In other reports a dilution of the hydroxyalkene should give better results,[263] so a highly diluted reaction was tested with the same substrate amounts and 50 mL toluene. However, both approaches showed hardly any conversions even after 16 h reaction time. A reaction with 5-bromo-1-pentene (**33**) (3 eq.) showed a conversions of about 30% in 10 mL toluene and 1 mol% catalyst. Since the conversion of 5-bromo-1-pentene (**33**) leads to better results, the optimization was continued with this substrate. Dichloromethane was used as a solvent and heated for reflux with 15 mol% catalyst, resulting in a conversion of 99% after 16 h. Furthermore, two reactions were performed with reduced catalyst loading 2 mol% and 10 mol%. After 16 h the reaction was completed with 10 mol%, while the reaction with 2 mol% showed only about 10% conversion (Table 14). In the following, all olefin metatheses were performed with 10 mol% Hoveyda-Grubbs catalyst, in dichloromethane, for 16 h at reflux (Scheme 55).

The products were purified by preparative thin layer chromatography with cyclohexane:EtOAc (3:1, *v/v*) as solvent. The bromo derivative **34** was prepared from 12-OPDA ethyl ester **30** with 5-bromo-1-pentene (**33**) with a yield of 40%.

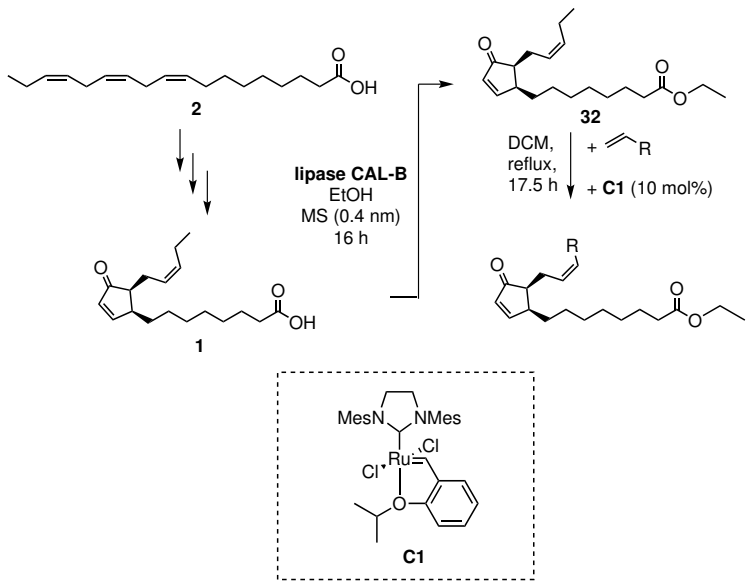

Scheme 55: Reaction cascade starts from linolenic acid (**2**) to 12-OPDA (**1**), followed by esterification with CAL-B. Metathesis reaction were performed in dichloromethane and reflux for 17.5 h.

In addition, an experiment with an increased amount (1.5 x) of starting material **1** was carried out for the reaction with 5-bromo-1-pentene (**33**). This, in turn, led to a doubling of the yield of the desired product **34**. The nitrile derivative **34** was formed with 5-hexennitrile (**36**) and a yield of 39%. The synthesis was carried out with 20 mol% $Ti(OiPr)_4$ added as an additive, since the cyano function can coordinate to the ruthenium and thus inhibit further reaction.[263] The LEWIS acid is used to complex the cyano group and thus prevent inhibition of the catalyst.

The ketone derivative **37** was prepared from 5-hexen-2-one (**38**) with a yield of 30%, the alcohol derivative as isolated with 24% yield.

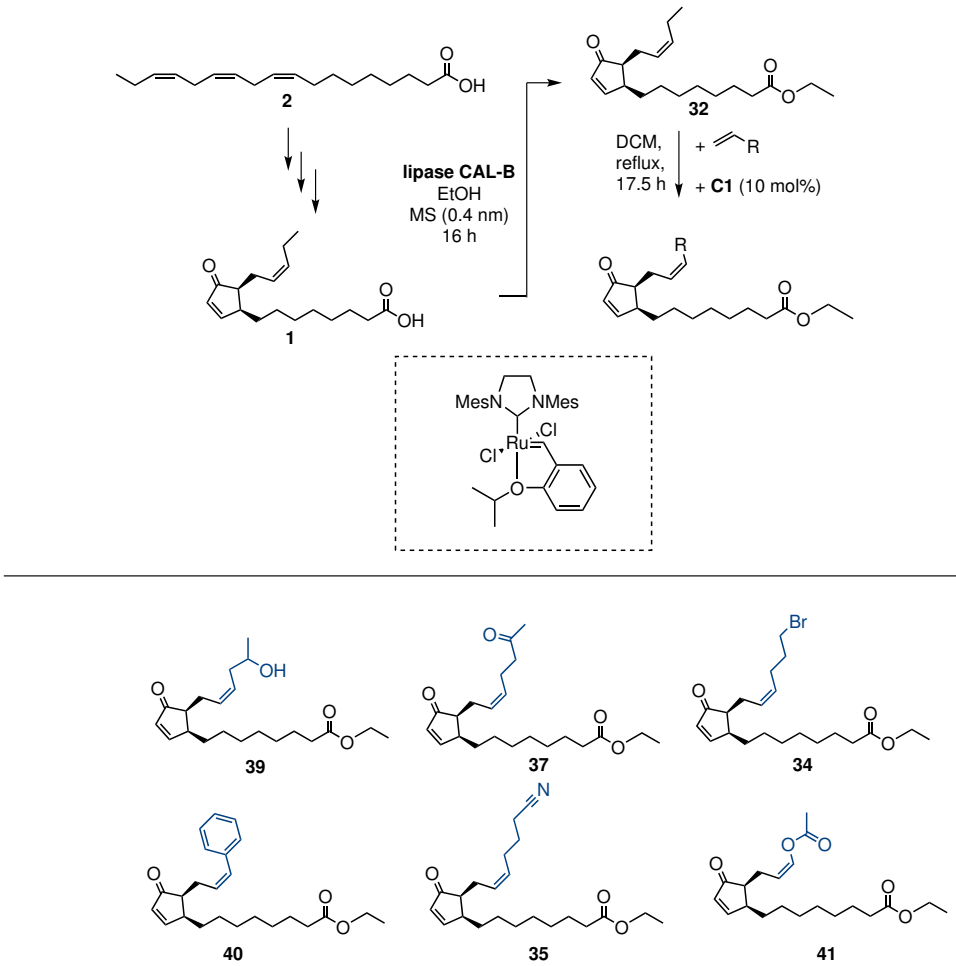

Scheme 56: Synthesis of 12- OPDA derivatives. Reaction cascade starts from linolenic acid (**2**) to 12-OPDA (**1**), followed by esterification with CAL-B. Metathesis reaction were performed in DCM and reflux for 17.5 h.

The attempt to synthesize a derivative with styrene (**30**) *via* metathesis with the above-mentioned conditions was unsuccessful. Possible reasons could be the high steric demand, due to the 12-OPDA-ester and the phenyl ring of styrene (**30**). As a result, the 12-OPDA **1** ester derivatives library has been established and is now available for further physiological functional tests (Scheme 56).

The results on the 12-OPDA (**1**) characterization were published in the journal Bioorganic and Medical Chemistry: D. Maynard, S. M. Müller, M. Hahmeier, **J. Löwe**, I. Feussner, H. Gröger, A. Viehhauser, K.–J. Dietz. One-pot synthesis of bioactive cyclopentenones from linolenic acid and docosahexaenoic acid, *Bioorganic Med. Chem.* **2018**, *26*, 1356-1364.

The results on the 12-OPDA (**1**) synthesis optimization in combination with metathesis accepted for publication in the journal Advanced Science: **J. Löwe**, K.-J. Dietz, H. Gröger, From a biosynthetic pathway toward a biocatalytic process and chemocatalytic modifications: Three-step enzymatic cascade to the plant metabolite 12-OPDA (**1**) and metathesis-derived products, *Adv. Sci.* **2020**, accepted.

7.7 Outlook for the biocatalytic access towards 12-OPDA (1)

For the cascade reaction towards 12-OPDA (**1**) the commercially available 13-LOX from *glycine max* was chosen, and the AtAOS and AtAOC2 as recombinantly produced enzymes from *Arabidopsis thaliana*. With the help of a spectrophotometric assays, it could be shown that the 13-LOX provides the optimal reaction conditions with NH_4Cl buffer, 100 mM buffer concentration, pH 9, 30 to 35 °C and 5% ethanol. For the AtAOS the best reaction conditions were NH_4Cl buffer, pH 8 and 20 °C. With the reaction catalyzed by 13-LOX towards 13-HPOT **3**, oxygen, as well as higher reaction temperatures, could be evaluated as important aspect. Afterward, a whole cell catalyst consisting of AtAOS in pQE30 and AtAOC2 in pET28a was constructed, leading to only 5-10% side product **27**. Furthermore it was also possible to do a scale-up experiment with 2 g L^{-1} 12-OPDA (**1**). Moreover, the side-product **27** can be easily separated *via* automatically reverse phase column chromatography. In this context further enzymes could be tested to make the reaction even more efficient (faster, less side-product **27**). A further shortcoming is the work-up, as only 61% of the desired product **1** can be isolated after optimization, other methods would have to be evaluated. Possibilities for the isolation are precipitation of the product **1** or work-up with ion exchangers. The flow-experiments were successful as well. It could also be shown that the conversion in flow is better compared to the batch, with isooctane and Tween 20 (1%, *v/v*). In addition, the yield could be increased by the segmented flow, which makes this a fantastic starting point for further experiments. It would be interesting to know, whether the 13-LOX can also be used in the flow experiment. In a tube-in-tube experiment the oxygen, required for the 13-LOX, could be supplied. For the metathesis reaction Hoveyda-Grubbs 2nd-generation catalyst was chosen, according to known literature synthesis. First, the 12-OPDA (**1**) was synthesized using a three-step enzyme cascade, afterward, **1** was esterified through the lipase B from *Candida antarctica* (CAL-B).

The chemical approach towards the *cis*-12-OPDA esters failed. The esterification *via* lipases has the advantage of mild reaction conditions. Afterward, alkene-cross metathesis was done with different, interesting olefins. The conversion was >80% for all olefins, expect vinyl acetate, which was not accepted at all. For 5-hexenenitrile (**36**) the addition of 20 mol% $Ti(OiPr)_4$ was necessary for successful conversion. Furthermore, no self-metathesis product of 12-OPDA ethyl ester (**32**) could be observed. Until now, four 12-OPDA (**1**) derivatives were available. In this part of research the substrate scope could be increased by testing additional olefins. Furthermore, the yields have to be optimized. It could already be shown that by increasing the starting material **1**, the yield could be doubled. Additionally, alternative isolation methods could be investigated. However, the catalyst loading is still very high, this is also a point that needs to be optimized.

8 Summary and outlook

The aim of this thesis was the establishment, processing and optimization of three independent enzymatic-catalyzed cascade reactions. The first cascade dealt with the synthesis of chiral and primary amines by using an amine dehydrogenase. The biocatalytic access to hydrated fatty acids for the synthesis of complex polyols as building blocks for polyurethane was the goal of the second cascade. The third cascade focused the synthesis of 12-OPDA (**1**), as a precursor of the hormone jasmonic acid (**26**), utilizing a three-enzyme component cascade.

The first cascade, in turn, had two areas of focus. Firstly, the synthesis of aryl-substituted chiral amines (Figure 57) was performed. Secondly, the amine dehydrogenase was used for the synthesis of primary amines. The highlight of the second part of the first cascade was the cofactor regeneration system. Here formate, produced by the alga *Chlamydomonas reinhardtii*, was converted by a formate dehydrogenase to CO_2.[109] This reaction reduces the required NAD^+ to NADH (Figure 58). The NADH is used for the reductive amination catalyzed by the amine dehydrogeanse.

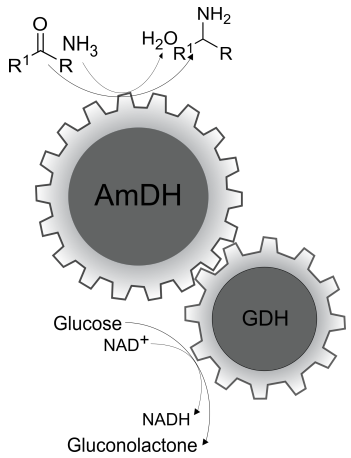

Figure 57: Amine dehydrogenase-catalyzed reductive amination with GDH and glucose as cofactor regeneration system.

The amine dehydrogenase from *Exiguobacterium sibiricum* (EsLeuDH-DM) developed by Chen *et al.* was used for the production of the chiral and primary amines, utilizing the mutations in accordance to the literature.[82] The activities towards aryl-substituted ketones were investigated. The highest activity was observed with acetophenone (**7a**), but also substituents with −M-effect, as well as diketones and bicyclic ketones were accepted as substrates. With acetophenone (**7a**) the K_M value (26.3 mM) and cosolvent tolerance (DMSO) were determined. Kinetics of 20-100 mM showed that even high substrate concentrations could be converted (50 mM). In a dosing experiment (13 ng min^{-1}) within 66 h the conversion could be increased from 21 to 50%.

The second topic was the synthesis of primary amines. Above all, the amines produced for the bulk sector must be accessible at low cost. Here enzymes, such as EsLeuDH-DM, are a desirable option. Due to the cofactor dependence of this enzyme and the high costs of stoichiometric quantities of cofactors, recycling of the cofactor is indispensable. For cofactor recycling, however, stoichiometric quantities of cosubstrate are required, which, in turn, is a major cost factor. To avoid this, algae metabolism was adopted. In the anaerobic fermentation of *Chlamydomonas reinhardtii* synthesizes formate from starch.[109] This formate can be used in combination with formate dehydrogenase for cofactor regeneration. The co-substrate is produced *in situ* and is thus more accessible at lower cost. The formate and the algae were provided by Wobbe from the working group Algae Biotechnology & Bioenergy. In this context it was possible to link amine dehydrogenase catalysis with algae biotechnology. On the one hand, the algae supernatant, in which the algae secrete the formate, as well as the formate which was produced *in situ* was used. In the range of 3 mM, hexylamine (**9**, >99%) and cyclohexylamine (**5**, >99%) could be successfully synthesized.

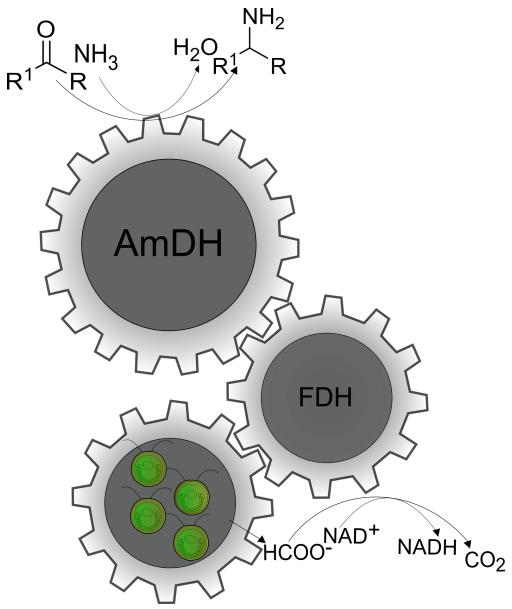

Figure 58: Amin Dehydrogenase catalyzed reductive amination with FDH and formate from the algae as cofactor regeneration system.

On the other hand, the established algae technology could be linked with new flavine monooxygenases (FMO) from *Pseudomonas sp.* The FMOs were isolated, cloned, expressed, and purified by the working group Algae Biotechnology & Bioenergy of Kruse and were thus accessible for the combination of the novel recycling system. In this context, bicyclo[3.2.0]hept-2-en-6-one (**11f**) could be successfully converted to its corresponding lactones ($\mathbf{11f}_{ABN}$) and ($\mathbf{11f}_{N}$).

When linking the amine hydrogenase and the flavin monooxygenase with the algae technology, a basis for avoiding the addition of organic cosubstrates in one-step oxidation reactions with NAD(P)H-dependent enzymes was established. This is particularly interesting in the production of bulk chemicals. In the context of amine hydrogenase, a more favorable access to primary amines could be generated. With flavin monooxygenase, for example, the production of ϵ-caprolactone in combination with the novel cofactor excitation system would be of great interest.

The second cascade involved the synthesis of hydroxylated fatty acids as building blocks for polyols (Figure 59). These polyols are, in turn, substrates for the synthesis polyurethanes, which are used by the cooperation partner WINDMÖLLER to produce flooring and impact sound mats.

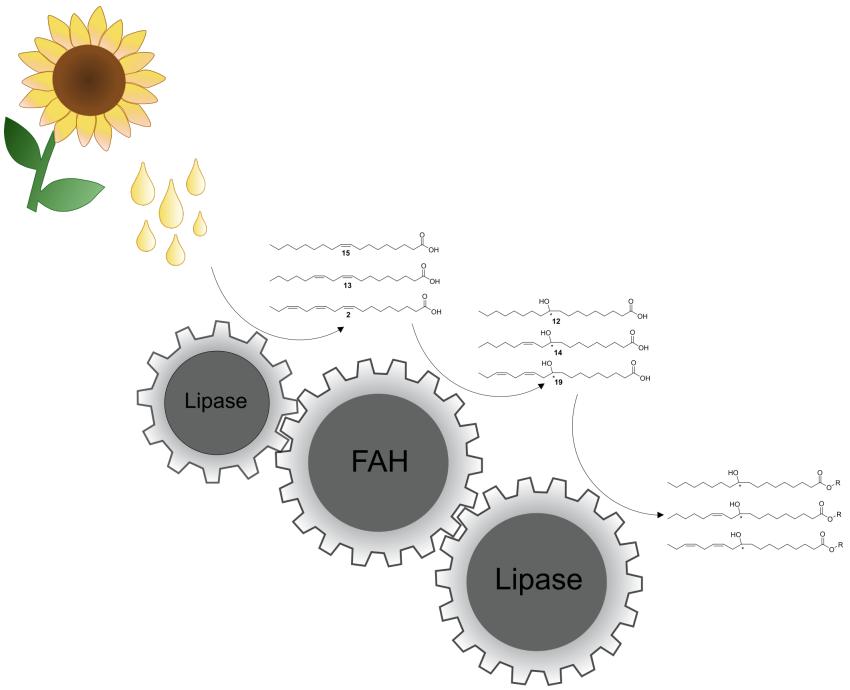

Figure 59: Production of polyols from oils, with the help of lipases and fatty acid hydratases.

For the project three oleate hydratases (Ohy) and two linoleate hydratases (Lhy) were selected, due to their substrate width and their applicability for the synthesis of large quantities: Cla-HY (Lp-Lhy from *Lactobacillus plantarum*), La-Ohy (from *Lactobacillus acidophilus*), Em-Ohy (from *Elizabethkingia meningoseptica*), La-Lhy (from *Lactobacillus acidophilus*) and Sn-Ohy (from *Stenotrophomonas nitritireducens*). Initially, analytical experiments were performed with these fatty acid hydratases (FAH).

For the Ohy oleic acid (**15**) and for the Lhy **13** was used with 10 mM substrate concentration. Yields between 79 and >99% could be determined after 22.5 h reaction time, which confirmed the activity of the hydratases. The following experiments focused on the oleic acid hydratases for the synthesis of 10-hydroxystearic acids (**12**).

Therefore, Sn-Ohy was selected, because it showed the most promising results in the preliminary experiments. Under optimal reaction conditions (Sn-Ohy crude extract, citrate buffer pH 6.3, 50 mM, 35 °C, 5% DMSO, *v/v*) within 48 h, a product-related conversion was obtained with an isolated yield of 72% and a purity of 97%. Furthermore, the Sn-Ohy has been successfully immobilized for a practical, cost-effective industrial application. After initial establishment of the immobilization of Sn-Ohy on the hydrophobic carrier *Lewatit*® VP OC 1600 by Pietrowski, these results were taken up and refined. The best results were obtained with a loading of 1:9 enzyme:carrier, an immobilization shaking rate of 80-180 rpm and time of 18 h. With the successfully immobilized FAH, scale-up experiments (400 g L^{-1}) with a yield of 59% could be performed.

To complete the cascade, the hydrated fatty acids were successfully esterified with different polyols in analytical approaches. This was catalyzed by lipase B from *Candida antarctica*. In a preparative approach the 10-hydroxystearic acid (**12**) was successfully esterified with 1,6-hexanediol (**20**) to the polyol (**21**, 7.8 g, 20%). Additionally, it was possible to produce hydrated fatty acids from sunflower oil in 50 g L^{-1}. For this purpose, the lipase from *Candida rugosa* was used.

In summary, the intention to make hydrated fatty acids accessible on a large scale was successfully completed. Compared with the to date established systems of other workgroups in the field of the synthesis of 10-hydroxystearic acid (**12**), in this work, higher yields could be achieved, as well as the possibility of isolating 10-hydroxystearic acid (**12**) in high purity. Furthermore, a separable and active biocatalyst for the synthesis of 10-hydroxystearic acid (**12**) could be developed, which is now accessible for future processes. Furthermore, it was possible to synthesize linked polyols in a two-step process starting from oleic acid (**15**). Thus, the basis for tailor-made polyols could be generated starting from 10-hydroxystearic acid (**12**) with different alcohol linkers.

In the last cascade 12-OPDA (**1**) was produced. 12-OPDA (**1**) is the first biological active intermediate in the plant synthesis of jasmonate (**26**) and therefore of great importance in agricultural science. Due to its similarity to the prostaglandins occurring in humans it is also of highest pharmacological relevance.[203] The major tasks were the optimization of the synthesis, because of difficulties in production,[212–215] as well as the isolation of the acid **1**. Furthermore, novel derivatives of 12-OPDA (**1**) using olefin cross-metathesis, were synthesized. For the synthesis of 12-OPDA (**1**) the commercial lipoxygenase from soybean was coupled with the recombinant allene oxide synthase (AOS) and cyclase (AOC2) from *Arabidopsis thaliana* (At) (Figure 60).

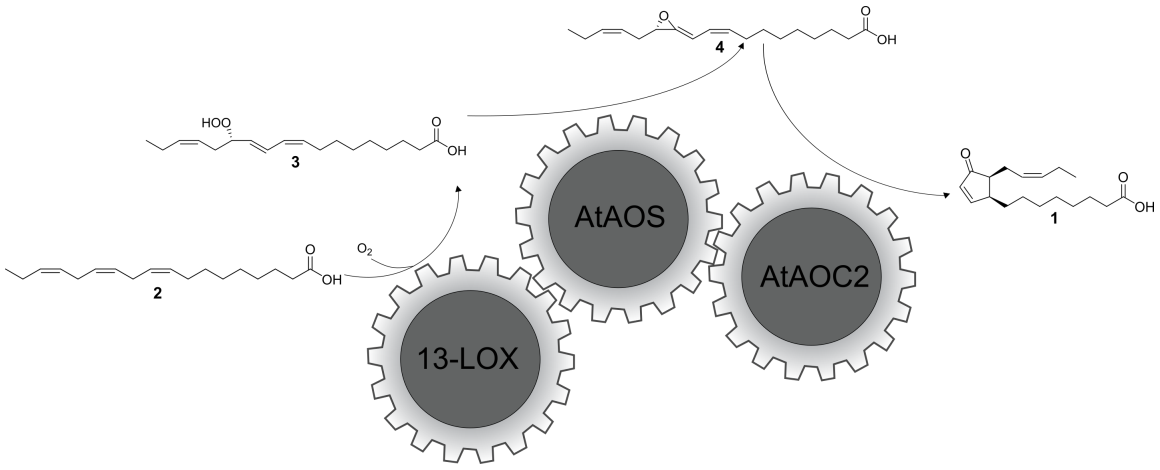

Figure 60: Synthesis of 12-OPDA (**1**), starting from linolenic acid (**2**) *via* lipoxygenase (13-LOX) from *Glycine max*, allene oxide synthase (AOS) and allen oxid cyclase (AOC2) from *Arabidopsis thaliana* (At).

In initial activity tests and biotransformations optimal conditions for the lipoxygenase could be found with NH_4Cl buffer, pH 9 and 100 mM, 25-30 °C, ethanol (5%) as cosolvent and the constant oxygen saturation of the system. For the two enzymes from *Arabidopsis thaliana* a whole cell system was chosen. For this purpose both enzymes were co-expressed in *E.coli*. In this context, the combination with BL21-CodonPlus(DE3)-RIL (pET28a-AtAOS and pQE30-AtAOC2), 13-LOX as a commercially available enzyme and a substrate concentration of 1 g L^{-1} in NH_4Cl- buffer, pH 9 and 100 mM, 25-30 °C, ethanol (5%, *v/v*) shows the best results.

12-OPDA (**1**) could be produced in a 12-OPDA (**1**) and α-ketol (**27**, side-product) 90:10 ratio and in a 91:9 *cis*:*trans* ratio with a conversion of 28%. Another focus was the isolation of 12-OPDA (**1**). Due to its hydrophobic properties, separation from the cell material was a major difficulty. Therefore, two approaches were focused to overcome this problem: the optimization of the extraction or the application in segmented flow. The extraction could be improved from 31% to 61% by additional ultrasonic treatment of the cell pellet in the batch setup in dichloromethane. Furthermore, it was possible to synthesize the 12-OPDA (**1**) in segmented flow successfully. For this purpose 13-hydroperoxy-9,11,15-octadecatrienoic acid (**3**, 13-HPOT) was synthesized from linolenic acid (**2**) and dissolved in isooctane. In addition, the AtAOS and AtAOC2 were dissolved in buffer (NaPi, pH 8, 100 mM, Tween 1%, *v/v*) (optimal parameters in previous studies for segmented flow). In segmented flow, 99% conversion was achieved in comparison to 34% in the batch process. Furthermore, in a scale-up experiment (7x amount of starting material **3**) the yield could be increased from 36% in batch to 61% in segmented flow. Finally, 12-OPDA (**1**) derivatives were synthesized using olefin cross-metathesis 12-OPDA. Therefore, the 12-OPDA (**1**) has to be esterified because the acid deactivates the catalyst. The 12-OPDA ester (**32**) was successfully esterified with the lipase CAL-B with a yield of 92%. The chemical esterification however, led to complete epimerization to the physiologically inactive *trans*-12-OPDA (**1**). For olefin cross-metathesis, dichloromethane, reflux and the 2nd generation Hoveyda-Grubbs catalyst (10%) were determined as optimal reaction conditions. With these conditions, a large number of 12-OPDA (**1**) derivatives with high conversions and moderate yields could be produced (Figure 61).

In the project of 12-OPDA (**1**) production, a major part of the defined goals could be achieved. It is now possible, with the established cascade, to isolate 12-OPDA (**1**) in large quantities and with high purity.

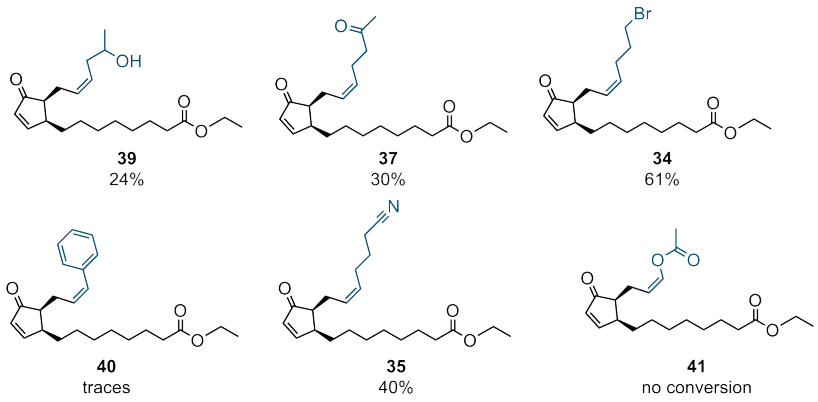

Figure 61: Products of olefin metathesis with 12-OPDA ethyl ester **32**.

Particularly in comparison with the so far accessible quantity of 12-OPDA (**1**) this is an outstanding development. Besides, both the extraction optimization and the segmented flow process have made it possible to improve the isolation of 12-OPDA (**1**), which, as a lipid-like molecule, is difficult to separate from aqueous reaction media. An additional intention of this work was the preparation of a 12-OPDA library using alkene cross-metathesis. This purpose could successfully be achieved with the methodology presented in this work. Thus, a foundation for the synthesis of further 12-OPDA derivatives could be created. The production of alternative 12-OPDA derivatives is particularly interesting concerning further investigations of the physiological structure-activity relationship in plants.

9 Zusammenfassung und Ausblick

Ziel dieser Arbeit war die Etablierung, Bearbeitung und Optimierung dreier voneinander unabhängiger enzymatisch katalysierter Kaskadenreaktionen. Die erste Kaskade thematisierte die Synthese von chiralen und primären Aminen mit Hilfe von Amindehydrogenasen. Der biokatalytischer Zugang zu hydratisierten Fettsäuren zur Synthese komplexer Polyole als Bausteine für Polyurethan war das Ziel der zweiten Kaskade. Die dritte Kaskade hatte die Synthese von 12-OPDA (**1**), einer Vorstufe des Pflanzenhormons Jasmonsäure **26**, mit Hilfe einer Drei-Enzym-Komponenten Kaskade als Fokus.

Die erste Kaskade wiederum hatte zwei Schwerpunkte. Einerseits sollten arylsubstituierte Ketone zu chiralen Aminen umgesetzt werden (Figure 62). Darüber hinaus wurde die Amindehydrogenase zur Synthese primärer Amine genutzt. Die Besonderheit dieser Kaskade bestand im Cofaktorregenerierungssystem. Hier wurde das sekretierte Formiat, produziert von der Alge *Chlamydomonas reinhardtii*, von einer Formiat Dehydrogenase zu CO_2 umgesetzt.[109] Diese Reaktion hat das für die Amindehydrogenase benötigte NAD^+ zu NADH reduziert (Figure 63). Das NADH wird für die reduktive Aminierung, katalysiert durch die Amindehydrogeanse, verwendet.

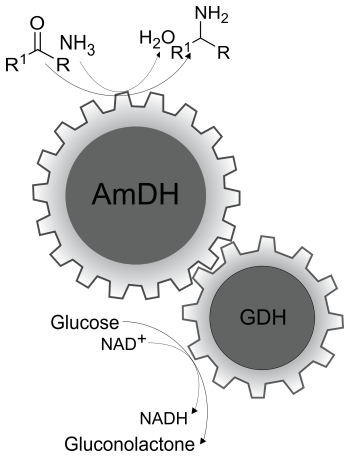

Figure 62: Amindehydrogenase-katalysierte reduktive Aminierung mit GDH und Glucose als Cofaktorregenerierungssystem.

Die Amindehydrogenase aus *Exiguobacterium sibiricum* (EsLeuDH-DM) von Chen *et al.* wurde für die Produktion der chiralen und primären Amine verwendet, wobei die Mutationen gemäß der Literatur eingeführt wurden.[82] Zunächst wurden die Aktivitäten hinsichtlich aryl-substituierter Ketone untersucht. Bezüglich Acetophenon (**7a**) hatte das Enzym die höchste Aktivität, doch auch Aromaten mit -M-Substituenten, als auch Diketone und bicyclische Ketone wurden von der Amindehydrogenase EsLeuDH-DM als Substrate akzeptiert. Mit Acetophenon (**7a**) wurden anschließend der K_M-Wert (26.3 mM) und Cosolvenztoleranz (DMSO) ermittelt. Kinetiken bei 20-100 mM zeigten, dass auch hohe Substratkonzentrationen umgesetzt werden konnten (50 mM). Mit einem Dosierexperiment, bei dem das Substrat innerhalb von 66 h in 13 ng min^{-1} zudosiert wurde, konnte der Umsatz von 21 auf 50% erhöht werden.

Der zweite Schwerpunkt der Amindehygrogenasen-Kaskade hingegen fokussierte sich auf die Synthese primärer Amine. Die für den Bulk-Bereich hergestellten Amine müssen vor allen Dingen preiswert zugänglich sein. Hier sind Enzyme, wie in diesem Fall die Amindehydrogenase EsLeuDH-DM eine erstrebenswerte Möglichkeit. Bei Cofaktorabhängigkeit von Enzymen ist ein Cofaktorregenerierungssystem aus Kostengründen unabdingbar. Hier ist besonders das Cosubstrat ein großer Kostenfaktor. Um diesen zu umgehen wurde sich der Algenmetabolismus aus *Chlamydomonas reinhardtii* zu Eigen gemacht. Die Alge sekretiert während des anaeroben Fermentationsprozesses, bei dem die synthetisierte Stärke abgebaut wird, Formiat.[109] Dieses Formiat kann in Kopplung mit der Formiatdehydrogenase (FDH) zur Cofaktorregneriung genutzt werden. Das Cosubstrat wird also *in situ* erzeugt und ist damit kostengünstiger zugänglich. Das Formiat und die Alge wurden Wobbe aus dem Arbeitskreis Algenbiotechnologie & Bioenergie um bereitgestellt. In diesem Zusammenhang war es möglich die Amindehydrogenase-katalysierten Reaktionen mit der Algenbiotechnologie zu verknüpfen.

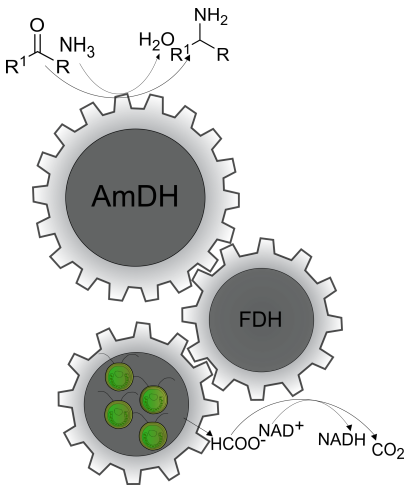

Figure 63: Amindehydrogenase-katalysierte reduktive Aminierung mit Formiatdehydrogenase (FDH) und Formiat aus der Alge *Chlamydomonas reinhardtii* als Cofaktorregenerierungssystem.

Einerseits wurde der Algenüberstad, in dem die Alge das Formiat sekretiert, als auch das Formiat, welches *in situ* produziert wurde genutzt. Im Bereich von 3 mM konnten Hexylamin (**9**, >99%) und Cyclohexylamin (**5**, >99%) erfolgreich synthetisiert werden. Die etablierte Algentechnologie konnte darüber hinaus mit neuen Flavinmonooxygenasen (FMO) aus *Pseudomonas sp.* verknüpft werden. Die FMOs wurden vom Arbeitskreis Algenbiotechnologie & Bioenergie von Kruse isoliert, umkloniert, exprimiert und aufgereinigt und waren so zugänglich für die Kombination des neuartigen Recyclingsystems. In diesem Zusammenhang konnte Bicyclo[3.2.0]hept-2-en-6-on (**11f**) erfolgreich in seine entsprechenden Lactone ($\mathbf{11f_a}$) und ($\mathbf{11f_b}$) umgesetzt werden.

Bei der Verknüpfung der Amindehydrogenase und der Flavinmonooxygenase mit der Algentechnologie, wurde ein Grundstein für die Vermeidung des Zusatzes von organischen Cosubstraten bei Einschritt-Oxidationsreaktionen mit NAD(P)H-abhängigen Enzymen gelegt. Dies ist besonders bei der Herstellung von Bulk-Chemikalien interessant. In Zusammenhang mit der Amindehydrogenase könnte so ein günstigerer Zugang zu primären Aminen geschaffen werden. Mit der Flavinmonooxygenase wäre beispielsweise die Herstellung von ϵ-Caprolacton in Kombination mit dem neuartigen Cofaktorregernierungssystem von großem Interesse.

Die zweite Kaskade umfasste die Synthese von hydratisierten Fettsäuren als Bausteine für Polyole (Figure 64). Diese Polyole sind wiederum Substrate für die Synthese von Polyurethane, die für den Kooperationspartner WINDMÖLLER zur Herstellung von Fußböden und Trittschallmatten dienen. Für das Projekt wurden drei Oleate-Hydratasen (Ohy) und zwei Linoleaet-Hydratasen (Lhy) ausgewählt, wobei folgende aufgrund ihrer Substratbreite und der Anwendbarkeit für die Synthese von großen Mengen ausgewählt wurden.

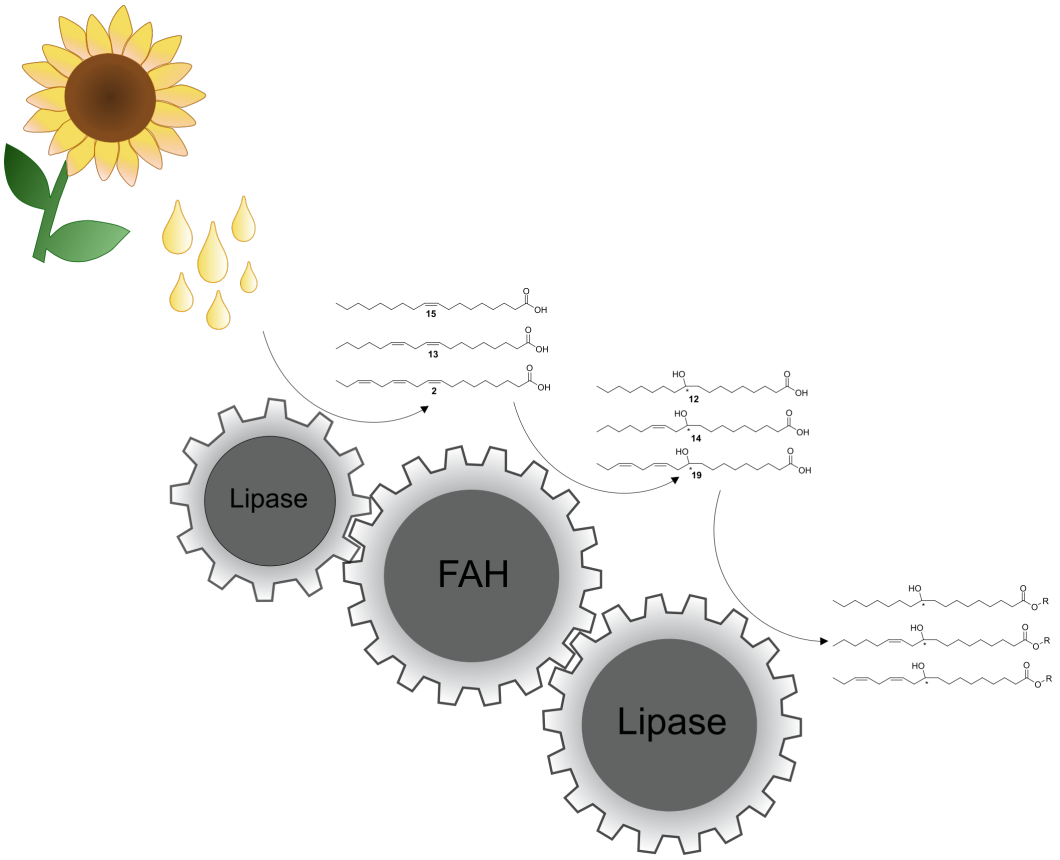

Figure 64: Herstellung von Polyolen ausgehend von Ölen, mit Hilfe von Lipasen und Fettsäurehydratasen.

Cla-HY (Lp- Lhy aus *Lactobacillus plantarum*), La-Ohy (aus *Lactobacillus acidophilus*), Em-Ohy (aus *Elizabethkingia meningoseptica*), La-Lhy (aus *Lactobacillus acidophilus*) and Sn-Ohy (aus *Stenotrophomonas nitritireducens*). Zunächst wurden analytische Experimente mit den Fettsäurehydratasen (FAH) durchgeführt. Für die Ohy wurde Ölsäure (**15**) und für die Lhy Linolsäure (**13**) mit 10 mM Substratkonzentration verwendet. Nach 22.5 h Reaktionszeit konnten Ausbeuten zwischen 79 und >99% erzielt werden, was die Aktivität der Hydratasen bestätigte. Der Fokus der folgenden Experimente lag auf den Ölsäurehydratasen. Diese sollten dazu genutzt werden 10-Hydroxystearinsäuren (**12**) zu synthetisieren. Hierfür wurde die Fettsäurehydratase Sn-Ohy ausgewählt, da sie die vielversprechendsten Ergebnisse in Vorversuchen zeigte. Unter den optimalen Reaktionsbedingungen (Citratpuffer pH 6.3, 50 mM, 35 °C, 5% DMSO bzw. kein Cosolvent) konnten mit dem Rohextrakt nach 48 h 90% Umsatz erzielt und eine Ausbeute von 72% mit einer Reinheit von 97% erreicht werden. Für eine praktikable, kostengünstige industrielle Anwendbarkeit wurde das oben genannte Enzym erfolgreich immobilisiert. Nach initialer Etablierung der Immobilisierung der Sn-Ohy auf den hydrophoben Carrier *Lewatit* VP OC 1600 von Pietrowski wurden diese Ergebnisse aufgegriffen und verfeinert.[184] Die besten Ergebnisse konnten mit einer Beladung von 1:9 Enzym:Carrier einer Immobilisierungsgeschwindigkeit von 80-180 rpm und Zeit von 18 h erzielt werden. Mit der erfolgreich immobilisierten FAH konnten schlussendlich *up-scaling* Experimente (400 g L^{-1}) mit einer Ausbeute von 59% durchgeführt werden. Um die Kaskade zu komplettieren wurden die hydratisierten Fettsäuren in analytischen Ansätzen erfolgreich mit verschiedenen Polyolen verestert. Katalysiert wurde dies durch die Lipase B aus *Candida antarctica*. Im präparativen Ansatz konnte die 10-Hydroxystearinsäure (**12**) mit 1,6-Hexandiol (**20**) erfolgreich zu einem Polyol (**21**, 7.8 g, 20%) verestert werden. Zusätzlich war es möglich hydratisierte Fettsäuren ausgehend von Sonnenblumenöl im 50 g L^{-1}L herzustellen.

Hierzu wurde die Lipase aus *Candida rugosa* als effizientes Enzym für die Hydrolyse des Triglycerids ermittelt.

Zusammenfassend lässt sich feststellen, dass die Intention, hydratisierte Fettsäuren in großem Maßstab zugänglich zu machen, erfolgreich umgesetzt wurde. Im Vergleich zu den *bis dato* etablierten Systemen anderer Arbeitsgruppen auf dem Gebiet der Synthese von 10-Hydroxystearinsäure (**12**), konnten in dieser Arbeit höhere Ausbeuten erreicht, sowie die Möglichkeit der Isolation der 10-Hydroxystearinsäure (**12**) in hoher Reinheit ermöglicht werden. Darüber hinaus konnte ein abtrennbarer und aktiver Biokatalysator für die Synthese von 10-Hydroxystearinsäure (**12**) entwickelt werden, der nun zugänglich für zukünftige Prozesse ist. Des Weiteren war es möglich in einem Zweistufenprozess ausgehend von Ölsäure (**15**), verlinkte Polyole zu synthetisieren. Somit konnte eine Basis für die Synthese maßgeschneiderter Polyole aus 10-Hydroxystearinsäure (**12**) mit verschiedenen Alkohollinkern gelegt werden.

Die letzte Kaskade hatte die Herstellung von 12-OPDA (**1**) als Ziel. 12-OPDA (**1**) ist das erste biologisch aktive Intermediat in der pflanzlichen Synthese von Jasmonat (**26**) und daher von großer agrarwissenschaftlicher Bedeutung. Aufgrund seiner Ähnlichkeit zu den im Menschen vorkommenden Prostaglandinen ist es auch pharmakologisch von höchster Relevanz.[203] Aufgrund der *bis dato* schwierigen Zugänglichkeit[212–215] wurde sich einerseits mit der Optimierung der Reaktionskaskade, als auch der Isolation beschäftigt. Darüber hinaus war ein Ziel die Herstellung neuartiger 12-OPDA-Derivate mittels Olefinkreuzmetathese. Für die Synthese von 12-OPDA (**1**) wurden die kommerzielle Lipoxygenase aus der Soyabohne mit der rekombinanten Allenoxidsynthase (AOS) und Allenoxidcyclase (AOC2) aus *Arabidopsis thaliana* (At) gekoppelt (Figure 65).

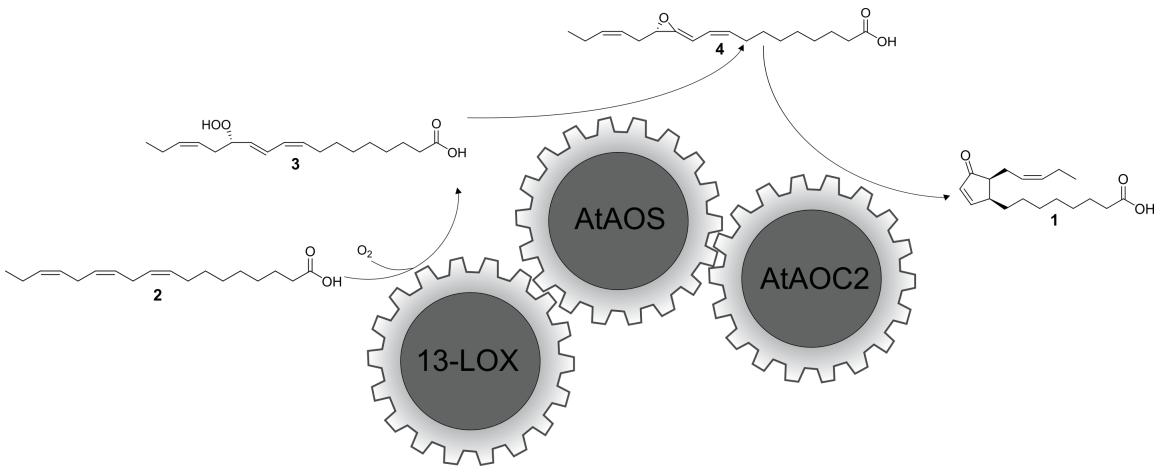

Figure 65: Synthese von 12-OPDA (**1**), ausgehend von Linolensäure (**2**) aus *Glycine max* über die Lipoxygenase (13-LOX), Allenoxidsynthase (AOS) und Allenoxidcyclase (AOC2) aus *Arabidopsis thaliana* (At).

In initialen Aktivitätstest und Biotransformationen konnte für die Lipoxygenase optimale Bedingungen gefunden werden mit NH_4Cl- Puffer, pH 9 und 100 mM, 25-30 °C, Ethanol (5 %) als Cosolvenz und die ständige Sauerstoffsättigung des Systems. Für die beiden Enzyme aus *Arabidopsis thaliana* wurde sich für ein Ganzzellsystem entschieden. Hierfür wurden beide Enzyme in *E.coli* coexprimiert. In diesem Zusammenhang lieferte die Kombination mit BL21-CodonPlus(DE3)-RIL (pET28a-AtAOS and pQE30-AtAOC2) in einer Konzentration von 1 g L^{-1} (NH_4Cl- Puffer, pH 9 und 100 mM, 25-30 °C, Ethanol (5%), *v/v*) 12-OPDA (**1**) und α-Ketol (Nebenprodukt) in einem 90:10 Verhältnis und in einem 91:9 *cis*:*trans* Verhältnis mit einer Ausbeite von 28%. Ein weiterer Schwerpunkt war die Aufarbeitung von 12-OPDA (**1**). Aufgrund seiner hydrophoben Eigenschaften stellte sich die Abtrennung vom Zellmaterial als große Schwierigkeit heraus. Um dieser Problematik Herr zu werden, wurden zwei Ansätze verfolgt: die Optimierung der Extraktion oder die Applikation im *segmented flow*. Die Extraktion konnte durch zusätzliche Ultraschallbehandlung des Zellpellets nach der Batch Reaktion in Dichlormethan von 31% auf 61% verbessert werden. Darüber hinaus war es möglich das 12-OPDA (**1**) erfolgreich im *segmented flow* zu synthetisieren. Hierfür wurde 13-HPOT (**3**) aus Linolensäure (**2**) synthetisiert und in Isooctan gelöst.

Außerdem wurden die AtAOS und AtAOC2 in Puffer (NaPi, pH 8, 100 mM, Tween 1%, *v/v*) gelöst. Diese Parameter konnte in vorherigen Studien zum *segmented flow* als optimal ermittelt werden. Im *segmented flow* konnte im Vergleich zum Batch (34%) 99% Umsatz erzielt werden. Darüber hinaus konnte in einem *up-scaling* Experiment (7 facher Ansatz) die Ausbeute von 36% im Batch auf 61% im *segmented flow* erhöht werden. Schlussendlich wurde mit Hilfe der Olefinkreuzmetathese 12-OPDA-Derivate synthetisiert. Dabei konnte gezeigt werden, dass für die Metathese der 12-OPDA-Ester (**32**) als Ausgangssubstrat genutzt werden muss, da die Säure den Katalysator deaktiviert. Der 12-OPDA Ester (**32**) konnte erfolgreich mit der Lipase CAL-B mit einer Ausbeute von 92% verestert werden. Die chemische Synthese hingegen führte zur kompletten Epimerisierung zum physiologisch inaktiven *trans*-12-OPDA (**1**). Für die Olefinkreuzmetathese wurden DCM, Reflux und der Hoveyda-Grubbs Katalysator der 2. Generation (10%) als optimale Reaktionsbedingungen ermittelt. Mit diesen Bedingungen konnte eine Vielzahl von 12-OPDA-Derivaten mit hohen Umsätzen und moderaten Ausbeuten hergestellt werden (Figure 66).

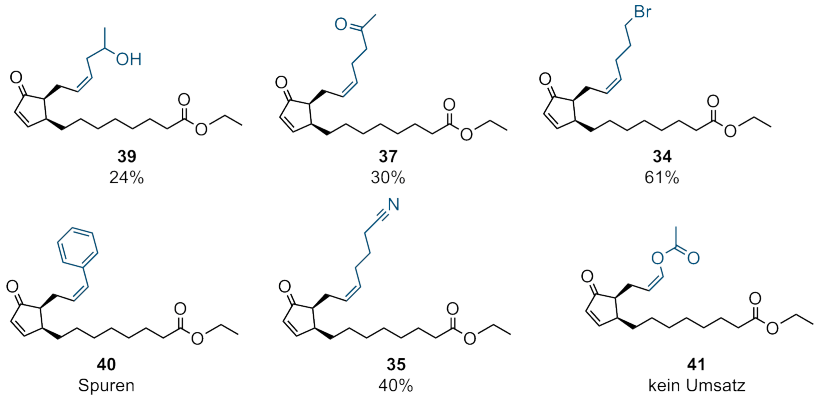

Figure 66: Produkte der Olefinmetathese mit 12-OPDA-Ethylester **32**.

In dem Projekt zur Herstellung von 12-OPDA (**1**), konnte ein großer Teil der festgelegten Ziele erreicht werde. So ist es nun möglich, mit der etablierten Kaskade, 12-OPDA (**1**) in großen Mengen und mit hoher Reinheit zu isolieren.

Dies ist, gerade im Vergleich mit der *bis dato* zugänglichen Menge von 12-OPDA (**1**), ein großer Fortschritt.

Des Weiteren konnte einerseits mit der Extraktionsoptimimierung, andererseits mit dem *segmented flow*-Prozess, eine Möglichkeit zur besseren Isolierung von 12-OPDA (**1**) erreicht werden, welches sich als Lipid-ähnliches Molekül schwer aus wässrigen Reaktionsmedien abtrennen lässt. Ein zusätzliches Ziel dieser Arbeit war die Herstellung einer 12-OPDA-Bibliothek mithilfe der Alken-Kreuzmetathese. Dieses Ziel konnte mit der hier dargestellten Methodik erfolgreich erreicht werden. Somit konnte ein Grundstein für die Synthese weiterer 12-OPDA-Derivate gelegt werden. Die Herstellung alternativer 12-OPDA-Derivate ist insbesondere in Hinblick auf weitere Untersuchungen der physiologischen Aktivitäts- Wirkungsbeziehung in Pflanzen interessant.

10 Experimental part

10.1 General

10.1.1 Chemicals

Commercially available reagents and chemicals were purchased from *Acros Organics*, *Alfa Aesar*, *ABCR*, *Carl Roth*, *Deutero*, *Fluorochem*, *Merck*, *Sigma-Aldrich*, *VWR*, *Thermo Fisher Scientific*, *TCI* in highest purity and used without further purification. Oleic acid (**15**) was purchased from *Sigma-Aldrich* and used in 90% purity. The restriction endonucleases, T4 DNA ligases and dNTPs were purchased from *Thermo Fisher Scientific*. The oligonucleotides were acquired from *Eurofins Genomics*. Dichloromethane and toluene for metathesis reactions were used as dried solvents. Water is used as deionized water (dH_2O) or ultrapure water.

10.1.2 Column chromatography

The automatic column chromatography was performed with the Isolera One from *Biotage*®. Silica gel columns "SNAP Ultra" with 10 g or 25 g of a "HP-Sphere 25 µm" quality were used. The substances were applied on silica gel cartridge with the same quality. The solvents used were mixtures with different gradients. Reverse-phase chromatography was performed with a 10 g or 30 g "SNAP KP-C18-HS", whereby the substances were applied on a cartridge with the same quality.

10.1.3 Thin layer chromatography

Thin layer chromatography was performed with DC aluminum foils ALUGRAM SILG/UV (0.22 mm silica gel with fluorescence indicator) from *Macherey-Nagel*. The analysis was carried out with heat treatment and UV light at 254 nm respectively dyed with potassium permanganate or molybdenum.

10.1.4 NMR spectroscopy

NMR spectra were recorded on *Bruker Avance* 500 spectrometer recorded at a frequency of 500 MHz for spectra or 126 MHz for ^{13}C NMR spectra. Chemical shifts (ppm) are given relative to a tetramethylsilane standard (TMS). The deuterated solvents present the reference for all spectra (chloroform-d: 7.26 ppm ^{1}H NMR, 77.16 ppm ^{13}C NMR). Multiplets were assigned as s (singlet), d (doublet), t (triplet), dd (doublet of doublet), m (multiplet), q (quintet). The obtained data were evaluated with the software *MestReNova* 8.1 (*Mestrelab Research*).

10.1.5 Mass spectrometry

Nano-ESI mass spectra were recorded using an Esquire 3000 ion trap mass spectrometer (*Bruker* Daltonik GmbH, Bremen, Germany), equipped with a nano-ESI source. Samples were dissolved in solvent (containing e.g. sodium perchlorate or similar compound to enhance adduct formation) and introduced by static nano-ESI using in-house pulled glass emitters. Nitrogen served both as nebulizer gas and dry gas. Nitrogen was generated by a *Bruker* nitrogen generator NGM 11. Helium served as cooling gas for the ion trap and collision gas for MS^n experiments. The mass axis was externally calibrated with ESI-L Tuning Mix (*Agilent Technologies*, Santa Clara, CA, USA) as a calibration standard. The spectra shown here are recorded with the *Bruker* Daltonik esquire NT 5.2 esquire. Control software by the accumulation and averaging of several single spectra. DataAnalysis^{TM} software 3.4 was used for processing the spectra.

10.1.6 High performance liquid chromatography (HPLC)

For analytical HPLC, a system of *Jasco* was used. The system consisted of a degasser LC-Net II/ADC device, pumps (PU-2080 plus), a multiwavelength detector MD-2010 plus, an autosampler AS-2059-SF, a thermostat CO-2060 and a backpressure controller BP-2080. The supercritical carbon dioxide was cooled *via* cryostat from *Julabo*F250. The samples were separated using *Chiralpak* columns from *Daicel*. The chromatograms were evaluated using the *Galaxy* Chromatography Data System software.

10.1.7 Gas chromatography (GC)

Gas chromatography analysis was performed with AOC-20i/s Auto Injector/Auto Sampler from *Shimadzu* on a GC-2010 Plus from *Shimadzu Phenomenex* ZB-SMS capillary column (polydimethylsiloxane with 5% polyphenylmethylsiloxane, 30 m, 0.25 mm i.d., 0.25 µm film thickness) using nitrogen as a carrier gas. GC analysis for the determination of enantioselectivity was conducted using a *MN Lipodex E* chiral column [octatakis(2,6-di-*O*-phenyl-3-*O*-butyryl)-γ-cyclodextrine] (25 m, 0.25 mm) (*Macherey–Nagel*, Düren, Germany) with a GC2010 (*Shimadzu*) and nitrogen as a carrier gas.

10.1.8 Optical rotation measurements

The optical rotation measurements were performed on a Perkin Elmer "Model 341" polarimeter. The measurements were performed in a cuvette with a layer thickness of 1 cm at room temperature and a wavelength of 589 nm (sodium D-line).

10.2 Biochemical, molecularbiological and microbiological methods

10.2.1 Bacterial strains and plasmids

The used bacterial strains and plasmids are shown in the table below:

Table 15: Bacterial strains and plasmids.

Bacterial strains and plasmids	Manufacturer/Resistenz
Escherichia coli BL21 (DE3)	*Novagen*
Escherichia coli BL21-CodonPlus(DE3)-RIL	*Novagen*
pET-21a(+)	Ampicilin
pET-24a(+)	Kanamycin
pET-28a(+)	Kanamycin
pUC18	Ampicilin
pQE30	Ampicilin

10.2.2 Antibiotics and IPTG

The used buffers, antibiotics and IPTG solutions are shown in the table below:

Table 16: Antibiotics and IPTG.

Solution	Composition
Ampicillin (*Roth*)	Stock solution 50 mg mL^{-1} Final concentration 0.05 mg L^{-1}
Kanamycin (*Roth*)	Stock solution 100 mg mL^{-1} Final concentration 0.1 mg mL^{-1}
IPTG (*Appli Chem*)	Stock solution 100 mmol L^{-1} Final concentration 0.2 mmol L^{-1}

10.2.3 Polymerase chain reaction (PCR)

The polymerase chain reactions were performed with the Labcycler Compact Gradient from *Sensoquest*. The phusion polymerase and dNTPs were obtained from *ThermoScientific*.

10.2.4 Agarose gel electrophoresis

The buffer for the agarose gel electrophoresis is shown in the table below:

Table 17: TBE buffer composition.

Compound	Concentration
Tris base	445 mM
Boric acid	445 mM
EDTA	10 mM
dH_2O	1 L

The agarose gel electrophoresis was performed with agarose gels (1%, *m/V*) in TBE buffer using the fluorescent dye *GelRed* Nucleic Acid Gel Stain 10.000x, diluted to a 1x concentration, performed with the *PowerPac* Basic Power Supply from *BioRad*.

10.2.5 Photometric DNA- and protein concentration measurement

The DNA and purified protein concentrations were determined using the *NanoDrop* One Microvolume UV/Vis spectrophotometer from *Thermo Scientific*. The protein concentrations of the crude extracts were determined using the *Thermo Scientific* Multiskan GO spectrophotometer at 595 nm.

10.2.6 Media and solutions

The used media and solutions are shown in the table below:

Table 18: Composition of LB-agar.

Media/Solutions	Composition
LB-Agar:	10 g LB medium 6 g Agar (1.5 %) 400 mL dH_2O autoclaved Antibiotika (1:1000)

10.2.7 Centrifugation

Centrifugation of 15 and 50 mL *Falcon* tubes was performed with the Multifuge 3S-R from *Heraeus* and Multifuge X3R from *Heraeus*. EPPENDORF tubes (0.5, 1.5 and 2.0 mL) were centrifuged with the CT 15RE from VWR.

10.2.8 Buffer for protein purification

The used buffers for the protein purification are shown in the table below:

Table 19: Solutions for protein purification.

Buffer	Composition
Binding buffer	50 mM Sodium dihydrogen phosphate 300 mM NaCl 10 mM Imidazole pH 8 in 250 mL H_2O
Wash buffer	50 mM Sodium dihydrogen phosphate 300 mM NaCl 20 mM Imidazole pH 8 in 250 mL H_2O
Elution buffer	50 mM Sodium dihydrogen phosphate 300 mM NaCl 250 mM Imidazole pH 8 in 250 mL H_2O

10.2.9 Marker

Figures of the markers used for SDS-PAGE and agarose gel electrophoresis are shown below:

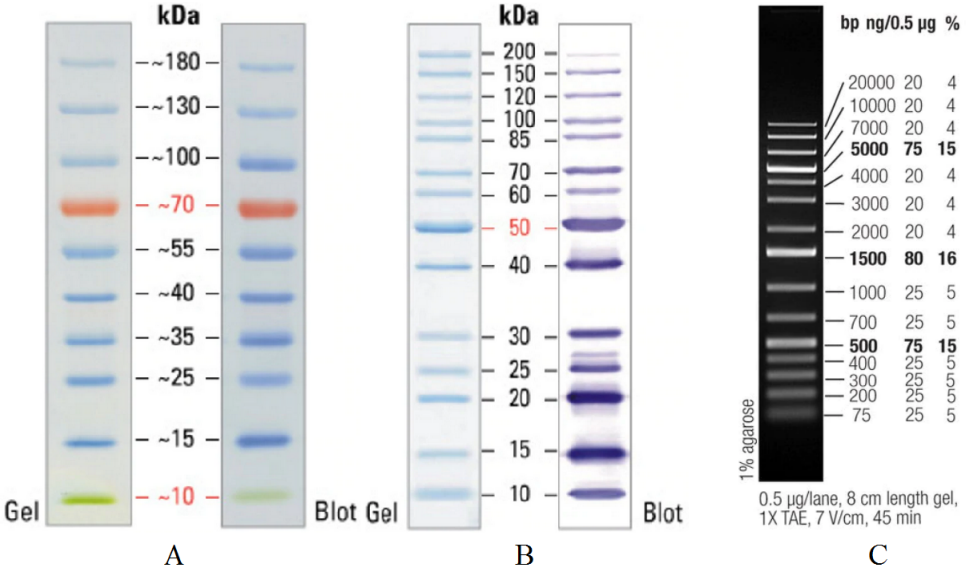

Figure 67: Used Markers. **A** shows the SDS-PAGE band profile of the *ThermoScientific* PageRuler Prestained Protein Ladder. **B** shows SDS-PAGE band profile of the *ThermoScientific* PageRuler Unstained Protein Ladder. **C** shows *Roth* GeneRuler 1 kb DNA Ladder.

10.2.10 Bradford Assay

The used Bradford assay solution is shown in the table below:

Table 20: Solution for Bradford Assay.

Buffer	Composition
Bradford-Reagent	59 mg mL^{-1} Comassie blue G250 50 mL Methanol (w=99 %) 100 mL *o*-Phosphoric acid (w=85 %) 1 L dH_2O

10.2.11 Sodium dodecyl sulfate-polyacrylamide gel electrophoresis (SDS-PAGE)

The composition for the buffer used for the SDS-PAGE is shown in the table below:

Table 21: Solution for SDS-PAGE.

Solution	Composition
Collecting gel (5%):	3.4 mL dH_2O
	1.26 mL TRIS buffer (1 M, pH 6.8)
	0.83 Acrylamide (10%)
	50 μL SDS (10%)
	50 μL APS
	5 μL TEMED
Separation gel (12%):	3.3 mL dH_2O
	2.5 mL TRIS buffer (1.5 M, pH 8.8)
	4 mL Acrylamide (10%)
	100 μL SDS (10%)
	100 μL APS
	10 μL TEMED
Staining solution:	Acetic acid (10%)
	Ethanol (30%)
	dH_2O (60 %)
	1 g L^{-1} Coomassie
Decolouring solution:	Acetic acid (10%)
	Ethanol (30%)
	dH_2O (60 %)
Laemmli buffer	1.2 g SDS
	6 mg Bromphenol blue
	4.7 mL Glycerol
	1.2 mL 0.5M TRIS pH 6.8
	2.1 mL dH_2O
SDS running buffer	30.3 g TRIS
	144 g Glycine
	10 g SDS
	1 L dH_2O pH 8.4

10.2.12 UV/Vis-Analytics

Enzyme activity was determined with the *Jasco* V-630 spectrophotometer. Raw data were evaluated using the *Jasco* Spectra Manager. Multiactivity determinations were done with the *Tecan* Reader Spark 10M and data evaluated using *Excel*.

10.2.13 General operating procedure 1 (GOP1): Polymerase chain reaction

The primer for the PCR amplification of EsLeuDH are shown in the table below:

Table 22: Used primers.

Direction	Sequence
5´ 3´	GCGGCGTCATATGGTTGAAACAAACGTAGAAGC
3´ 5´	GCGCCAACTCGAGTTAACCGCGTGATCCTAAAATG

The composition for the PCR amplification are shown in the table below:

Table 23: Composition of PCR samples.

Compound	Volume	Final concentration
Template-DNA	100 ng	
Oligonucletides (100 pmol µL)		1 pmol/µL
HF buffer (5x)/GC buffer (5x)	2 µL	1x
dNTPs (10 mM)	1 µL	0.2 mM
Phusion-Polymerase	0.2 µL	
DMSO	0.4 µL	
ddH_2O	to 20 µL	

The Quik-Change PCR-program is shown in the table below:

Table 24: QuikChange PCR program for amplification.

	T/°C	t	Cyclus
Initial denaturation	98	10 min	1
Denaturation	95	30 s	23
Primer annealing	60	40 s	23
Elongation	72	4 min	23
Final elongation	72	10 min	1

10.2.14 General operating procedure 2 (GOP2): Restriction digestion

The restriction digest was carried out with 10 U of restriction enzymes in *ThermoScientific* FastDigest buffer (1x). For AtAOC in pQE30 BamHI/SalI and in pUC18 XbaI/EcoRI were used. The reaction mixtures with plasmids were incubated for three hours at 37 °C, reaction mixtures with inserts for 30 minutes. DNA was first purified using agarose gel electrophoresis and afterward by using GE Gel Purification Kit from *GE Healthcare*.

10.2.15 General operating procedure 3 (GOP3): Ligation

For ligation two samples were prepared (1:1 and 1:3 plasmid:insert) with ligase buffer (1x) and ligase (5 U). The reaction mixture was incubated for 30 minutes at room temperature. The ligation mixture reaction was transformed in *E. coli* DH5α.

10.2.16 General operating procedure 4 (GOP4): Transformation of competent cells with plasmid-DNA

Plasmid-DNA (1 µL) was added to the chemical competent cells (100 µL) and incubated for 30 minutes on ice. The cells were heated to 42 °C for 90 seconds, and incubated again for five minutes on ice. Afterward, 1 mL of LB media was added. The mixture was incubated for three hours at 37 °C (Kanamycin) or one hour at 37 °C (Ampicillin, Chloramphenicol) and 800 rpm. Subsequently, the cells were streaked over the agar surface, with suitable antibiotics and incubated overnight at 37 ° C.

10.2.17 General operating procedure 5 (GOP5): Test digestion

For validation of the ligation, the transformed ligation product was streaked over the agar surface with a suitable antibiotic. A clone was isolated from the plate and cultured in the liquid culture medium.

The plasmid was isolated according to *innu PREP* Plasmid Mini Kit and digested with suitable restriction enzyme in *ThermoScientific* FastDigest buffer (1x) for three hours at room temperature. Positive ligation was monitored using agarose gel electrophoresis.

10.2.18 General operating procedure 6 (GOP6): Preparation of precultures

For the overexpression in *E. coli*, precultures were prepared in test tubes (160x16 mm) or ERLENMEYER flasks (100 mL). For this purpose, antibiotics in a dilution of 1:1000 (5 µL in test tube, 20 µL in Erlenmeyer flasks) and a colony *E. coli* were added to LB medium (5 mL in test tube, 20 mL in ERLENMEYER flasks). The cultures were shaken overnight at 37 °C and 170-180 rpm.

10.2.19 General operating procedure 7 (GOP7): Plasmid isolation

For plasmid isolation from precultures of *E. coli* DH5α cells the protocol of the Wizard Plus SV Minipreps DNA Purification System Kit from *Promega* was used. The elution was performed with 50 µL ultrapure H_2O, heated to 50 °C.

10.2.20 General operating procedure 8 (GOP8): Expression of enzymes in TB-Medium

TB medium (20% of flask volume) with antibiotic (1:1000) were transferred in autoclaved flasks. The medium was inoculated with 1% preculture. The cultures were grown at 37 °C and 180 rpm. When the culture reached an OD of 0.4-0.8, cell cultures were induced with 200 µL of IPTG (1 M). For expression, the temperature was reduced and the culture was shaken at 160-180 rpm overnight. Afterward, cells were harvested (4000x g, 4 °C, 30 minutes) and stored at -20 °C.

10.2.21 General operating procedure 9 (GOP9): Expression of enzymes in AI-Medium

For autoinduction (AI) expression, AI medium was used. The composition of the AI medium is shown in the table below:

Table 25: Composition of autoinduction medium.

Solution	V/%
TB-Medium	89
Lactose (20 g L^{-1})	10
Glucose (50 g L^{-1})	1

The medium was transferred (20% of flask-volume) with antibiotic (1:1000) in autoclaved flasks. The medium was inoculated with 1% overnight culture. The cultures were grown at 37 °C and 180 rpm. After two hours, temperature was reduced to 15 °C, and the culture was shaken at 160-180 rpm overnight. Afterward, cells were harvested (4000x g, 4 °C, 30 minutes) and stored at -20 °C.

10.2.22 General operating procedure 10 (GOP10): Cell digestion

The cells were suspended in buffer (25% cell suspension). The cells were digested under ultrasound (3x 3 minutes, 5x 10 cycles for volumes up to 10 mL; 3x 5 minutes, 5x 10 cycles for volumes up to 20 mL; 3x 10 minutes, 5x 10 cycles for volumes up to 50 mL). Afterward, the suspension was centrifuged (20.000x g, 30 minutes).

10.2.23 General operating procedure 11 (GOP11): Bradford Assay

The protein concentrations of the crude extracts were determined by the means of Bradford assay.[264] First, two dilutions (1:25, 1:40) of the samples were prepared and thoroughly mixed. Subsequently, 5 µL of the diluted samples were transferred into a microtiter plate and mixed with 250 µL of the Bradford reagent. After an incubation period of 15 min at 25 °C, the absorbance was measured at a wavelength of 595 nm.

In addition, BSA standards were determined with known protein concentration. Thus, the protein concentration could be determined by the means of a standard curve. For each sample, a triplicate determination was performed.

10.2.24 General operating procedure 12 (GOP12): SDS-PAGE

The cells were digested *via* ultrasound, according to GOP 10. One sample (10 µL) was taken (insoluble fraction). The solution was first centrifuged (4000x g, 5 minutes). The pellets are inclusion bodies, and dissolved in 5 M urea (same volume as supernatant). The supernatant was centrifuged again (20000x g, 5 minutes). The supernatant is the crude extract. The protein content was determined *via* Bradford assay (GOP 11). For the preparation of the samples, a protein concentration of 1 µg mL^{-1} is required. Samples were mixed with Laemmli buffer (1x) and incubated for five minutes at 95 °C for protein denaturation. The samples were centrifuged and the supernatant (10 µL) and marker (5 µL) were applied to SDS-PAGE. The proteins were separated at 100 V until separating gel is reached. Subsequently, the voltage was increased to 120 V. After separation, the SDS-PAGE was colored *via* staining solution for one hour, purified with ddH_2O and finally decolorized with s decolourising solution.

10.2.25 General operating procedure 13 (GOP13): Protein purification

The cells were suspended in digestion buffer (25% cell suspension) and digested, according GOP 8. The suspension was centrifuged (20.000x g for 20 min). The pellet was discarded, and the crude extract was used for further purification. The Ni^{2+}-NTA column was washed with 5x 5 mL dH_2O and 5x 5 mL binding buffer. The crude extract (6-8 mL) was added to the column and the flow-through (FT) was collected after incubation for 5 min. The column was rinsed with wash buffer (7x 5 mL), the washing fraction (W) was collected. In the next step, the protein of interest could be eluted with elution buffer.

The column was regenerated for further uses with 5x 5 mL wash buffer, 0.5 M NaOH and dH_2O. Afterwards, the elution fraction was concentrated *via* centrifugal concentrator. Therefore, concentrator was equilibrated with 10 mL water. Next, elution fraction was concentrated to 2.5 mL. A SiO_2 column was washed with 5x 5 mL NaPi buffer (100 mM, pH 7) or rather NaPi buffer (20 mM, pH 7). The concentrated elution fraction was applied to the column and subsequently eluted with 3.7 mL of NaPi buffer (100 mM, pH 7) or rather NaPi buffer (20 mM, pH 7).

10.2.26 General operating procedure 14 (GOP14): Activity assay

With an optical test, it is possible to determine the activity of enzymes. On this occasion, the oxidation of NADH to NAD^+ is measured by the decrease in absorbance at 340 nm for 60 seconds. The enzyme activity is defined as µmol min^{-1} and is calculated according to the following formula:

$$U = \frac{\Delta_{Abs} \cdot V_t}{t \cdot V_P \cdot d \cdot \epsilon} \cdot F \tag{1}$$

Δ_{Abs} is the change in absorption, V_t is the total volume of the sample, t is the time and V_p is the total volume of the enzyme sample. d is the thickness of the cuvette and F is the dilution factor. ϵ is the extinction coefficient (6.3 10^3 L mol^{-1} cm^{-1}).

10.2.27 General operating procedure 15 (GOP15): Determination of K_M-value

For determination of the Michaelis-Menten constant (K_M) the activity was measured according to GOP 14 in a microtiter plate *via TecanReader*®. The activity was examined at various substrate concentrations and a fixed enzyme amount. The conversion from NADH to NAD^+ is measured in absorbance at 340 nm for 60 seconds.

The enzyme activity is defined as µmol min^{-1} and calculated according to the following formula:

$$U = \frac{\Delta_{Abs} \cdot V_t}{t \cdot V_P \cdot d \cdot \epsilon} \cdot F \quad (2)$$

Δ_{Abs} is the change in absorption, V_t is the total volume of the sample, t is he time and V_p is the total volume of the enzyme sample. d is the thickness of the cuvette and F is the dilution factor. ϵ is the extinction coefficient (6.3 10^3 L mol^{-1} cm^{-1}).

10.3 Experimental part for amine dehydrogenase

10.3.1 Activity assay EsLeuDH-DM of aryl-substituted ketones

The activity assay was done according to GOP 14. EsLeuDH-DM was prepared according to GOP 10. The composition for the assay is shown in the table below:

Table 26: Composition of EsLeuDH-DM activity assay.

Solution	V/mL
Buffer (NH_4Cl, pH 9.5, ketone (20 mM))	980
NADH (10 mM)	10
Enzym (crude extract)	10

The results for the activity assay are shown in the table below:

Table 27: Results of EsLeuDH-DM activity assay.

Substrate	U/mL
Acetophenone (**7a**)	3.24
Propiophenone (**7b**)	0.47
1-Phenylbutan-1-one (**7c**)	0.62
para-Nitrophenone (**7d**)	1.04
4-Acetylbenzoic acid (**7e**)	0.89
para-Bromophenone (**7f**)	0.32
para-Methoxyphenone (**7g**)	0.13
1-Phenylpropane-1,2-dione (**7h**)	0.47
2-Oxo-2-phenylacetic acid (**7i**)	0.36
Methyl 2-oxo-2-phenylacetate (**7j**)	0.75
1-Phenylbutane-1,3-dione (**7k**)	3.01
Ethyl 3-oxo-3-phenylpropanoate (**7l**)	0.55
α-Tetralon (**7m**)	0.78

10.3.2 Composition of EsLeuDH-DM K_M value measurement for acetophenone

The activity assay was done according to GOP 15. EsLeuDH-DM was prepared according to GOP 10. The composition for the assay is shown in the table below:

Table 28: Composition of EsLeuDH-DM K_M-value determination.

Solution	V/mL	Final concentration
Buffer (NH_4Cl, pH 9.5, ketone)	250	
NADH (5 mM)	10	0.2 mM
Enzym (purified enzyme)	10	58 µg
Acetophenone **7a**: Concentrations 0.5-80 mM		

The results for the activity assay are shown in the table below:

Table 29: Results of EsLeuDH-DM K_M-value determination.

Conc./mM	U/mg
0.5	$7.18\ 10^{-4}$
1	$7.85\ 10^{-4}$
10	$2.76\ 10^{-3}$
15	$5.55\ 10^{-3}$
20	$1.33\ 10^{-2}$
30	$2.03\ 10^{-2}$
40	$1.95\ 10^{-2}$
50	$2.93\ 10^{-2}$
60	$2.62\ 10^{-2}$
70	$2.96\ 10^{-2}$
80	$2.85\ 10^{-2}$

10.3.3 General operating procedure 16 (GOP16): Biotransformation with EsLeuDH-DM (analytic scale)

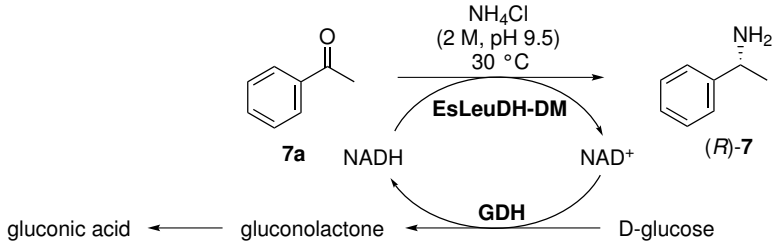

Acetophenone (**7a**) was dissolved in ammonium chloride buffer (2 M, pH 9.5). EsLeuDH-DM (0.69 U) prepared according to GOP 10, glucose (150 mM final concentration), NAD^+ (1 mM final concentration) and GDH (3.6 U) were added and the mixture was heated to 30 °C. The total volume of the reaction mixture was 1 mL. At fixed times, samples were taken. The conversion was measured *via* gas chromatography. The gas chromatographic analyses were performed with the GC-2010 Plus from *Shimadzu* with the autoinjector AOC-20i on the non-chiral column *Phenomenex* ZB-SMS. Start 90 °C, 20 °C min^{-1} to 107 °C, 15 °C min^{-1} to 150 °C, R_t= 2.01 min.

For measurement of enantiomeric excess, the samples were acetylated with acetyl chloride (1.1 eq) and triethylamine (1.5 eq) in dichloromethane for one hour.

The suspension was washed with hydrogen chloride (1:1, *v/v*). The solvent was removed *in vacuo*. Enantiomeric excess was determined *via* HPLC. Therefore, the *Chiralpak* AD H-column was used for the separation. The mobile phase was a mixture of CO_2 and isopropanol in a 95:5 ratio, with a flow rate of 1.5 mL min^{-1} at 20 °C, R_{t1}=14.9 min, R_{t2}=20.9 min.

10.3.4 Biotransformation with EsLeuDH-DM (analytic scale)

The reaction was performed according to GOP 16. Acetophenone (**7a**, 2.4 mg (0.02 mmol), 6.0 mg (0.05 mmol), 8.5 mg (0.07 mmol), 11.3 mg (0.09 mmol)) was dissolved in ammonium chloride buffer (585 µL, 2 M, pH 9.5). EsLeuDH-DM (250 µL, 0.69 U), prepared according to GOP 10, 50 µL glucose (100 µL, 1.5 M, 150 mM final concentration), NAD^+ (20 µL, 50 mM, 1 mM final concentration) and GDH (20 µL, 3.6 U) were added and the mixture was heated to 30 °C. The total volume of the reaction mixture was 1 mL. The samples were purified and analyzed according to GOP 16.

Table 30: Results of biotransformations with EsLeuDH-DM using different substrate **7a** concentrations.

t/h	conv.(20 mM)/%	conv.(50 mM)/%	conv.(75 mM)/%	conv.(100 mM)/%
1	1.30	2.70 1.72	1.20	
3.5	15.54	-	-	-
6	33.64	-	-	-
15	53.36	17.68	15.52	5.86
24	73.10	30.02	27.27	-
31	80.45	38.59	27.65	-
46	-	-	18.06	-
66	98.74	43.92	-	20.98
100	98.45	76.94	45.84	43.11

10.3.5 Biotransformation with EsLeuDH-DM (dosing experiment)

The reaction was performed according to GOP 16. Acetophenone (**7a**) was added in a rate of 13 ng min^{-1} in a 5 mL solution, consisting of ammonium chloride buffer (2 M, pH 9.5, 3 mL), EsLeuDH-DM (1.25 mL, 3.45 U), 500 µL glucose (1.5 M, 150 mM final concentration), 100 µL NAD^+ (50 mM) and GDH (100 µL). The reaction mixture was heated to 30 °C for 75 h. The samples were purified and analyzed according to GOP 16. After 66 h a conversion of 50% was achieved.

10.3.6 Activity assay EsLeuDH-DM with cosolvent

Into a microtiter plate 190/175/150 µL ammonium chloride buffer (2 M, pH 9.5), 20 mM acetophenone (**7a**) and EsLeuDH-DM (15 µL crude extract) and water-soluble cosolvent (25/50/75 µL) were added. The activity assay was prepared according to GOP 10. The suspension was incubated for 0/1/3/24 h and the assay was started by the addition of 10 µL NADH (5 mM, final concentration 0.2 mM). The activity was measured according to the enzyme activity assay (GOP 14).

Table 31: Activities for EsLeuDH-DM with different DMSO amounts.

t/h	slope (0/%)	slope (10/%)	slope (20/%)	slope (30/%)
0	$7.60\ 10^{-4}$	$1.07\ 10^{-3}$	$1.41\ 10^{-3}$	$1.27\ 10^{-3}$
1	$4.28\ 10^{-4}$	$1.21\ 10^{-3}$	$1.31\ 10^{-3}$	$1.14\ 10^{-3}$
3	$7.10\ 10^{-4}$	$1.11\ 10^{-3}$	$4.53\ 10^{-4}$	$7.82\ 10^{-4}$
24	$6.39\ 10^{-4}$	$7.10\ 10^{-4}$	$3.72\ 10^{-4}$	0

Table 32: Activities for EsLeuDH-DM with different EtOH amounts.

t/h	slope (0/%)	slope (10/%)	slope (20/%)	slope (30/%)
0	$7.60\ 10^{-4}$	$1.67\ 10^{-3}$	0	0
1	$4.28\ 10^{-4}$	0	0	0
3	$7.10\ 10^{-4}$	0	0	0
24	$6.39\ 10^{-4}$	0	0	0

Table 33: Activities for EsLeuDH-DM with different MeOH amounts.

t/h	slope (0/%)	slope (10/%)	slope (20/%)	slope (30/%)
0	$7.60\ 10^{-4}$	$1.11\ 10^{-3}$	$1.11\ 10^{-3}$	0
1	$4.28\ 10^{-4}$	$5.24\ 10^{-4}$	$1.15\ 10^{-3}$	0
3	$7.10\ 10^{-4}$	0	0	0
24	$6.39\ 10^{-4}$	0	0	0

Table 34: Activities for EsLeuDH-DM with different isopropanol amounts.

t/h	slope (0/%)	slope (10/%)	slope (20/%)	slope (30/%)
0	$7.60\ 10^{-4}$	$9.00\ 10^{-4}$	$3.37\ 10^{-4}$	$1.33\ 10^{-4}$
1	$4.28\ 10^{-4}$	$3.20\ 10^{-4}$	0	0
3	$7.10\ 10^{-4}$	0	0	0
24	$6.39\ 10^{-4}$	0	0	0

10.3.7 General operating procedure 17 (GOP17): Immobilization methodology

10.3.8 Calculation loading and immobilization yield

The immobilization yields (IY) were calculated from the masses of the bound protein (m_{bp}) on the carrier, divided through the masses of the protein used for immobilization (m_e) (equation 3). The masses of the crude extract and of the supernatant were determined by the means of a Bradford assay.

$$IY = \frac{m_{bp}}{m_e} \tag{3}$$

The loading (CL) was calculated according to the mass of the bound protein (m_{bp}) and the amount of used carrier (m_c) material, which was used. The loading is given in mg enzyme/g carrier (equation 4).

$$CL = \frac{m_{bp}}{m_c} \tag{4}$$

10.3.9 Immobilization on hydrophobic carrier

The purchased carrier material was washed with KPi buffer (50 mM, pH 7.0). The ratio of carrier to the buffer was 1:1 (m/v). Subsequently, the washed carrier material was suspended in an enzyme solution (in KPi buffer (5 mM, pH 7.0)) and shaken for 18 h at 20 °C and 80 rpm. The supernatant was removed with a pipette and the carrier was washed once with KPi buffer (10 mM, pH 7.0). The protein concentration was validated *via* Bradford assay.

10.3.10 Immobilization on covalent carrier

The purchased carrier material was washed three times with KPi buffer (50 mM, pH 7.0). The ratio of carrier to buffer corresponds to 1:1 (m/V). The washed carrier was suspended in an enzyme solution in KPi buffer (50 mM, pH 7.0) and shaken for 18 h at 20 °C and 80 rpm. The supernatant was removed with a pipette and the carrier was washed three times with KPi buffer (10 mM, pH 7.0). The protein concentration was validated *via* Bradford assay.

10.3.11 Examination of leaching-process for EsLeuDH-DM

For the examination of the leaching process the heterogenized catalyst was incubated in NH_4Cl buffer, 0.65 M NH_4Cl buffer and dH_2O for seven days.

The protein concentration was validated *via* BRADFORD assay.

Table 35: Results of leaching experiment with immobilized EsLeuDH-DM.

Carrier	Buffer/M	Amount resin/mg	Loaded protein/mg	Protein in supernatant
Hydrophobic	0.00	213	13.2	<1%
Hydrophobic	0.65	220	13.7	<1%
Hydrophobic	1.30	216	13.4	<1%
Covalent	0.00	229	18.4	<1%
Covalent	0.65	221	17.7	<1%
Covalent	1.30	225	18.1	<1%

10.3.12 Stability of EsLeuDH-DM at different substrate 7a concentrations

For the stability examination an activity assay was done, according to GOP 14. The activity was examined at various substrate concentrations and a fixed enzyme amounts. EsLeuDH-DM was prepared according to GOP 10. The decrease in NADH is monitored photometrically at 340 nm for 60 seconds after 0/8/22/33/58/82/143 h. The composition for the assay is shown in the table below:

Table 36: Composition of EsLeuDH-DM activity assay.

Solution	V/mL	final concentration
Buffer (NH_4Cl, pH 9.5, 2 M)	250	
NADH (5 mM)	10	0.2 mM
Enzym (crude extract)	10	4.5 µg
Acetophenone (**7a**): 20 mM, 50 mM, 100 mM		

The results are shown in the table below:

Table 37: Results of EsLeuDH-DM stability test.

t/h	20 mM	50 mM	100 mM
	U/mg	U/mg	U/mg
0	0.20	0.11	0.04
22	0.14	0.11	0.03
33	0.08	0.09	-
58	0.07	0.05	0.02
82	0.05	0.05	0.02
143	0.05	0.05	0.03

10.3.13 Stability of NADH and NAD^+ in NH_4Cl-buffer

For determination of cofactor stability of NADH and NAD^+ in NH_4Cl-buffer (pH 9.5, 2 M), the cofactors were incubated for 0/3/23/32/55 h at 30 °C with 990 µL NH_4Cl buffer (pH 9.5, 2 M) and 10 µL cofactor (10 mM, 0.1 mM final concentration).

Table 38: Results of cofactor stability test.

t/h	NADH (absorption at 340 nm)	NAD^+ (absorption at 260 nm)
0	1.29-1.29	2.19-2.02
3	1.24-1.26	2.17-2.19
23	1.24-1.24	2.05-2.05
32	1.16-1.16	2.21-2.20
58	1.12-1.14	1.97-1.97
140	0.90-0.90	1.95-1.97

10.3.14 Activity assay EsLeuDH-DM for different aldehydes

The activity assay was done according to GOP 14. EsLeuDH-DM was prepared according to GOP 10. The composition for the assay is shown in the table below:

Table 39: Composition of EsLeuDH-DM activity assay.

Solution	V/mL
Buffer (NH_4Cl, pH 9.5, aldehyde, ketone (5, 20 mM))	980
NADH (10 mM)	10
Enzym (crude extract)	10

The results for the activity assay are shown in the table below:

Table 40: Results of EsLeuDH-DM activity assay.

Substrate	U/mg
Propanal (**8a**)	0.49
Butanal (**8b**)	1.16
Pentanal (**8c**)	0.15
Hexanal (**8d**)	0.32
Heptanal (**8e**)	0.19
Octanal (**8f**)	0.09
Butanone (**8g**)	0.69
Isopropyl methyl ketone (**8h**)	2.15
Cyclohexanone (**8i**)	2.06

10.3.15 Composition of EsLeuDH-DM K_M-value measurement for hexanal (8d)

The activity assay was done according to GOP 15. EsLeuDH-DM was prepared according to GOP 10. The composition for the assay is shown in the table below:

Table 41: Composition of EsLeuDH-DM KM-value determination for hexanal (**8d**).

Solution	V/mL	Final concentration
Buffer (NH_4Cl, pH 9.5)	250	
NADH (5 mM)	10	0.2 mM
Enzym (purified enzyme)	10	58 µg
Acetophenone (**7a**): 0.5-25 mM		

The results for the activity assay are shown in th table below:

Table 42: Results of the EsLeuDH-DM K_M-value determination for hexanal (**8d**).

Conc./mM	U/mg
0.5	0.13
1	0.39
2	0.52
5	0.81
7.5	0.79
10	0.76
15	0.74
20	0.72
25	0.78

10.3.16 General operating procedure 18 (GOP18): Biotransformation with EsLeuDH-DM with aldehyds

The aldehyde was dissolved in ammonium chloride buffer (2 M, pH 9.5). EsLeuDH-DM was prepared according to GOP 10, cosubstrate (glucose, formate), NAD^+ and commercially available cbFDH (*Candida boidinii* formate dehydrogenase) (*Sigma Aldrich* F8649, lyophilized powder) or GDH were added and the mixture was incubated at 30 °C. The reaction solution was extracted with MTBE (3x 5 mL). The gas chromatographic analyses were performed with the GC-2010 Plus from *Shimadzu* with the autoinjector AOC-20i on the non-chiral column *Phenomenex* ZB-SMS. The temperature programs and retention times were shown in the table below:

Table 43: Temperature programs for gas chromatographic analysis of primary amines.

Substrate	Temperature program	R_t/min
Hexylamine (**9**)	50 °C, 3 °C/min to 80 °C, 30 °C/min to 220 °C	3.6
Octylamine (**10**)	120 °C, 10 °C/min to 300 °C	2.2
Cyclohexylamine (**5**)	3 °C/min to 80 °C, 30 °C/min to 220 °C	3.0
Butylamine	40 °C, 3 °C/min to 50 °C, 30 °C/min to 220 °C	4.6
2-Butylamine	40 °C, 3 °C/min to 50 °C, 30 °C/min to 220 °C	2.0

10.3.17 Biotransformation with EsLeuDH-DM and GDH

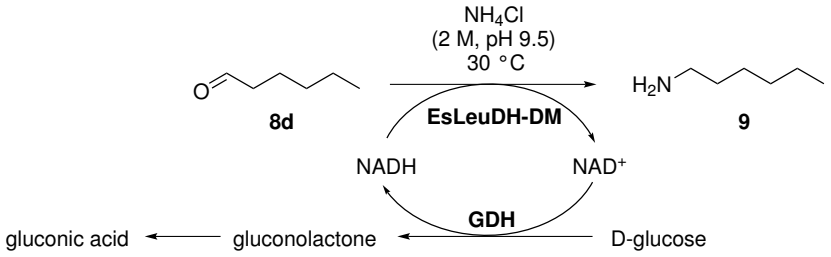

Hexanal (**8d**, 0.12 mg (1.20 µmol, 1 mM), 0.30 mg (3.00 µmol, 3 mM), 0.50 mg (5.00 µmol, 5 mM) was dissolved in ammonium chloride buffer (0.73 mL, 2 M, pH 9.5). EsLeuDH-DM (0.20 mL, 7.3 U, 1.5 U final activity), prepared according to GOP 10, glucose (33 µL, 1.5 M, 50 mM final concentration), NAD^+ (20 µL, 10 mM, 0.2 mM final concentration) and GDH (6 µL, 42 U) were added and the mixture was heated to 30 °C. The total volume of the reaction mixture was 1 mL. At fixed times, samples were taken (1/4/20/24 h). The reaction solution was extracted with MTBE (3x 1 mL). The conversion was measured *via* gas chromatography according to GOP 18.

Table 44: Kinetics for the biotransformation with hexanal (**8d**) and EsLeuDH-DM with glucose dehydrogenase (GDH) cofactor recycling system.

Conc./mM	Conv./% (1 h)	Conv./% (4 h)	Conv./% (20 h)	Conv./% (24 h)
1	6	27	71	84
3	4	32	68	80
5	0	22	-	74

10.3.18 Biotransformation with algae supernatant

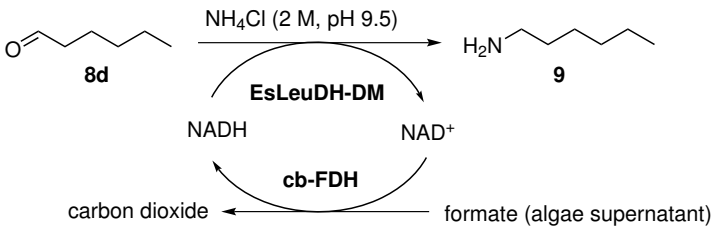

Hexanal (**8d**, 0.25 mg, 2.50 µmol), octanal (**8f**, 0.32 mg, 2.50 µmol), cyclohexanone (**8i**, 0.25 mg, 2.50 µmol) were dissolved in ammonium chloride buffer (1 mL, 100 mM, pH 9.5). EsLeuDH-DM (300 µL, 7.3 U, 2.2 U final) prepared according to GOP 10 was added to the reaction mixture. Algae supernatant (1 mL, 3 mM formate) was isolated according to literature[265] and kindly provided by Wobbe from Algae Biotechnology & Bioenergy Research Group was also added to the reaction mixture. NAD^+ (1 µL, 1 mM, 1 µmol final concentration) and commercially available cbFDH (*Sigma Aldrich* F8649, lyophilized powder, 5 mg, 3.30 U) were added and the reaction mixture, which was finally heated to 30 °C. The total volume of the reaction mixture was 2 mL. After 40 h the reaction was stopped. The reaction solution was extracted with MTBE (2x 1 mL). The conversion was measured *via* gas chromatography according to GOP 18.

Table 45: Results for biotransformations with algae supernatant and EsLeuDH-DM.

Substrate	Conv./%
Hexanal (**8d**)	>99
Octanal (**8f**)	>99
Cyclohexanone (**8i**)	>99

10.3.19 Biotransformations during algae fermentation, with various salt concentrations

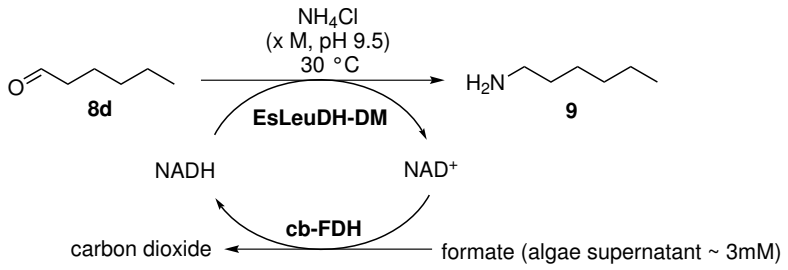

Hexanal (**8d**, 0.25 mg, 2.50 µmol) was dissolved in ammonium chloride buffer (1 mL, 248 mM, 122 mM, 50 mM, pH 9.5). EsLeuDH-DM ((300 µL, 7.3 U, 2.2 U final), prepared according to GOP 10, was added to the reaction mixture. Photoautrophically grown *C. reinhardtii* cells (1 mL, 3 mM formate, cell suspension in SUEOKA'S HIGH-SALT MEDIUM (HSM) medium; 10^8 cells) were prepared according to literature.[265] The algae was kindly provided by WOBBE from Algae Biotechnology & Bioenergy Research Group and added to the reaction mixture. Finally, NAD^+ (1 µL, 1 mM, 1 µmol final concentration) and commercially available cbFDH (*Sigma Aldrich* F8649, lyophilized powder, 5 mg, 3.30 U) were added and the reaction mixture was heated to 30 °C. After 40 h the reaction was stopped. The reaction solution was extracted with MTBE (2x 1 mL). The conversion was measured *via* gas chromatography according to GOP 18.

Table 46: Results for biotransformations during algae fermentation with various salt concentrations.

Conc./mM	Consumption/%
248	65
122	>99
50	>99
25	>99

10.3.20 Biotransformations during algae fermentation

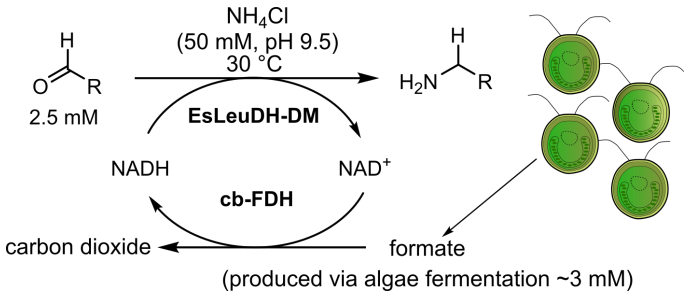

Hexanal (**8d**, 0.25 mg, 2.50 µmol) was dissolved in ammonium chloride buffer (1 mL, 100 mM, pH 9.5). EsLeuDH-DM (300 µL, 7.3 U, 2.2 U final), prepared according to GOP 10, was added to the reaction mixture. Photoautrophically grown *C. reinhardtii* cells (1 mL, 3 mM formate, cell suspension in Sueoka's high-salt medium (HSM) medium; 10^8 cells) prepared according to literature[265] and kindly provided by Wobbe from Algae Biotechnology & Bioenergy Research Group, were added as well. NAD^+ (1 µL, 1 mM, 1 µmol final concentration) and commercially available cbFDH (*Sigma Aldrich* F8649, lyophilized powder, 5 mg, 3.30 U) were finally added. The reaction mixture was heated to 30 °C. After 40 h the reaction was stopped. The reaction solution was extracted with MTBE (2x 1 mL). The conversion was measured *via* gas chromatography according to GOP 18.

Table 47: Results for biotransformations during algae fermentation with different substrates.

Sample	Consumption/%
Hexanal (**8d**) (1)	>99
Hexanal (**8d**) (2)	>99
Hexanal (**8d**) (3)	>99
Hexanal (**8d**) (4)	>99
Butanone (**8g**) (1)	>99
Butanone (**8g**) (2)	>99
Butanal (**8b**) (1)	>99
Butanal (**8b**) (2)	>99
Octanal (**8f**)	>99
Cyclohexanone (**8i**)	>99

10.3.21 Activity assay for FMOs

The activity assay was prepared according to GOP 14 and the composition for the activity assay was done to literature.[124] The enzymes were used in their purified form and kindly provided by Kruse from Algae Biotechnology & Bioenergy Research Group. All activity tests were performed with NADH unless otherwise specified. The composition for the assay is shown in the table below:

Table 48: Composition of FMO activity assay.

Solution	V/mL
Buffer (TRIS-HCl, pH 7.5, 50 mM 1 mM DTT, 1 mM EDTA 10 µM FAD, 10% glycerol, 5% 1,4-dioxane)	250
NADH (15 mM) or NADPH (15 mM)	5 (75 µM final concentration)
FMO (purified enzyme)	10 (36 µg L^{-1} final concentration)
3-Phenylcyclobutanone (**11a**) Cyclopentanone (**11b**) Cyclohexanone (**8i**) 3-Methylcyclohexanone (**11c**) 2-Heptanone (**11d**) Acetophenone (**7**) 4-Hydroxy-acetophenone (**11e**) Bicyclo[3.2.0]hept-2-en-6-one (**11f**) Camphor (**11g**) Cyclobutanone (**11h**) (1.25 mM)	10 (50 µM final concentration)

The results are shown in the following table:

Table 49: Results for the FMO activity test.

Substrate	Enzyme	U/mg
3-Phenylcyclobutanone (**11a**) (NADH)	*Ps*FMO-A	15 10^{-2}
3-Phenylcyclobutanone (**11a**) (NADH)	*Ps*FMO-B	3 10^{-2}
3-Phenylcyclobutanone (**11a**) (NADH)	*Ps*FMO-C	7 10^{-2}
3-Phenylcyclobutanone (**11a**) (NADPH)	*Ps*FMO-A	10 10^{-2}
3-Phenylcyclobutanone (**11a**) (NADPH)	*Ps*FMO-B	17 10^{-2}
3-Phenylcyclobutanone (**11a**) (NADPH)	*Ps*FMO-C	2 10^{-2}
Cyclopentanone (**11b**)	*Ps*FMO-A	0
Cyclopentanone (**11b**)	*Ps*FMO-B	0
Cyclohexanone (**8i**)	*Ps*FMO-A	24 10^{-2}
Cyclohexanone (**8i**)	*Ps*FMO-B	0
3-Metylcyclohexanone (**11c**)	*Ps*FMO-A	8 10^{-2}
3-Metylcyclohexanone (**11c**)	*Ps*FMO-B	0
2-Heptanone (**11d**)	*Ps*FMO-A	0
2-Heptanone (**11d**)	*Ps*FMO-B	0
Acetophenone (**7a**)	*Ps*FMO-A	12 10^{-2}
Acetophenone (**7a**)	*Ps*FMO-B	9 10^{-2}
4-Hydroxyacetophenone (**11e**)	*Ps*FMO-A	16 10^{-2}
4-Hydroxyacetophenone (**11e**)	*Ps*FMO-B	0
Bicyclo[3.2.0]hept-2-en-6-one (**11f**)	*Ps*FMO-A	40 10^{-2}
Bicyclo[3.2.0]hept-2-en-6-one (**11f**)	*Ps*FMO-B	0
Bicyclo[3.2.0]hept-2-en-6-one (**11f**)	*Ps*FMO-C	0
Camphor (**11g**)	*Ps*FMO-A	49 10^{-2}
Cyclobutanone (**11h**)	*Ps*FMO-A	27 10^{-2}

10.3.22 Composition of FMO K_M-value measurement for bicyclo[3.2.0]hept-2-en-6-one (11f)

The activity assay was done according to GOP 14. The enzymes were used in their purified form and kindly provided by Kruse from Algae Biotechnology & Bioenergy Research Group. The composition for the assay is shown in the table below:

Table 50: Composition of the FMO K_M-value measurement.

Solution	V/mL	Final concentration
Buffer (TRIS-HCl, pH 7.5, 50 mM, 1 mM DTT, 1 mM EDTA, 10 µM FAD, 10 % glycerol, 5 % 1,4-dioxane)	250	
NADH (5 mM)	10	0.2 mM
Enzym (purified enzyme)	10	36 µg L^{-1}

The results are shown in the following table:

Table 51: Results for the FMO K_M-value measurement.

Area	c/mM
523814	0.77
816340	1.35
1157884	2.16
2182956	3.9

10.3.23 General operating procedure 19 (GOP19): Biotransformation with FMO

Conversions were performed according to literature[124] in a total volume of 500 µL, with buffer (50 mM Tris/HCl pH 7.5, 10% glycerol, 1 mM DTT, 1 mM EDTA, 10 µM FAD), bicyclo[3.2.0]hept-2-en-6-one (**11f**) (5 mM final concentration) or cyclohexanone (**8i**) (5 mM final concentration), (5%, 1,4-dioxane, *(*v/v), NAD^+ (100 µM), glucose (20 mM, final concentration), GDH (2 U) and crude extract of the purified FMO 1534 (0.18 mg mL^{-1}), which were kindly provided by Kruse from Algae Biotechnology & Bioenergy Research Group.

The reaction solutions were shaken at 25 °C for 66 h. The gas chromatographic analyses were performed with the GC-2010 Plus from *Shimadzu* with the autoinjector AOC-20i on the non-chiral column *Phenomenex* ZB-SMS.

The injector and detector temperatures were set to 300 °C, and the column flow was 2.30 mL min^{-1} with a pressure of 144.0 kPa and a split ratio of 15. GC analysis for the determination of enantioselectivity was conducted using a *MN Lipodex E* chiral column. The injector and detector temperatures were set to 220 °C, and the column flow was 1.86 mL min^{-1} with a pressure of 112.8 kPa and a split ratio of 1. The consumption of the substrate bicyclo[3.2.0]hept-2-en-6-one (**11f**) was calculated by means of a standard curve ranging from 0.5 to 4 mM.

Table 52: GC analysis programs for **11f** and ϵ-caprolactone.

Substrate	analytic	Temperature program	R_t/min
11f	Conv.[a]	40 °C, 30 °C min^{-1} to 280 °C	2.2
11f	*ee*[b]	60 °C , 10 °C min^{-1} to 130 °C (15 min)	(-)-**11f** 20.5
		20 °C min^{-1} to 200 °C (4 min)	(+)-**11f** 21.0
			(+)-**11f**$_N$ 31.6
			(-)-**11f**$_{ABN}$ 32.9
			(-)-**11f**$_N$ 33.3
			(+)-**11f**$_{ABN}$ 34.5[c]
ϵ-Caprolactone	Conv.[a]	50 °C, 3 °C min^{-1} to 110 °C	22.9
		25 °C $^{-1}$ to 200 °C	

[a] Conversion, [b] Enantiomeric excess, [c] Absolute configurations of products were determined on the basis of literature data[131]

10.3.24 Biotransformation with FMOs and GDH with purified enzyme

Reactions were performed according to GOP 19 in a total volume of 500 µL, with 398 µL buffer (50 mM Tris/HCl pH 7.5, 10% glycerol, 1 mM DTT, 1 mM EDTA, 10 µM FAD), bicyclo[3.2.0]hept-2-en-6-one (**11f**) (5 mM final concentration) or cyclohexanone (**8i**) (5 mM final concentration), (5%, 1,4-dioxane, *v/v*), NAD^+ (100 µM), glucose (20 mM, final concentration), GDH (5 µL, 2 U) and crude extract of the purified FMO 1534 (50 µL, 0.18 mg mL^{-1}). The reactions were shaken at 25 °C for 66 h.

10.3.25 Biotransformation with FMOs and GDH with crude extract (reaction 1)

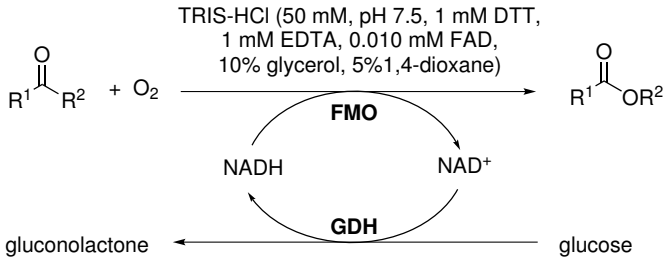

Reactions were performed according to GOP 19 in a total volume of 700 µL, with 386 µL buffer (50 mM Tris/HCl pH 7.5, 10% glycerol, 1 mM DTT, 1 mM EDTA, 10 µM FAD),bicyclo[3.2.0]hept-2-en-6-one (**11f**) (5 mM final concentration) or cyclohexanone (**8i**) (5 mM final concentration), (5%, 1,4-dioxane, *v/v*), NAD^+ (100 µM), glucose (20 mM, final concentration), GDH (5 µL, 2 U) and crude extract of the PsFMO-A (250 µL, 0.18 mg mL^{-1}). The reactions were carried out at 25 °C for 66 h.

10.3.26 Biotransformation with FMOs, FDH and commercially available formate (reaction 2)

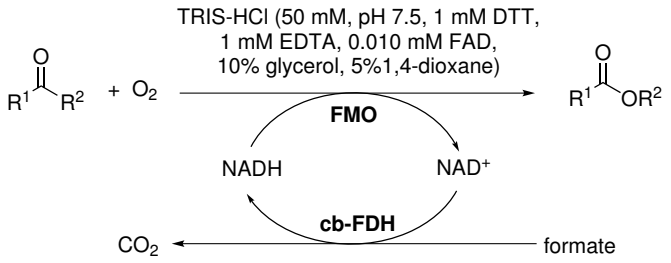

Reactions were performed according to GOP 19 in a total volume of 557 µL with 398 µL buffer (50 mM Tris/HCl pH 7.5, 10% glycerol, 1 mM DTT, 1 mM EDTA, 10 µM FAD), bicyclo[3.2.0]hept-2-en-6-one (**11f**) (2.5 mM final concentration), (5%, 1,4-dioxane, *v/v*), NAD^+ (100 µM), formate (5 mM, final concentration), commercially available cbFDH (*Sigma Aldrich* F8649, lyophilized powder, 2 mg, 1.7 U).

Finally, purified PsFMO-A 1534 (50 µL, 0.18 mg mL^{-1}) was added. The reactions were carried out at 25 °C for 66 h.

10.3.27 Biotransformation with FMOs, FDH and algae supernatant (reaction 3)

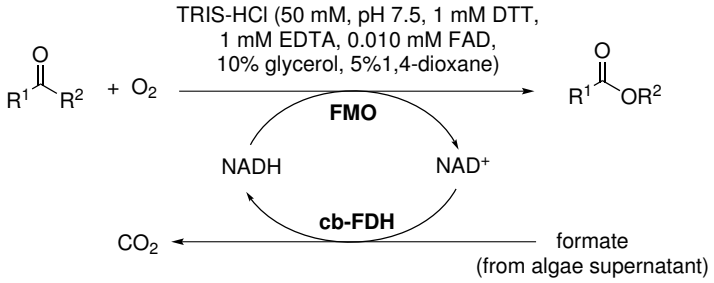

Reactions were performed according to GOP 19 in a total volume of 500 µL with 378 µL buffer (50 mM Tris/HCl pH 7.5, 10% glycerol, 1 mM DTT, 1 mM EDTA, 10 µM FAD), bicyclo[3.2.0]hept-2-en-6-one (**11f**) (2.5 mM final concentration), (5%, 1,4-dioxane, *v/v*), NAD^+ (100 µM), algae supernatant (1 mL, 3 mM, end concentration), commercially available cbFDH (*Sigma Aldrich* F8649, lyophilized powder, 2 mg, 1.7 U) and purified PsFMO 1534 (50 µL, 0.18 mg mL^{-1}). The reactions were carried out at 25 °C for 66 h.

Table 53: Regiodivergent oxidation of racemic bicyclo[3.2.0]hept-2-en-6-one (**11f**).

Reaction	Consumption/% (N/ABN)	ee_N/% ee_{ABN}/%
1	89	99 (1*R*,5*S*)
	1.5:3	30 (1*R*,5*S*)
2	85	99 (1*R*,5*S*)
	1.5:3.5	34 (1*R*,5*S*)
3	94	99 (1*R*,5*S*)
	2:3	57 (1*R*,5*S*)

10.4 Experimental part for fatty acid hydratases

10.4.1 General operating procedure 20 (GOP20): Biotransformation with fatty acid hydratase

For the reaction hydratase (crude extract prepared according to GOP 10 or whole cells) was added with fatty acid, fatty acid ester or sunflower oil to buffer (50 mM, pH 6.3). The reactions were stirred for at 35 °C and monitored by TLC (R_f= 0.4 (Cyclohexane/EtOAc/AcOH 3:1:0.5, *v/v*). The crude product was extracted with $CDCl_3$ (2x 700 µL) and analyzed by the means of ^{1}H NMR-spectroscopy.

10.4.2 Enzymatic reactions towards hydroxy-substituted fatty acids in analytical scale

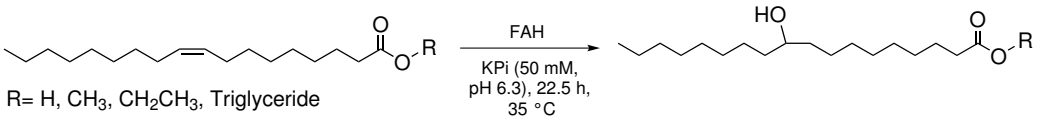

For the reaction hydratase (100 µL crude extract prepared according to GOP 10, 15 mg mL^{-1} protein concentration or 100 mg whole cells) were added with fatty acid, fatty acid ester or sunflower oil (20 mM) in KPi buffer (50 mM, pH 6.3, 1 mL final volume). For the reaction with Lp-Lhy NADH (25 µmol) and FAD (0.1 µmol) were used. The reactions were stirred for 22.5 h at 35 °C and 850 rpm and monitored by TLC (R_f= 0.4 (Cyclohexane/EtOAc/AcOH 3:1:0.5, *v/v*). The crude product was extracted with $CDCl_3$ (2x 700 µL) and analyzed by the means of ^{1}H NMR-spectroscopy. For the analytics of the hydroxylated poly-unsaturated fatty acids, (*Z*)-10-hydroxyoctadec-12-enoic acid (**18**) and (*Z*)-13-hydroxyoctadec-9-enoic acid (**14**) were purified by the means of preparative TLC (Cyclohexane/EtOAc/AcOH, 3:1:0.5, *v/v*) and subsequently analyzed *via* ^{1}H NMR-spectroscopy. For the esters and the oil no conversion was detected.

Table 54: Composition of fatty acid hydratase reactions in analytic scale for fatty acids.

Hydratase	Substrate	Formulation	NADH	FAD	Conv/%
Lp-Lhy	**13**	whole cells	25 mmol $\cdot L^{-1}$	0.1 mmol $\cdot L^{-1}$	83
Sn-Ohy	**15**	crude extract	-	-	> 99
Em-Ohy	**15**	crude extract	-	-	> 99
La-Lhy	**13**	crude extract	-	-	79

10-Hydroxyoctadecanoic acid (12)

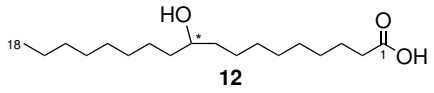

12

$C_{18}H_{36}O_3$

300.27 g mol^{-1}

^{1}H-NMR (500 MHz, $CDCl_3$): δ[ppm]= 3.61 (m, 1H, (C10)*H*), 2.37 (t, ^3J= 7.5 Hz, 2H, (C2)*H*), 1.66 (q, ^3J= 7.2 Hz, 2H, (C3)*H*), 1.47 (m, 4H, (C8,11)*H*), 1.31 (m, 22H, H_{alkyl}), 0.90 (t, ^3J= 6.8 Hz, 3H, (C18)*H*).

The spectroscopical data corresponds to the literature data.[266]

(*Z*)-10-Hydroxyoctadec-12-enoic acid (18)

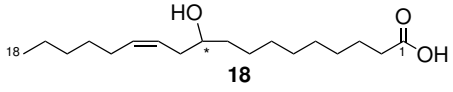

18

$C_{18}H_{34}O_3$

298.25 g mol^{-1}

^{1}H-NMR (500 MHz, $CDCl_3$): δ[ppm]= 5.64 – 5.54 (m, 1H, *H12,13*), 5.48 – 5.38 (m, 1H, (C12,13)*H*), 3.64 (p, ^3J= 6.1 Hz, 1H, (C10)*H*), 2.37 (t, ^3J= 7.5 Hz, 2H, (C2)*H*), 2.24 (t, ^3J= 6.8 Hz, 2H, (C11)*H*), 2.07 (m, 2H, (C14)*H*), 1.66 (p, ^3J= 7.6 Hz, 2H, (C3)*H*), 1.48 (h, ^3J= 8.2, 6.8 Hz, 2H, (C9)*H*), 1.43 – 1.31 (m, 16H, H_{alkyl}), 0.91 (t, ^3J= 6.8 Hz, 3H, (C18)*H*).

The spectroscopical data corresponds to the literature data.[165]

(*Z*)-13-Hydroxyoctadec-9-enoic acid (14)

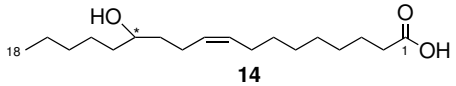

14

$C_{18}H_{34}O_3$

298.25 g mol^{-1}

^{1}H-NMR (500 MHz, $CDCl_3$): δ[ppm]= 5.38 (q, ^3J= 6.6 Hz, 2H, (C9,10)*H*), 3.66 – 3.60 (m, 1H, (C13)*H*), 2.35 (t, ^3J= 7.2 Hz, 2H, (C2)*H*), 1.70 – 1.62 (m, 2H, (C3)*H*), 1.49 – 1.41 (m, 2H, (C8)*H*), 1.33 (s, 20H, H_{alkyl}), 0.89 (t, ^3J= 6.4 Hz, 3H, (C18)*H*).

The spectroscopical data corresponds to the literature data.[177]

10.4.3 Enzymatic reactions towards hydroxy-substituted fatty acids, kinetic studies

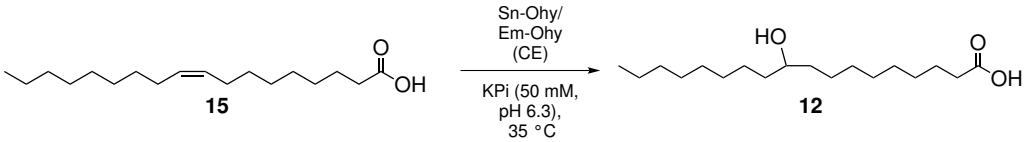

15 **12**

For the reaction (prepared according to GOP 20) hydratase (50 µL crude extract prepared according to GOP 10, 15 mg mL^{-1} protein concentration), was dissolved with fatty acid (**15**, 2.82 mg, 0.01 mmol, 10 mM) in KPi buffer (50 mM, pH 6.3, 5% isopropanol (*v/v*), 1 mL final volume). The reactions were incubated for 5/15/30/45/60/150/240/360 min at 35 °C and 850 rpm. The crude product was extracted with $CDCl_3$ (2x 700 µL) and analyzed by the means of ^{1}H NMR-spectroscopy.

The results are shown in the table below:

Table 55: Results for Sn-Ohy and Em-Ohy kinetics.

Reaction	t/min	Conv.(Sn-Ohy)/%	Conv.(Em-Ohy)/%
1	5	7	10
2	15	7	13
3	30	16	23
4	45	26	37
5	60		44
6	150		79
7	240	46	96
3	360	44	96

10.4.4 Cosolvent screening for Em-Ohy and Sn-Ohy

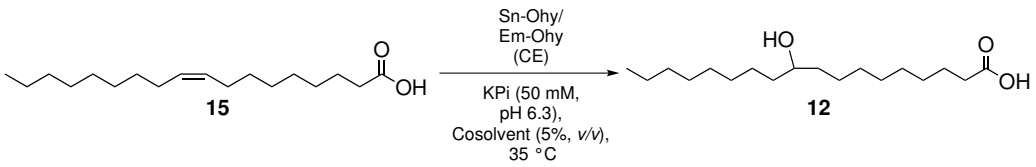

For the reaction (prepared according to GOP 20) hydratase (50 µL crude extract prepared according to GOP 10, 15 mg mL^{-1} protein concentration) was dissolved in KPi buffer (50 mM, pH 6.3, 1 mL final volume, the addition of 5% cosolvent and the addition of 25 µM NADH and 25 µM FAD or no addition of cofactor). The reaction solution was incubated for 22 h. After incubation fatty acid (**15**, 2.78 mg, 10 mM) was added and the reaction performed for 60 minutes at 35 °C and 850 rpm. The crude product was extracted with $CDCl_3$ (2x 700 µL) and analyzed by the means of ^{1}H NMR-spectroscopy.

The results are shown in the table below:

Table 56: Results for Sn-Ohy and Em-Ohy colsolvent screening.

Cosolvent	Conv.(Sn-Ohy)/%	Conv.(Em-Ohy)/%
DMSO	65	72
Isopropanol	45	46
Isopropanol + Cofactors	30	57
Cyclohexane	0	0
MTBE	0	19

10.4.5 Enzymatic reactions towards hydroxy-substituted fatty acids, parameter study for Em-Ohy

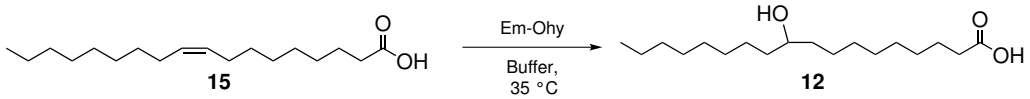

For the reaction (prepared according to GOP 20) Em-Ohy crude extract prepared according to GOP 10 (100 µL, 15 mg mL^{-1} protein concentration) or whole cells (40 mg), were added with oleic acid (**15**, 99% purity, 2.78 mg, 0.01 mmol, 10 mM) to buffer (50 mM, pH 6.3, 5% DMSO, 1 mL final volume). The reactions were incubated for 60 min at 35 °C and 850 rpm. The crude product was extracted with $CDCl_3$ (2x 700 µL) and analyzed by the means of ^1H NMR-spectroscopy. The composition of the reactions are shown in the table below:

Table 57: Reaction composition of Em-Ohy in different solvents.

Reaction-Nr.	Component	Volume
1	KPi buffer (50 mM, pH 6.3, 5% DMSO, *v/v*)	850 µL
	Crude extract	100 µL
2	KPi buffer (50 mM, pH 6.3, 5% DMSO, *v/v*)	830 µL
	NADH (2.5 mM)	10 µL
	FAD (0.2 mM)	10 µL
	Crude extract	100 µL
3	Citrate buffer (50 mM, pH 6.3, 5% DMSO, *v/v*)	850 µL
	Crude extract	100 µL
4	KPi buffer (50 mM, pH 6.3, 5% DMSO, *v/v*)	
	Whole cells	40 mg
5	KPi buffer (50 mM, pH 6.3, 5% DMSO, *v/v*)	
	Whole cells	40 mg
	Glucose (2.5 M)	20 µL

The results are shown in the table below:

Table 58: Results of Em-Ohy in different solvents.

Reaction-Nr.	Conv./%
1	53
2	28
3	53
4	22
5	53

10.4.6 Enzymatic reactions towards hydroxy-substituted fatty acids, parameter study for Sn-Ohy

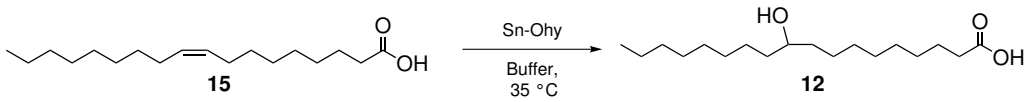

For the reaction (prepared according to GOP 20) Sn-Ohy crude extract prepared according to GOP 10 (100 µL, 15 mg mL^{-1} protein concentration) or whole cells (40 mg), were added with oleic acid (**15**, 99% purity, 2.78 mg, 0.01 mmol, 10 mM) to buffer (50 mM, pH 6.3, 5% DMSO, 1 mL final volume). The reactions were incubated for 60 min at 35 °C and 850 rpm. The crude product was extracted with $CDCl_3$ (2x 700 µL) and analyzed by the means of ^1H NMR-spectroscopy. The compositions of the reactions are shown in the table below:

Table 59: Reaction composition of Sn-Ohy in different solvents.

Reaction-Nr.	Component	Volume
1	KPi buffer (50 mM, pH 6.3, 5% DMSO, *v/v*)	850 µL
	Crude extract	100 µL
2	KPi buffer (50 mM, pH 6.3, 5% DMSO, *v/v*)	830 µL
	NADH (2.5 mM)	10 µL
	FAD (0.2 mM)	10 µL
	Crude extract	100 µL
3	Citrate buffer (50 mM, pH 6.3, 5% DMSO, *v/v*)	850 µL
	Crude extract	100 µL
4	KPi buffer (50 mM, pH 6.3, 5% DMSO, *v/v*)	
	Whole cells	40 mg
5	KPi buffer (50 mM, pH 6.3, 5% DMSO, *v/v*)	
	Whole cells	40 mg
	Glucose (2.5 M)	20 µL

The results are shown in the table below:

Table 60: Results of Sn-Ohy in different solvents.

Reaction-Nr.	Conv./%
1	11
2	67
3	36
4	10
5	15

10.4.7 Oleate hydratase catalyzed reaction with poly-unsaturated fatty acids and Em-Ohy

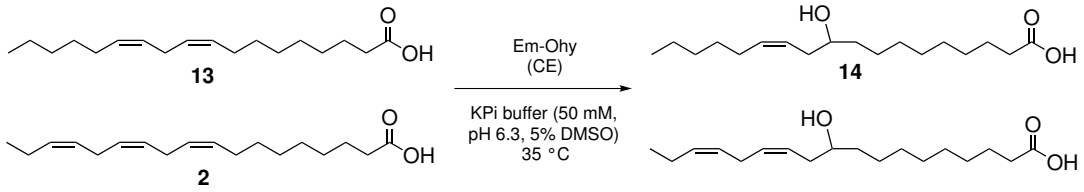

Linoleic acid (**13**) or linolenic acid (**2**) (5.6 mg, 0.02 mmol, 20 mM) were dissolved in DMSO (50 µL). Afterwards, KPi buffer (pH 6.3, 100 mM, 850 µL), Em-Ohy crude extract prepared according to GOP 10 (100 µL, 15 mg mL^{-1} protein concentration) were added to the reaction mixture and stirred at 35 °C and 850 rpm for 0.5/1/6/23 h. The crude product was extracted with $CDCl_3$ (2x 700 µL) and analyzed by the means of ^1H NMR-spectroscopy. The results are shown in the table below:

Table 61: Results for the conversion of linoleic acid (**13**) or linolenic acid (**2**) using Em-Ohy.

t/h	Linolic acid (**13**) Conv./%	Linolenic acid (**2**) Conv./%
0	0	0
0.5	7	6
1	11	15
6	11	15
23	13	17

10.4.8 Oleate hydratase catalyzed reaction with poly-unsaturated fatty acids and Sn-Ohy

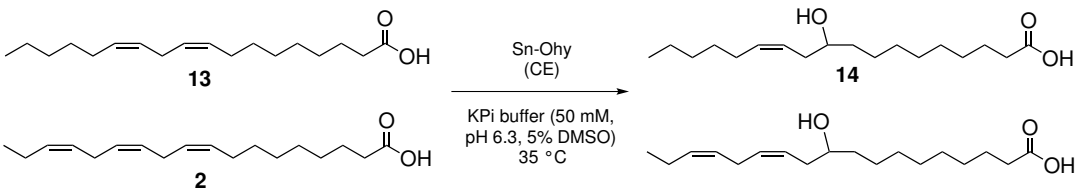

Linoleic acid (**13**) or linolenic acid (**2**) (5.6 mg, 0.02 mmol, 20 mM) were dissolved in DMSO (50 µL). Afterwards, KPi buffer (pH 6.3, 100 mM, 850 µL), Sn-Ohy crude extract prepared according to GOP 10 (100 µL, 15 mg mL^{-1} protein concentration) were added to the reaction mixture and stirred at 35 °C and 850 rpm for 0.5/1/6/23 h. The crude product was extracted with $CDCl_3$ (2x 700 µL) and analyzed by the means of ^1H NMR-spectroscopy. The results are shown in the table below:

Table 62: Results for the conversion of linoleic acid (**13**) or linolenic acid (**2**) using Sn-Ohy.

t/h	Linoleic acid (**13**) Conv./%	Linolenic acid (**2**) Conv./%
0	0	0
0.5	38	24
1	38	39
6	45	31
23	43	42

10.4.9 Oleate hydratase stability tests at different incubation times

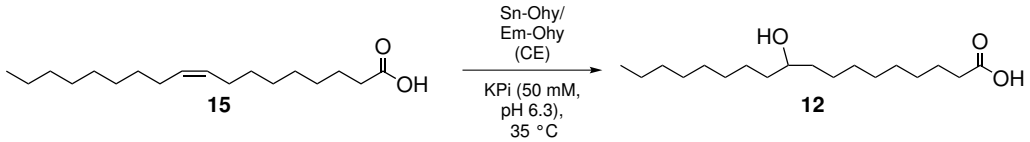

The reaction was performed according to GOP 20. KPi buffer (pH 6.3, 100 mM, 850 µL) and oleate hydratase crude extract, prepared according to GOP 10, (100 µL, protein concentration 15 mg mL^{-1}) were given together.

The reaction was stirred at 35 °C for 1.35/3.35/5.50/22/46 h. Afterward, oleic acid (**15**, 90% purity, 5.6 mg, 0.019 mmol, 20 mM) was added to DMSO (50 µL, 5%, *v/v*) and given to the reaction solution. The reaction was stirred for one hour, at 35 °C and 850 rpm. The crude product was extracted with $CDCl_3$ (2x 700 µL) and analyzed by the means of ^{1}H NMR-spectroscopy.

Table 63: Reaction conditions and results for oleate hydatase stability tests at different incubation times.

t/h	Conv.(Em-Ohy)/%	Conv.(Sn-Ohy)/%
1.35	43	33
3.35	37	30
5.5		26
22	26	14
46	6	0

10.4.10 Oleate hydratase stability tests at different storage temperatures

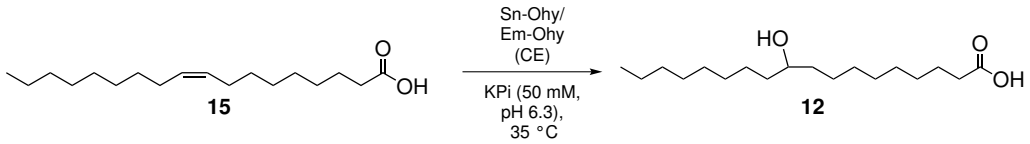

The reaction was performed according to GOP 20. KPi buffer (pH 6.3, 100 mM, 850 µL), and oleate hydratase crude extract, prepared according to GOP 10, (100 µL, protein concentration 15 mg mL^{-1}) given together and stored at 4/10/20/-20 °C for 22 h. Afterwards, oleic acid (**15**, 90% purity, 5.6 mg, 0.019 mmol, 20 mM) was dissolved in DMSO (50 µL, 5%, (*v/v*)) and given to the reaction mixture. The reaction was stirred for one hour at 35 °C. The crude product was extracted with $CDCl_3$ (2x 700 µL) and analyzed by the means of ^{1}H NMR-spectroscopy.

Table 64: Reaction conditions and results for oleate hydatase stability tests at different storage temperatures.

T/°C	Conv.(Em-Ohy)/%	Conv.(Sn-Ohy)/%
-20	35	32
4	42	61
10	38	47
20	45	47

10.4.11 Enzymatic reactions towards hydroxy-substituted fatty acids, influence of NaCl

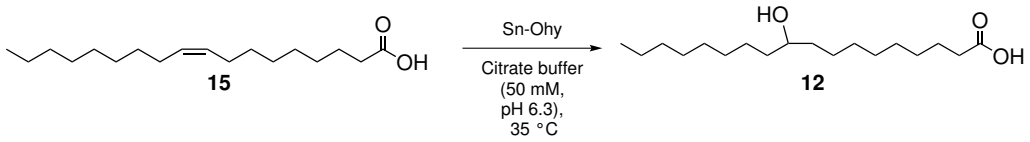

The reactions were performed according to GOP 20. Oleic acid (**15**, 99% purity, 10 mg, 0.04 mmol, 40 mM) was dissolved in citrate buffer (890 µL, pH 6.3, 50 mM, with the addition of 50 mM NaCl or without NaCl) and Sn-Ohy crude extract, prepared according to GOP 10, (100 µL, protein concentration 30 mg mL^{-1}) was added to the reaction mixture. The reaction mixture was stirred for 2 h at 35 °C. The crude product was extracted with $CDCl_3$ (2x 700 µL) and analyzed by the means of ^1H NMR-spectroscopy.

Table 65: Reaction conditions and results for oleate hydatase stability tests with NaCl influence.

Component	Conv./%
Without NaCl	48
With NaCl	52

10.4.12 Enzymatic reactions towards hydroxy-substituted fatty acids, influence purity

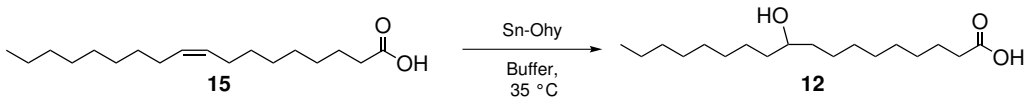

The reactions were performed according to GOP 20. Oleic acid (**15**, 99% purity or 90% purity, 10 mg, 0.04 mmol, 40 mM) was added to citrate buffer (890 µL, pH 6.3, 50 mM) and Sn-Ohy crude extract, prepared according to GOP 10, (100 µL, protein concentration 30 mg mL^{-1}) was added to the reaction mixture. The reaction mixture was stirred for 2 h at 35 °C. The crude product was extracted with $CDCl_3$ (2x 700 µL) and analyzed by the means of ^1H NMR-spectroscopy.

Table 66: Results for the influence of the oleic acid **15** purity.

Component	Conv./%
90% oleic acid (**15**) purity	26
99% oleic acid (**15**) purity	25

10.4.13 Sn-Ohy reaction kinetics in different buffers

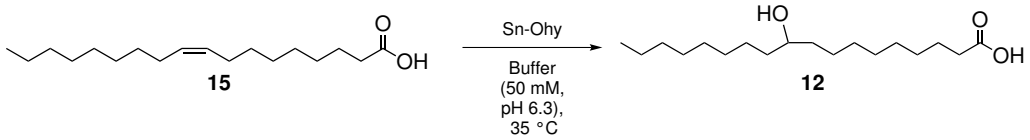

The reaction were performed according to GOP 20. Buffer (pH 6.3, 100 mM, 850 µL), oleate hydratase crude extract prepared according to GOP 10 or whole cells (2 mL crude extract, protein concentration 30 mg mL^{-1}, whole cells 500 mg) and oleic acid (**15**, 90% purity, 1.1 g, 3.89 mmol) were added to the reaction mixture and stirred at 35 °C for 24 h or 48 h.

The crude product was extracted with toluene (90 mL) dried over $MgSO_4$ and the solvent was removed *in vacuo*. The crude product was analyzed by the means of ^1H NMR-spectroscopy.

Table 67: Reaction conditions and results for oleate hydratase scale-up experiment.

t/h	Buffer	Conv./% (Crude extract)	Conv./% (Whole cells)
24 (4 mmol **15**)	KPi	66	55
48 (4 mmol **15**)	KPi	84	78
24 (4 mmol **15**)	Citrate	86	64
48 (4 mmol **15**)	Citrate	83	90
48 (40 mmol **15**)	Citrate	87	48

10.4.14 Immobilization of Sn-Ohy on hydrophobic carrier

The immobilization was done according to GOP 17 and the immobilized enzyme stored at 4 °C.

10.4.15 Immobilization of Sn-Ohy on hydrophobic carrier with different ratios

The immobilization was done according to GOP 17 and the immobilized enzyme stored at 4 °C. The purchased carrier material from *Lewatit*® VP OC 1600 (550 mg) was first washed in a ratio of about 1:1 (*w/v*, carrier:buffer) with KPi buffer (pH 7.5, 50 mM). Subsequently, crude extract, prepared according to GOP 10, (30 mg mL^{-1} in KPi buffer, pH 6.3, 50 mM) was added in different ratios (1:4, 1:9, 1:15, 1:20 enzyme:carrier, *w/w*) to the washed carrier material and immobilized for 18 h at 20 °C and 80 rpm. The supernatant was removed and the carrier was washed in a ratio of about 1:1 (*w/v*, carrier:buffer) with KPi buffer (pH 7.5, 10 mM). The protein concentration in the supernatant was determined by means of a Bradford assay (see GOP 11).

Table 68: Results of immobilization on hydrophobic carrier with different ratios.

Reaction-Nr.	Carrier	Loading/%
1	1:4	55
2	1:9	53
3	1:15	72
4	1:20	67

10.4.16 Immobilization of Sn-Ohy on hydrophobic carrier at different immobilization times

The immobilization was done according to GOP 17 and the immobilized enzyme stored at 4 °C. The purchased carrier material from *Lewatit*® VP OC 1600 (550 mg) was first washed in a ratio of about 1:1 (*w/v*, carrier:buffer) with KPi buffer (pH 7.5, 50 mM). Subsequently, crude extract prepared according to GOP 10 (30 mg mL^{-1} in KPi buffer, pH 6.3, 50 mM) in different ratios (1:9, 1:15 enzyme:carrier, *w/w*) was added to the washed carrier material and immobilized for 18 h or 24 h at 20 °C and 80 rpm. The supernatant was removed and the carrier was washed in a ratio of about 1:1 (*w/v*, carrier:buffer) with KPi buffer (pH 7.5, 10 mM). The protein concentration in the supernatant was determined by means of a Bradford assay (see GOP 11).

Table 69: Results of immobilization on hydrophobic carrier with different immobilization times.

Reaction-Nr.	Carrier	Loading/%
5	1:9	72
6	1:15	70

10.4.17 Immobilization on hydrophobic carrier at different immobilization rate

The immobilization was done according to GOP 17 and the immobilized enzyme stored at 4 °C. The purchased carrier material from *Lewatit*® VP OC 1600 (550 mg) was first washed in a ratio of about 1:1 (*w/v*, carrier:buffer) with KPi buffer (pH 7.5, 50 mM).

Subsequently, crude extract prepared according to GOP 10 (30 mg mL^{-1}, in KPi buffer, pH 6.3, 50 mM) in a ratio 1:9 (enzyme:carrier, *w/w*) was added to the washed carrier material and immobilized for 18 h at 20 °C and 80 rpm or 180 rpm. The supernatant was removed and the carrier was washed in a ratio of about 1:1 (*w/v*, carrier:buffer) with KPi buffer (pH 7.5, 10 mM). The protein concentration in the supernatant was determined by means of a BRADFORD assay (see GOP 11).

Table 70: Results of immobilization on hydrophobic carrier with different immobilization rates.

Reaction-Nr.	Shaking rate/rpm	Loading/%
7	80	85
8	160	80

10.4.18 Immobilized enzymatic reactions towards hydroxy-substituted fatty acids (hydrophobic carrier) – analytic scale

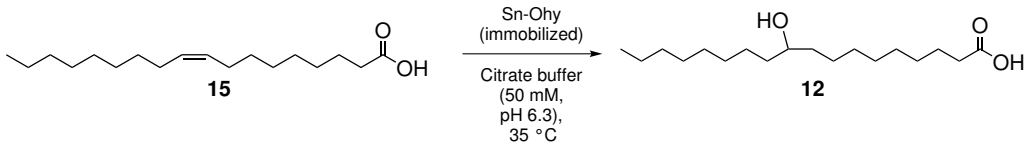

The immobilized enzyme (550 mg immobilized enzymes on *Lewatit*® VP OC 1600) was prepared according GOP 17. For the reaction 0.9 µL (3.54 µmol) oleic acid (**15**, 90% purity)/mg immobilized enzyme was used. The immobilized enzyme (550 mg immobilized enzymes on *Lewatit*® VP OC 1600) was added to citrate buffer (100 µL buffer/µL substrate, 50 mM, pH 6.3). The reaction was done for 24 h at 35 °C.

The results are shown in the table below:

Table 71: Results of hydration reaction of **15** on hydrophobic carrier with different parameters.

Reaction-Nr.	Conv./%
1	40
2	53
3	64
4	-
5	63
6	35
7	85
8	80

10.4.19 Immobilized enzymatic reactions towards hydroxy-substituted fatty acids (hydrophobic carrier) – preparative scale

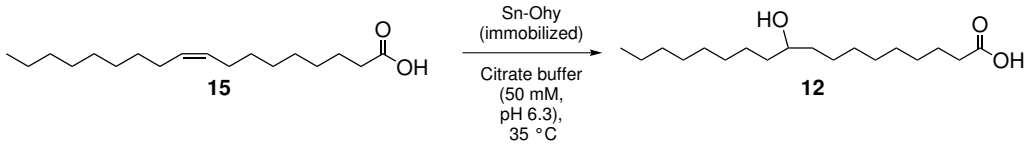

The immobilized carrier (or 7 g (reaction 1) or 14 g (reaction 2), 97 mg/g enzyme/carrier) was prepared according GOP 17. For the reaction oleic acid (**15**, 90% purity, 39.7 g, 0.14 mol) was diluted in citrate buffer (95 mL, pH 6.3, 50 mM). The reaction was done for 48 h at 35 °C, afterwards the crude product **12** was filtered and washed with warm MTBE (2x 20 mL). The solid colorless crude product was dried in *vacuo*, and analyzed by means of ^{1}H NMR-spectroscopy. The results are shown in the table below:

Table 72: Results of hydration reaction of **15** with Sn-Ohy in preparative scale.

Reaction	Conv./%
1	59
2	46

10.4.20 General operating procedure 21 (GOP21): *SpinChem*® reactor reactions

The immobilized enzyme (97 mg/g enzyme/carrier) was prepared according GOP 17. For the reaction oleic acid (**15**, 90% purity) was diluted in citrate buffer (100 mL, pH 6.3, 50 mM). The carrier was stored in the *SpinChem*® rotating bed reactor. The reaction was done at 35 °C, afterwards a sample (5 mL) was isolated, the water removed *in vacuo* and analyzed by the means of ^{1}H NMR-spectroscopy.

10.4.21 Immobilized enzymatic reactions towards hydroxy-substituted fatty acids (hydrophobic carrier) – *SpinChem*® reactor reactions

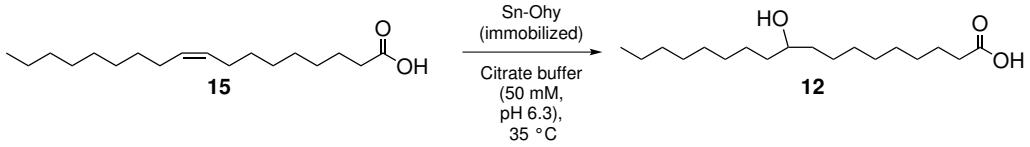

The immobilized enzyme (97 mg/g enzyme/carrier) was prepared according GOP 17. For the reaction oleic acid (**15**, 90% purity) was diluted in citrate buffer (100 mL, 50 mM, pH 6.3) or either dosed into the buffer. The carrier was stored in the *SpinChem*® rotating bed reactor. The reaction was done at 35 °C. Reaction 1-3 were stirred for 48 h, reaction 4 was stirred for 96 h. Afterwards, a sample (5 mL) was isolated, the water removed *in vacuo* and analyzed by the means of ^{1}H NMR-spectroscopy.

Table 73: Results of hydration reaction of **15** using *SpinChem*® reactor.

Nr.	Carrier/g	Substrate **15**/g	rpm	Dosing/mL min^{-1}	Glassballs	Conv./%
1	17.7	17.9 (63.3 mmol)	400	no	no	2
2	7.3	7.7 (27.3 mmol)	400	no	no	7
3	7.0	8.9 (31.5 mmol)	400	7.0 10^{-3}	no	<1
4	4.0	8.9 (31.5 mmol)	850	3.5 10^{-4}	yes	42

10.4.22 Modification of hydroxy fatty acids

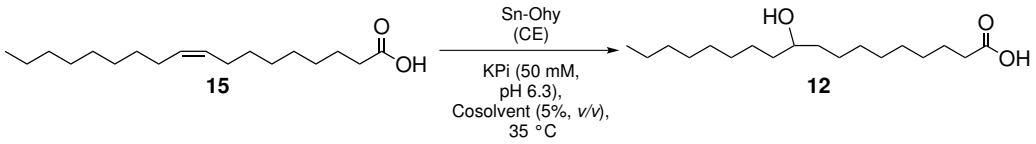

Oleic acid (**15**, 90% purity, 52 g, 0.18 mol) was dissolved in DMSO (12.5 mL). Afterward, KPi buffer (237.5 mL, pH 6.3, 100 mM), Sn-Ohy crude extract, prepared according to GOP 10, (20 mL, protein concentration 15 mg mL^{-1}) were added. The suspension was stirred at 35 °C for six days. The crude product was filtered and washed with dichloromethane (20 mL). Afterward, the crude product **12** was recrystallized from dichloromethane (50 mL) and dried *in vacuo*. 10-Hydroxystearic acid (**12**) was isolated with a yield of 31% (15 g, 50 mmol) and the formation of the product **12** analyzed *via* ^{1}H NMR-spectroscopy.

^{1}H-NMR (500 MHz, $CDCl_3$): δ[ppm]= 3.61 (m, 1H, (C10)H), 2.37 (t, ^3J= 7.5 Hz, 2H, (C2)H), 1.66 (q, ^3J= 7.2 Hz, 2H, (C3)H), 1.47 (m, 4H, (C8,11)H), 1.31 (m, 22H, H_{alkyl}), 0.90 (t, ^3J= 6.8 Hz, 3H, (C18)H).

The spectroscopical data corresponds to the literature data.[266]

10.4.23 Modification of hydroxy fatty acids - dosing experiment

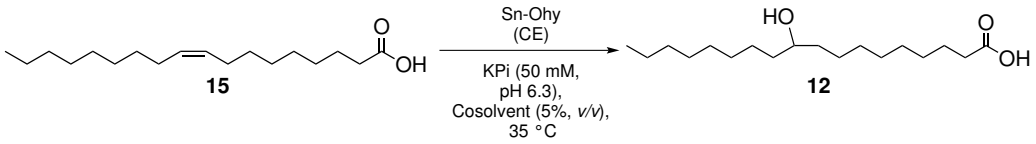

Oleic acid (**15**, 90% purity, 11 g, 0.04 mol) was dissolved in DMSO (5 mL). Afterward, KPi buffer (95 mL, pH 6.3, 100 mM), Sn-Ohy crude extract, prepared according to GOP 10, (7.3 mL, protein concentration 15 mg mL^{-1}) was dissolved in the reaction mixture and stirred for 35 °C for 7 h, afterward again Sn-Ohy crude extract prepared according to GOP 10 (3.5 mL, protein concentration 15 mg mL^{-1}) was added and after 14 h again Sn-Ohy crude extract prepared according to GOP 10 (8.5 mL, protein concentration 15 mg mL^{-1}) was added. The reaction mixture was stirred for 21 h at 35 °C. The crude product was filtered and washed with MTBE (20 mL). Afterward, the crude product **12** was recrystallized from MTBE (50 mL) and dried *in vacuo*. 10-Hydroxystearic acid (**12**) was isolated with a yield of 72% (7.8 g, 53 mmol, 97% purity) and the formation of the product **12** was analyzed *via* ^{1}H NMR-spectroscopy.

^{1}H-NMR (500 MHz, $CDCl_3$): δ[ppm]= 3.61 (m, 1H, (C10)H), 2.37 (t, ^3J= 7.5 Hz, 2H, (C2)H), 1.66 (q, ^3J= 7.2 Hz, 2H, (C3)H), 1.47 (m, 4H, (C8,11)H), 1.31 (m, 22H, H_{alkyl}), 0.90 (t, ^3J= 6.8 Hz, 3H, (C18)H).

The spectroscopical data corresponds to the literature data.[266]

10.4.24 General operating procedure 22 (GOP 22): Esterification of hydroxy-substituted fatty acids

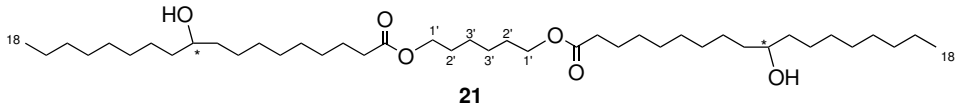

21
$C_{42}H_{82}O_6$
683.11 g mol^{-1}

10-Hydroxystearinic acid (**12**, 15 g, 50 mmol) was dissolved in MTBE and *n*-hextane (125 mL, 1:1, *v/v*) in a *SpinChem*® reactor. Afterward, hexane-1,6-diol (**20**, 5.61 g, 0.05 mmol), CAL-B (54326 *Sigma-Aldrich* Lipase B *Candida antarctica* immobilized on Immobead 150, recombinant from *Aspergillus oryzae*, 1.5 g) and molecular sieve (0.4 nm, 20 g) were transferred into the reaction solution and stirred for 14 h at 35 °C. The solvent was removed under reduced vacuum. The crude product was purified by the means of column chromatography (Cyclohexane:EtOAc, 3:1, *v/v*) and washed with EtOAc several times. Hexane-1,6-diyl-bis(10-hydroxyoctadecanoate) (**21**) was isolated with a yield of 20% (7 g, 0.01 mol).

^{1}H-NMR (500 MHz, $CDCl_3$): δ[ppm]= 4.08 (t, ^3J= 6.7 Hz, 4H, (C1′)*H*), 3.60 (q, ^3J= 5.8, 5.1 Hz, 2H, (C10)*H*), 2.31 (t, ^3J= 7.5 Hz, 8H, (C8,11)*H*), 1.69 – 1.59 (m, 8H, (C2,2′)*H*), 1.46 – 1.38 (m, 16H, H_{alkyl}), 1.31 (d, ^3J= 9.2 Hz, 36H, H_{alkyl}), 0.90 (t, ^3J= 6.7 Hz, 6H, (C18)*H*).

^{13}C-NMR (126 MHz, $CDCl_3$): δ[ppm]= 173.96 (*C1*), 64.17(*C1´*), 29.73 (C_{alkyl}), 29.64 (C_{alkyl}), 29.61 (C_{alkyl}), 29.43 (C_{alkyl}), 29.29 (C_{alkyl}), 29.21 (C_{alkyl}), 29.14 (C_{alkyl}), 28.56 (C_{alkyl}), 25.66 (C_{alkyl}), 24.99 (C_{alkyl}), 22.68 (C_{alkyl}), 14.12 (*C18*).

MS(ESI): m/z = 706.2 [M+Na^+].

HRMS (ESI) calculated for $[C_{42}H_{84}O_5+Na]^+$ 705.6004, found 705.5992.

FT-IR/cm^{-1}: 3275 (OH-ν), 2953 (CH-ν), 248 (CH-ν), 1730 (C=O-ν), 1469 (CH_3/CH_2-δ).

10.4.25 Esterification of 10-hydroxysteranic acid (12) with alcohols

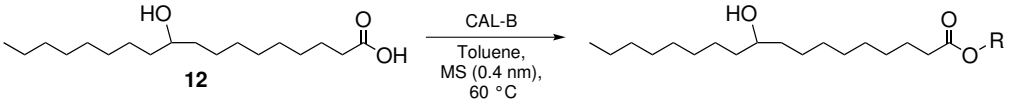

10-Hydroxystearinic acid (**12**, 92 mg, 0.03 mol) was added to toluene (3 mL). Afterwards, the alcohol, CAL-B (54326 *Sigma-Aldrich* Lipase B *Candida antarctica* immobilized on Immobead 150, recombinant from *Aspergillus oryzae*) and molecular sieve (0.4 nm) were transferred into the reaction mixture and stirred for 14 h at 60 °C. The solvent was removed under reduced vacuum and analyzed *via* mass spectrometry, where the starting material, as well as the mono-, di-, or triesters, could be detected. The compositions are shown in the following table:

Table 74: Composition of esterification reaction of 10-hydroxysteranic acid (**12**) with different alcohols.

Alcohol	Alcohol amount	MS/mg	CAL-B/mg
1,3-Propanediol	12.1 µL (0.17 mmol)	136	11
1,1,1-Trimethylolpropane	15.1 mg (0.11 mmol)	101	12
2,2-Dimethyl-1,3-propanediol	18.0 mg (0.17 mmol)	128	12
2-Methyl-1,3-propanediol	14.7 µL (0.17 mmol)	105	13

Propane-1,3-diyl bis(10-hydroxyoctadecanoate) (22).

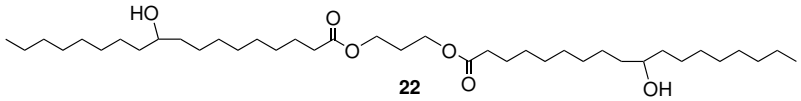

22
$C_{39}H_{76}O_6$
641.03 g mol^{-1}

MS(ESI): m/z = 663.5 [M+Na$^+$], 381.3 [M+Na$^+$] (Monoester), 323.3 [M+Na$^+$] 10-Hydroxystearic acid (**12**).

2-Methylpropan-1,3-diyl-bis(10-hydroxyoctadecanoat) (23).

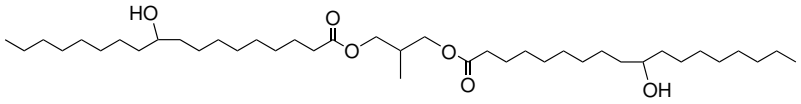

23
$C_{40}H_{78}O_6$
654.58 g mol^{-1}

MS(ESI): m/z = 677.6 [M+Na$^+$], 395.3 [M+Na$^+$] (Monoester), 323.3 [M+Na$^+$] 10-Hydroxystearic acid (**12**).

2,2-Dimethylpropan-1,3-diyl-bis(10-hydroxyoctadecanoat) (24).

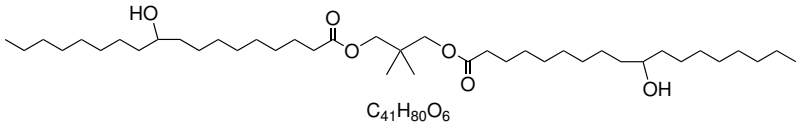

$C_{41}H_{80}O_6$
669.09 g mol^{-1}

MS(ESI): m/z = 692.6 [M+Na$^+$], 409.4 [M+Na$^+$] (Monoester), 323.3 [M+Na$^+$] 10-Hydroxystearic acid (**12**).

2-Ehyl-2-(((10-hydroxyoctadecanoyl)oxy)methyl)propane-1,3-diyl bis(10-hydroxyoctadecanoate (25).

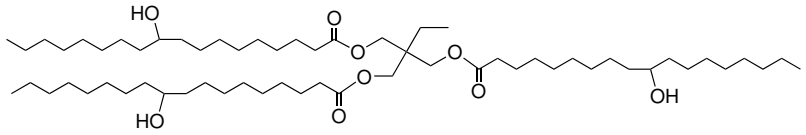

25
$C_{60}H_{116}O_9$
981.58 g mol^{-1}

MS(ESI): m/z = 1004.0 [M+Na$^+$], 722.6 [M+Na$^+$], 439.4 [M+Na$^+$] (Monoester), 323.3 [M+Na$^+$] 10-Hydroxystearic acid (**12**).

10.4.26 General operating procedure 23 (GOP 23): Hydrolysis of triglycerides by the means of lipases

For the hydrolysis, sunflower oil and commercially available lyophilized or immobilized lipases (30 mg mL^{-1}), were used. The reaction was performed in buffer with sunflower oil at 35 °C.

10.4.27 Hydrolysis of triglycerides by the means of different lipases

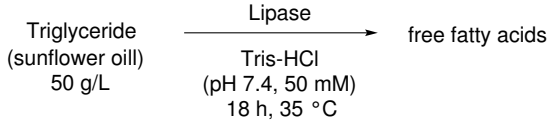

Sunflower oil (50 g L^{-1}) was dissolved in TRIS-HCl buffer (10 mL, pH 7.4, 50 mM). *C. rugosa* lipase (L1754 *Sigma-Aldrich* Lipase from *Candida rugosa* Type VII, 30.7 mg), CAL-B (54326 *Sigma-Aldrich* Lipase B *Candida antarctica* immobilized on Immobead 150, recombinant from *Aspergillus oryzae*, 31.1 mg), CAL-A (41658 *Sigma-Aldrich* Lipase A *Candida antarctica* immobilized on Immobead 150, recombinant from *Aspergillus oryzae*, 31.6 mg) and *B. cepacia* lipase (534641 *Sigma-Aldrich* Amano Lipase PS, from

Burkholderia cepacia, 30.3 mg) were added. The reaction mixtures were incubated at 35 °C for 18 h. Afterwards, the reaction mixtures were extracted with dichloromethane (3x 10 mL), dried over $MgSO_4$ and the solvent was removed *in vacuo*. The conversion was determined *via* ^{1}H NMR-spectroscopy.

Table 75: Results of sunflower oil hydrolysis catalyzed by lipases.

Lipase	Conv./%
CAL-B	8
CAL-A	85
C. rugosa	>99
B. cepacia	88

10.4.28 Hydrolysis of triglycerides with *C. rugosa* lipase, kinetic studies

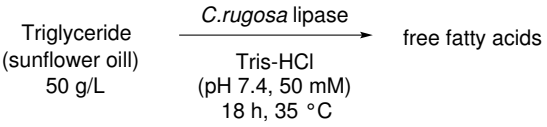

Sunflower oil (500 µL) and *C. rugosa* lipase (L1754 *Sigma-Aldrich* Lipase from *Candida rugosa* Type VII, 32 mg) were added to TRIS-HCl buffer (10 mL, 50 mM, pH 7.4). The reaction mixtures were incubated at 35 °C for 3/6/9 h. The crude product was extracted with $CDCl_3$ (2x 700 µL) and analyzed by the means of ^{1}H NMR spectroscopy. For all reactions a full conversion was observed.

10.4.29 Hydrolysis of triglycerides with *C. rugosa* lipase with citrate buffer

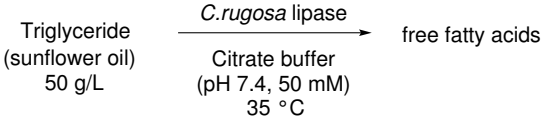

Sunflower oil (500 µL) was added to citrate buffer (10 mL, 50 mM, pH 7.4). *C. rugosa* lipase (32 mg) was added. The reaction mixtures were incubated at 35 °C for 3 h.

The crude product was extracted with $CDCl_3$ and analyzed by the means of ^{1}H NMR-spectroscopy. Full conversion was observed.

10.4.30 Combination of oil hydrolysis and hydration of free fatty acids

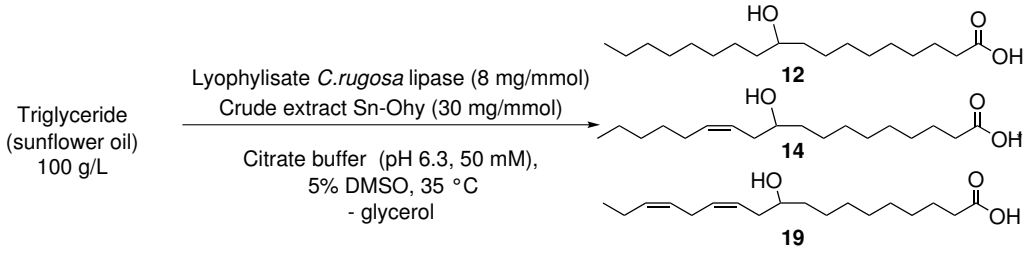

Sunflower oil (5.5 mL) was dissolved in citrate buffer (50 mM, pH 7.4, 47.5 mL). *C. rugosa* lipase (L1754 *Sigma-Aldrich* Lipase from *Candida rugosa* Type VII, 50 mg) and Sn-Ohy crude extract, prepared according to GOP 10, (10 mL, Protein concentration 22 mg mL^{-1}) were added. The reaction mixtures were incubated for 18 h at 35 °C. Afterward, the reaction mixtures were extracted with dichloromethane (3x 10 mL), dried over $MgSO_4$ and the solvent was removed *in vacuo*. The conversion was determined *via* ^{1}H NMR-spectroscopy. The exact conversion could not be determined because no exact composition of the oil was available. In addition, it cannot be said which fatty acid has been hydrated in which percentage.

10.5 Experimental part for 12-OPDA (1) synthesis

10.5.1 General operating procedure 24 (GOP 24): Biocatalytic synthesis of 13-HPOT 3

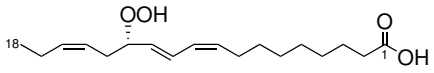

3
$C_{18}H_{30}O_4$
310.21 g mol^{-1}

Linolenic acid (**2**) was diluted in degassed ethanol. The solution was dissolved in ammonium chloride buffer (100 mM, pH 9). Commercially available lipoxygenase from *Glycine max* (*Sigma Aldrich* L7395, Type I-B, lyophilized powder) was dissolved in ammonium chloride buffer (100 mM, pH 9) and dissolved in the reaction mixture. The reaction was carried out under constant oxygen stream. Reaction was controlled *via* TLC (Cyclohexane/EtOAc/AcOH, 3:1:0.1, *v/v*, R_f= 0.25). Afterwards the reaction mixture was acidified with 2 M hydrochloric acid and extracted twice with MTBE or DCM (1:1, *v/v*). Magnesium sulfate was added to remove residual water. The solvent was removed *via* rotary evaporator.

10.5.2 Initial synthesis of 13-HPOT (3)

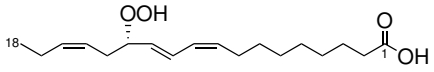

3
$C_{18}H_{30}O_4$
310.21 g mol^{-1}

The reaction was carried out according to GOP 24. Linolenic acid (**2**, 220 mg, 0.80 mmol) was diluted in degassed ethanol (6.4 mL). The solution was dissolved in ammonium chloride buffer (100 mL, 100 mM, pH 9).

Commercially available lipoxygenase from *Glycine max* (*Sigma Aldrich* L7395, Type I-B, lyophilized powder, 7.3 mg) was dissolved in 1 mL ammonium chloride buffer (100 mM, pH 9) and dissolved in the reaction mixture. The reaction was carried according to GOP 24 and extracted twice with MTBE (1:1, *v/v*). Further workup was done according to GOP 24. The product **3** could be isolated as a yellow oil with a yield of 20% (49.6 mg, 0.16 mmol).

^{1}H NMR (500 MHz, $CDCl_3$): δ[ppm]= 6.58 (ddt, ^4J= 15.3, 11.1, 1.0 Hz, 1H, (C11)*H*), 5.99 (t, ^3J= 11.0 Hz, 1H, (C12)*H*) 5.58 (dd, ^3J= 8.0 Hz, ^4J= 15.2, 1H, (C10)*H*), 5.53 – 5.47 (m, 2H, (C15,16)*H*), 5.33 (dtt, ^3J= 7.3 Hz, ^4J= 10.7, 1.7 Hz, 1H, (C9)*H*), 4.43 (dt, ^3J= 8.2, 6.6 Hz, 1H, (C13)*H*), 2.50 – 2.44 (m, 1H, (C8a)*H*), 2.34 (t, ^3J= 7.4 Hz, 2H, (C2)*H*), 2.32 – 2.28 (m, 1H, (C8b)*H*), 2.18 (dtd, ^3J=7.4 Hz, ^4J= 1.5, 15.0 Hz, 2H, (C14)*H*), 2.05 (pd, ^3J= 7.4 Hz, ^4J= 1.5 Hz, 2H, (C17)*H*), 1.63 (p, ^3J= 7.3 Hz, 2H, (C7)*H*), 1.25 (td, ^3J= 7.1, 4.6 Hz, 8H, (C3-6)*H*), 0.96 (t, ^3J= 7.5 Hz, 3H, (C18)*H*).

^{13}C NMR (126 MHz, $CDCl_3$): δ[ppm]= 178.46 (*C1*), 134.53 (*C12*), 134.26 (*C9*), 130.42 (*C16*), 130.36 (*C10*), 127.68 (*C11*), 123.22 (*C15*), 86.36 (*C13*), 58.65 (*C14*), 33.89 (*C2*), 30.76 (*C7*), 29.42 – 27.94 (*C4-6*), 27.80 (*8*), 24.77 (*C3*), 20.85 (*C17*), 14.25 (*C18*).

EI-MS [m/z]: 333.26 $[M+Na]^+$, 349.17 $[M+K]^+$.

HRMS (ESI) calculated for $[C_{18}H_{30}O_4+Na]^+$ 333.2036, found 333.2043.

FT-IR/cm^{-1}: 3500-3000 (OH-ν), 2924 (CH-ν), 2853 (CH-ν), 1704 (C=O-ν), 1456-1409 (CH_3/CH_2-δ), 1243 (CH_3-δ), 1200 ((*E*)-CH_2-progression bands).

10.5.3 Optimization of 13-HPOT (3) synthesis

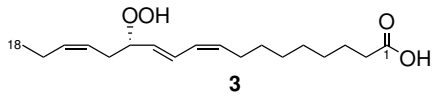

3

$C_{18}H_{30}O_4$

310.21 g mol^{-1}

The reaction was carried out according to GOP 24. Linolenic acid (**2**) was dissolved in ethanol (5 mL). The solution was dissolved in ammonium chloride buffer (100 mL, 100 mM, pH 9). Commercially available lipoxygenase from *Glycine max* (*Sigma Aldrich* L7395, Type I-B, lyophilized powder) was dissolved in ammonium chloride buffer (1 mL, 100 mM, pH 9) and afterward in the reaction solution. The reaction was carried according to GOP 24. The reaction compositions and results are shown in detail in the following table:

Table 76: Composition and results for the optimized synthesis of 13-HPOT (**3**) using 13-LOX.

Experiment	NH_4Cl/mL	LA/mg	13-LOX/mg	O_2	t/min	Conv./%
A	25	12 (0.04 mmol)	0.35	-	180	15
B	250	100 (0.34 mol)	3.12	+	60	20
C	250	100 (0.34 mol)	3.16	+	30	32
D	250	100 (0.34 mol)	3.00	++	30	56
E[a]	250	100 (0.34 mol)	3.00	++	20	76

[a] Reaction at room temperature

10.5.4 Determination of extinction factor for 13-HPOT (3)

An absorption spectrum (200-500 nm) was recorded from a stock solution of 1 µL mL^{-1} purified 13-HPOT (different concentrations) in sodium phosphate buffer (50 mM, pH 7).

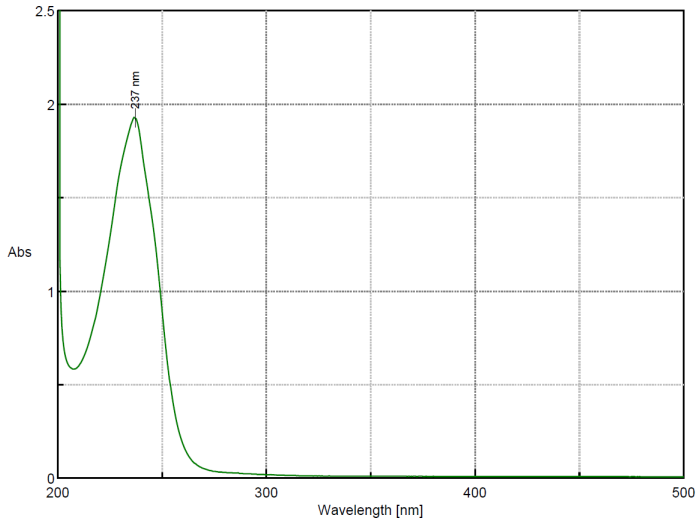

Table 77: Absorption of 13-HPOT (**13**) at different concentrations.

13-HPOT/ mg mL^{-1}	Absorption	ϵ/ L mol^{-1} cm^{-1}
4.1	0.28	21432
5.9	0.49	25887
8.5	0.69	25281
8.8	0.81	28572
11.3	0.94	25660

The extinction factor was calculated according to equation (**1**) with a total value of 25383 L mol^{-1} cm^{-1}.

10.5.5 Activity assay for 13-LOX

The activity assay for 13-LOX was done according to GOP 14, tracing the formation of 13-HPOT at 237 nm within 60 seconds. Therefore, the extinction factor of 13-HPOT was used with ϵ= 25383 L mol^{-1} cm^{-1}. The temperature was changed from 25 to 40 °C in 5 °C steps. The composition of the assay is shown in the table below:

Table 78: Composition of the activity assay for 13-LOX.

Compound	V/µL	final concentration/volume
NH_4Cl-buffer, pH 9; 20, 50, 100 mM		
NH_4Cl-buffer, 100 mM, pH 7, 8, 9		
NaPi buffer, 100 mM		
TRIS-HCl, 100 mM		
NH_4Cl, 100 mM, 0/5/10% ethanol	890	-
Linolenic acid (**2**, 1 mg/25 mL (Buffer))	100	14 nmol
13-LOX (3 mg/ 25 mL(Buffer))	20	1.2 µg

The results for the activity assay are shown in the table below:

Table 79: Results for the activity assay for 13-LOX with **2**.

Buffer	pH	c/mM	T/°C	EtOH/%	A/min	U/mg
NH_4Cl	7	100	25	0	0	0
NH_4Cl	8	100	25	0	23.8 10^{-2}	2.47
NH_4Cl	9	100	25	0	52.7 10^{-2}	5.84
NH_4Cl	9	20	25	0	17.4 10^{-2}	1.80
NH_4Cl	9	50	25	0	37.8 10^{-2}	3.82
NH_4Cl	9	100	25	0	52.7 10^{-2}	5.84
NaPi	9	100	25	0	47.5 10^{-2}	4.52
TRIS-HCl	9	100	25	0	21.5 10^{-2}	2.23
NH_4Cl	9	100	20	0	29.5 10^{-2}	3.06
NH_4Cl	9	100	30	0	64.8 10^{-2}	6.70
NH_4Cl	9	100	35	0	64.5 10^{-2}	6.69
NH_4Cl	9	100	40	0	44.8 10^{-2}	4.54
NH_4Cl	9	100	35	5	64.3 10^{-2}	6.72
NH_4Cl	9	100	35	10	16.5 10^{-2}	1.46

Table 80: Aktivity of 13-HPOT (**3**) with linolenic acid esters.

Buffer	pH	A/min	U/mg
LA **2**	7	1.9 10^{-2}	0.20
LA **2**	8	4.3 10^{-2}	0.45
LA **2**	9	77.5 10^{-2}	8.03
Methyl-LA **28**	7	2.2 10^{-2}	0.22
Methyl-LA **28**	8	2.2 10^{-2}	0.23
Methyl-LA **28**	9	3.3 10^{-2}	0.35
Ethyl-LA **29**	7	4.6 10^{-2}	0.48
Ethyl-LA **29**	8	4.4 10^{-2}	0.56
Ethyl-LA **29**	9	4.7 $^{-2}$	0.48

10.5.6 Purification of AtAOS

E. coli BL21(DE3)containing AtAOS cells were digested by ultrasound sonification according to GOP 10. For the purification the supernatant, after the first centrifugation step (4000x g, 30 minutes, 4 °C), was used and centrifuged again (20000x g, 30 minutes, 4 °C), the pellet contains the AtAOS. The AtAOS pellet of the last centrifugation step was resuspended in sodium phosphate buffer (50 mM, pH 7) and analyzed by means of SDS-PAGE (GOP12) or used for activity tests (GOP14).

10.5.7 Activity assay of AtAOS

E. coli BL21(DE3)containing AtAOS cells were digested by ultrasound sonification according to GOP 10. For the isolation the supernatant, after the first centrifugation step (4000x g, 30 minutes, 4 °C), was used and centrifuged again (20000x g, 30 minutes, 4 °C), the pellet contains the AtAOS. The AtAOS pellet was resuspended in sodium phosphate buffer (50 mM, pH 7). The protein concentration was determined by Bradford assay (0.31 mg mL^{-1}).

The composition of the assay is shown in the table below:

Table 81: Composition of activity assay for AtAOS.

Compound	V/µL	final concentration/volume
NH_4Cl-buffer, pH 9; 20, 50, 100 mM		
NH_4Cl-buffer, 100 mM, pH 7, 8, 9		
NaPi buffer, 100 mM		
TRIS-HCl, 100 mM		
NH_4Cl, 100 mM, 0/5/10% ethanol	890	-
13-HPOT (0.13 mg/25 mL (Buffer))	100	13 µg
AtAOS (0.31 mg/ 1 mL(Buffer))	20	3.1 µg

The results for the activity assay are shown in the table below:

Table 82: Results of activity assay for AtAOS.

Buffer	pH	c/mM	T/°C	EtOH/%	A/min	U/mg
NH_4Cl	9	20	25	0	0.18	5.62
NH_4Cl	9	50	25	0	0.15	4.75
NH_4Cl	9	100	25	0	0.14	4.32
TRIS-HCl	9	100	25	0	0.24	7.52
NaPi	9	100	25	0	0.24	7.61
NaPi	9	100	25	0	0.18	5.64
NaPi	9	100	20	0	0.13	4.12
NaPi	9	100	30	0	0.13	3.91
NaPi	9	100	35	0	0.10	3.01
NaPi	9	100	40	0	0.15	4.77
NaPi	9	100	25	5	0.14	4.35
NaPi	9	100	25	10	0.18	5.62

10.5.8 General operating procedure 25 (GOP 25): Biocatalytic synthesis of 12-OPDA (1)

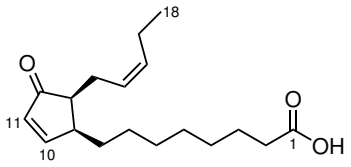

1
$C_{18}H_{28}O_3$
292.42 g mol^{-1}

Between each reaction step the solution was saturated with oxygen for five minutes, by the means of an oxygen balloon. *E.coli* with AOS and AOC2 were dissolved in ammonium chloride buffer (100 mM, pH 9). Commercially available lipoxygenase from *Glycine max* (*Sigma Aldrich* L7395, Type I-B, lyophilized powder) was dissolved in ammonium chloride buffer and added to the reaction mixture. Linolenic acid (**2**) was dissolved in ethanol and then added to the reaction mixture. The reaction was performed under oxygen saturation at room temperature. The completeness of the reaction was controlled by TLC (Cyclohexane/EtOAc/AcOH 6:2:0.1 *v/v*, R_f= 0.32). In the following the reaction mixture was centrifuged (10.000x g, 15 min, 4 °C). The supernatant was acidified with 2 M hydrochloric acid and extracted. Magnesium sulfate was added to remove the residual water. The solvent was removed under vacuum and the ratio between α-ketol **27** and 12-OPDA (**1**), as well as the *cis*:*trans* ratio were determined from the resulting crude product by ^{1}H NMR spectroscopy.[267] The crude product was purified by automated column chromatography with a gradient (ACN/H_2O, gradient 0 - 100 % ACN and AcOH (0.1%, *v/v*)) resulting in 12-OPDA (**1**) as isolated product.

10.5.9 Synthesis of 12-OPDA (1) with WCC 1

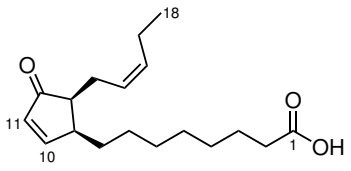

1
$C_{18}H_{28}O_3$
292.42 g mol^{-1}

The reaction was prepared according to GOP 25. Ammonium chloride buffer (100 mL, 100 mM, pH 9) in a flask was saturated with O_2. Cells of whole cell catalyst (400 mg or 1000 mg *E.coli* BL21-CodonPlus(DE3)-RIL, pET24a(+)-AtAOS and pQE30-AtAOC2, WCC1) were weighed, suspended in buffer and stirred for five minutes under oxygen. Commercially available lipoxygenase from *Glycine max* (*Sigma Aldrich* L7395, Type I-B, lyophilized powder, 3 mg, 40 U) were weighed and dissolved in cold buffer (1 mL). Ethanol (5 mL) was then added to the solution and stirred under O_2 saturation for another 5 min. Linolenic acid (**2**, 100 mg, 0.359 mmol) was weighed, dissolved in ethanol (1 mL) and cooled to 4 °C, then added to the reaction mixture. The reaction mixture was stirred at room temperature under oxygen saturation. The reaction was performed according to GOP 25 and extracted with MTBE (3x 50 mL). The solvent was dried over magnesium sulfate and the solvent removed under reduced vacuum. The analytics were performed according to GOP 25.

The results are shown in the table below:

Table 83: Results for the synthesis of **1** with WCC1.

Reaction	Conv. to **1**/%	*cis*:*trans* ratio	**27**/**1** ratio
400 mg	>99	98:2	58:42
1000 mg	>99	99:1	95:5

^{1}H-NMR (500 MHz, $CDCl_3$): δ[ppm]= 7.73 (dd, ^{3}J= 6.0, 2.7 Hz, 1H, (C10)*H*, (*cis*-12-OPDA **1**)), 7.60 (d, ^{3}J= 5.7 Hz, 1H, (C10)*H*, (*trans*-12-OPDA **1**)), 6.18 (dd, ^{3}J= 5.9, ^{4}J= 1.7 Hz, 1H, (C11)*H*, (*cis*-12-OPDA **1**)), 6.12 (d, ^{3}J= 5.9 Hz, 1H, (C11)*H*, (*trans*-12-OPDA **1**)), 5.46 – 5.32 (m, 2H, (C15,16)*H*), 2.97 (ddt, ^{3}J= 10.8, 7.6, 3.6 Hz, 1H, (C9)*H*), 2.50 (dt, ^{3}J= 15.3, 5.4 Hz, 1H, (C14)*Ha*), 2.47 – 2.41 (m, 1H, (C13)*H*), 2.35 (t, ^{3}J= 7.5 Hz, 2H, (C2)*H*), 2.17 – 2.10 (m, 2H, (C17)*H*), 2.06 (d, ^{3}J= 7.5 Hz, 1H, (C14)*Hb*), 1.72 (td, ^{3}J= 11.1, 5.0 Hz, 2H, (C8)*H*), 1.63 (p, ^{3}J= 7.2 Hz, 2H, (C3)*H*), 1.15 (dtd, ^{4}J= 14.3, ^{3}J= 9.6, 4.5 Hz, 8H, (C4,7)*H*), 0.97 (t, ^{3}J= 7.5 Hz, 3H, (C18)*H*).

^{13}C-NMR (126 MHz, $CDCl_3$): δ[ppm]= 211.05 (*C12*), 171.35 (*C1*), 167.28 (*C10*), 133.13 (*C11*), 132.59 (*C16*), 127.10, (*C15*), 50.00 (*C13*), 44.43 (*C9*), 34.02 (*C2*), 30.90 (*C8*), 29.70 – 27.27 (*C4-7*), 24.75 (*C3*), 23.93 (*C14*), 20.94 (*C17*), 14.15 (*C18*).

The ^{1}H NMR-spectrum for this compound is in accordance with the data reported in literature.[213]

10.5.10 Synthesis of 12-OPDA (1) with WCC 2 and WCC 3

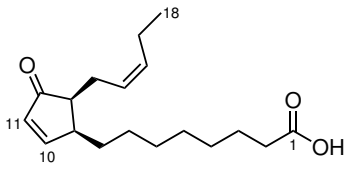

1
$C_{18}H_{28}O_3$
292.42 g mol^{-1}

The reaction was prepared according to GOP 25. Ammonium chloride buffer (100 mL, 100 mM, pH 9) in a flask was saturated with O_2. Cells of whole cell catalyst (300 mg, *E.coli* BL21-CodonPlus(DE3)-RIL, pET28a(+)-AtAOS and pUC18-AtAOC2, WCC2 and pET28a(+)-AtAOS and pQE30-AtAOC2, WCC 3) were weighed and suspended in buffer. Commercially available lipoxygenase from *Glycine max* (*Sigma Aldrich* L7395, Type I-B, lyophilized powder, 3 mg, 40 U) were weighed and dissolved in cold buffer (1 mL). The 13-LOX buffer solution was added to the buffer. Ethanol (5 mL) was added to the reaction suspension. Linolenic acid (**2**, 100 mg, 0.359 mmol) was weighed, dissolved in ethanol (1 mL) and cooled to 4 °C, then added to the reaction mixture. The reaction mixture was stirred at room temperature under oxygen saturation. The reaction was performed according to GOP 25. The supernatant was extracted with dichloromethane (3x 50 mL). The solvent was dried over magnesium sulfate and removed under vacuum. The analytics were performed according to GOP 25. The results are shown in the table below:

Table 84: Results for the synthesis of **1** with WCC 2 and WCC 3.

Reaction	Conv. to **1**/%	*cis*:*trans* ratio	**27**/**1** ratio
WCC 2	>99	97:3	69:31
WCC 3	>99	91:9	90:10

The crude product of WCC 3 was purified according to GOP 25, leading to 12-OPDA (**1**) as an isolated product with a yield of 28% (27.8 mg, 0.10 mmol).

10.5.11 Synthesis of 12-OPDA (1) with separate cells

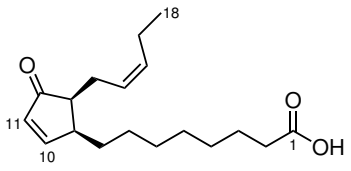

1
$C_{18}H_{28}O_3$
292.42 g mol^{-1}

The reaction was performed according to GOP 25. Ammonium chloride buffer (100 mL, 100 mM, pH 9) in a flask was saturated with O_2. Cells of whole cell catalyst 150 mg, *E.coli* BL21-CodonPlus(DE3)-RIL pET28a(+)-AtAOS and 150 mg *E.coli* BL21-CodonPlus(DE3)-RIL pET21a(+)-AtAOC2 were weighed and suspended in buffer and stirred for five minutes under oxygen. Commercially available lipoxygenase from *Glycine max* (*Sigma Aldrich* L7395, Type I-B, lyophilized powder, 3 mg, 40 U) was weighed and dissolved in cold buffer (1 mL). The 13-LOX buffer solution was added to the buffer saturated with O_2 was stirred on under O_2 for five minutes. Ethanol (5.4 mL) was added to the solution and under O_2 for another 5 min. Linolenic acid (**2**, 100 mg, 0.359 mmol) was weighed, dissolved in ethanol (1 mL) and cooled to 4 °C, then added to the reaction mixture. The reaction mixture was stirred at room temperature under oxygen saturation. The reaction was performed according to GOP 25. The supernatant was extracted with dichloromethane (3x 50 mL). The solvent was dried over magnesium sulfate and removed under vacuum. The analytics were performed according to GOP 25. A full conversion was detected and a ratio between α-ketol **27** and 12-OPDA (**1**) of 69:31 was determined and a *cis*:*trans* ratio of 95:5.

10.5.12 Synthesis of 12-OPDA (1) with WCC 3 in preparative scale

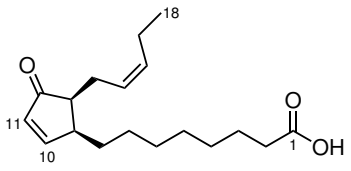

1
$C_{18}H_{28}O_3$
292.42 g mol^{-1}

The reaction was performed according to GOP 25. Ammonium chloride buffer (500 mL, 100 mM, pH 9) in a flask was saturated with O_2. Cells of whole cell catalyst (1.5 g, *E.coli* BL21-CodonPlus(DE3)-RIL, pET28a(+)-AtAOS and pQE30-AtAOC2, WCC 3) were weighed and suspended in buffer. Commercially available lipoxygenase from *Glycine max* (*Sigma Aldrich* L7395, Type I-B, lyophilized powder, 15 mg, 200 U) was weighed and dissolved in cold buffer (1 mL). The 13-LOX buffer solution was added to the buffer. Linolenic acid (**2**, 500 mg, 1.80 mmol) was weighed, dissolved in ethanol (27 mL) and cooled to 4 °C, then added to the reaction mixture. The reaction mixture was stirred at room temperature under oxygen saturation. The reaction was performed according to GOP 25. The supernatant was extracted with dichloromethane (3x 250 mL). The solvent was dried over magnesium sulfate and removed under vacuum. The analytics were performed according to GOP 25. A full conversion was detected and a ratio between α-ketol **27** and 12-OPDA (**1**) of 95:5 and a *cis*:*trans* ratio of 92:8. The crude product was purified according GOP 25, leading to 12-OPDA (**1**) as an isolated product with a yield of 31% (155 mg, 0.56 mmol).

10.5.13 Extraction optimization

Between each reaction step the solution was saturated with oxygen for five minutes by the means of an oxygen balloon. Cells of whole cell catalyst (2.7 g, pET28a(+)-AtAOS and pQE30-AtAOC2, WCC 3) were weighed and suspended in ammonium chloride buffer (900 mL, 100 mM, pH 9). Commercially available lipoxygenase from *Glycine max* (*Sigma Aldrich* L7395, Type I-B, lyophilized powder, 27 mg, 360 U) was weighed and dissolved in cold buffer (1 mL). The 13-LOX buffer solution was added to the buffer. Linolenic acid (**2**, 900 mg, 3.23 mmol) was weighed, dissolved in the ethanol (45 mL) and cooled to 4 °C, then added to the reaction mixture and the reaction was stirred at room temperature under oxygen saturation. Afterward, the reaction was divided into three parts (I, II, III), centrifuged (10,000 xg, 15 min, 4 °C) and stopped by addition of HCl (2 M, 4 mL).

Part I was extracted with DCM (3x 250 mL). Magnesium sulfate was added to remove residual water. The solvent was removed *in vacuo* and 51% crude product was isolated. The crude product was purified according to GOP 25 and a yield of 31% was isolated (**1**, 93 mg, 0.33 mmol).

For part II the cell pellet was dissolved in DCM (15 mL) and disrupted under ultrasound sonification (1x 5 minutes, 5x 10 cycles, 10-20% power), afterward the mixture was centrifuged (10.000x g, 5 min). The procedure was repeated twice. The supernatants and the reaction medium were combined and the solvent was removed *in vacuo* and 75% crude product was isolated. The crude product was purified according to GOP 25 and a yield of 61% was isolated (**1**, 183 mg, 0.65 mmol) with *cis*:*trans* ratio of 96:4. Optical rotation: $\alpha_D{}^{20} = +104°$ (c = 10.0, $CHCl_3$).

Part III was purified by the means of Bligh and Dyer extraction method,[253] therefore the pellet was dissolved in a mixture (MeOH, $CHCl_3$, H_2O, 2:1:1, *v/v*). After centrifugation (5000x g, 5 min) the chloroform phase was isolated and the solvent was removed *in vacuo* and 52% crude product **1** was isolated.

10.5.14 Esterification of 12-OPDA (1)

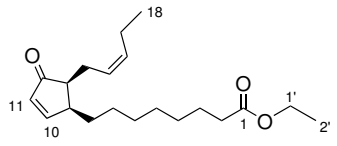

32
$C_{20}H_{32}O_3$
320.47 g mol^{-1}

12-OPDA (**1**, 126 mg, 0.43 mmol) was dissolved in EtOH (5 mL), molecular sieve (0.4 nm, 770 mg) and CAL-B (54326 *Sigma-Aldrich* Lipase B *Candida antarctica* immobilized on Immobead 150, recombinant from *Aspergillus oryzae*, 97 mg) were added. The reaction was stirred for 16 h at room temperature. The molecular sieve was filtered off and washed with EtOH (2x 5 mL), the reaction mixture was extracted with *n*-hexane (2x 5 mL). The solvent was removed *in vacuo* and the product **32** was isolated as an oil with a yield of 92% (127 mg, 0.39 mmol).

^{1}H-NMR (500 MHz, $CDCl_3$): δ[ppm]= 7.73 (dd, ^3J= 6.0, 2.7 Hz, 1H, (C10)*H*, (*cis*-12-OPDA **1**)), 7.59 (d, ^3J= 5.7 Hz, 1H, (C10)*H*, (*trans*-12-OPDA **1**)), 6.17 (dd, ^3J= 5.9, ^4J= 1.7 Hz, 1H, (C11)*H*, (*cis*-12-OPDA **1**)), 6.11 (d, ^3J= 5.9 Hz, 1H, (C11)*H*, (*trans*-12-OPDA **1**)), 5.46 – 5.32 (m, 2H, (C15,16)*H*), 4.11 (q, ^3J= 7.1 Hz, 2H, (C1′)*H*), 2.97 (ddt, ^3J= 10.8, 7.6, 3.6 Hz, 1H, (C9)*H*), 2.49 (dt, ^3J= 15.3, 5.4 Hz, 1H, (C14)*Ha*), 2.46 – 2.41 (m, 1H, (C13)*H*), 2.28 (t, ^3J= 7.5 Hz, 2H, (C2)*2*), 2.16 – 2.07 (m, 2H, (C17)*H*), 2.06 (d, ^3J= 7.5 Hz, 1H, *H14b*), 1.72 (m, 2H, (C8)*H*), 1.63 (p, ^3J= 7.2 Hz, 2H, (C3)*H*), 1.24 (t, ^3J= 7.1 Hz, 3H, (C2′)*H*), 1.15 (dtd, ^4J= 14.3, ^3J= 9.6, 4.5 Hz, 8H, (C4-7)*H*), 0.96 (t, ^3J= 7.5 Hz, 3H, (C18)*H*).

^{13}C-NMR (126 MHz, $CDCl_3$): δ[ppm]= 211.05 (*C12*), 171.35 (*C1*), 167.28 (*C10*), 133.13 (*C11*), 132.59 (*C16*), 127.10, (*C15*), 60.20 (*C2´*), 50.00 (*C13*), 44.43 (*C9*), 34.02 (*C2*), 30.90 (*C8*), 29.70 – 27.27 (*C4-7*), 24.75 (*C3*), 23.93 (*C14*), 20.94 (*C17*), 20.60 (*C1´*), 14.15 (*C18*).

MS (ESI): m/z = 343.27 $[M+Na]^+$.

HRMS (ESI) calculated for $[C_{20}H_{32}O_3+Na]^+$ 343.2244, found 343.2241.

IR(neat)/cm^{-1}: 2926 (s, ν, -CH_2), 2921 (m, ν, -CH_3), 1730 (s, -ν, -C=O), 1707 (m, -ν, -C=C).

10.5.15 Synthesis of 12-OPDA (1) in a two-phase batch system, analytic scale

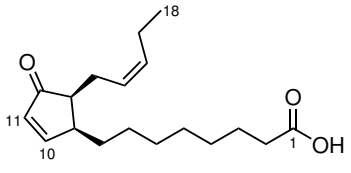

1
$C_{18}H_{28}O_3$
292.42 g mol^{-1}

E.coli BL21-CodonPlus(DE3)-RIL cells containing AtAOS and AtAOC2 (10/20/30 mg) were diluted in NaPi-buffer (1 mL, 100 mM, pH 8). 13-HPOT (**3**, 7.50 mg, 0.02 mmol) was dissolved in 1 mL solvent (either with the addition of Tween 20 (1%, *m/V*) or without additive). Both, organic and aqueous phases were combined to start the reaction. The reaction was done at room temperature for 30 minutes in a 10 mL vial at 400 rpm, respectively 1400 rpm. Afterward, the reaction was quenched with HCl (2 M, 500 µL). The organic phases were combined and the solvent was removed *in vacuo* and analyzed by the means of ^{1}H NMR-spectroscopy.

Table 85: Reaction conditions and results for 12-OPDA (**1**) synthesis in a two-phase batch system.

Buffer/Cosolvent	Whole cells/mg	Stirrer/rpm	Conv./%
NaPi, pH 8	30	400	99
NH_4Cl, pH 8	30	400	35
NH_4Cl, pH 9	30	400	99
5x Wet cell mass in NaPi, pH 8	150	400	99
Cyclohexane	30	400	50
Cyclohexane + Tween 20 (1%, *m/V*)	30	400	74
Cyclohexane + 10% MTBE	30	400	85
Cyclohexane + 50% MTBE	30	400	31
Isooctane	30	400	99
Ethylacetate	30	400	14
Cyclohexane + 10% MTBE	10	400	8
Cyclohexane + 10% MTBE + Tween 20 (1%, *m/V*)	10	400	8
Isooctane	10	400	9
Isooctane + Tween 20 (1%, *m/V*)	10	400	9
Isooctane + Tween 20 (1%, *m/V*)	20	400	34
Isooctane + Tween 20 (1%, *m/V*)	20	1400	0

10.5.16 Synthesis of 12-OPDA (1) in a two-phase batch system, preparative scale

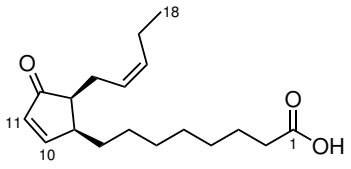

1
$C_{18}H_{28}O_3$
292.42 g mol^{-1}

E.coli BL21-CodonPlus(DE3)-RIL cells containing AtAOS and AtAOC2 (200 mg) were diluted in NaPi-buffer (5 mL, 100 mM, pH 8, 5 mg Tween 20, *m/V*). 13-HPOT (**3**, 53 mg, 0.17 mmol) was dissolved in isooctane (5 mL). Both, organic and aqueous phases were combined to start the reaction. The reaction was done at room temperature in a 10 mL vial at 400 rpm and for 30 minutes. Afterward, the reaction was quenched with HCl (2 M, 500 µL) and centrifuged (10.000x g, 5 min).

The aqueous phase was extracted with dichloromethane (5 mL). The organic phases were combined and the solvent was removed *in vacuo* and analyzed by the means of ^{1}H NMR-spectroscopy. The crude product **1** was isolated with a yield of 36% (19 mg, 0.07 mmol).

10.5.17 Synthesis of 12-OPDA (1) in segmented flow, analytical scale

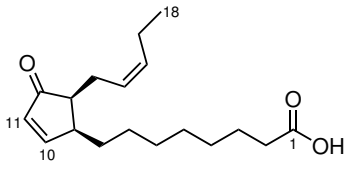

1
$C_{18}H_{28}O_3$
292.42 g mol^{-1}

E.coli BL21-CodonPlus(DE3)-RIL cells containing AtAOS and AtAOC2 (20 mg_{wcm} mL_{aq} $^{-1}$) were diluted in 5 mL saturated NaPi-buffer (100 mM, pH 8) and Tween 20 (5 mg). The reaction solution was transferred into a syringe (5 mL, S.G.E., gas tight, 10.3 mm ID). A second solution of 13-HPOT (**3**, 7.50 mg, 0.02 mmol) was dissolved in 5 mL isooctane and transferred into a syringe (5 mL, S.G.E., gas tight, 10.3 mm ID). The feed of the two solutions (each Q: 1 mL h^{-1}, pumped with a syringe pump) were mixed in a Y mixer (0.5 mm ID). The produced segments were led into a tubular reactor (PFE, 0.8 mm ID, 1 mL). To start the reaction, the syringe pump was set up (0.5 mL h^{-1}, τ= 60 min). Fractions were collected in a glass vial containing HCl (2 M, 1 mL). The aqueous was extracted with dichloromethane (1 mL). The organic phases were combined and the solvent was removed *in vacuo* and analyzed by the means of ^{1}H NMR-spectroscopy.

Table 86: Results for 12-OPDA (**1**) synthesis in segmented flow.

Entry	fraction time/h	Conv. to **1**/%
1	0.5 – 1.5	>99
2	1.5 – 2.5	>99
3	2.5 – 3.5	>99
4	3.5 – 4.5	>99
5	4.5 – 5.5	>99

10.5.18 Synthesis of 12-OPDA (1) in segmented flow, preparative scale

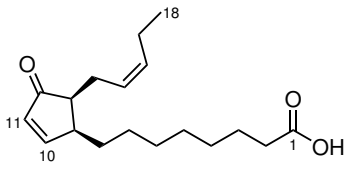

1
$C_{18}H_{28}O_3$
292.42 g mol^{-1}

E.coli BL21-CodonPlus(DE3)-RIL cells containing AtAOS and AtAOC2 (200 mg_{wcm} mL_{aq} $^{-1}$) were diluted in 5 mL saturated NaPi-buffer (100 mM, pH 8) and Tween 20 (5 mg, *(m/V)*). The reaction solution was transferred into a syringe (5 mL, S.G.E., gas tight, 10.3 mm ID). A second solution of 13-HPOT (**3**, 53 mg, 0.17 mmol) was dissolved in 5 mL isooctane and transferred into a syringe (5 mL, S.G.E., gas tight, 10.3 mm ID). The feed of the two solutions (each Q: 1 mL h^{-1}, pumped with a syringe pump) were mixed in a Y mixer (0.5 mm ID). The produced segments were led into a tubular reactor (PFE, 0.8 mm ID, 1 mL). To start the reaction, the syringe pump was set up (0.5 mL h^{-1}, τ= 60 min). Fractions were collected in a glass vial containing HCl (2 M, 1 mL). The aqueous was extracted with dichloromethane (1 mL). The organic phases of all fractions were combined and the solvent was removed in *vacuo* and analyzed by the means of ^{1}H NMR-spectroscopy. The crude product **1** was isolated with a yield of 65% (44 mg, 0.15 mmol).

10.6 Chemical synthesis

10.6.1 2-oxabicyclo[3.3.0]oct-6-en-3-one and 3-oxabicyclo-[3.3.0]oct-6-en-2-one $\mathbf{11f}_{N/ABN}$

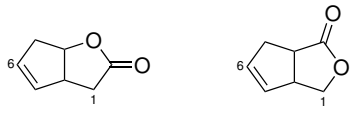

-/+ **11f$_N$**
$C_7H_8O_2$
124.14 g mol^{-1}
main isomer
9:1

-/+ **11f$_{ABN}$**
$C_7H_8O_2$
124.14 g mol^{-1}
minor isomer
1:9

The reaction was performed with bicyclo[3.2.0]hept-2-en-6-one (**11f**) (200 mg, 1.61 mmol) and *m*-chlorobenzoperoxoic acid (492 mg, 2.85 mmol) in dichloromethane (15 mL). The reaction mixture was stirred at 25 °C for 24 h. Afterwards, saturated K_2CO_3 solution (15 mL) was added. The aqueous phase was extracted with dichloromethane (2x 15 mL). The solvent was removed *in vacuo* and the crude products $\mathbf{11f}_{N/ABN}$ were purified *via* flash chromatography using the Isolera One from *Biotage*® on silica (Cyclohexane/EtOAc, 1:1, *v/v*). The product $\mathbf{11f}_{N/ABN}$ was successfully isolated as a colorless solid (20 mg, 0.16 mmol, 10%, 9:1 $\mathbf{11f}_N$:$\mathbf{11}_{ABN}$).

^{1}H-NMR (500 MHz, $CDCl_3$): δ[ppm]= (2-oxabicyclo[3.3.0]oct-6-en-3-one $\mathbf{11f}_N$) 5.81 – 5.77 (m, 1H, (C7)*H*), 5.58 (dq, ^3J= 6.0, ^4J= 2.0 Hz, 1H, *H*), 5.13 (dddd, ^3J = 5.8, 4.4, ^4J = 3.0, 1.9 Hz, 1H, (C4)*H*), 3.52 – 3.49 (m, 1H, (C8)*H*), 2.73 – 2.68 (m, 2H, (C5)*H*), 2.44 (dd, ^4J = 18.0, 1.6 Hz, 2H, (C1)*H*).

^{1}H-NMR (500 MHz, $CDCl_3$): δ[ppm]= (3-oxabicyclo[3.3.0]oct-6-en-2-one $\mathbf{11f}_{ABN}$) 5.88 – 5.86 (m, 1H, (C7)*H*), 5.66 (dq, ^3J = 5.9, 2.1 Hz, 1H, (C6)*H*), 4.43 (dd, ^3J = 9.3, 7.2 Hz, 1H, (C1)*H*), 4.24 (dd, ^4J= 9.3, 1.5 Hz, 1H, (C1)*H*), 3.59 (dd, ^4J= 4.6, 2.5 Hz, 1H, (C8)*H*), 3.13 – 3.08 (m, 1H, (C4)*H*), 2.74 – 2.69 (m, 2H, (C5)*H*).

The ^{1}H NMR-spectra for **11f**$_{N/ABN}$ were in accordance with the data reported in literature.[268]

Achiral GC: *Phenomenex ZB-SMS*, method: 40 °C followed by a gradient of 30 °C min^{-1} to 280 °C, R$_t$: *rac*-(**11f**) 2.2 min.

Chiral GC: MN Lipodex E chiral column [octatakis(2,6-di-*O*-phenyl-3-*O*-butyryl)-γ-cyclodextrine] (25 m, 0.25 mm), method: 60 °C for 15 min followed by a gradient of 10 °C min^{-1} to 130 °C (15 min), followed by a gradient of 20 °C min^{-1} to 200 °C (4 min). R$_t$: (-)-**11f** 20.5 min, (+)-**11f** 21.0 min, (+)-**11f**$_N$ 31.6 min, (-)-**11f**$_{ABN}$ 32.9 min, (-)-**11f**$_N$ 33.3 min, (+)-**11f**$_{ABN}$ 34.5 min.

10.6.2 General operating procedure 26 (GOP 26): Esterification of fatty acids

The fatty acid was dissolved in toluene with methanol (188 eq.), HCl (46 eq.) and molecular sieve (0.3 nm). Everything was stirred at 110 °C for 1.5 h. Afterward, the crude product was filtered, and the solvent removed *in vacuo*. Next, water was added and extract twice with *n*-hexane. The reaction mixture was dried and the solvent removed *in vacuo*.

10.6.3 Esterification of oleic acid (15)

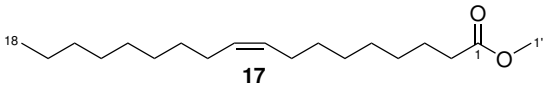

17
$C_{19}H_{36}O_2$
296.50 g/mol

Oleic acid (**15**, 150 mg, 0.51 mmol), toluene (20 mL), methanol (20 mL), HCl (0.48 mL), molecular sieve (0.3 nm, 1.25 g) were stirred together at 110 °C for 1.5 h.

The progress of the reaction was verified by TLC (Cyclohexane/EtOAc/AcOH, 3:1:0.5 *v/v*, R_f= 0.5). Afterwards, the crude product was filtered, and the solvent removed *in vacuo*. Next, 20 mL of water was added and extract twice with *n*-hexane (20 mL). The reaction mixture was dried and the solvent removed *in vacuo*. The product (**17**, 106 mg, 0.36 mmol, 70%) was isolated as a yellowish oil.

^{1}H-NMR (500 MHz, $CDCl_3$): δ[ppm]= 5.41 – 5.28 (m, 2H, C(9,10)*H*,), 3.67 (s, 3H, C(1′)*H*), 2.30 (t, ^3J= 7.5 Hz, 2H, (C2)*H*), 2.01 (q, ^3J= 16.7, 7.4 Hz, 4H, C(8,11)*H*), 1.61 (q, ^3J= 7.3 Hz, 2H, (C3)*H*), 1.30 (m, 20H, (C4-7, 12-17)*H*), 0.88 (t, ^3J= 6.8 Hz, 3H, (C18)*H*).

The spectroscopical data are according to the literature data.[269]

10.6.4 Esterification of linoleic acid (2)

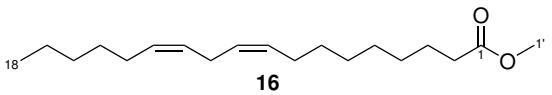

16
$C_{19}H_{34}O_2$
294.26 g/mol

Linoleic acid (**2**, 150 mg, 0.52 mmol), toluene (20 mL), methanol (20 mL), HCl (0.48 mL), molecular sieve (0.3 nm, 1.25 g) were stirred together at 110 °C for 1.5 h. The progress of the reaction was verified by TLC (Cyclohexane/EtOAc/AcOH 3:1:0.5, *v/v*, R_f= 0.5). Afterwards, the crude product was filtered, and the solvent removed *in vacuo*. Next, 20 mL of water was added and extract twice with *n*-hexane (20 mL). The reaction mixture was dried and the solvent removed *in vacuo*. The product (**17**, 125 mg, 0.42 mmol, 82%) was isolated as a yellowish oil.

^{1}H-NMR (500 MHz, $CDCl_3$): δ[ppm]= 5.43 – 5.42 (m, 4H, (C9, 10, 12, 13)*H*,), 3.67 (s, 3H, (C1′)*H*), 2.77 (t, ^3J= 7.6, 2H, (C11)*H*), 2.30 (t, ^3J= 7.5 Hz, 2H, (C2)*H*), 2.01 (q, ^3J= 16.7, 7.4 Hz, 4H, (C8,14)*H*), 1.61 (q, ^3J= 7.3 Hz, 2H, (C3)*H*), 1.41 – 1.23 (m, 14H, C(4-7,15-17)*H*), 0.88 (t, ^3J= 6.8 Hz, 3H, (C18)*H*).

The spectroscopical data are according to the literature data.[270]

10.6.5 Esterification of linolenic acid (2) with methanol

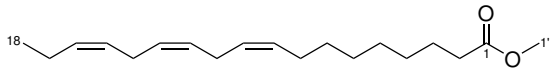

28
$C_{19}H_{32}O_2$
292.46 g mol^{-1}

Linolenic acid (**2**, 524 mg, 1.71 mmol), toluene (75 mL), methanol (130 mL), HCl (2.4 mL), molecular sieve (0.3 nm, 1.25 g) were stirred together at 110 °C for 1.5 h. The progress of the reaction was verified by TLC (Cyclohexane/EtOAc/AcOH 3:1:0.5, *v/v*, R_f = 0.5). Afterwards, the crude product was filtered, and the solvent removed *in vacuo*. Next, 20 mL of water was added and extract twice with *n*-hexane (20 mL). The reaction mixture was dried and the solvent removed *in vacuo*. The product (**28**, 408 mg, 1.40 mmol, 72%.) was isolated as a yellowish oil.

^{1}H-NMR (500 MHz, $CDCl_3$): δ[ppm]= 5.48 – 5.25 (m, 6H, (C9-10, 12, 13, 15, 16)*H*,), 3.67 (s, 3H, (C1′)*H*), 2.86 – 2.75 (m, 4H, (C11,14)*H*), 2.30 (t, ^3J= 7.5 Hz, 2H, (C2)*H*), 2.06 (q, ^3J= 16.7, 7.4 Hz, 4H, (C8,17)*H*), 1.62 (q, ^3J= 7.3 Hz, 2H, (C3)*H*), 1.30 (m, 8H, (C4-7)*H*), 0.98 (t, ^3J= 6.8 Hz, 3H, (C18)*H*).

The spectroscopical data are according to the literature data.[271]

10.6.6 Esterification of linolenic acid (2) with ethanol

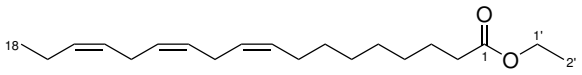

29
$C_{20}H_{34}O_2$
306.49 g mol^{-1}

Linolenic acid (**2**, 100 mg, 0.40 mmol), toluene (20 mL), ethanol (130 mL), HCl (2.4 mL), molecular sieve (0.4 nm, 0.11 g) were stirred together at 110 °C for 2 h. The progress of the reaction was verified by TLC (Cyclohexane/EtOAc/AcOH 3:1:0.5, *v/v*, R_f= 0.5). Afterwards, the crude product was filtered, and the solvent removed *in vacuo*. Next, 20 mL of water was added and extract twice with *n*-hexane (10 mL). The reaction mixture was dried and the solvent removed *in vacuo*. The product (**29**, 58 mg, 0.21 mmol, 58%.) was isolated as a yellowish oil.

^{1}H-NMR (500 MHz, $CDCl_3$): δ[ppm]= 5.37 – 5.18 (m, 6H, (C9, 10, 12, 13, 15, 16)*H*,), 4.12 (q, ^3J= 7.1 Hz, 2H, (C2′)*H*), 2.86 – 2.75 (m, 4H, (C11,14)*H*), 2.30 (t, ^3J= 7.5 Hz, 2H, (C2)*H*), 2.06 (q, ^3J= 16.7, 7.4 Hz, 4H, (C8,17)*H*), 1.62 (q, ^3J= 7.3 Hz, 2H, (C3)*H*), 1.31 (m, 8H, (C4-7)*H*), 1.25 (t, ^{3}J= 7.1 Hz, 3H, (C1′)*H*), 0.98 (t, ^3J= 6.8 Hz, 3H, (C18)*H*).

The spectroscopical data are according to the literature data.[272]

10.6.7 General operating procedure 27 (GOP 27): Metathesis reaction

The reaction was done with 12-OPDA-ethylester and olefine in degassed solvent (DCM, toluene) with Hoveyda-Grubbs catalyst 2nd generation (C1). Afterwards the solvent was removed, and the crude product purified *via* thin layer chromatography (Cyclohexane/EtOAc, 3:1, *v/v*).

10.6.8 Optimization of metathesis reaction

The reaction was performed with 12-OPDA-ethylester (**32**, 1 eq.) and olefine in degassed solvent (DCM, toluene) and with HOVEYDA-GRUBBS catalyst 2nd generation (C1). Afterward, the solvent was removed. The conversion was determined by the means of ^{1}H NMR-spectroscopy.

Table 87: Reaction cascade starting from 12-OPDA (**1**), esterification with CAL-B and metathesis reactions with different parameters.

Exp.	Substrate/mg	Olefin/µL	Eq.	Solvent/mL	Cat./mg	T/°C
1[a]	16.3 (90 µmol)	15 (0.15 mmol)	2	10 (TolH[c])	0.31 (0.5 mol/%)	rt
2[a]	12.3 (40 µmol)	11 (0.11 mmol)	3	50 (TolH[c])	0.34 (1 mol/%)	rt
3[a]	9.3 (30 µmol)	1000 (9.63 mmol)	300	-	0.31 (1.5 mol/%)	rt
4[b]	12.1 (30 µmol)	11 (0.09 mmol)	3	10 (TolH[c])	0.29 (1.5 mol/%)	rt
5[b]	40.0 (120 µmol)	46 (0.37 mmol)	3	6 (DCM)	11.60 (15 mol/%)	40
6[b]	16.9 (50 µmol)	23 (0.19 mmol)	4	15 (DCM)	3.66 (10 mol/%)	40
7[b]	19.4 (60 µmol)	23 (0.19 mmol)	3	15 (DCM)	0.88 (2 mol/%)	40

[a] 4-Penten-2-ol (**31**), [b] 5-Bromo-1-penten (**34**), [c] Toluene

Table 88: Results for reaction cascade starting from 12-OPDA **1**, esterification with CAL-B and metathesis reactions with different parameters.

Experiment	Conv.%
1	10
2	1
3	5
4	30
5	99
6	99
7	20

10.6.9 Ethyl 8-((1S,5S)-5-((Z)-5-hydroxyhex-2-en-1-yl)-4-oxocyclopent-2-en-1-yl)octanoate (39)

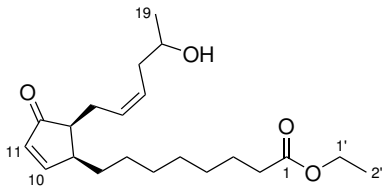

39
$C_{21}H_{34}O_4$
350.25 g mol^{-1}

The reaction was done with 12-OPDA-ethylester (**32**, 23 mg, 70 µmol) and 4-penten-2-ol (**31**, 22 µL, 210 µmol, 3 eq.) in degassed dichloromethane (10 mL) with HOVEYDA-GRUBBS catalyst 2nd generation (C1, 4.5 mg, 6 µmol, 10 mol%) for 17.5 h. Afterward, the solvent was removed, and the crude product purified according to GOP 27. The product was successfully isolated with a yield of 24% (**39**, 6.1 mg, 17 µmol).

^{1}H-NMR (500 MHz, $CDCl_3$): δ[ppm]= 7.71 (ddt, ^3J= 5.8 Hz, ^4J= 11.8, 3.2 Hz, 1H, (C10)*H*,), 6.19 – 6.14 (m, 1H, (C11)*H*,), 5.61 (dq, ^4J= 13.2, ^3J= 6.4 Hz, 1H, (C18)*H*), 5.47 (ddt, ^3J= 7.5 Hz, ^4J= 29.7, 15.0, 2H, (C15,16)*H*), 4.12 (q, ^3J= 7.1 Hz, 2H, (C1′)*H*,), 3.83 (dt, ^4J= 12.6, ^3J= 6.4 Hz, 2H, (C17)*H*,), 2.98 (m, 1H, (C9)*H*), 2.45 (dt, ^3J= 6.5, ^4J= 16.4 Hz, 1H, (C14)*Ha*), 2.41 – 2.36 (m, 1H, (C13)*H*), 2.29 (t, ^3J= 7.5 Hz, 2H, (C2)*H*), 2.26 – 2.18 (m, 1H, (C14)*Hb*), 1.76 - 1.68 (m, 2H, (C8)*H*), 1.62 (t, ^3J= 7.3 Hz, 2H, (C3)*H*), 1.32 (m, 8H, (C4-7)*H*), 1.26 (t, ^3J= 7.1 Hz, 3H, (C2′)*H*), 1.20 (dd, ^3J= 6.3, ^4J= 3.4 Hz, 3H, C(19)*H*).

^{13}C-NMR (126 MHz, $CDCl_3$): 210.86 (*C12*), 173.85 (*C1*), 167.15 (*C10*), 133.12 (*C11*), 132.43 (*C16*) ,127.15 (*C15*), 67.21 (*C18*), 60.20 (*C2´*), 49.45 (*C13*), 44.35 (*C9*), 34.33 (*C2*), 30.76, (*C8*), 29.60 – 28.66 (*C4-7*), 27.57 (*C3*), 25.68 (*C14*), 24.91 (*C19*), 20.63 (*C17*), 14.26 (*C1´*).

MS (ESI): m/z = 373.27 $[M+Na]^+$.

HRMS (ESI) calculated for $[C_{21}H_{34}O_4+H]^+$ 351.25299, found 351.25366.

IR (neat)/cm^{-1}: 3439 (s, -ν, OH) 2925 (s, -ν, -CH_2), 2921 (m, -ν, -CH_3), 1732 (s, -ν, -C=O), 1702 (m, -ν, -C=C) 1347 (w, δ, -CH_2).

10.6.10 Ethyl 8-((1*S*,5*S*)-5-((*Z*)-6-bromohex-2-en-1-yl)-4-oxocyclopent-2-en-1-yl)octanoate (34)

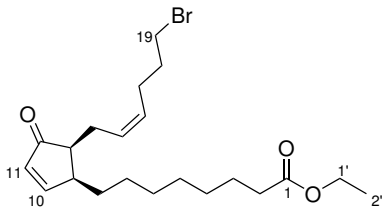

34
$C_{21}H_{33}BrO_3$
413.40 g mol^{-1}

The reaction was done with 12-OPDA-ethylester (**32**, 19.4 mg, 60 µmol or 30.0 mg, 90 µmol) and 5-bromopentene (**33**, 22 µL, 180 µmol, 3 eq. or 41.0 µL, 0.34 mmol, 4 eq.) in degassed dichloromethane (10 mL) with Hoveyda-Grubbs catalyst 2nd generation (C1, 3.8 mg, 6 µmol, 10 mol% or C1, 13.3 mg, 16 µmol, 18 mol%) for 17.5 h. Afterward, the solvent was removed, and the crude product purified according to GOP 27. The product **34** was successfully isolated with a yield of 10 mg (24 µmol), 40% or 23 mg (56 µmol), 61%.

^{1}H-NMR (500 MHz, $CDCl_3$): δ[ppm]= 7.72 (dd, ^{3}J= 5.8 Hz, ^{4}J= 2.7 Hz, 1H, (C10)*H*), 6.16 (d, ^{3}J= 5.8 Hz, 1H, (C11)*H*), 5.61 – 5.36 (m, 2H, (C15,16)*H*), 4.11 (q, ^{3}J= 7.2 Hz, 2H, (C2′)*H*), 3.38 (dt, ^{4}J= 15.1, ^{3}J= 6.6 Hz, 2H, (C19)*H*), 3.01 – 2.94 (m, 1H, (C9)*H*), 2.60 (m, 2H, (C18)*H*), 2.50 (m, 1H, (C14)*Ha*), 2.41 – 2.36 (m, 1H, (C13)*H*), 2.28 (t, ^{3}J= 7.5 Hz, 2H, (C2)*H*), 2.20 -2.15 (m, 1H, (C14)*Hb*), 1.90 (m, 2H, (C17)*H*), 1.77 – 1.68 (m, 2H, (C8)*H*), 1.67 – 1.58 (m, 2H, (C3)*H*), 1.31 (s, 8H, (C4-7)*H*), 1.25 (t, ^{3}J= 7.1 Hz, 3H, (C1′)*H*).

^{13}C-NMR (126 MHz, $CDCl_3$): 210.86 (*C12*), 173.85 (*C1*), 167.15 (*C10*), 133.12 (*C11*), 132.43 (*C16*), 127.15 (*C15*), 60.20 (*C2´*), 49.45 (*C13*), 44.32 (*C9*), 34.33 (*C2*), 33.20 (*C19*), 32.28 (*C18*), 30.76, (*C8*), 29.60 – 28.66 (*C4-7*), 27.57 (*C17*), 25.68 (*C14*), 24.91 (*C3*), 14.26 (*C1´*).

MS (ESI): m/z = 435.229 m/z $[M+Na]^+$, 437.186 m/z $[M+Na]^+$.

HRMS (ESI) calculated for $[C_{21}H_{33}BrO_3+Na]^+$ 435.1505, found 435.1506.

IR (neat)/cm^{-1}: 2925 (s, -ν, CH_2), 2854 (m, -ν, CH_2), 1732 (s, -ν, C=O-Ester), 1702 (vs, -ν, C=O-carbonyl), 1586 (w, -ν, C=C), 600 (w, -ν, C-Br).

10.6.11 Ethyl 8-((1*S*,5*S*)-5-((*Z*)-6-cyanohex-2-en-1-yl)-4-oxocyclopent-2-en-1-yl)octanoate (35)

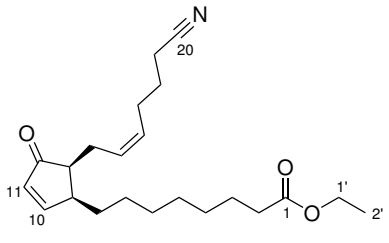

35
$C_{22}H_{33}NO_3$
359.51 g mol^{-1}

The reaction was done with 12-OPDA-ethylester (**32**, 24.0 mg, 60 µmol) and hex-5-enenitril (**36**, 21.7 µL, 0.19 mmol, 3 eq.) in degassed dichloromethane (10 mL) with HOVEYDA-GRUBBS catalyst 2nd generation (C1, 3.80 mg, 6 µmol, 10 mol%) for 17.5 h. Afterward, the solvent was removed, and the crude product purified according to GOP 27. The product **35** was successfully isolated with a yield of 40% (9.0 mg, 25 µmol).

^{1}H-NMR (500 MHz, $CDCl_3$): δ[ppm]= 7.72 (dd, ^3J= 6.0 Hz, ^4J= 2.7 Hz, 1H, (C10)*H*), 6.16 (dd, ^3J= 5.9, ^4J= 1.7 Hz, 1H, (C11)*H*), 5.47 – 5.38 (m, 2H, (C15, 16)*H*), 4.11 (q, ^3J= 7.1 Hz, 2H, (C1′)*H*), 3.61 (m, 2H, (C19)*H*), 2.98 (tt, ^3J= 8.4, ^4J= 3.7 Hz, 1H, (C9)*H*), 2.60 (q, ^3J= 8,4 Hz, 2H, (C18)*H*) 2.49 (dd, ^3J= 5.5, ^4J= 15.3 Hz, 1H, (C13)*H*), 2.43 (m, 1H, (C14)*Ha*), 2.33 (t, ^3J= 7.0 Hz, 2H, (C17)*H*), 2.28 (t, ^3J= 7.5 Hz, 3H, (C2)*H*), 2.18 (m, 1H, (C14)*Hb*), 1.72 – 1.68 (m, 2H, (C8)*H*), 1.61 (q, 2H, (C3)*H*), 1.33 (s, 8H, (C4-7)*H*), 1.25 (t, ^3J= 7.2 Hz, 3H, (C2′)*H*).

^{13}C-NMR (126 MHz, $CDCl_3$): δ[ppm]= 210.86 (*C12*), 173.85 (*C1*), 167.15 (*C10*), 132.43 (*C11*), 130.84 (*C16*), 127.15 (*C15*), 119.52 (*C20*), 60.20 (*C2´*), 49.45 (*C13*), 44.31 (*C9*), 34.33 (*C2*), 30.76 (*C8*), 29.60 - 28.66 (*C4-7*), 25.68 - 24.89 (*C17-18,14,3*), 16.42 (*C19*), 14.26 (*C1´*).

MS (ESI): m/z = 382.30 $[M+Na]^+$.

HRMS (ESI) calculated for $[C_{22}H_{33}NO_3+Na]^+$ 382.23526, found 382.2348.

IR (neat)/cm^{-1}: 2925 (s, -ν, CH_2), 2854 (m, -ν, CH_2), 2250 (w, -ν, CN), 1732 (s, -ν, C=O-ester), 1702 (vs, -ν, C=O-carbonyl), 1586 (w, -ν, C=C).

10.6.12 Ethyl 8-((1*S*,5*S*)-4-oxo-5-((*Z*)-6-oxohept-2-en-1-yl)cyclopent-2-en-1-yl)octanoate (37)

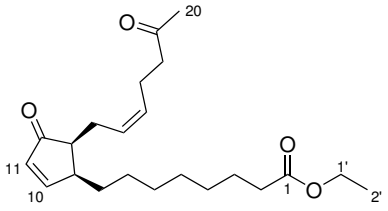

37
$C_{22}H_{34}O_4$
362.25 g mol^{-1}

The reaction was done with 12-OPDA-ethylester (**32**, 24.0 mg, 70 µmol) and hexen-5-one (**38**, 22.0 µL, 0.22 mmol, 3 eq.) in degassed dichloromethane (10 mL) with HOVEYDA-GRUBBS catalyst 2nd generation (C1, 4.7 mg, 6 µmol, 10 mol%) for 17.5 h. Afterward, the solvent was removed, and the crude product purified according to GOP 27. The product **37** was successfully isolated with a yield of 30% (8.0 mg, 22 µmol).

^{1}H-NMR (500 MHz, $CDCl_3$): δ[ppm]= 7.72 (dd, ^{3}J= 6.0, ^{4}J= 2.7 Hz, 1H, (C10)*H*), 6.20 (m, 1H, (C11)*H*), 5.40 – 5.30 (m, 2H, (C15,16)*H*), 4.12 (q, ^{3}J= 7.1 Hz, 2H, (C1′)*H*), 2.97 (m, 1H, (C9)*H*), 2.52 - 2.48 (m, 1H, (C14)*Ha*), 2.46 (dt, ^{3}J= 7.1, ^{4}J= 14.3 Hz, 1H, (C13)*H*), 2.32 (t, ^{3}J= 6.4 Hz, 2H, (C18)*H*), 2.28 (t, ^{3}J= 7.4 Hz, 2H, (C2)*H*), 2.16 – 2.07 (m, 1H, (C14)*Hb*), 2.12 (s, 3H, (C20)*H*), 2.03 (dq, ^{4}J = 24.9, ^{3}J= 7.9 Hz, 2H, (C17)*H*), 1.75-1.70 (m, 2H, (C8)*H*), 1.60 (q, ^{3}J= 7.1 Hz, 2H, (C3)*H*), 1.30 (s, 8H, (C4-7)*H*), 1.25 (t, ^{3}J= 7.1 Hz, 3H, (C2′)*H*).

^{13}C-NMR (126 MHz, $CDCl_3$): δ[ppm]= 210.62 (*C12*), 208.49 (*C19*), 173.96 (*C1*), 167.19 (*C10*), 132.92 (*C11*), 132.57 (*C16*), 127.66 (*C15*), 60.34 (*C2´*), 49.42 (*C13*), 44.43 (*C9*), 43.47 (*C18*), 34.46 (*C2*), 30.80 (*C20*), 30.11 (*C8*), 28.67 - 26.80 (*C4-7*), 24.91 (*C3*), 22.57 (*C14*), 21.71 (*C17*), 14.41 (*C1´*).

MS (ESI): m/z = 385.30 $[M+Na]^+$.

HRMS (ESI) calculated for $[C_{22}H_{34}O_4+H]^+$ 363.25299, found 363.25271.

IR (neat)/cm^{-1}: 2925 (s, -ν, CH_2), 2854 (m, -ν, CH_2), 1715 (vs, -ν, C=O-Ester), 1586 (w, -ν, C=C).

10.6.13 Ethyl 8-((1*S*,5*S*)-4-oxo-5-((*Z*)-3-phenylallyl)cyclopent-2-en-1-yl)octanoate (40)

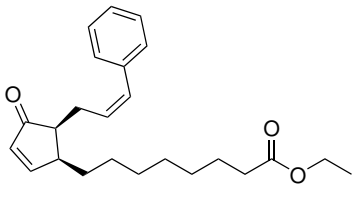

40
$C_{24}H_{32}O_3$
368.24 g mol^{-1}

The reaction was done with 12-OPDA-ethylester (10 mg, 30 µmol) and vinylacetate (8.60 µL, 0.10 mmol, 3 eq.) in degassed toluene (10 mL) with Hoveyda-Grubbs catalyst 2nd generation (C1, 0.39 mg, 4 µmol, 2 mol%) for 17 h. Afterward, the solvent was removed, no product could be detected.

10.6.14 Ethyl 8-((1*S*,5*S*)-5-((*Z*)-3-acetoxyallyl)-4-oxocyclopent-2-en-1-yl)octanoate (41)

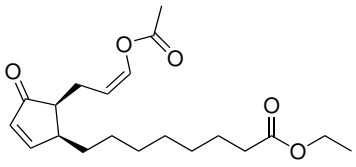

41
$C_{20}H_{30}O_5$
350.21 g mol^{-1}

The reaction was done with 12-OPDA-ethylester (**32**, 10 mg, 0.03 mmol) and stryrene (10.6 µL, 0.11 mmol, 3 eq.) in degassed toluene (10 mL) with Hoveyda-Grubbs catalyst 2nd generation (C1, 250 µg, 4 µmol, 2 mol%) for 17 h. Afterward, the solvent was removed, no product could be detected.

11 Appendix-I Ozanimod: Enzymatic synthesis of the key intermediate

11.1 Introduction

The topic of the appendix describes the completion of the enzyme-catalyzed synthesis step of ozanimod production, in which the lipase-catalyzed key step to the enantiomerically pure amine was further optimized. Ozanimod is a sphingosine-1-phosphate receptor-1 (S1P1) and receptor-5 (S1P5) agonist. Sphingosine-1-phosphate receptors are one possible target for addressing the therapy of autoimmune diseases, like multiple sclerosis.[273] The current chemical synthesis[274] of ozanimod, developed by the company *Receptos* is shown below (Scheme 57):

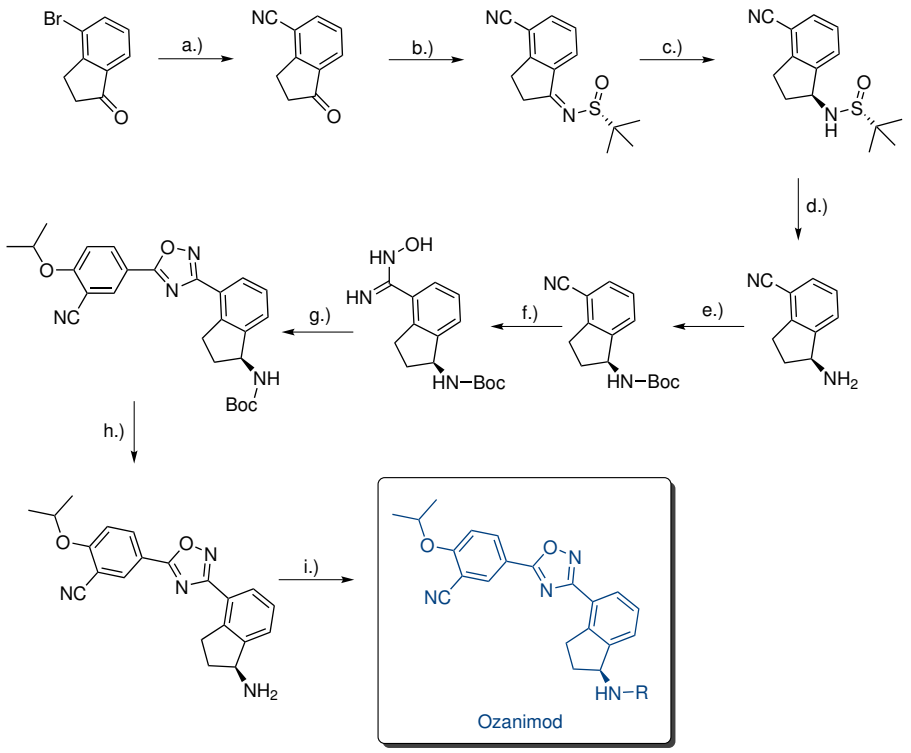

Scheme 57: Chemical Synthesis of Ozanimod, developd by the company *Receptos*. a.) $Zn(CN)_2$, $Pd(PPh_3)_4$, NMP; b.) 2-methylpropan-2-sulfamide, $Ti(OEt)_4$, toluene; c.) $NaBH_4$, THF; d.) 4 M HCl in dioxan, MeOH; e.) Boc_2O, TEA, DCM; f.) NH_2OH HCl, TEA, EtOH; g.) HOBt, EDC, substituted benzoic acid, DMF h.) 4 M HCl in dioxane; i.) R.

In the current synthesis of ozanimod by *Receptos* the chirality center is introduced using 2-methylpropane-2-sulfamide as a chiral auxiliary, starting from the 4-bromo-1-indanone.[274] In order to make this step more efficient, economical and cost-effective, the kinetic resolution of the racemic amine by the means of a lipase was chosen as a starting point. The following works are based on the work of the author of this thesis. In this work it could be demonstrated that the kinetic resolution of *rac*-1-aminoindane (**45**) and its derivatives towards (*S*)-1-aminoindane (**45**) could be performed and leads to high E-values and high enantioselectivity. In this context the racemic amines were prepared by reductive amination (yields between 27% and 37%). Furthermore, the kinetic resolution was optimized by evaluating the influence of *rac*-1-aminoindane (**45**) residues, different acyl donors, temperatures, solvent and substrate loading.

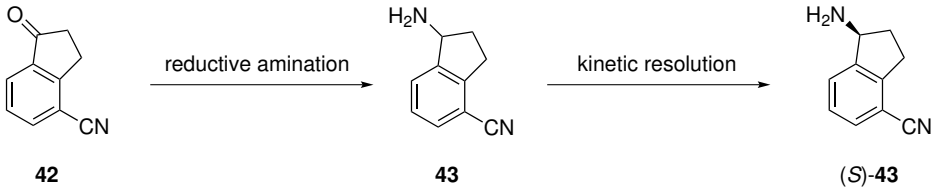

Figure 68: Reductive amination and lipase-catalyzed resolution towards the (*S*)-amine (**43**).

Finally, it was shown that (*S*)-**43** could be successfully produced from the ketone precursor by reductive amination and kinetic resolution (Scheme 68).[117]

In theory, the kinetic resolution describes a reaction, in which two enantiomers reacts at different reaction rate (Figure 69). The lipase distinguish between two enantiomers in a racemic mixture and therefore one enantiomer is faster converted than the other.[275]

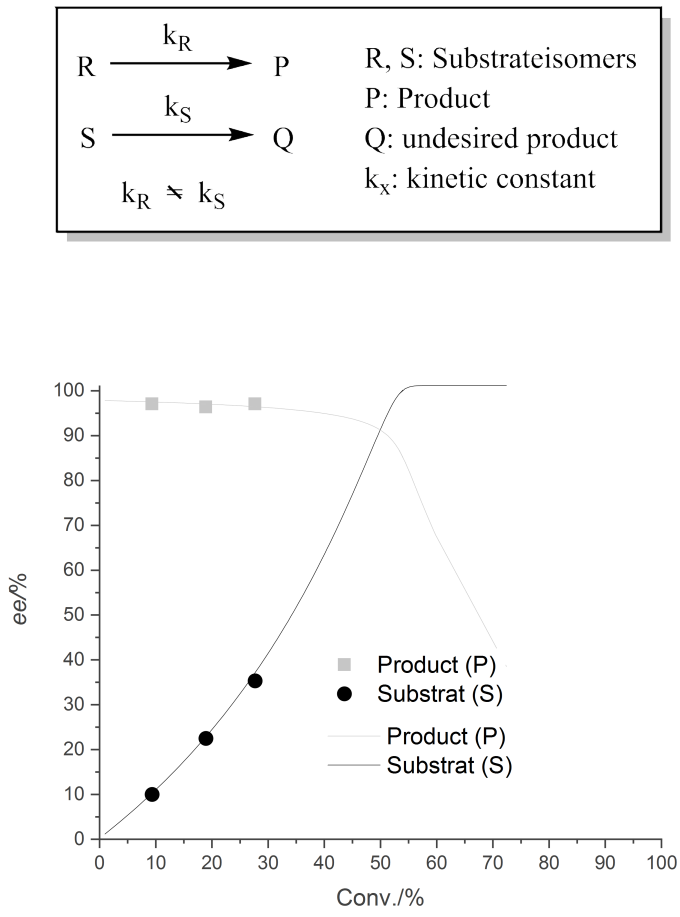

Figure 69: Theoretical backround for kinetic resolution.

To implement a kinetic resolution to obtain the enantiomerically pure (*S*)-amine **43**, lipases were tested showing Lipase B from *Candida antartica* CAL-B as the most promosing enzyme for aminoacylation of *rac*-1-aminoindane (**45**).[117] The CAL-B can be used for many different applications, including kinetic racemate splitting of racemic alcohols and amines or the desymmetrization of diols and diacetates. Industrial processes catalyzed by CAL-B include the synthesis of isopropyl myristate or the production of fats and oils.[49,56,276] CAL-B is furthermore used industrially for the synthesis of chiral products, as well as for the production of various pharmaceuticals and plant protection products.[277] Another example of the industrial use of lipases is the kinetic racemic cleavage of racemic amines established by BASF.[51,52,278]

With CAL-B in hand, the route was already implemented and optimized by preliminary work of the author of this thesis.[117] Therefore, the respective prochiral ketone was converted to the (*S*)-amine **43** with the best reaction conditions.

11.2 Results and diskussion

The main focus of research was the reduction of CAL-B amount for racemization of *rac*-4-cyano-1-aminoindane (**43**) (Figure 11.2) and the recycling of CAL-B.

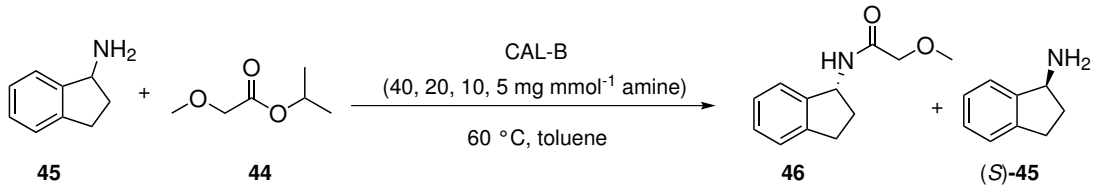

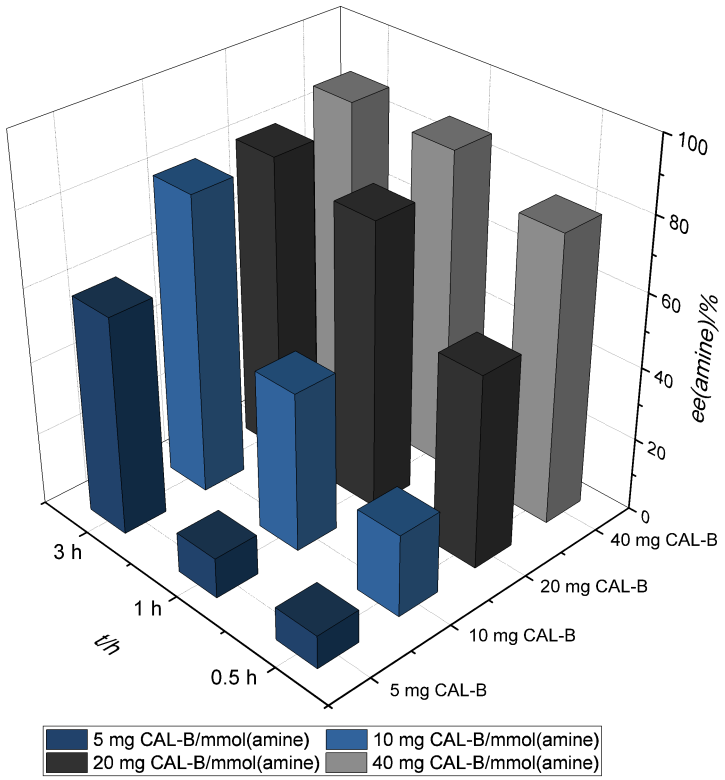

Figure 70: Reduction of catalyst amount in CAL-B-catalyzed resolution 1-aminoindane (**45**).

In recent works of the author of this thesis 40 mg $mmol^{-1}$ enzyme per substrate was used for biotransformation.[117] In further experiments the CAL-B amount was reduced to 20 mg $mmol^{-1}$, 10 mg $mmol^{-1}$ and 5 mg $mmol^{-1}$ enzyme per substrate, addressing a better manageability for industrial use, as well as for cost reduction. The reaction was representativly done with 1-aminoindane (**45**) and isopropyl methoxyacetate (**44**).

The reaction also proceeds with a decreased amount of CAL-B. The *ee*-values of 40 to 10 $mg \cdot mmol^{-1}$ do not really differ after 3 h. There is a slight decrease in the *ee*-value to about 60%, using 5 $mg \cdot mmol^{-1}$ CAL-B. A full conversion could probably be achieved by longer reaction time. With this reduced CAL-B amount, the reaction was also performed with 4-cyano-1-aminoindane **43**, and after 5 h a conversion of 57% and a *ee*-value of 99% for the the (*S*)-amine (*S*)-**43** could be reached.

Additionally, a recycling experiment was done (Figure 71), therefore the acylation of *rac*-1-aminoindane (**45**) was performed with isopropyl methoxyacetate (**44**) at 60 °C in toluene. The enzyme was reused for six times. The results are shown in Figure 71. The recycling experiment shows reusability of CAL-B with no significant loss in activity after six times. This result, as well as the reduction of the CAL-B amount, indicates a great major improvement of the system.

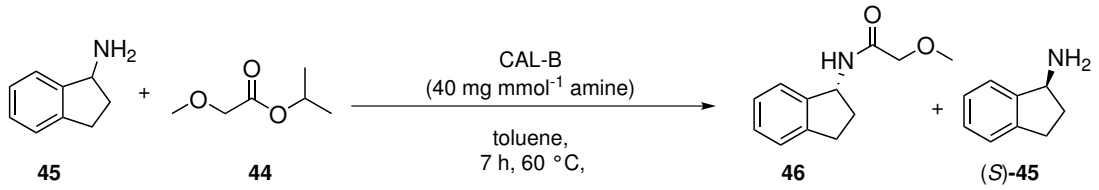

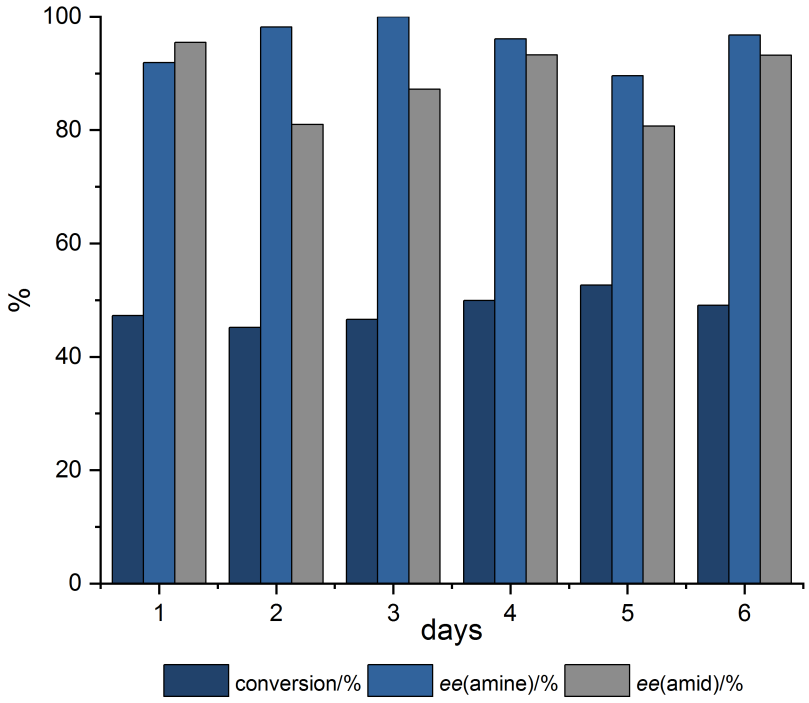

Figure 71: Recycling experiment with CAL-B.

In recent works of the author of this thesis racemization of *rac*-4-cyano-1-aminoindane (**43**) was carried out with ethyl methoxyacetate. Furthermore, it was shown that racemization of *rac*-1-aminoindane (**45**) with isopropyl methoxyacetate (**44**) leads to higher E-values compared to ethyl methoxyacetate.[117] In this regard the synthesis of (*S*)-4-cyano-1-aminoindane (**43**) was carried out with isopropyl methoxyacetate (**44**) and toluene instead of 2-MTHF.

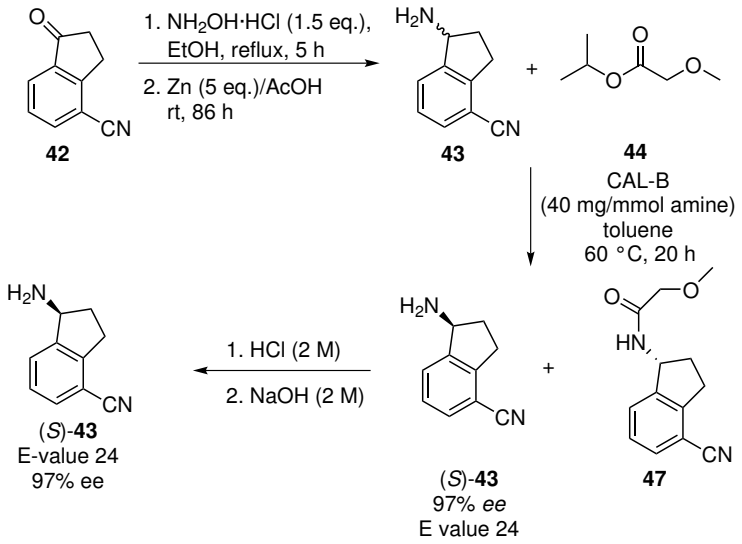

Figure 72: Chemoenzymatic synthesis of enantiomerically pure 4-cyano-1 aminoindane (**43**).

Compared to the racemization of *rac*-1-aminoindane (**45**) with ethyl methoxyacetate (E-values 22) the E-value for racemization of 1-aminoindane with isopropyl methoxyacetate (**44**) (E-value 24) is not as high as expected, compared to literature data.[56]

11.3 Experimental part

11.4 Substrate synthesis

11.4.1 Isopropyl methoxyacetate (44)

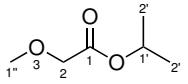

44

$C_6H_{12}O_3$

132.16 g mol^{-1}

2-Propanol (1.58 g, 26.3 mmol) and 2-methoxy acetyl chloride (2.11 g, 19.4 mmol) were dissolved in 10 mL methylene chloride. Triethylamine (3.19 g, 36.5 mmol) was added to the mixture and stirred for 1 h. The suspension was washed with 2 M hydrogen chloride (2x 10 mL). The organic phase was dried over $MgSO_4$. The solvent was removed *in vacuo*. The desired product **44** was isolated with a yield of 36% (0.92 g, 6.96 mmol).

^{1}H NMR (500 MHz, $CDCl_3$): δ/ppm = 1.26 (d, ^3J= 6.3 Hz, 6H, (C2′)H), 3.44 (s, 3H, (C1″)H), 3.98 (s, 2H, (C2)H), 5.11 (p, 1H, (C1″)H).

The ^{1}H NMR-spectrum for this compound is in accordance with the data reported in literature.[279]

11.4.2 *rac*-4-cyano-1-aminoindane (43)

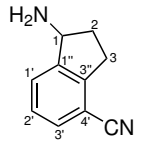

43

$C_{10}H_{10}N_2$

158.20 g mol^{-1}

4-Cyano-1-indanone (**42**, 0.40 g, 2.55 mmol) and hydroxylamine hydrochloride (0.27 g, 3.84 mmol) were dissolved in 10 mL ethanol and water (1:1, *v/v*). Meanwhile sodium hydroxide (0.17 g, 4.51 mmol), dissolved in 1 mL water, was added to the suspension. The mixture was heated to reflux for 1.5 h. The crude product was filtered over celite and washed with water. The oxime was dissolved in 10 mL acetic acid. Under argon atmosphere, zinc-dust (0.83 g, 12.77 mmol) was added and the suspension was stirred at room temperature for 86 h. The reaction mixture was filtered over celite, washed with ethyl acetate and the solvent was removed *in vacuo*. The oil was dissolved in 10 mL ethyl acetate and HCl (1:1,*v/v*) and extracted with 2 M hydrogen chloride (2x 10 mL). The pH value of the aqueous phase was adjusted to 10 and afterward extracted with ethyl acetate (3x 10 mL). The organic phase was washed with brine and dried over $MgSO_4$. The solvent was removed *in vacuo*.

^{1}H NMR (500 MHz, $CDCl_3$): δ/ppm = 7.71 (d, ^3J= 7.9 Hz, 1H, (C1′,3′)*H*), 7.56 (d, ^3J= 7.5 Hz, 1H, (C1′,3′)*H*), 7.36 (t, ^3J= 7.6 Hz, 1H, (C2′)*H*), 4.70 (t, ^3J= 7.5 Hz, 1 H, (C1)*H*), 3.28-3.30 (m, 1H, (C3)*H*), 3.00-3.06 (m, 1H, (C2)*H*), 2.60-2.67 (m, 1H, (C2)*H*), 2.09-2.19 (m, 1H, (C3)*H*).

The ^{1}H NMR-spectrum for this compound is in accordance with the data reported in literature.[280]

11.4.3 (*S*)-4-cyano-1-aminoindane (*S*)-(43)

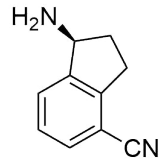

$C_{10}H_{10}N_2$
158.20 g mol^{-1}

4-Cyano-1-aminoindane (**43**, 76 mg, 0.46 mmol), isopropyl methoxyacetate (**44**, 67 mg, 0.51 mmol) and CAL-B (54326 *Sigma-Aldrich* Lipase B *Candida antarctica* immobilized on Immobead 150, recombinant from *Aspergillus oryzae*, 19 mg) was added to toluene (0.92 mL) and stirred at 60 °C for 20 h. The sample was acetylated with acetyl chloride (39.7 mg, 0.51 mmol) and triethylamine (69.8 µL, 0.69 mmol) in dichloromethane for one hour. The suspension was washed with HCl (1:1, *v/v*) and sodium hydrogen carbonate. The solvent was removed *in vacuo*. Enantiomeric excess and conversion were determined *via* HPLC. (*S*)-4-cyano-1-aminoindane ((*S*)-**43**, 23 mg, 0.15 mmol, 4% in two steps) was isolated as a yellow oil.

^{1}H NMR (500 MHz, $CDCl_3$): δ/ppm = 7.71 (d, ^3J= 7.9 Hz, 1H, (C1,3′)*H*), 7.56 (d, ^3J= 7.5 Hz, 1H, (C1,3′)*H*), 7.36 (t, ^3J= 7.6 Hz, 1H, (C2′)*H*), 4.70 (t, ^3J= 7.5 Hz, 1H, (C1)*H*), 3.28-3.30 (m, 1H, (C3)*H*), 3.00-3.06 (m, 1H, (C2)*H*), 2.60-2.67 (m, 1H, (C2)*H*), 2.09-2.19 (m, 1H, (C3)*H*).

^{13}C-NMR (500 MHz, $CDCl_3$): δ/ppm = 148.8 (*C1″*), 147.4 (*C3″*), 130.9 (C_{aryl}), 128.2 (C_{aryl}), 127.5 (C_{aryl}), 117.9 (*C4′*), 109.0 (C_{aryl}), 57.4 (*C1*), 37.1 (*C2,3*), 30.0 (*C2,3*).

MS (ESI): m/z = 159.0 $[M+H]^+$, 298.1 $[2M+H]^+$.

NP-HPLC: Daicel Chiracel OJ-H, CO_2/isopropanol 95:5, 1.5 mL · min^{-1}, 20 °C, 210 nm, R_{t1} = 19.0 min.

The ^{1}H NMR-spectrum for this compound is in accordance with the data reported in literature.[280]

11.4.4 *(R)*-4-Cyano-1-indanyl-(2-methoxyacetamid) (47)

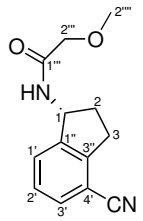

46
$C_{13}H_{14}N_2O_2$
230.27 g mol^{-1}

(*R*)-4-Cyano-1-indanyl-(2-methoxyacetamid) (*R*)-**47** (78 mg, 0.20 mmol, 5% in two steps) was isolated as a brown solid.

^{1}H NMR (500 MHz, $CDCl_3$): δ/ppm: 7.51 (tt, ^3J= 7.7, 0.9 Hz, 2H, (C1,3′)*H*), 7.30 (dd, ^3J= 7.7 Hz, 1H, (C2′)*H*), 5.58 (q, ^3J= 8.1 Hz, 1H, (C1)*H*), 3.96 (d, ^4J= 2.5 Hz, 2H, (C2‴)*H*), 3.40 (s, 3H, (C2⁗)*H*), 3.21-3.25 (m, 1H, (C3)*H*), 3.07-3.12 (m, 1H, (C2)*H*), 2.67-2.71 (m, 1H, (C3)*H*), 1.92-2.00 (m, 1H, (C2)*H*).

^{13}C-NMR (500 MHz, $CDCl_3$): δ/ppm = 169.6 (*C1‴*), 147.3 (*C1″*), 144.7 (*C3″*), 131.6 (C_{aryl}), 128.8 (C_{aryl}), 127.7 (C_{aryl}), 117.4 (*C4′*), 109.2 (C_{aryl}), 71.8 (*C2‴*), 59.2 (*C1⁗*), 53.7 (C_{aryl}), 33.2 (*C2,3*), 29.9 (*C2,3*).

MS (EI): m/z = 253.1 $[M+Na]^+$, 483.1 $[2M+Na]^+$.

IR (neat)/cm^{-1}: 3216 (m, *v*, -NH), 2920 (m, *v*, -CH_3), 2850 (w, *v*, -O-CH_3), 2222 (m, *v*, -CN), 1654 (s, *v*, -C=O), 1541 (w, *v* , HN-C=O-), 1447 (w, δ, -CH2), 795 (m, δ, -Ar).

EA: calculated for $C_{13}H_{14}N_2O_2$: C, 67.81; H, 6.13; N, 12.17. Found: C, 67.83; H, 6.21; N, 11.73.

NP-HPLC: Daicel Chiracel OJ-H, CO_2/isopropanol 95:5, 1.5 mL · min^{-1}, 20 °C, 210 nm, R_{t1} = 22.4 min.

11.5 General operating procedure (GOP 28): Kinetic resolution catalyzed by lipases

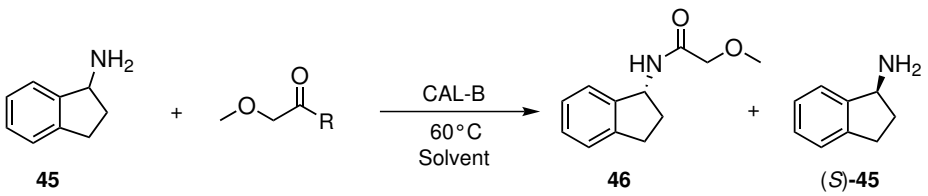

1-Aminoindane (**45**, 1.0 eq) and the acyldonor (1.1 eq) were dissolved in organic solvent. CAL-B (54326 *Sigma-Aldrich* Lipase B *Candida antarctica* immobilized on Immobead 150, recombinant from *Aspergillus oryzae*) was added and heated to 60 °C. At fixed times, samples were taken. The samples were acetylated with acetyl chloride (1.1 eq) and triethylamine (1.5 eq) in methylene chloride for one hour for HPLC-analysis. The suspension was washed with hydrogen chloride (1:1, *v/v*). The solvent was removed *in vacuo*. Enantiomeric excess and conversion were determined *via* HPLC.

11.5.1 Stepwise reduction of catalyst amount

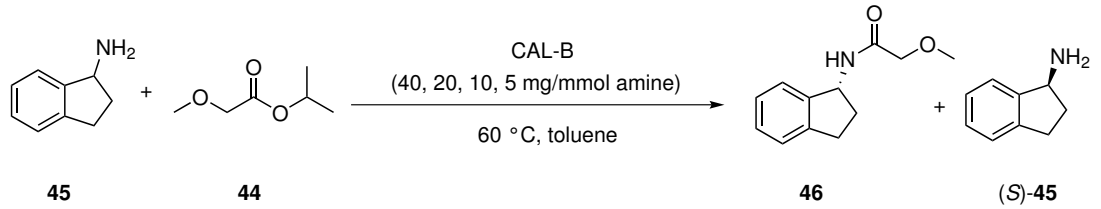

The reaction was performed according to GOP 28. 1-Aminoindan (**45**, 83 mg, 0.63 mmol), isopropyl methoxyacetate (**44**, 91 g, 0.69 mmol) and CAL-B (54326 *Sigma-Aldrich* Lipase B *Candida antarctica* immobilized on Immobead 150, recombinant from *Aspergillus oryzae*, 25 mg, 13 mg, 6 mg and 3 mg) were dissolved in 1.25 mL toluene and stirred at 60 °C. After 0.5 h, 1 h and 3 h, 100 µL samples were taken. The samples were acylated with acetyl chloride (4 mg, 0.04 mmol) and triethylamine (8 mg, 0.08 mmol). The samples were purified and analyzed according to GOP 28.

Table 89: Conversion and *ee*-value for racemization of *rac*-**43** with reduced CAL-B amount.

CAL-B/mg · mmol^{-1}	t/h	conv/%[a]	*ee*-amine/%[a]	*ee*-amide/%[a]
5	0.5	9	9	91
5	1	10	11	91
5	2	29	38	92
5	3	39	59	90
5	5	44	74	91
5	7	48	85	91
10	0.5	19	22	95
10	1	31	43	94
10	3	46	81	95
20	0.5	45	52	93
20	1	47	78	94
20	3	48	81	91
40	0.5	45	78	93
40	1	47	86	94
40	3	48	87	91

[a] Determinded by the means of HPLC

11.6 Recycling of CAL-B

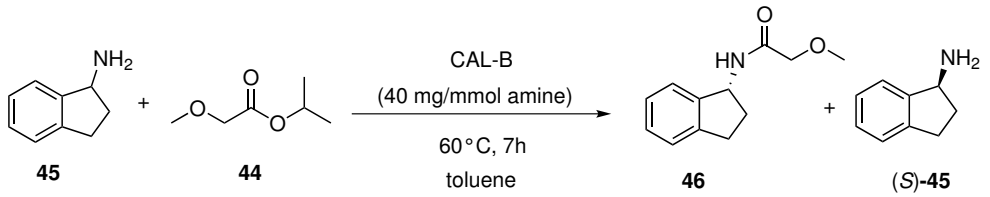

The reaction was performed according to GOP 28. 1-Aminoindane (**45**, 67 mg, 0.50 mmol), isopropyl methoxyacetate (**44**, 73 mg, 0.55 mmol) and CAL-B (54326 *Sigma-Aldrich* Lipase B *Candida antarctica* immobilized on Immobead 150, recombinant from *Aspergillus oryzae*, 20 mg) were dissolved in 5 mL toluene and stirred at 60 °C. After 7 h, 200 µL of a sample was taken. The sample was acylated with acetyl chloride (9 mg, 0.11 mmol) and triethylamine (15 mg, 0.15 mmol). The sample was purified and analyzed according to GOP 28. The reaction was repeated six times.

Table 90: Conversion and *ee*-value for racemization with recycled CAL-B.

Day	conv/%[a]	*ee*-amine/%[a]	*ee*-amide/%[a]
1	47	91	95
2	45	98	80
3	46	99	87
4	49	96	93
5	52	89	80
6	49	96	93
7	47	91	95

[a] Determinded by the means of HPLC

The results of the new approach towards ozanimod of kinetic resolution as a key step were published in Journal of Organic Chemistry: F. Uthoff, J. Löwe, C. Harms, K. Donsbach, H. Gröger, Total Synthesis of Ozanimod Based on a Biocatalytic Key Step, *J. Org Chem* **2019**, *8*, 4856-4866 and as a patent J. Löwe, F. Uthoff, C. Harms, K. Donsbach, H. Gröger, 2018, Enantioselective Biocatalytic Preparation of 4-Cyano-Substituted 1-Aminoindane and Ozanimod, EP 18167058.9, 06.06.2018.

12 Appendix-II

12.1 Sequences and plasmid cards

All plasmids that were not provided with a literature reference were purchased from *ThermoScientific*.

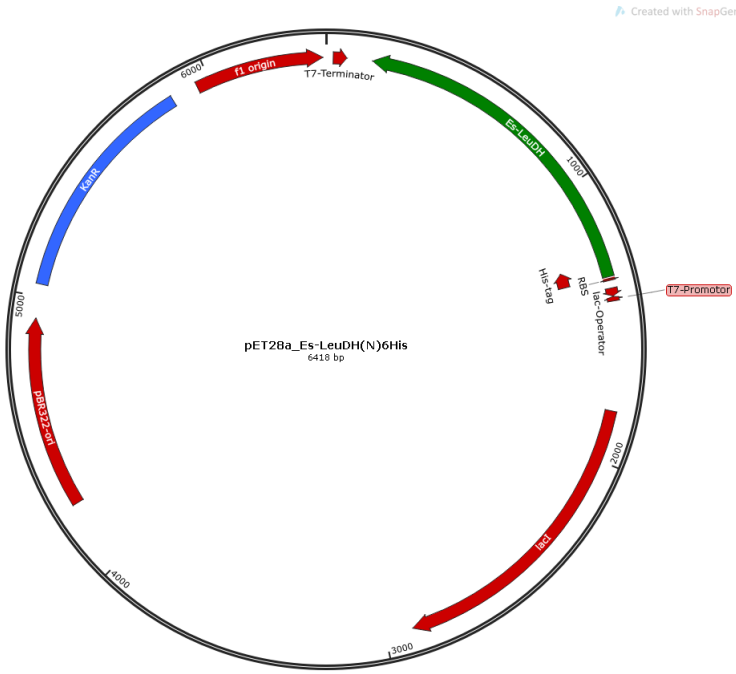

Leucine dehydrogenase from *Exiguobacterium sibiricum* - EsLeuDH Uniprot: B1YLR3, Nucleotid sequence (1125 bp):[117]

ATGGTTGAAACAAACGTAGAAGCACGATTCAGTATTTTCGAAACGATGG
CAATGGAAGATTACGAACAAGTCGTATTTTGTCACGATAAAGTCTCAGGAT
TAAAGGCGATTATCGCGATTCATGATACGACACTCGGACCAGCACTCGGCG
GACTCCGTATGTGGAACTATGCGTCTGACGAGGAAGCATTGATCGACGCG
CTTCGTTTGGCAAAAGGCATGACGTATAAAAATGCGGCAGCCGGTCTGAAC
CTTGGCGGCGGGAAAGCGGTCATCATCGGTGATGCGAAAACGCAAAAATC
AGAAGCTCTGTTCCGTGCATTCGGTCGTTACGTACAGTCGTTAAACGGACG
TTACATCACTGCGGAAGACGTCAACACAACAGTCGCCGACATGGATTATAT
CCACATGGAAACAGATTTCGTAACCGGTGTCAGCCCGGCATTCGGATCAAG
CGGCAATCCGTCACCAGTCACGGCTTATGGCGTTTACCGCGGAATGAAGGC
AGCCGCTAAAGAAGTATATGGCACAGATTCACTCGGAGGAAAAACAGTTG

CGATTCAAGGTGTTGGTAACGTTGCTTTCAACCTATGCCGTCACTTGCATG
AAGAAGGCGCAAAATTGATTGTCACAGACATCAATCAAGATGCATTACGCC
GTGCAGAAGAAGCGTTTGGCGCTCTCGTCGTCGGACCGGATGAAATTTAC
AGCGTCGATGCCGATATCTTTGCGCCGTGTGCCTTAGGTGCGACATTGAAC
GATGAGACGATTCCACAACTGAAAGTGAAAATCATTGCCGGAGCAGCAAAC
AACCAACTCAAAGAAGATCGTCACGGAGATATGCTCCAGGAACGCGGTATT
TTATATACACCGGACTTCGTCATCAACGCAGGAGGTGTCATCAATGTGGCC
GACGAACTCGACGGGTACAACCGTGAGCGGGCGATGAAAAAAGTCGAACT
CGTCTATGATGCGGTAGCAAAAGTCATCGAAATTGCCAAACGTGACCATCT
GCCGACTTACCGGGCAGCAGAGAAGATGGCAGAAGAACGGATCGCGACAA
TGGGCAGTGCCCGCAGCCAGTTCTTACGCCGGGATAAAAACATTTTAGGAT
CACGCGGTTAA

Amino acid sequence (374 AS; 40.5 kDa):

MVETNVEARFSIFETMAMEDYEQVVFCHDKVSGLKAIIAIHDTTLGPALGGL
RMWNYASDEEALIDALRLAKGMTYKNAAAGLNLGGGKAVIIGDAKTQKSEALF
RAFGRYVQSLNGRYITAEDVNTTVADMDYIHMETDFVTGVSPAFGSSGNPSPV
TAYGVYRGMKAAAKEVYGTDSLGGKTVAIQGVGNVAFNLCRHLHEEGAKLIV
TDINQDALRRAEEAFGALVVGPDEIYSVDADIFAPCALGATLNDETIPQLKVKII
AGAANNQLKEDRHGDMLQERGILYTPDFVINAGGVINVADELDGYNRERAMK
KVELVYDAVAKVIEIAKRDHLPTYRAAEKMAEERIATMGSARSQFLRRDKNILG
SRG

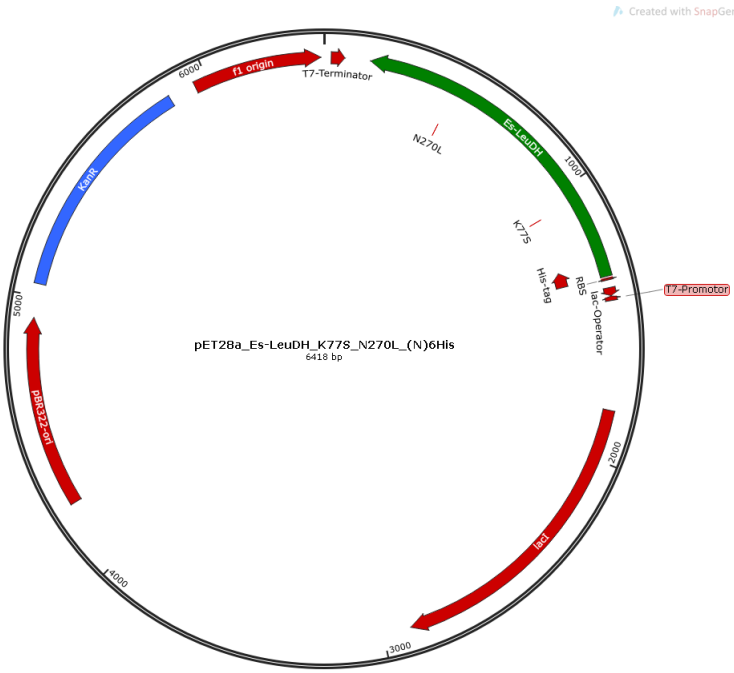

Amine dehydrogenase from *Exiguobacterium sibiricum* EsLeuDH-DM in pET28(a)+ and N-terminal his tag with K77S,N270L: pET28(a)+EsLeuDH-

DM(N)His$_6$, Nucleotide sequence (1185 bp):[82]

ATGGGCAGCAGCCATCATCATCATCATCACAGCAGCGGCCTGGTGCCGCG
CGGCAGCCATATGGTTGAAACAAACGTAGAAGCACGATTCAGTATTTTCGA
AACGATGGCAATGGAAGATTACGAACAAGTCGTATTTTGTCACGATAAAGT
CTCAGGATTAAAGGCGATTATCGCGATTCATGATACGACACTCGGACCAGC
ACTCGGCGGACTCCGTATGTGGAACTATGCGTCTGACGAGGAAGCATTGA
TCGACGCGCTTCGTTTGGCAAAAGGCATGACGTATAGCAATGCGGCAGCC
GGTCTGAACCTTGGCGGCGGGAAAGCGGTCATCATCGGTGATGCGAAAAC
GCAAAAATCAGAAGCTCTGTTCCGTGCATTCGGTCGTTACGTACAGTCGTT
AAACGGACGTTACATCACTGCGGAAGACGTCAACACAACAGTCGCCGACAT
GGATTATATCCACATGGAAACAGATTTCGTAACCGGTGTCAGCCCGGCATT
CGGATCAAGCGGCAATCCGTCACCAGTCACGGCTTATGGCGTTTACCGCGG
AATGAAGGCAGCCGCTAAAGAAGTATATGGCACAGATTCACTCGGAGGAA
AAACAGTTGCGATTCAAGGTGTTGGTAACGTTGCTTTCAACCTATGCCGTC
ACTTGCATGAAGAAGGCGCAAAATTGATTGTCACAGACATCAATCAAGATG
CATTACGCCGTGCAGAAGAAGCGTTTGGCGCTCTCGTCGTCGGACCGGAT
GAAATTTACAGCGTCGATGCCGATATCTTTGCGCCGTGTGCCTTAGGTGCG
ACATTGAACGATGAGACGATTCCACAACTGAAAGTGAAAATCATTGCCGGA
GCAGCACTAAACCAACTCAAAGAAGATCGTCACGGAGATATGCTCCAGGAA
CGCGGTATTTTATATACACCGGACTTCGTCATCAACGCAGGAGGTGTCATC
AATGTGGCCGACGAACTCGACGGGTACAACCGTGAGCGGGCGATGAAAAA
AGTCGAACTCGTCTATGATGCGGTAGCAAAAGTCATCGAAATTGCCAAACG
TGACCATCTGCCGACTTACCGGGCAGCAGAGAAGATGGCAGAAGAACGGA
TCGCGACAATGGGCAGTGCCCGCAGCCAGTTCTTACGCCGGGATAAAAACA
TTTTAGGATCACGCGGTTAA

Amino acid sequence (394 AS; 42.7 kDa):

MGSSHHHHHHSSGLVPRGSHMVETNVEARFSIFETMAMEDYEQVVFCHDKV
SGLKAIIAIHDTTLGPALGGLRMWNYASDEEALIDALRLAKGMTYSNAAAGLNL
GGGKAVIIGDAKTQKSEALFRAFGRYVQSLNGRYITAEDVNTTVADMDYIHME
TDFVTGVSPAFGSSGNPSPVTAYGVYRGMKAAAKEVYGTDSLGGKTVAIQGV
GNVAFNLCRHLHEEGAKLIVTDINQDALRRAEEAFGALVVGPDEIYSVDADIFA
PCALGATLNDETIPQLKVKIIAGAALNQLKEDRHGDMLQERGILYTPDFVINAG
GVINVADELDGYNRERAMKKVELVYDAVAKVIEIAKRDHLPTYRAAEKMAEER
IATMGSARSQFLRRDKNILGSRG-

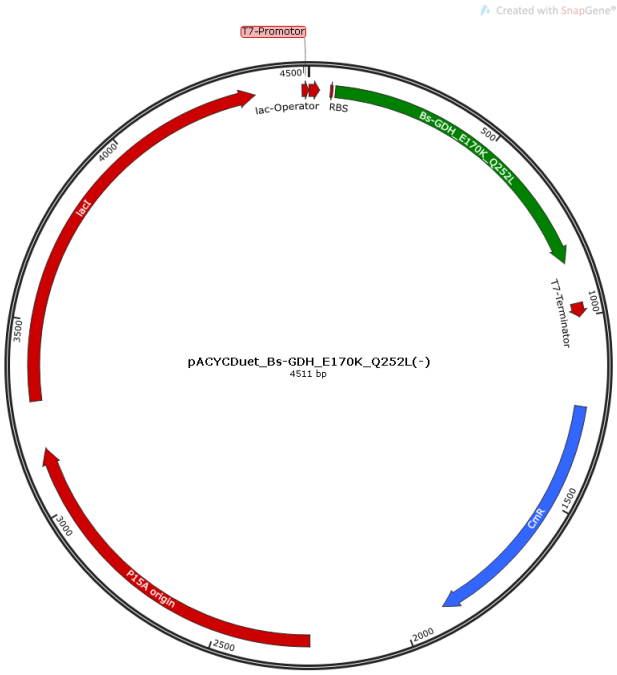

Glucose dehydrogenase from *Bacillus subtilis* Bs-GDH in pACYCDuet with E170K,Q252L heat stable enzyme: pACYCDuetBs-GDH, Nucleotide sequence (786 bp):[111]

ATGTATCCGGATTTAAAAGGAAAAGTCGTCGCTATTACAGGAGCTGCTT
CAGGGCTCGGAAAGGCGATGGCCATTCGCTTCGGCAAGGAGCAGGCAAAA
GTGGTTATCAACTATTATAGTAATAAACAAGATCCGAACGAGGTAAAAGAA
GAGGTCATCAAGGCGGGCGGTGAAGCTGTTGTCGTCCAAGGAGATGTCAC
GAAAGAGGAAGATGTAAAAAATATCGTGCAAACGGCAATTAAGGAGTTCG
GCACACTCGATATTATGATTAATAATGCCGGTCTTGAAAATCCTGTGCCAT
CTCACGAAATGCCGCTCAAGGATTGGGATAAAGTCATCGGCACGAACTTAA
CGGGTGCCTTTTTAGGAAGCCGTGAAGCGATTAAATATTTCGTAGAAAACG
ATATCAAGGGAAATGTCATTAACATGTCCAGTGTGCACGAAGTGATTCCTT
GGCCGTTATTTGTCCACTATGCGGCAAGTAAAGGCGGGATAAAGCTGATG
ACAAAGACATTAGCGTTGGAATACGCGCCGAAGGGCATTCGCGTCAATAAT
ATTGGGCCAGGTGCGATCAACACGCCAATCAATGCTGAAAAATTCGCTGAC
CCTAAACAGAAAGCTGATGTAGAAAGCATGATTCCAATGGGATATATCGGC
GAACCGGAGGAGATCGCCGCAGTAGCAGCCTGGCTTGCTTCGAAGGAAGC
CAGCTACGTCACAGGCATCACGTTATTCGCGGACGGCGGTATGACACTCTA
TCCTTCATTCCAGGCAGGCCGCGGTTAA

Amino acid sequence (261 AS; 28.1 kDa):

MYPDLKGKVVAITGAASGLGKAMAIRFGKEQAKVVINYYSNKQDPNEVKEE
VIKAGGEAVVVQGDVTKEEDVKNIVQTAIKEFGTLDIMINNAGLENPVPSHEMP
LKDWDKVIGTNLTGAFLGSREAIKYFVENDIKGNVINMSSVHEVIPWPLFVHYA

ASKGGIKLMTKTLALEYAPKGIRVNNIGPGAINTPINAEKFADPKQKADVESMI
PMGYIGEPEEIAAVAAWLASKEASYVTGITLFADGGMTLYPSFQAGRG-

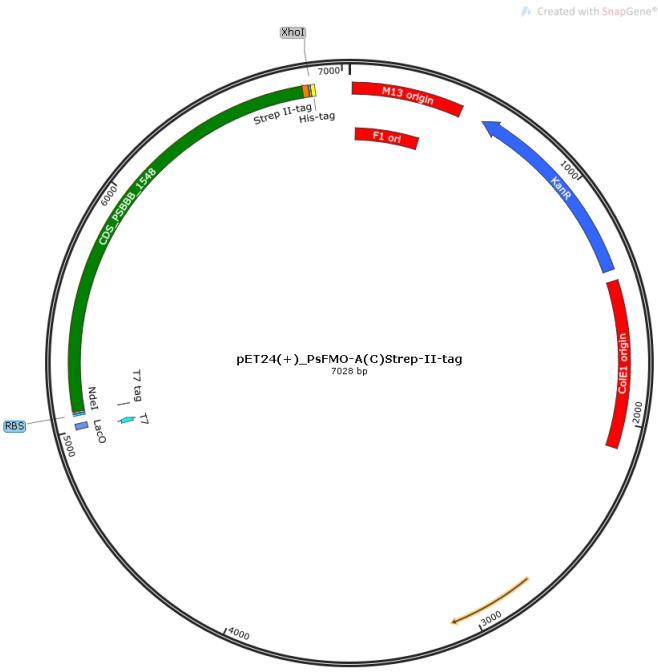

Flavinmonooxygenase from *Pimelobacter sp.* *Bb-B* PsFMO-A (PSBBB1548) in pET24(a)+ with C-terminal strep-II-tag: pET24(a)+PsFMO-A(*C*)Strep-II-tag, Nucleotide sequence (1794 bp):[265]

ATGAAAGTTGACACTGGTAGTAGTCCTGACGAAGTGAAAGCGGCATTCG
AGGCATGGCTTGCCGACTTTGCGGACGCTCTTGCTACGGCTGACACTGGTG
CGACCACTGATTTACTGGACGCAGGTTGCTGGTGGCGTGACTTGCTTGCGC
TTAGTTGGGACCTGGGAACCTATCACGGAACGGACCGCATCGCGGGATTG
CTGGATGAACATTTAAAACCCGCGCAAGTTTCAGGAGTGCGCGTGGTAACC
GAGTTTGGGCCACGTTTTGTTGCGGAAGAGGGTGGGAGCGGAACAATCGA
AGGGTTCTTCACCTTCGAAACAGCAGGCGCCTGGTGTCGTGGAGTTGCTCG
CTTGCGTCAAGGGGATGACGGGTGGCGTGCATGGACGGTAATGACTGGGG
TGGAAGACCTGAAAGGTCATGAGCGCGCTCTTGGAGAGCGTCGCCCGACA
GGGCCGCGTCACGAAGTAGGGGCTACCACTCAGCGCAACTGGAAGGATAA
GCGTGAAGCAGCTCAGGCGTACGACGACCGCGAGCCGGAAGTGGTCATTT
TGGGCGCAGGACAAGGAGGCTTGGCGCTTGCAGCAAACCTGCGTCTGATG
GGGGTGGACGCCCTGATCCTTGAGAAAAGTGCACGCATCGGGGACGGGTG
GCGTCGCCGCTACCACTCCCTGGTGTTGCATGATCCTGTTTGGGCAGACCA
TTTGCCGTACCTTCCTTTTCCACAATCTTGGCCAATCTATAGCCCGAAGGA
TAAAATCGCGGACTGGTTTGAGTTTTATGCCCAGGCAATGGAACTTAATGT
CTGGTGCAGCGCCGAAATGACGGACGCGGCTTACGATGAACAGGCCGGAG

CGTGGACCTTGACGGTCCGCACCGAACAGGGGGAACGCACACTGCGTCCG
CGTAATGTAGTATTGGCGACAGGAGCTGCAGGCGAACCGAACATTCCGGA
TTTCCCAGGGCGTGATGAATTTGCTGGCACCGTATATCACTCGTCCCAACA
TGGAGCCGGTGGGTCATGGGCCGGGAAGAAGGCGATTGTTGTGGGGGCCT
GCAACTCGGGGCATGATATTGCACAAGACCTGCATGAGGCCGGAGCGGAA
GTCACGCTTGTCCAGCGCAGTAGTACCCACATTATTAGTCAACAACACGGG
ATTCCCGCAATTTTTGGTGCTAATTTCACAGAGTCGGGTCCTCCTACAGAA
TACGCAGACTTGCTTGCGTCTGCGTTTCCTTGGCCGTTAGTACTGGAAGCA
GCTAAGGAAGGCGTCAAACAAACTGCCGAAAAGGATGCAGAGCTTTTAGC
ATCGTTAGAGGCGGTCGGGTTCCAACTGAATGACGGGCCAGATGGAACGG
GATTAATGGGTTTTGCGTTAGCGAAAGGTGGAGGCTATTACATCGACGTA
GGAGCATCTGGCTTGATTGCTTCAGGCCGCATTGCGCTTGCTCAGGGGTCC
GGGCTGGCGGAGTTCACCCCGTCCGGCATTCGCCTTGCTGATGGGCGTGA
GCTTGATGCTGATCTGGTTGTGCTTGCTACTGGGTATTCGAACATGCGCGA
AACAGCTCGTCGTCTGTTTGGGGATGGAGTAGCAGACCGCCTGCCAAGCG
TACTGGGGATTGGGGAGGACGGCGAGATCGGAGGCCTTTACCGTCGTACA
GGGCAACCCGGCTTTTGGTTTATGGGCGGTCCTTTAGCCTGGGTCCGCGTA
TATAGCAAGCACTTAGCGCTGCAAATCACTGCTGACCTGAATGGGGTGCGT
TCATGG TCTCACCCACAATTCGAGAAGTGA

Amino acid sequence (597 AS; 64.4 kDa):

MKVDTGSSPDEVKAAFEAWLADFADALATADTGATTDLLDAGCWWRDLLA
LSWDLGTYHGTDRIAGLLDEHLKPAQVSGVRVVTEFGPRFVAEEGGSGTIEGF
FTFETAGAWCRGVARLRQGDDGWRAWTVMTGVEDLKGHERALGERRPTGP
RHEVGATTQRNWKDKREAAQAYDDREPEVVILGAGQGGLALAANLRLMGVD
ALILEKSARIGDGWRRRYHSLVLHDPVWADHLPYLPFPQSWPIYSPKDKIADWF
EFYAQAMELNVWCSAEMTDAAYDEQAGAWTLTVRTEQGERTLRPRNVVLAT
GAAGEPNIPDFPGRDEFAGTVYHSSQHGAGGSWAGKKAIVVGACNSGHDIAQD
LHEAGAEVTLVQRSSTHIISQQHGIPAIFGANFTESGPPTEYADLLASAFPWPLV
LEAAKEGVKQTAEKDAELLASLEAVGFQLNDGPDGTGLMGFALAKGGGYYID
VGASGLIASGRIALAQGSGLAEFTPSGIRLADGRELDADLVVLATGYSNMRETA
RRLFGDGVADRLPSVLGIGEDGEIGGLYRRTGQPGFWFMGGPLAWVRVYSKH
LALQITADLNGVRS WSHPQFEK

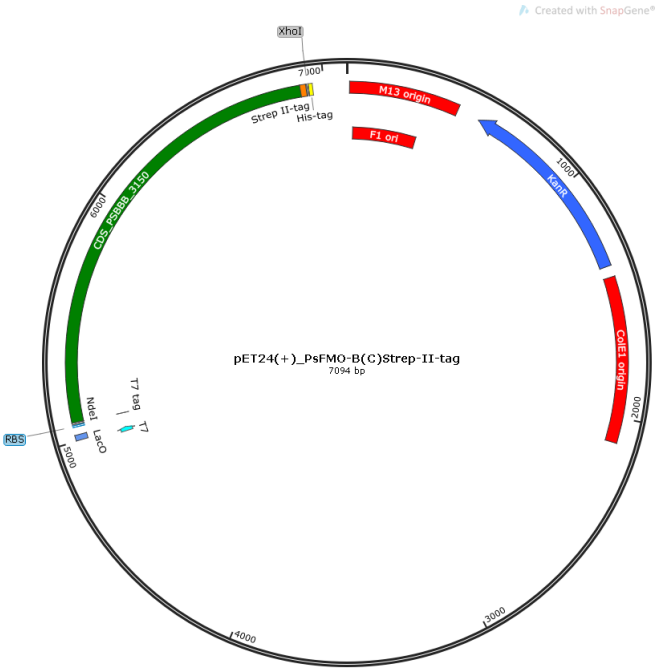

Flavinmonooxygenase from *Pimelobacter sp.* *Bb-B* PsFMO-B (PSBBB3150) in pET24(a)+ with C-terminal strep-II-tag+: pET24(a)+PsFMO-B(*C*)Strep-II-tag, Nucleotide sequence (1860 bp):[265]

ATGACTCAATTGGATGACCGCCCGGTAACAGCAGCGGACACCACAGAAG
CCTTAGACCCGGCGACGGCTTGGTTCGCCGCGTTCGAGGATGCCTTAACTG
CGCGCGACGTGGACCGCGCCGCCGGTCTGTTCGCCGCCACCTCATTTTGGC
GCGACTTAATTGCGTTTACTTGGAATTTGACTACGGTCGAGAATCCGGACG
GTGTAGCCGGCTTACTTACTTCTACATTAGATCGCGTCGATCCACGCGGAT
TCCGCCTGACCGAACCCGCTGCGACGGCTGACGGGGTCACGACCGCGTGG
TTCGAGTTCGAGACAAGCGTAGGACGCGGCCGCGGACTTGTTCGCATCGT
AGACGAAGATGGTCCTAAAGCCTGGACATTTTTGACAACCCTTTATGAACT
TACTGGGCACGAGGAACCTCGCGGAACACGTCGCCCAATGGGTGCTGAAC
ACGGGGCGACCAAAGAGCGTGTCACATGGCTTGAAAAGCGCCAGGCCGAA
GATGCTGCGTTAGGCGTCGACACACAACCTTATGTATTAGTTGTCGGGGG
GGGTCAGGGGGGCATCGCTTTAGGCGCTCGCTTACGTCAATTGGGTGTGC
CTGCCTTAGTCATCGACAAACACCCTCGTCCGGGCGACCAATGGCGCAACC
GCTACAAATCGTTATGTCTTCACGATCCTGTTTGGTACGATCACCTGCCAT
ATCTTAAATTTCCGGACAATTGGCCAGTATTCGCGCCTAAAGATAAAGTCG
GAGACTGGCTTGAGTTCTATACTCGCGTTATGGAAGTCCCTTATTGGTCCA
GTACAGTAGCGACAGATGCCTCTTACGACGAAGAGACAGGCGAATGGACC
GTTCACCTTGAGCGCGAGGGGAAACCGTTAGTGCTGAAACCTACTCACTTG
GTCATGGCCACTGGGATGTCCGGCAAACCTAACATCCCGGTTGTCCCTGGT
GCGGATGTTTTTCAGGGGGAACAACACCACTCGTCTCAACATCCTGGGCCT

GATGCCTACGCAGGAAAACGTGTAGTAGTTATTGGATCCAACAACAGTGCT
TTTGATATTTGTGGCGCACTGTGGGAGACGGGAGCCGACGTTACAATGGT
CCAACGCTCTTCTACTCATATTGTGAAATCAGACACCCTGATGGACATTGG
ACTTGGTGACCTTTATTCCGAGCGTGCAGTAGAAGCCGGTATGACGACTGA
AAAAGCCGACCTGGTCTTCGCGTCGCTTCCGTATCGTATCATGCACGAATT
CCAAATCCCTCTTTACGATCAGATGCGCGAACGCGACAAAGATTTTTATGA
CCGTATGGAAGCAGCGGGTTTTGACTTAGACTGGGGAGACGACGGATCCG
GTTTGTTCATGAAATACCTTCGTCGTGGATCAGGGTATTACATCGATGTCG
GCGCGGCGGAACTGGTTGCGTCCGGTGATGTCAAATTAGCCCACGGACAA
GTCGACCATCTGACTGAAACTGCAGTCGTTCTGGAGGATGGGACTGAACT
GCCAGCTGATCTTGTGGTGTACGCGACAGGCTATGGTAGTATGAATGGTT
GGGCTGCCGACTTAATTAGTCAAGAGGTTGCTGATCGCGTTGGAAAAGTG
TGGGGGCTTGGCAGCGACACGACAAAGGACCCGGGTCCGTGGGAAGGTGA
ACAACGTAACATGTGGAAACCGACTCAGCAAGAAAACCTTTGGTTCCATGG
TGGTAACCTTCATCAGTCGCGTCACTATTCATTATATTTGGCCTTGCAATT
AAAGGCACGTCACGCCGGAATCGAAACACCCGTGCATGGCTTACAAGAAGT
ACACCATTTAGGGTGTCTCACCCACAATTCGAGAAGTGA

Amino acid sequence (619 AS; 68.7 kDa):

MTQLDDRPVTAADTTEALDPATAWFAAFEDALTARDVDRAAGLFAATSFW
RDLIAFTWNLTTVENPDGVAGLLTSTLDRVDPRGFRLTEPAATADGVTTAWF
EFETSVGRGRGLVRIVDEDGPKAWTFLTTLYELTGHEEPRGTRRPMGAEHGA
TKERVTWLEKRQAEDAALGVDTQPYVLVVGGGQGGIALGARLRQLGVPALVI
DKHPRPGDQWRNRYKSLCLHDPVWYDHLPYLKFPDNWPVFAPKDKVGDWL
EFYTRVMEVPYWSSTVATDASYDEETGEWTVHLEREGKPLVLKPTHLVMATG
MSGKPNIPVVPGADVFQGEQHHSSQHPGPDAYAGKRVVVIGSNNSAFDICGAL
WETGADVTMVQRSSTHIVKSDTLMDIGLGDLYSERAVEAGMTTEKADLVFASL
PYRIMHEFQIPLYDQMRERDKDFYDRMEAAGFDLDWGDDGSGLFMKYLRRGS
GYYIDVGAAELVASGDVKLAHGQVDHLTETAVVLEDGTELPADLVVYATGYGS
MNGWAADLISQEVADRVGKVWGLGSDTTKDPGPWEGEQRNMWKPTQQENL
WFHGGNLHQSRHYSLYLALQLKARHAGIETPVHGLQEVHHLWSHPQFEK

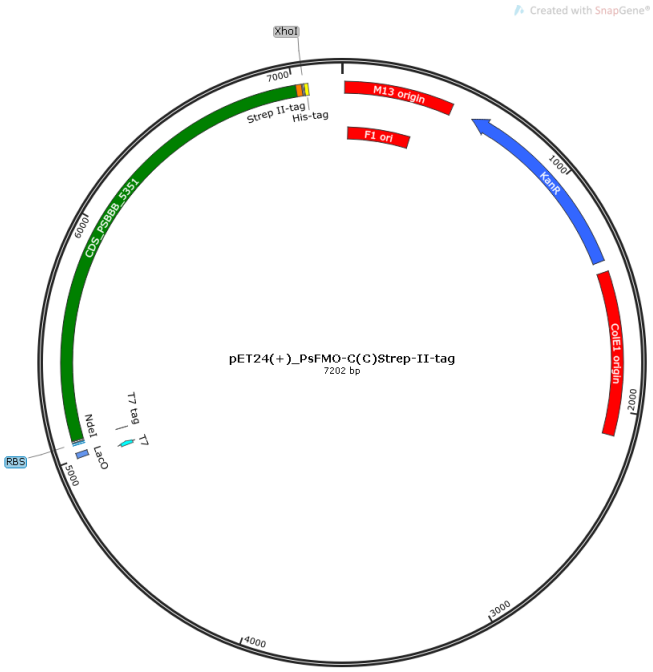

Flavinmonooxygenase from *Pimelobacter sp.* *Bb-B* PsFMO-C (PSBBB5351) in pET24(a)+ with C-terminal strep-II-tag: pET24(a)+PsFMO-C(*C*)Strep-II-tag, Nucleotide sequence (1968 bp):[265]

ATGACTCAATTGGATGACCGCCCGGTAACAGCAGCGGACACCACAGAAG
CCTTAGACCCGGCGACGGCTTGGTTCGCCGCGTTCGAGGATGCCTTAACTG
CGCGCGACGTGGACCGCGCCGCCGGTCTGTTCGCCGCCACCTCATTTTGGC
GCGACTTAATTGCGTTTACTTGGAATTTGACTACGGTCGAGAATCCGGACG
GTGTAGCCGGCTTACTTACTTCTACATTAGATCGCGTCGATCCACGCGGAT
TCCGCCTGACCGAACCCGCTGCGACGGCTGACGGGGTCACGACCGCGTGG
TTCGAGTTCGAGACAAGCGTAGGACGCGGCCGCGGACTTGTTCGCATCGT
AGACGAAGATGGTCCTAAAGCCTGGACATTTTTGACAACCCTTTATGAACT
TACTGGGCACGAGGAACCTCGCGGAACACGTCGCCCAATGGGTGCTGAAC
ACGGGGCGACCAAAGAGCGTGTCACATGGCTTGAAAAGCGCCAGGCCGAA
GATGCTGCGTTAGGCGTCGACACACAACCTTATGTATTAGTTGTCGGGGG
GGGTCAGGGGGGCATCGCTTTAGGCGCTCGCTTACGTCAATTGGGTGTGC
CTGCCTTAGTCATCGACAAACACCCTCGTCCGGGCGACCAATGGCGCAACC
GCTACAAATCGTTATGTCTTCACGATCCTGTTTGGTACGATCACCTGCCAT
ATCTTAAATTTCCGGACAATTGGCCAGTATTCGCGCCTAAAGATAAAGTCG
GAGACTGGCTTGAGTTCTATACTCGCGTTATGGAAGTCCCTTATTGGTCCA
GTACAGTAGCGACAGATGCCTCTTACGACGAAGAGACAGGCGAATGGACC
GTTCACCTTGAGCGCGAGGGGAAACCGTTAGTGCTGAAACCTACTCACTTG
GTCATGGCCACTGGGATGTCCGGCAAACCTAACATCCCGGTTGTCCCTGGT
GCGGATGTTTTTCAGGGGGAACAACACCACTCGTCTCAACATCCTGGGCCT

GATGCCTACGCAGGAAAACGTGTAGTAGTTATTGGATCCAACAACAGTGCT
TTTGATATTTGTGGCGCACTGTGGGAGACGGGAGCCGACGTTACAATGGT
CCAACGCTCTTCTACTCATATTGTGAAATCAGACACCCTGATGGACATTGG
ACTTGGTGACCTTTATTCCGAGCGTGCAGTAGAAGCCGGTATGACGACTGA
AAAAGCCGACCTGGTCTTCGCGTCGCTTCCGTATCGTATCATGCACGAATT
CCAAATCCCTCTTTACGATCAGATGCGCGAACGCGACAAAGATTTTTATGA
CCGTATGGAAGCAGCGGGTTTTGACTTAGACTGGGGAGACGACGGATCCG
GTTTGTTCATGAAATACCTTCGTCGTGGATCAGGGTATTACATCGATGTCG
GCGCGGCGGAACTGGTTGCGTCCGGTGATGTCAAATTAGCCCACGGACAA
GTCGACCATCTGACTGAAACTGCAGTCGTTCTGGAGGATGGGACTGAACT
GCCAGCTGATCTTGTGGTGTACGCGACAGGCTATGGTAGTATGAATGGTT
GGGCTGCCGACTTAATTAGTCAAGAGGTTGCTGATCGCGTTGGAAAAGTG
TGGGGGCTTGGCAGCGACACGACAAAGGACCCGGGTCCGTGGGAAGGTGA
ACAACGTAACATGTGGAAACCGACTCAGCAAGAAAACCTTTGGTTCCATGG
TGGTAACCTTCATCAGTCGCGTCACTATTCATTATATTTGGCCTTGCAATT
AAAGGCACGTCACGCCGGAATCGAAACACCCGTGCATGGCTTACAAGAAGT
ACACCATTTAGTCTCACCCACAATTCGAGAAGTGA

Amino acid sequence (655 AS; 73.2 kDa):

MGTQPQTFDEATLREAIESANLPTLLMVMFQLTGDRRWIAEPYRPKRAKGM
SDNDTGGFAPEIQDEVRAAAYDILQEWRGGRPVAVPLPDDEMLVELIATCVGE
EVPSEFGPMFAEDMRASLEGDRPHPHVEDGAVLSVIIVGAGISGLAAAVELNAA
GIRATIFEKNPDVGGTWWENRYPGCGVDTPSHVYSLSYQPRRWSTYYGKRDE
VLDYVRDVARKTGVVDQVQFETAVESAVWDEGTQRWTVTTRTAEGVVSEHV
ANVVITAVGQLNRPAVPAIPGAETFTGRQFHSAEWPEGFDVAGLRVGVVGSGA
SAMQIVPAVADRVSSLTVFQRSPQWIAPSFNYSSPVPEPVHWLMDNVPNYRLW
YRLRLSWLINDRLYPSLEIDPAWPHPERSINAHNDGHRRALTRYIQEELAGRDDL
LEKSLPTYPPFGKRMLIDNGWYAALRKEGVELVTDGVASIDETGLTTTAGQHV
ELDVIVYATGFEAKKMLYPMDIRGRDGVSIRDRWGDEDAKAYLGLTVPDFPNL
MVMYGPNLNLGHGGSYMFAGECQARYIAQMCALLTERHVASFEVRRDVHDDY
NQRVDAQHARMIWSHRGMDTWYRNSAGRIVTNSPWRVVDYWNMTRTVNPD
DFVLAPAAEGELVEAGSWSHPQFEK

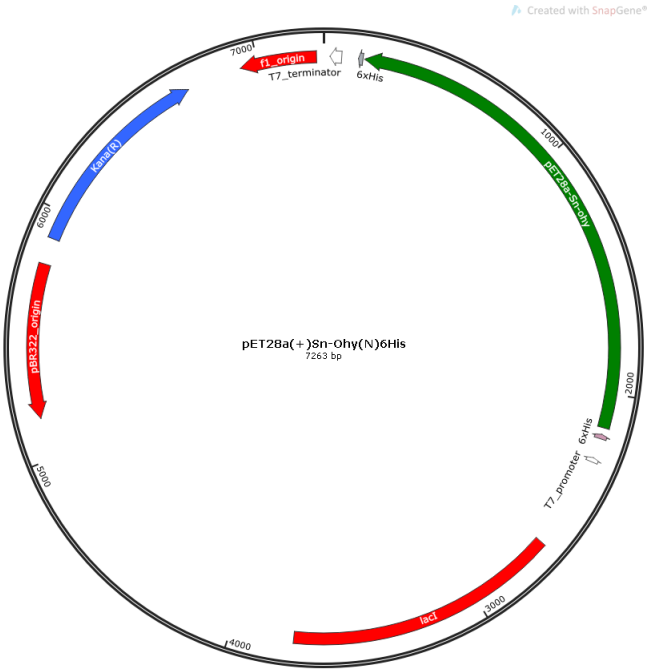

Oleate hydratase from *Stenotrophomonas nitritireducens* Sn-Ohy in pET28(a)+ and N-terminal his tag: pET28(a)+SnOhy(N)His$_6$, Uniprot: A0A172MLH9 , Nucleotide sequence (2022 bp):

ATGGGCAGCAGC CATCATCATCATCATCAC AGCAGCGGCCTGGTGCCGC
GCGGCAGCCATATGGAAGAAGTGAGTTATCCCAAAGCTGGACCGAGCATT
GAAGCGAACGTAGGGGATGGGCACTGGCGAAAGGGGCCCTCGGATACGCT
GCCGCCTCCGGACACTGTTGGACCCTATATGCGCAACCGCCCCCTGCCTGT
GGATCAAGTGGAAGGCAGGAAAGCATGGATCATCGGAAGTGGAATCGCGG
GTCTGGCCTCTGCCTTTTACTTGATCCGCGACGGGCGGATGAAGGGGCAG
GACATAACCATCCTCGATGCCGTGGGCACTCCAGGCGGATCACTGGACGGC
TCAGGGAACGCCGAAGATGGCTACCTGATCCGAGGCGGGCGCGAGATGAA
CTGGAACTACGATCACTTTTGGGATCTCTTCCAGGACATTCCCGCGCTGGA
GTACCCGTCCCCTTACTCGGTCTTGGATGAGTATCGGGCGGTGAACGACAA
TGATCCTAATTGGTCCAAGTCCCGATTGATGCACAAGCAAGGCCAAATTCG
GGATTTCAGCACCTTGGGGCTTTCTTCCGCCCACCAATGGGAATTGATCAA
GCTTCTCCTGAAGCGCAAGGAGGACCTCGATGACATCACCATCGAACAGTA
CTTCAGCGATAGCTTTCTGGAGACCAACTTCTGGTACCTCTGGCGCTCGAT
GTTTGCGTTCCAGAACTGGCAAAGTCTGCTGGAAGTGAAGTTGTACATGCA
TCGCTTTTTGGATGCAATCGACGGCTTGACGGATATGTCAGCGCTCGTGTT
CCCAAAATACAACCAGTACGACAGCTTCGTCGTCCCCCTGGTCAACTACCT
CAAGGGCCAAGGCGTCAACGTAGAATTCGGCACGCGCGTCTACGACCTGG
ACATGACGGACAACAACGGCGAGCGTACCGTGACCTCCATTCTTGCGAAGG
TAGACGGGCGGGATCAGAAGATTGACATCGGCGCGAAGGACGTGGTTTTT

GCCCTGACTGGATCGATGACGGAGGGTACAGCCTACGGCGATCTGGATAC
TGCTCCCGACCTCACTCGAGCCACCACGCCCCCTGGCGACTCAAGCGATTG
GGCGTTGTGGCAGAACCTGGCCAAGAAGTCCCACGTCTTTGGTAAGCCTGA
AAAGTTCTGCGGGCAACCCAGTCGCTCGATGTGGGAGTCTGCCACCCTGAC
GTGCAAGCCTTCGCCGTTGACCGAGCGCCTCAAAGATCTCTCAATCAATGA
CCCTTATTCGGGAAAAACGGTGACCGGTGGAATCATCACCTTTACCGACTC
GAACTGGGTTCTCAGCTTCACCTGCAATCGTCAACCGCATTTCCCCACACA
ACCAGACGACGTACTGGTGCTTTGGGTCTATGCCTTGGTCATGGACAGCAA
AGGCAACCATGTACTAAAACCAATGCCTGAGTGTACGGGCCGCGAAATTCT
TGCTGAGCTTTGCTACCACCTCGGCATTGTGGATCAGGTGGATGAAGTGG
CCAGACAGACCAAGGTTCGCCTTGCCCTGATGCCATTCATCACGGCTCAAT
TTATGCCACGAGCTGCTGGAGATCGACCGCGTGTTGTTCCAGCCGGGTGCA
CCAATCTCGCTCTGCTGGGCCAATTCGTGGAGACGTCTAATGACATCATCT
TCACCATGGAGAGTTCCGTCAGGACTGCGCGGATTGGCGTGTACACGCTTC
TGGGGCTACGAAAGCAGGTCGCCGATATCAGCCCCACGCAATACGACGTCC
GAAATCTGATCAAGGGTGCTCGTGCCCTGAACAACAACGAGCCGTTCATGG
GCGAGCGGCTGCTCCATCGACTGCTCGACAACACCTACTTCGCCCACATCC
TCCCGCCGCTGCCAGCAGGAGACGGTGGATCCAGCGATCAAGCGGCAAGC
TCGCGTATGAAGGCCAACCACACTGCGGCGGCGGCACTTGGAGCGGTGTC
TGATTGGATCCATCATGTTCGGGATAAACTGAAGCCGGGCGCCTGA

Amino acid sequence (674 AS; 75.0 kDa):

MGSS HHHHHHSSGLVPRGSHMEEVSYPKAGPSIEANVGDGHWRKGPSDTLP
PPDTVGPYMRNRPLPVDQVEGRKAWIIGSGIAGLASAFYLIRDGRMKGQDITIL
DAVGTPGGSLDGSGNAEDGYLIRGGREMNWNYDHFWDLFQDIPALEYPSPYSV
LDEYRAVNDNDPNWSKSRLMHKQGQIRDFSTLGLSSAHQWELIKLLLKRKEDL
DDITIEQYFSDSFLETNFWYLWRSMFAFQNWQSLLEVKLYMHRFLDAIDGLTD
MSALVFPKYNQYDSFVVPLVNYLKGQGVNVEFGTRVYDLDMTDNNGERTVTS
ILAKVDGRDQKIDIGAKDVVFALTGSMTEGTAYGDLDTAPDLTRATTPPGDSS
DWALWQNLAKKSHVFGKPEKFCGQPSRSMWESATLTCKPSPLTERLKDLSIND
PYSGKTVTGGIITFTDSNWVLSFTCNRQPHFPTQPDDVLVLWVYALVMDSKGN
HVLKPMPECTGREILAELCYHLGIVDQVDEVARQTKVRLALMPFITAQFMPRA
AGDRPRVVPAGCTNLALLGQFVETSNDIIFTMESSVRTARIGVYTLLGLRKQVA
DISPTQYDVRNLIKGARALNNNEPFMGERLLHRLLDNTYFAHILPPLPAGDGGS
SDQAASSRMKANHTAAAALGAVSDWIHHVRDKLKPGA

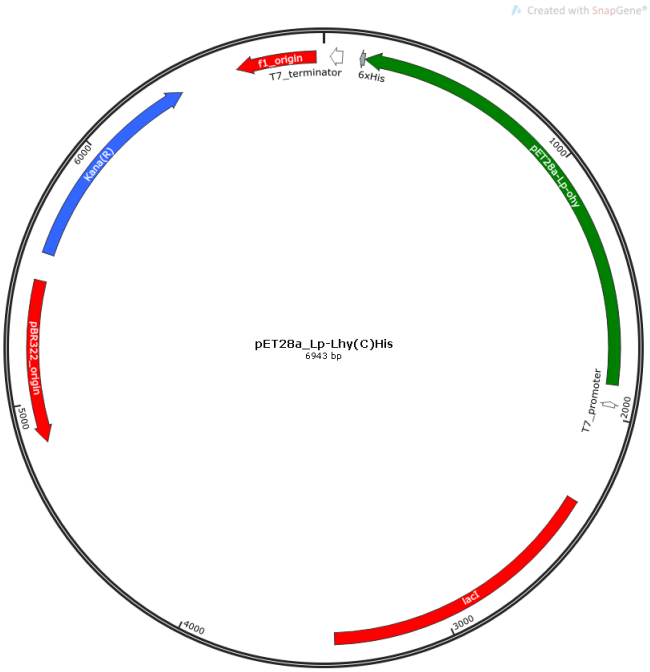

Linoleate hydratase from *Lactobacillus plantarum* Lp-Lhy in pET28(a)+ and C-terminal his tag: pET28(a)+LpOhy(*C*)His_6, Uniprot: A0A1I9RYU9 , Nucleotide sequence (1734 bp):

ATGGGGGCGTTATTTATGGTTAAAAGTAAAGCAATTATGATTGGTGCCG
GGCTATCAAATATGGCTGCGGCGGTCTACTTGATTCAAGATGGTCATTGG
GATGGTAAGGACATCACATTCTATGGTGTTGATATGCACGGTGCGAATGA
TGGTGGTGCTACGACTGATTTTACCAATGAGTATTGGAATAAGAATCATC
CGATGGCTAACACGACTGGGTATGTTGCCCGGGGTGGTCGGATGCTGAAT
TACCGGACGTACGTTGACTTAATGGATTTATTGGACCGGATTCCATCGGT
AACTGAACCGGGGATGACGGCGGCCGAAGATACGCGTGATTTTGATGCGA
AACATCGGACGTATGATATTGCCCGCTTGATGCAGGGTGGTAAAGGCATT
ATTAATGCTGGTAAGTTAGGATTCAATAATAAGGATCGGACTTTGCTGAC
TAAGTTGATCATGATGCCAGATAGTGAAGAAACGAAGCTCGACAACGTTT
CGATTGCTGAGTACTTCAAGGATGATCCGCATATGTTCCAAACGAATTTCT
GGTATATGTGGGAAACAACCTTTGCCTTTAGAACGCAAAGCTCTGCTCAAG
AACTGCGGCGTTACATGCATCAAATGATTTATGAATTTACACAAATTGAAC
ACTTAGTTGGTGTCAACCGGACGCGTTACAATCAATTCGAAAGCATGATTT
TGCCATTAATTAAGTACTTGCAAGGGCAAGGTGTGACTTTCATTGATAATA
AGATTGTTAAGGATTGGCAATTTAAAGACACGCCAATGCAAGACGAAATT
ACGGTGACTGGCTTAGTCATTGAGGATGCGCAGACTGGCGAAACGGAAGA
AGTTGAAGTTGATGAGGACACAGCGGTGATCTTCACTAACGGTTCAATTA
CCGATTCTGCAACGATGGGTGATTACAACACGCCTGCTCCTGAAAATATGG
ATTATGGTGTTAGTGCTAGTTTGTGGAAGAAGGCTACTGAGCGGTTCTAT

AACTTAGGGACGCCAGATAAGTTCTTCAACGATCGGAATGCTAGCGAATG
GGTCAGCTTCACGTTGACGACTAAGAATCATTTATTCTTAAATGAAATCGT
TCGGATCACCACCCAGGAACCCGGGAATGCGTTGAACTCCTTCTTATCAAC
TACGCCAATTACGCCGTTGAACCAAAAGGATGTTAATATGTCGATCGTGG
TGCACCACCAACCACACTTTACGACACAGCAACCAAACGAAACAGTTCTGT
GGGGCTACTTCTTGTATCCACGGCGTCAAGGTGAGTTTGTTAACAAGCCG
TATATCAAGATGACGGGTAAGGAAATGGCTCAAGAATTAATTGGTCAACT
TTCCAAAGTAGATCCGGGTCCAGGCAATATTAAGGACAAGGAAAAGGAAA
ATTTGGACAGTATCGTGAACAATATTCCGGTATACATGCCATATGCTTCCG
CACTCTTTAATAACCGGGCTAAGTCTGATCGGCCAGAAGTCTTACCAAAGC
ACTCAACGAACCTAGCCTTTACGGGTGAATTTGCGGAACAACCATACCAGA
TGATCTTCACGGAACAGAGTGCGGTCCGCTCTGGTGAGATTGCCGCTTATC
ACTTTGCTGGGGTCCCAATGGATAACTTGGTCAAGACACCACGGTACGATA
AGGATCCAAAGACCTTGCTCAAGGCAACTAAGAAGATGTTTGATCTCGAG
CACCACCACCACCACCAC

Amino acid sequence (577 AS; 65.8 kDa):

MGALFMVKSKAIMIGAGLSNMAAAVYLIQDGHWDGKDITFYGVDMHGAND
GGATTDFTNEYWNKNHPMANTTGYVARGGRMLNYRTYVDLMDLLDRIPSVT
EPGMTAAEDTRDFDAKHRTYDIARLMQGGKGIINAGKLGFNNKDRTLLTKLIM
MPDSEETKLDNVSIAEYFKDDPHMFQTNFWYMWETTFAFRTQSSAQELRRYM
HQMIYEFTQIEHLVGVNRTRYNQFESMILPLIKYLQGQGVTFIDNKIVKDWQFK
DTPMQDEITVTGLVIEDAQTGETEEVEVDEDTAVIFTNGSITDSATMGDYNTPA
PENMDYGVSASLWKKATERFYNLGTPDKFFNDRNASEWVSFTLTTKNHLFLN
EIVRITTQEPGNALNSFLSTTPITPLNQKDVNMSIVVHHQPHFTTQQPNETVLW
GYFLYPRRQGEFVNKPYIKMTGKEMAQELIGQLSKVDPGPGNIKDKEKENLDSI
VNNIPVYMPYASALFNNRAKSDRPEVLPKHSTNLAFTGEFAEQPYQMIFTEQSA
VRSGEIAAYHFAGVPMDNLVKTPRYDKDPKTLLKATKKMFDLE HHHHHH

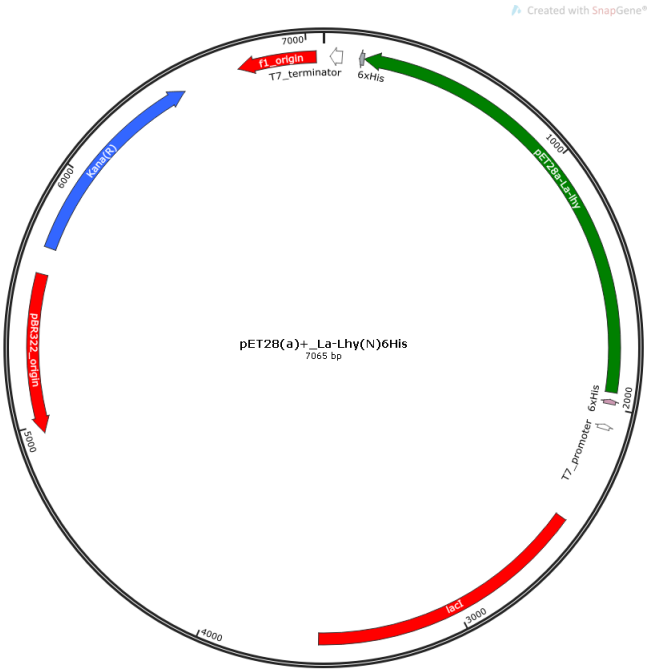

Linoleate hydratase from *Lactobacillus acidophilus* La-Lhy in pET28(a)+ and N-terminal his tag: pET28(a)+LaLhy(N)His$_6$, Uniprot: X5GEZ4 , Nucleotide sequence (1773 bp):

ATGGGCAGCAGC CATCATCATCATCATCAC AGCAGCGGCCTGGTGCCGC
GCGGCAGCCATATGCATTATAGTAGTGGTAATTATGAAGCTTTTGTAAACG
CAAGTAAACCTAAGGATGTCGATCAGAAGTCCGCATATCTTGTTGGTTCAG
GTTTGGCATCGCTTGCTAGTGCTGTATTTTTAATTCGTGATGGTCACATGA
AGGGTGATAGAATTCATATCCTTGAAGAATTGAGCCTTCCAGGTGGTTCAA
TGGATGGGATCTATAATAAGCAAAAAGAAAGCTACATCATTCGTGGTGGT
CGTGAAATGGAAGCCCATTTTGAATGCTTGTGGGACTTGTTTAGATCGATT
CCATCAGCTGAAAATAAAGATGAATCGGTCCTGGATGAATTTTACCGTTTA
AATAGAAAAGATCCAAGTTTCGCAAAGACTCGTGTCATTGTTAACCGCGGA
CATGAACTTCCAACTGACGGTCAATTACTTCTTACTCCCAAGGCTGTTAAA
GAAATTATTGATCTTTGCTTAACTCCTGAAAAAGATTTACAAAATAAAAAA
ATTAATGAAGTCTTTAGTAAAGAATTTTTTGAATCAAACTTCTGGCTTTAC
TGGTCAACGATGTTTGCCTTTGAGCCATGGGCAAGTGCGATGGAAATGCG
TCGTTACTTAATGCGTTTTGTTCAACACGTTTCTACACTTAAGAATTTATC
ATCACTACGCTTTACTAAGTATAACCAATATGAATCATTAATTTTACCAAT
GGTTAAATACTTGAAAGATCGCGGCGTGCAATTCCATTACAACACCGTTGT
TGATAATATCTTTGTTAACCGTTCAAATGGTGAAAAGATTGCTAAGCAAAT
TCTTTTAACTGAAAACGGTGAAAAAAAGAGCATCGATTTAACAGAAAATGA
CCTCGTCTTCGTTACTAACGGTTCAATTACTGAAAGTACAACTTATGGTGA
TAACTTGCACCCAGCTTCTGAGGAACATAAATTAGGTGCTACTTGGAAATT

ATGGCAAAACTTGGCAGCGCAAGATGATGACTTCGGTCACCCAGATGTCTT
CTGCAAGGATATTCCAAAGGCTAACTGGGTAATGTCTGCTACAATTACTTT
TAAGAATAATGATATTGTGCCATTCATTGAAGCAGTTAATAAGAAGGATCC
ACACAGCGGCTCAATTGTAACTAGTGGGCCTACTACGATTAAGGATTCTAA
CTGGCTACTTGGTTATTCAATCAGTCGTCAGCCTCACTTTGAAGCACAAAA
GCCTAACGAATTGATTGTATGGCTTTATGGTTTGTTCTCAGACACCAAAGG
TAACTATGTTGAAAAGACTATGCCTGACTGTAACGGTATTGAATTATGTGA
AGAATGGCTTTACCACATGGGTGTTCCTGAAGAAAGAATCCCAGAAATGGC
TTCAGCTGCTACGACTATTCCAGCACACATGCCATATATTACTTCATACTT
CATGCCAAGAGCATTAGGCGACAGACCCAAGGTTGTGCCAGACCACTCAAA
GAACTTGGCCTTCATTGGTAACTTTGCTGAAACGCCAAGAGACACTGTCTT
TACCACTGAATACTCTGTCAGAACTGCGATGGAAGCTGTATACACCTTGCT
TAACATTGATCGTGGTGTGCCAGAAGTATTTGCATCTGCCTTCGATGTCAG
AATGCTCATGAACGCAATGTACTACTTGAATGATCAAAAGAAGCTTGAAGA
TCTTGATTTGCCTATTGCTGAAAAGTTGGCAATTAAGGGGATGCTCAAGAA
AGTTAAGGGCACTTATATAGAGGAATTGCTTAAGAAGTATAAGTTGGTTTA
G

Amino acid sequence (590 AS; 67.5 kDa):

MGSS HHHHHH SSGLVPRGSHMHYSSGNYEAFVNASKPKDVDQKSAYLVGSG
LASLASAVFLIRDGHMKGDRIHILEELSLPGGSMDGIYNKQKESYIIRGGREMEA
HFECLWDLFRSIPSAENKDESVLDEFYRLNRKDPSFAKTRVIVNRGHELPTDGQ
LLLTPKAVKEIIDLCLTPEKDLQNKKINEVFSKEFFESNFWLYWSTMFAFEPWA
SAMEMRRYLMRFVQHVSTLKNLSSLRFTKYNQYESLILPMVKYLKDRGVQFHY
NTVVDNIFVNRSNGEKIAKQILLTENGEKKSIDLTENDLVFVTNGSITESTTYGD
NLHPASEEHKLGATWKLWQNLAAQDDDFGHPDVFCKDIPKANWVMSATITFK
NNDIVPFIEAVNKKDPHSGSIVTSGPTTIKDSNWLLGYSISRQPHFEAQKPNELIV
WLYGLFSDTKGNYVEKTMPDCNGIELCEEWLYHMGVPEERIPEMASAATTIPA
HMPYITSYFMPRALGDRPKVVPDHSKNLAFIGNFAETPRDTVFTTEYSVRTAM
EAVYTLLNIDRGVPEVFASAFDVRMLMNAMYYLNDQKKLEDLDLPIAEKLAIK
GMLKKVKGTYIEELLKKYKLV--

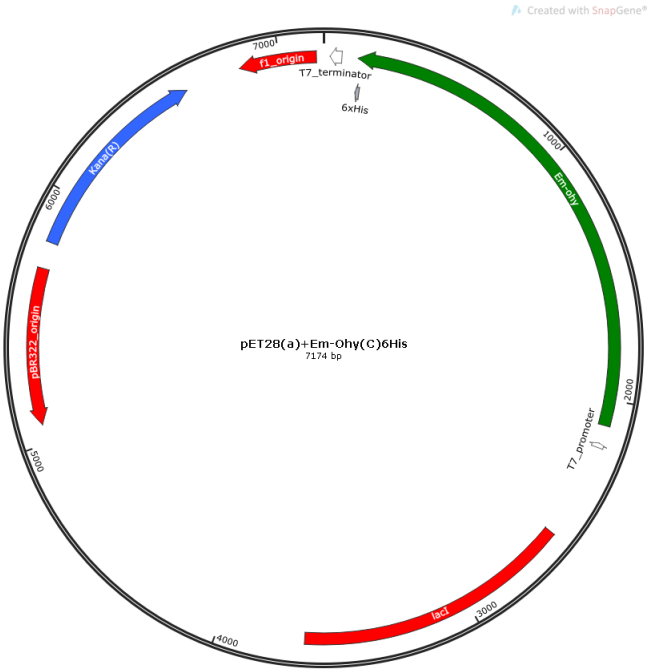

Oleate hydratase from *Elizabethkingia meningoseptica* Em-Ohy in pET28(a)+ and C-terminal his tag: pET28(a)+EmOhy(C)His_6, Uniprot: C7DLJ6 , Nucleotide sequence (1965 bp):

ATGAACCCAATAACTTCAAAATTTGACAAAGTACTTAATGCTTCTTCCGA
ATACGGACATGTAAACCATGAACCGGATTCCAGTAAAGAACAGCAACGAAA
CACCCCGCAAAAATCAATGCCCTTTTCTGATCAGATTGGAAATTATCAGAG
AAACAAAGGGATTCCTGTACAATCATATGACAATAGTAAGATTTACATTAT
AGGCAGTGGAATCGCAGGTATGTCGGCAGCTTATTATTTTATACGCGATG
GGCATGTTCCTGCAAAAAACATCACCTTCTTGGAACAATTGCATATCGATG
GCGGTTCATTAGATGGTGCCGGAAATCCGACAGACGGCTATATTATCCGTG
GCGGTCGTGAAATGGACATGACGTACGAAAATCTTTGGGATATGTTTCAG
GATATACCTGCCTTAGAAATGCCTGCTCCTTACAGTGTACTGGACGAATAC
AGATTAATTAATGATAACGACTCCAATTATTCTAAAGCCCGGTTAATCAAC
AATAAAGGTGAGATAAAAGACTTTAGCAAGTTCGGCCTAAATAAAATGGA
CCAGTTAGCTATTATCAGATTACTTCTGAAAAATAAAGAAGAACTGGACGA
TTTAACCATTGAGGATTACTTCAGCGAATCCTTCCTGAAAAGTAATTTCTG
GACTTTTTGGAGAACGATGTTTGCCTTTGAAAACTGGCATAGCTTATTGGA
ACTGAAACTTTACATGCACCGTTTCCTTCACGCCATAGACGGACTGAACGA
TCTGTCTTCACTGGTATTCCCTAAATACAACCAATACGACACCTTCGTAAC
TCCTCTGCGCAAATTCCTTCAGGAAAAAGGTGTTAATATCCACCTGAACAC
TCTGGTAAAAGATCTGGATATCCACATCAATACCGAAGGAAAAGTTGTAGA
AGGAATTATCACCGAACAGGATGGTAAGGAAGTAAAAATCCCTGTTGGTA
AAAATGACTATGTCATTGTAACTACAGGTTCCATGACGGAAGATACCTTCT
ACGGAAATAATAAAACTGCTCCTATTATTGGCATAGACAACAGCACAAGCG

GACAAAGTGCCGGATGGAAGTTGTGGAAAAATCTGGCTGCAAAATCAGAA
ATTTTTGGGAAACCAGAGAAATTCTGCAGCAATATCGAGAAATCTGCATGG
GAATCTGCAACGCTAACCTGTAAACCTTCAGCCCTTATCGACAAGCTGAAA
GAATACTCTGTTAACGATCCATATTCCGGAAAAACTGTTACCGGCGGTATT
ATTACCATTACAGATTCCAACTGGCTGATGAGTTTCACCTGCAACAGACAG
CCACACTTCCCGGAACAGCCGGATGATGTACTGGTACTTTGGGTATATGCC
TTATTCATGGACAAAGAGGGAAACTATATCAAAAAAACAATGCTGGAATGT
ACAGGAGATGAAATTCTTGCAGAATTATGCTACCATTTAGGTATTGAAGAT
CAGCTGGAAAATGTACAGAAAAATACAATTGTAAGAACTGCATTCATGCCC
TATATAACTTCTATGTTTATGCCAAGAGCTAAAGGCGATCGCCCTAGAGTA
GTGCCTGAAGGCTGTAAAAATCTGGGACTGGTAGGTCAGTTTGTAGAAAC
CAATAATGATGTGGTATTTACAATGGAAAGCTCTGTAAGAACAGCGAGAAT
TGCTGTCTACAAATTACTAAACCTCAACAAACAGGTTCCTGATATCAATCC
TTTACAGTATGATATCCGACATCTGCTAAAAGCAGCAAAAACACTGAATGA
TGACAAACCATTTGTAGGTGAAGGCTTGTTGAGAAAAGTCCTTAAAGGAA
CTTACTTTGAACATGTGTTACCTGCCGGTGCAGCAGAGGAAGAAGAACATG
AATCCTTTATCGCTGAACATGTAAATAAGTTCAGAGAATGGGTAAAAGGAA
TAAGAGGACTCGAG CACCACCACCACCACCACTGA

Amino acid sequence (654 AS; 74.6 kDa):

MNPITSKFDKVLNASSEYGHVNHEPDSSKEQQRNTPQKSMPFSDQIGNYQRN
KGIPVQSYDNSKIYIIGSGIAGMSAAYYFIRDGHVPAKNITFLEQLHIDGGSLDGA
GNPTDGYIIRGGREMDMTYENLWDMFQDIPALEMPAPYSVLDEYRLINDNDSN
YSKARLINNKGEIKDFSKFGLNKMDQLAIIRLLLKNKEELDDLTIEDYFSESFLKS
NFWTFWRTMFAFENWHSLLELKLYMHRFLHAIDGLNDLSSLVFPKYNQYDTFV
TPLRKFLQEKGVNIHLNTLVKDLDIHINTEGKVVEGIITEQDGKEVKIPVGKNDY
VIVTTGSMTEDTFYGNNKTAPIIGIDNSTSGQSAGWKLWKNLAAKSEIFGKPEK
FCSNIEKSAWESATLTCKPSALIDKLKEYSVNDPYSGKTVTGGIITITDSNWLMS
FTCNRQPHFPEQPDDVLVLWVYALFMDKEGNYIKKTMLECTGDEILAELCYHL
GIEDQLENVQKNTIVRTAFMPYITSMFMPRAKGDRPRVVPEGCKNLGLVGQFV
ETNNDVVFTMESSVRTARIAVYKLLNLNKQVPDINPLQYDIRHLLKAAKTLNDD
KPFVGEGLLRKVLKGTYFEHVLPAGAAEEEEHESFIAEHVNKFREWVKGIRGL
E HHHHHH

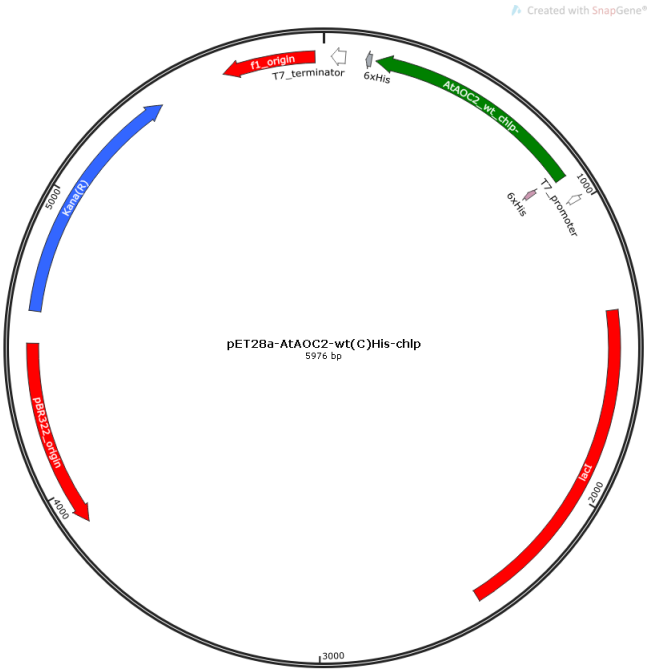

Allen oxid cyclase 2 from *Arabidopsis thaliana* Without chloroplast target sequence, AtAOC2 in pET21(a)+ and N-terminal his tag: pET21(a)+AtAOC2(N)His$_6$, Uniprot: Q9LS02, Nucleotide sequence (735 bp):

ATGGGCAGCAGC CATCATCATCATCATCAC AGCAGCGGCCTGGTGCCGC
GCGGCAGCCATATGCTTGGTTCCTCTAAATCCTTCCAAAATCTTGGTATCT
CATCTAACGGTTCAGATTTCTCCTATCCATCAAGTTTCACTGCCAAGAAGA
ACCTCACTGCTTCTCGAGCTCTCTCCCAAAACGGGAATATCGAAAACCCTA
GACCAAGCAAAGTTCAAGAACTGAGTGTGTACGAAATCAACGAATTAGATC
GACACAGCCCCAAGATTCTTAAAAACGCATTCAGCTTAATGTTCGGTCTCG
GAGATCTCGTACCATTCACAAACAAACTCTACACAGGCGATCTCAAGAAAC
GCGTGGGCATCACGGCAGGTCTCTGCGTCGTCATCGAACACGTCCCAGAGA
AGAAAGGTGAAAGATTCGAAGCTACTTATAGCTTCTACTTCGGAGACTATG
GCCACTTGTCCGTTCAAGGACCATACTTGACTTACGAGGATTCGTTCCTCG
CCATCACTGGTGGTGCTGGAATCTTTGAAGGTGCCTACGGACAGGTCAAGC
TTCAACAGCTTGTGTATCCGACAAAACTGTTCTACACTTTTTACCTTAAAG
GGTTGGCTAATGATTTGCCGTTGGAGCTCACCGGAACACCGGTACCGCCGT
CTAAGGACATAGAGCCGGCGCCGGAAGCTAAGGCACTGGAGCCTAGCGGA
GTTATAAGTAACTATACCAACTAA

Amino acid sequence (235 AS; 25.8 kDa):

MGSS HHHHHH SSGLVPRGSHMLGSSKSFQNLGISSNGSDFSYPSSFTAKKNLT
ASRALSQNGNIENPRPSKVQELSVYEINELDRHSPKILKNAFSLMFGLGDLVPFT
NKLYTGDLKKRVGITAGLCVVIEHVPEKKGERFEATYSFYFGDYGHLSVQGPY

LTYEDSFLAITGGAGIFEGAYGQVKLQQLVYPTKLFYTFYLKGLANDLPLELTG
TPVPPSKDIEPAPEAKALEPSGVISNYTN-

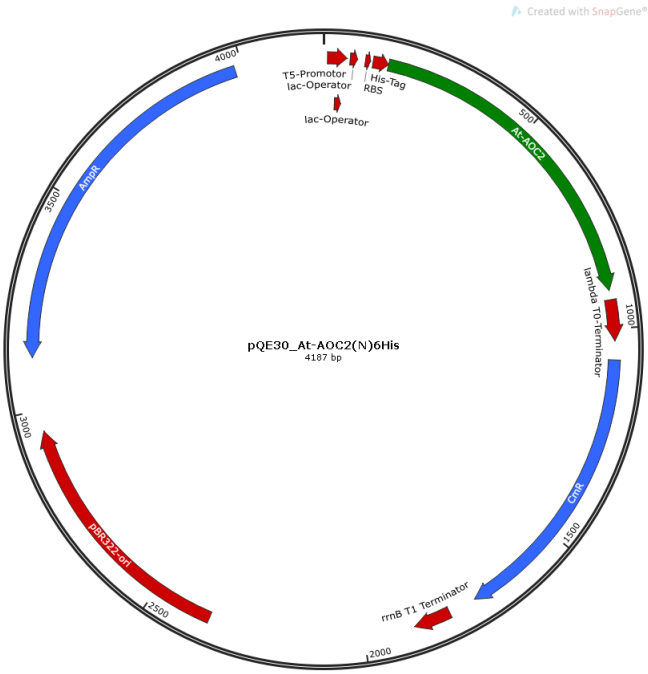

Allen oxid cyclase 2 from *Arabidopsis thaliana* Without chloroplast target sequence, AtAOC2 in pQE30 and N-terminal his tag: pQE30AtAOC2(N)His_6, Uniprot: Q9LS02, Nucleotide sequence (711 bp)[215]

ATGAGAGGATCG CATCACCATCACCATCAC GGATCCATGCTTGGTTCCT
CTAAATCCTTCCAAAATCTTGGTATCTCATCTAACGGTTCAGATTTCTCCT
ATCCATCAAGTTTCACTGCCAAGAAGAACCTCACTGCTTCTCGAGCTCTCT
CCCAAAACGGGAATATCGAAAACCCTAGACCAAGCAAAGTTCAAGAACTGA
GTGTGTACGAAATCAACGAATTAGATCGACACAGCCCCAAGATTCTTAAAA
ACGCATTCAGCTTAATGTTCGGTCTCGGAGATCTCGTACCATTCACAAACA
AACTCTACACAGGCGATCTCAAGAAACGCGTGGGCATCACGGCAGGTCTCT
GCGTCGTCATCGAACACGTCCCAGAGAAGAAAGGTGAAAGATTCGAAGCT
ACTTATAGCTTCTACTTCGGAGACTATGGCCACTTGTCCGTTCAAGGACCA
TACTTGACTTACGAGGATTCGTTCCTCGCCATCACTGGTGGTGCTGGAATC
TTTGAAGGTGCCTACGGACAGGTCAAGCTTCAACAGCTTGTGTATCCGACA
AAACTGTTCTACACTTTTTACCTTAAAGGGTTGGCTAATGATTTGCCGTTG
GAGCTCACCGGAACACCGGTACCGCCGTCTAAGGACATAGAGCCGGCGCC
GGAAGCTAAGGCACTGGAGCCTAGCGGAGTTATAAGTAACTATACCAACTA
A

Amino acid sequence (236 AS; 25.9 kDa):
MRGSHHHHHH GSMLGSSKSFQNLGISSNGSDFSYPSSFTAKKNLTASRALSQN
GNIENPRPSKVQELSVYEINELDRHSPKILKNAFSLMFGLGDLVPFTNKLYTGDL
KKRVGITAGLCVVIEHVPEKKGERFEATYSFYFGDYGHLSVQGPYLTYEDSFLA
ITGGAGIFEGAYGQVKLQQLVYPTKLFYTFYLKGLANDLPLELTGTPVPPSKDI
EPAPEAKALEPSGVISNYTN-

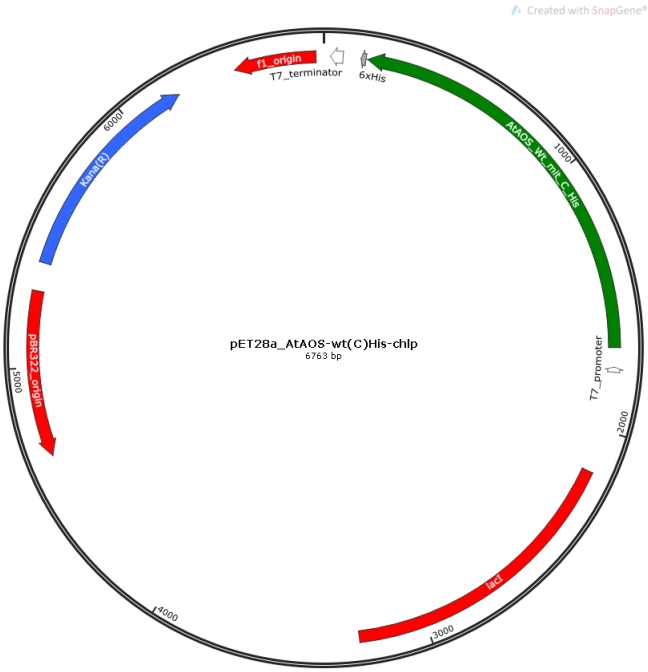

Allen oxid synthase from *Arabidopsis thaliana* Without chloroplast target sequence and solubility-sequence GCAAAAAAAACATCATCA, AtAOS in pET28(a)+ and C-terminal his tag: pET28(a)+AtAOS(C)His_6, Uniprot: Q96242, Nucleotide sequence (1527 bp):

ATG GCAAAAAAAACATCATCA GCATCAGGATCAGAAACACCAGACCTAA
CAGTAGCGACACGAACCGGATCCAAAGATCTCCCGATCCGAAACATACCGG
GAAACTACGGTTTACCAATCGTAGGACCAATCAAAGACCGTTGGGATTACT
TTTACGACCAAGGAGCTGAAGAGTTCTTCAAATCACGAATCCGTAAATACA
ACTCCACGGTGTACAGAGTCAACATGCCACCGGGAGCTTTTATCGCCGAGA
ATCCACAAGTCGTGGCTTTACTCGACGGTAAAAGCTTCCCGGTTTTATTCG
ATGTCGATAAAGTCGAAAAGAAAGATCTTTTCACCGGTACTTACATGCCGT
CAACGGAACTAACCGGAGGCTACCGTATCCTCTCGTACCTCGATCCATCGG
AGCCTAAACACGAAAAGCTCAAAAATCTCCTTTTCTTCCTCCTCAAGTCAT
CTCGAAACCGGATCTTCCCTGAGTTTCAAGCTACTTACTCCGAGCTTTTCG
ATTCTTTGGAGAAAGAGCTTTCCCTTAAAGGGAAAGCGGATTTCGGCGGT
TCCAGCGACGGAACCGCCTTTAATTTCTTGGCTCGGGCTTTCTACGGGACG

AATCCCGCAGATACAAAGCTCAAAGCCGACGCTCCGGGTTTGATCACTAAA
TGGGTTTTATTCAATCTCCATCCATTACTCTCTATTGGTTTACCGAGAGTT
ATAGAAGAACCTCTCATCCATACATTTAGTCTACCACCGGCGTTAGTCAAA
TCTGATTACCAGAGACTCTACGAGTTTTTCTTAGAATCCGCCGGTGAGATT
CTCGTTGAAGCCGATAAATTGGGTATCTCACGAGAAGAAGCTACTCACAAT
CTTCTCTTCGCCACGTGCTTCAACACGTGGGGTGGGATGAAGATTTTGTTT
CCGAATATGGTTAAACGTATCGGGCGGGCGGGTCATCAAGTTCATAACCG
ATTAGCGGAGGAGATTAGATCTGTGATTAAATCCAACGGCGGAGAACTCA
CGATGGGAGCGATTGAGAAAATGGAGTTAACCAAATCAGTGGTTTACGAA
TGTCTCCGGTTTGAACCACCGGTTACGGCTCAATACGGTAGAGCGAAGAA
GGATCTGGTTATCGAAAGCCACGACGCGGCGTTTAAAGTCAAAGCCGGTG
AAATGCTTTACGGTTATCAACCGTTGGCGACGAGAGATCCGAAGATTTTTG
ATCGGGCGGATGAGTTTGTGCCGGAGAGATTCGTCGGAGAAGAAGGAGAG
AAGCTTTTGAGGCATGTGTTGTGGTCGAATGGACCGGAGACGGAGACTCC
GACGGTGGGGAATAAACAATGCGCCGGTAAGGATTTTGTTGTTTTGGTGG
CGAGGTTGTTTGTGATTGAGATTTTCCGGCGATATGATTCGTTTGATATTG
AGGTTGGTACGTCGCCGTTAGGAAGCTCCGTTAATTTCTCGTCGTTAAGGA
AAGCTAGCTTTGTCGACAAGCTTGCGGCCGCACTCGGG CACCACCACCAC-
CACCACTAA

Amino acid sequence (508 AS; 57.0 kDa):

M AKKTSS ASGSETPDLTVATRTGSKDLPIRNIPGNYGLPIVGPIKDRWDYFY
DQGAEEFFKSRIRKYNSTVYRVNMPPGAFIAENPQVVALLDGKSFPVLFDVDK
VEKKDLFTGTYMPSTELTGGYRILSYLDPSEPKHEKLKNLLFFLLKSSRNRIFPE
FQATYSELFDSLEKELSLKGKADFGGSSDGTAFNFLARAFYGTNPADTKLKAD
APGLITKWVLFNLHPLLSIGLPRVIEEPLIHTFSLPPALVKSDYQRLYEFFLESAG
EILVEADKLGISREEATHNLLFATCFNTWGGMKILFPNMVKRIGRAGHQVHNRL
AEEIRSVIKSNGGELTMGAIEKMELTKSVVYECLRFEPPVTAQYGRAKKDLVIES
HDAAFKVKAGEMLYGYQPLATRDPKIFDRADEFVPERFVGEEGEKLLRHVLW
SNGPETETPTVGNKQCAGKDFVVLVARLFVIEIFRRYDSFDIEVGTSPLGSSVNF
SSLRKASFVDKLAAALG HHHHHH

13 List of abbreviations

12,13-EOT - (*S*)-12,13-Epoxyoctadecatrienoic acid
13-HPOT - (*S*)-13-Hydroperoxylinolenic acid
12-OPDA - 12-Oxophytodienoic acid
13-HOD - 13-Hydroxy-9(*Z*)-octadecenoic acid
10-HOD - 10-Hydroxy-12(*Z*)-octadecenoic acid
10-HSA - 10-Hydroxystearic acid
ABN - Abnormal
ACN - Acetonitrile
AcOH - Acetic acid
AI medium - Autoinduction medium
AmDH - Amine dehydrogenase
AOC - Allene oxide cyclase
AOS - Allene oxide synthase
APS - Ammonium peroxodisulphate
At - *Arabidopsis thaliana*
ATA - Amine transaminases
ATP - Adenosine triphosphate
AS - Amino acid
BSA - Bovine serum albumin
BVMO - Baeyer-Villiger monooxygenases
CAL-B - *Candida antarctica* Lipase B
CAST - Combinatorial active-site saturation
CbFDH - *Candida boidinii* formate dehydrogenase
CHMO - Cyclohexanone monooxygenase
CLEA - Cross-linked enzyme aggregates
CLEC - Cross-linked enzyme crystals
conv. - Conversion
δ - Chemical shift/ppm (NMR)
d - Doublet (NMR)
DCM - Dichloromethane
dH_2O - Distilled water
ddH_2O - Double distilled water
DMSO - Dimethyl sulfoxide
DNA - Deoxyribonucleic acid
DTT - Dithiothreitol
E. coli - *Escherichia coli*
ee - Enantiomeric excess
Em-Ohy - *Elizabethkingia meningoseptica* oleate hydratase
ESI - Electrospray ionization
EsLeuDH - *Exiguobacterium sibiricum* leucine dehydrogenase
EsLeuDH-DM - *Exiguobacterium sibiricum* leucine dehydrogenase double mutant

EtOAc - Ethyl acetate
et al. - *Et alteri* (and others)
EtOH - Ethanol
eq. - Equivalent
FA - Fatty acid
FAD - Flavin adenine dinucleotide
FAH - Fatty acid hydratase
FDH - Formate dehydrogenase
g - Acceleration due to gravity
GC - Gas chromatography
GDH - Glucose dehydrogenase
h - Hours
HCl - Hydrochloric acid
HPLC - High performance liquid chromatography
Hz - Hertz (unit of coupling constant in NMR)
iPrOH - Isopropanol
IPTG - Isopropyl β-D-1-thiogalactopyranoside
IRED - Imine reductase
J - Coupling constant/Hz (NMR)
JA - Jasmonic acid
k_{cat} - Turnover number of enzyme
kDa - Kilodalton
K_i - Dissociation constant of enzyme
K_M - Michaelis–Menten constant
KOH - Potassium hydroxide
KPi - Potassium phosphate buffer
LA - Linoleic acid
L. kefir - *Lactobacillus kefir*
La-Lhy - *Lactobacillus acidophilus* linoleate hydratase
LB medium - Lysogeny broth medium
LiOH - Lithium hydroxide
LOX - Lipoxygenase
Lp-Lhy - *Lactobacillus plantarum* linoleate hydratase
m - Multiplet (NMR)
MAO - Monoamine oxidase
MeOH Methanol
min - Minutes
mM - Millimolar
MPA - Methiopropamine
MS - Mass spectrometry
MTBE - Methyl *tert*-butyl ether
N - Normal
NaCl - Sodium chloride
NAD^+/NADH - Nicotinamide adenine dinucleotide

$NADP^+$/NADPH - Nicotinamide adenine dinucleotide phosphate
NaOH - Sodium hydroxide
Ni-NTA – Nickel nitrilotriacetate
NMR - Nuclear magnetic resonance spectroscopy
OA - Oleic acid
OD - Optical density
PCC - Pyridinium chlorochromate
PCR - polymerase chain reaction
PEA - Phenethylamine
PheDH - Phenylalanine dehydrogenase
ppm - Parts per million (NMR)
Ps - *Pseudomonas species*
R - Residue, rest
Ra-Ni - RANEY-Nickel
rpm - Rounds per minute
rt - Room temperature
R_t - Retention time
s - Singlet (NMR)
SDS-PAGE - Sodium dodecyl sulfate polyacrylamide gel electrophoresis
Sn-Ohy - Oleic acid hydratase from *Stenotrophomonas nitritireducens*
t - Triplet (NMR)
TA - Transaminase
TB medium - Terrific broth medium
T. brockii - *Thermoanaerobacter brockii*
TEMED - Tetramethylethylendiamin
TLC - Thin layer chromatography
THF - Tetrahydrofuran
TolH - Toluene
TRIS - Tris(hydroxymethyl)aminomethane
U - Unit ($\mu mol \cdot min^{-1}$)
UV - Ultraviolet
Vis - Visible spectral range
v_{max} - Maximal velocity of an enzyme
WCC - Whole cell catalyst
% *v/v* - Percent by volume
% *w/w* - Mass percent

References

[1] G. Hughes and J. C. Lewis, *Chemical Reviews*, 2018, **118**, 1–3.

[2] J. T. Sime, *Journal of Chemical Education*, 1999, **76**, 1658–1661.

[3] E. M. Abdelraheem, H. Busch, U. Hanefeld and F. Tonin, *Reaction Chemistry & Engineering*, 2019, **4**, 1878–1894.

[4] P. E. V. Paul, V. Sangeetha and R. G. Deepika, *Emerging Trends in the Industrial Production of Chemical Products by Microorganisms*, Elsevier Inc., 2019, pp. 107–125.

[5] P. N. Devine, R. M. Howard, R. Kumar, M. P. Thompson, M. D. Truppo and N. J. Turner, *Nature Reviews Chemistry*, 2018, **2**, 409–421.

[6] U. T. Bornscheuer, *Philosophical Transactions of the Royal Society A*, 2018, **376**, 1–7.

[7] J. A. Littlechild, *Frontiers in Bioengineering and Biotechnology*, 2015, **3**, 1–9.

[8] M. T. Reetz, J. D. Carballeira, J. Peyralans, H. Höbenreich, A. Maichele and A. Vogel, *Chemistry – A European Journal*, 2006, **12**, 6031–6038.

[9] U. T. Bornscheuer and M. Pohl, *Current Opinion in Chemical Biology*, 2001, **5**, 137–143.

[10] L. Pritchard, D. Corne, D. Kell, J. Rowland and M. Winson, *J. Theor. Biol.*, 2005, **234**, 497–509.

[11] M. Olsen, B. Iverson and G. Georgiou, *Current Opinion in Biotechnology*, 2000, **11**, 331–337.

[12] S. Jemli, D. Ayadi-Zouari, H. B. Hlima and S. Bejar, *Critical Reviews in Biotechnology*, 2016, **36**, 246–258.

[13] A. J. Straathof and P. Adlercreutz, *Applied Biocatalysis*, CRC Press, 2nd edn., 2019, pp. 1689–1699.

[14] L. Poppe and B. G. Vértessy, *ChemBioChem*, 2018, **19**, 284–287.

[15] A. Schmid, J. S. Dordick, B. Hauer, A. Kiener, M. G. Wubbolts and B. Witholt, *Nature*, 2001, **414**, 112–117.

[16] H. Griengl, H. Schwab and M. Fechter, *Trends in Biotechnolology*, 2000, **18**, 252–256.

[17] T. Nagasawa, H. Shimizu and H. Yamada, *Applied Microbiology and Biotechnology*, 1993, **40**, 189–195.

[18] G. Hills, *European Journal of Lipid Science and Technology*, 2003, **105**, 601–607.

[19] W. P. Stemmer, *Proceedings of the National Academy of Sciences*, 1994, **91**, 10747–10751.

[20] F. H. Arnold, *Nature*, 2001, **32**, 253–257.

[21] U. T. Bornscheuer, G. W. Huisman, R. J. Kazlauskas, S. Lutz, J. C. Moore and K. Robins, *Nature*, 2012, **485**, 185–194.

[22] J. Liang, J. Lalonde, B. Borup, V. Mitchell, E. Mundorff, N. Trinh, D. A. Kochrekar, R. N. Cherat and G. Ganesh Pai, *Organic Process Research and Development*, 2010, **14**, 193–198.

[23] W. R. Jarvis, J. C. Colbeck, A. Krebber, F. J. Fleitz and J. Brands, *Science*, 2010, **329**, 305–310.

[24] S. Atsumi, T. Hanai and J. C. Liao, *Nature*, 2008, **451**, 86–89.

[25] M. Jeschek, R. Reuter, T. Heinisch, C. Trindler, J. Klehr, S. Panke and T. R. Ward, *Nature*, 2016, **537**, 661–665.

[26] F. Schwizer, Y. Okamoto, T. Heinisch, Y. Gu, M. M. Pellizzoni, V. Lebrun, R. Reuter, V. Köhler, J. C. Lewis and T. R. Ward, *Chemical Reviews*, 2018, **118**, 142–231.

[27] V. Sabatino and T. R. Ward, *Journal of Organic Chemistry*, 2019, **15**, 445–468.

[28] S. Studer, D. A. Hansen, Z. L. Pianowski, P. R. Mittl, A. Debon, S. L. Guffy, B. S. Der, B. Kuhlman and D. Hilvert, *Science*, 2018, **362**, 1285–1288.

[29] V. Erdmann, B. R. Lichman, J. Zhao, R. C. Simon, W. Kroutil, J. M. Ward, H. C. Hailes and D. Rother, *Angewandte Chemie - International Edition*, 2017, **56**, 12503–12507.

[30] J. Zdarta, A. S. Meyer, T. Jesionowski and M. Pinelo, *Catalysts*, 2018, **8**, 1–27.

[31] R. Karande, A. Schmid and K. Buehler, *Advanced Synthesis & Catalysis*, 2011, **353**, 2511–2521.

[32] R. K. Kuipers, H. J. Joosten, W. J. van Berkel, N. G. Leferink, E. Rooijen, E. Ittmann, F. van Zimmeren, H. Jochens, U. Bornscheuer, G. Vriend, V. A. Martins Dos Santos and P. J. Schaap, *Proteins: Structure, Function, and Bioinformatics*, 2010, **78**, 2101–2113.

[33] H. R. Beller, E. B. Goh and J. D. Keasling, *Applied and Environmental Microbiology*, 2010, **76**, 1212–1223.

[34] H. G. Menzella, R. Reid, J. R. Carney, S. S. Chandran, S. J. Reisinger, K. G. Patel, D. A. Hopwood and D. V. Santi, *Nature Biotechnology*, 2005, **23**, 1171–1176.

[35] D. Ghislieri and N. J. Turner, *Topics in Catalysis*, 2014, **57**, 284–300.

[36] C. K. Savile, J. M. Janey, E. C. Mundorff, J. C. Moore, S. Tam, W. R. Jarvis, J. C. Colbeck, A. Krebber, F. J. Fleitz, J. Brands, P. N. Devine, G. W. Huisman and G. J. Hughes, *Science*, 2010, **329**, 305–310.

[37] C. Bornschein, S. Werkmeister, B. Wendt, H. Jiao, E. Alberico, W. Baumann, H. Junge, K. Junge and M. Beller, *Nature Communications*, 2014, **5**, 1–11.

[38] P. Roose, K. Eller, E. Henkes, R. Rossbacher and H. Höke, *Amines, Aliphatic*, Wiley-VCH, Weinheim, 2015, pp. 1–55.

[39] S. Yoon, M. D. Patil, S. Sarak, H. Jeon, G. H. Kim, T. P. Khobragade, S. Sung and H. Yun, *ChemCatChem*, 2019, 1898–1902.

[40] M. S. Bradshaw and R. W. Gibson, *Angewandte Chemie - International Edition*, 1968, **7**, 919–913.

[41] E. R. Alexander and R. B. Wildman, *Journal of the American Chemical Society*, 1948, **70**, 1187–1189.

[42] K. Kinbara, Y. Hashimoto, M. Sukegawa, H. Nohira and K. Saigo, *Journal of the American Chemical Society*, 1996, **118**, 3441–3449.

[43] M. Breuer, K. Ditrich, T. Habicher, B. Hauer, M. Kesseler, R. Stürmer and T. Zelinski, *Angewandte Chemie - International Edition*, 2004, **43**, 788–824.

[44] A. Johansson, *Contemporary Organic Synthesis*, 1995, **2**, 393–407.

[45] L. Storace, L. Anzalone, P. N. Confalone, W. P. Davis, J. M. Fortunak, M. Giangiordano, J. J. Haley, K. Kamholz, H. Y. Li, P. Ma, W. A. Nugent, R. L. Parsons, P. J. Sheeran, C. E. Silverman, R. E. Waltermire and C. C. Wood, *Organic Process Research and Development*, 2002, **6**, 54–63.

[46] (*a*) M. Höhne and U. T. Bornscheuer, *ChemCatChem*, 2009, **1**, 42–51; (*b*) N. J. Turner, *Current Opinion Chemical Biology*, 2004, **8**, 114–119; (*c*) G. W. Zheng and J. H. Xu, *Current Opinion in Biotechnology*, 2011, **22**, 784–792; (*d*) E. E. Ferrandi and D. Monti, *World Journal of Microbiology and Biotechnology*, 2018, **34**, 1–10; (*e*) E. O'Reilly and N. J. Turner, *Perspectives on Science*, 2015, **4**, 55–61; (*f*) L. K. Thaløn, D. Zhao, J.-B. Sortais, J. Paetzold, C. Hoben and J.-E. Bäckvall, *Chemistry - A European Journal*, 2009, **15**, 3403–3410; (*g*) S. P. France, L. J. Hepworth, N. J. Turner and S. L. Flitsch, *ACS Catalysis*, 2017, **7**, 710–724; (*h*) J. H. Schrittwieser, S. Velikogne, M. Hall and W. Kroutil, *Chemical Reviews*, 2018, **118**, 270–348; (*i*) M. Fuchs, J. E. Farnberger and W. Kroutil, *European Journal of Organic Chemistry*, 2015, **32**, 6965–6982; (*j*) M. Breuer, K. Ditrich, T. Habicher,

B. Hauer, M. Keßeler, R. Stürmer and T. Zelinski, *Angewandte Chemie - International Edition*, 2004, **43**, 788–824; (*k*) G. Strohmeier, H. Pichler, O. May and M. Gruber-Khadjawi, *Chemical Reviews*, 2011, **111**, 4141–4164.

[47] C.-E. Jäger and T. Eggert, *Current Opinion in Biotechnology*, 2002, **13**, 390–397.

[48] L. Brady, A. M. Brzozowski, Z. S. Derewenda, E. Dodson, G. Dodson, S. Tolley, J. P. Turkenburg, L. Christiansen, B. Huge-Jensen, L. Norskov, L. Thim and U. Menge, *Nature*, 1990, **343**, 767–770.

[49] R. Gupta, N. Gupta and P. Rathi, *Applied Microbiology and Biotechnology*, 2004, **64**, 763–781.

[50] C.-E. Jaeger, *Trends in Biotechnology*, 1998, **16**, 396–403.

[51] M. T. Reetz, *Current Opinion in Chemical Biology*, 2002, **6**, 145–150.

[52] P. Trodler, R. D. Schmid and J. Pleiss, *BMC structural biology*, 2009, **9**, 1–13.

[53] D. Guerrand, *Oilseeds and fats, Crops and Lipids*, 2017, **24**, 1–7.

[54] F. Balkenhohl, K. Ditrich, B. Hauer and W. Ladner, *Journal für Praktische Chemie*, 1997, **339**, 381–384.

[55] K. Ditrich, *Separation of Optically Active Amides*, WO1997010201A1, 1997.

[56] K. Ditrich, *Synthesis*, 2008, **14**, 2283–2287.

[57] V. F. Batista, J. L. Galman, D. C. Pinto, A. M. Silva and N. J. Turner, *ACS Catalysis*, 2018, **8**, 11889–11907.

[58] H. Gaweska and P. F. Fitzpatrick, *BioMolecular Concepts*, 2011, **2**, 365–377.

[59] (*a*) G. Grogan and N. J. Turner, *Chemistry - A European Journal*, 2016, **22**, 1900–1907; (*b*) J. Mangas-Sanchez, S. P. France, S. L. Montgomery, G. A. Aleku, H. Man, M. Sharma, J. I. Ramsden, G. Grogan and N. J. Turner, *Current Opinion in Chemical Biology*, 2017, **37**, 19–25; (*c*) M. Lenz, J. Meisner, L. Quertinmont, S. Lutz, J. Kästner and B. M. Nestl, *ChemBioChem*, 2017, **18**, 253–256; (*d*) M. Lenz, N. Borlinghaus, L. Weinmann and B. M. Nestl, *World Journal of Microbiology and Biotechnology*, 2017, **33**, 1–10.

[60] N. Zumbrägel, H. Gröger, D. Wetzl and H. Iding, *Heterocycles*, 2017, **95**, 1261–1271.

[61] K. Mitsukura, M. Suzuki, K. Tada, T. Yoshida and T. Nagasawa, *Organic and Biomolecular Chemistry*, 2010, **8**, 4533–4535.

[62] S. Hussain, F. Leipold, H. Man, E. Wells, S. P. France, K. R. Mulholland, G. Grogan and N. J. Turner, *ChemCatChem*, 2015, **7**, 579–583.

[63] D. Wetzl, M. Berrera, N. Sandon, D. Fishlock, M. Ebeling, M. Müller, S. Hanlon, B. Wirz and H. Iding, *ChemBioChem*, 2015, **16**, 1749–1756.

[64] H. Li, P. Tian, J. H. Xu and G. W. Zheng, *Organic Letters*, 2017, **19**, 3151–3154.

[65] N. Zumbrägel, C. Merten, S. M. Huber and H. Gröger, *Nature Communications*, 2018, **9**, 1949.

[66] S. P. France, R. M. Howard, J. Steflik, N. J. Weise, J. Mangas-Sanchez, S. L. Montgomery, R. Crook, R. Kumar and N. J. Turner, *ChemCatChem*, 2018, **10**, 510–514.

[67] (*a*) A. Gomm and E. O'Reilly, *Current Opinion in Biotechnology*, 2018, **43**, 106–112; (*b*) M. D. Patil, G. Grogan, A. Bommarius and H. Yun, *Catalysts*, 2018, **8**, 1– 25; (*c*) S. A. Kelly, S. Pohle, S. Wharry, S. Mix, C. C. Allen, T. S. Moody and B. F. Gilmore, *Chemical Reviews*, 2018, **118**, 349–367; (*d*) F. Guo and P. Berglund, *Green Chemistry*, 2017, **19**, 333–360; (*e*) D. Koszelewski, K. Tauber, K. Faber and W. Kroutil, *Trends in Biotechnolology*, 2010, **28**, 324–332.

[68] S. W. Han, E. S. Park, J. Y. Dong and J. S. Shin, *Advanced Synthesis & Catalysis*, 2015, **357**, 2712–2720.

[69] M. Fuchs, J. E. Farnberger and W. Kroutil, *European Journal of Organic Chemistry*, 2015, 6965–6982.

[70] M. T. Gundersen, P. Tufvesson, E. J. Rackham, R. C. Lloyd and J. M. Woodley, *Organic Process Research & Development*, 2016, **20**, 602–608.

[71] D. Zhu and L. Hua, *Biotechnology Journal*, 2009, **4**, 1420–1431.

[72] A. P. Green, N. J. Turner and E. O'Reilly, *Angewandte Chemie - International Edition*, 2014, **53**, 10714–10717.

[73] H. Schuette, W. Hummel, H. Tsai and M.-R. Kula, *Applied Microbiology and Biotechnology*, 1985, **22**, 306–317.

[74] R. R. Eady and P. J. Large, *Biochemical Journal*, 1968, **106**, 245–255.

[75] N. Itoh, C. Yachi and T. Kudome, *Biochemical Journal*, 2000, **11**, 281–290.

[76] D. Sun, K. Ono, T. Okajima, K. Tanizawa, M. Uchida, Y. Yamamoto, F. S. Mathews and V. L. Davidson, *Biochemistry*, 2003, **42**, 10896–10903.

[77] M. T. Reetz, D. Kahakeaw and R. Lohmer, *ChemBioChem*, 2008, **9**, 1797–1804.

[78] M. J. Abrahamson, E. Vázquez-Figueroa, N. B. Woodall, J. C. Moore and A. S. Bommarius, *Angewandte Chemie - International Edition*, 2012, **51**, 3969–3972.

[79] M. J. Abrahamson, J. W. Wong and A. S. Bommarius, *Advanced Synthesis and Catalysis*, 2013, **355**, 1780–1786.

[80] B. R. Bommarius, M. Schürmann and A. S. Bommarius, *Chemical Communications*, 2014, **50**, 14953–14955.

[81] S. K. Au, B. R. Bommarius and A. S. Bommarius, *ACS Catalysis*, 2014, **4**, 4021–4026.

[82] F. F. Chen, Y. Y. Liu, G. W. Zheng and J. H. Xu, *ChemCatChem*, 2015, **7**, 3838–3841.

[83] L. J. Ye, H. H. Toh, Y. Yang, J. P. Adams, R. Snajdrova and Z. Li, *ACS Catalysis*, 2015, **5**, 1119–1122.

[84] F. Mutti, N. S. G. Scrutton, N. J. Turner, M. Breuer, F. G. Mutti and T. Knaus, *Science*, 2015, **349**, 1525–1529.

[85] T. Knaus, W. Böhmer and F. G. Mutti, *Green Chemistry*, 2017, **19**, 453–463.

[86] H. Jeon, S. Yoon, M. Ahsan, S. Sung, G.-H. Kim, U. Sundaramoorthy, S.-K. Rhee and H. Yun, *Catalysts*, 2017, **7**, 251.

[87] J. Liu, B. Q. Pang, J. P. Adams, R. Snajdrova and Z. Li, *ChemCatChem*, 2017, **9**, 425–431.

[88] H. Ren, Y. Zhang, J. Su, P. Lin, B. Wang, B. Fang and S. Wang, *Journal of Biotechnology*, 2017, **241**, 33–41.

[89] G. Zhang, M. B. Quin and C. Schmidt-Dannert, *ACS Catalysis*, 2018, **8**, 5611–5620.

[90] W. Böhmer, T. Knaus and F. G. Mutti, *ChemCatChem*, 2018, **10**, 731–735.

[91] J. Löwe, A. A. Ingram and H. Gröger, *Bioorganic and Medical Chemistry*, 2018, **26**, 1387–1392.

[92] M. P. Thompson, S. R. Derrington, R. S. Heath, J. L. Porter, J. Mangas-Sanchez, P. N. Devine, M. D. Truppo and N. J. Turner, *Tetrahedron*, 2019, **75**, 327–334.

[93] (*a*) A. Basso and S. Serban, *Molecular Catalysis*, 2019, **479**, 110607; (*b*) U. Hanefeld, L. Gardossi and E. Magner, *Chemical Society Reviews*, 2009, **38**, 453–468; (*c*) U. Hanefeld, L. Cao and E. Magner, *Chemical Society Reviews*, 2013, **42**, 6211–6212.

[94] Y. Zhang, J. Ge and Z. Liu, *ACS Catalysis*, 2015, **5**, 4503–4513.

[95] C. Mateo, J. M. Palomo, G. Fernandez-Lorente, J. M. Guisan and R. Fernandez-Lafuente, *Enzyme and Microbial Technology*, 2007, **40**, 1451–1463.

[96] R. A. Sheldon and S. van Pelt, *Chemical Society Reviews*, 2013, **42**, 6223–6235.

[97] M. Mrksich, J. R. Grunwell and G. M. Whitesides, *Journal of the American Chemical Society*, 1995, **117**, 12009–12010.

[98] X. Tao, A. Li and H. Yang, *Environmental Pollution*, 2017, **222**, 348–355.

[99] T. Jesionowski, J. Zdarta and B. Krajewska, *Adsorption*, 2014, **20**, 801–821.

[100] R. Mahajan, V. K. Gupta and J. Sharma, *Indian Journal of Pharmaceutical Sciences*, 2010, **2**, 223–228.

[101] R. Di Cosimo, J. Mc Auliffe, A. J. Poulose and G. Bohlmann, *Chemical Society Reviews*, 2013, **42**, 6437–6474.

[102] A. K. Chandel, L. V. Rao, M. L. Narasu and O. V. Singh, *Enzyme and Microbial Technology*, 2008, **42**, 199–207.

[103] L. Wobbe and C. Remacle, *Journal of Biotechnology*, 2014, **201**, 28–42.

[104] R. H. Wijffels, O. Kruse and K. J. Hellingwerf, *Current Opinion in Biotechnology*, 2013, **24**, 405–413.

[105] M. L. Ghirardi, M. C. Posewitz, P.-C. Maness, A. Dubini, J. Yu and M. Seibert, *Annual Review of Plant Biology*, 2007, **58**, 71–91.

[106] O. Blifernez-Klassen, V. Klassen, A. Doebbe, K. Kersting, P. Grimm, L. Wobbe and O. Kruse, *Nature Communications*, 2012, **3**, 1214–1219.

[107] W. Khetkorn, R. P. Rastogi, A. Incharoensakdi, P. Lindblad, D. Madamwar, A. Pandey and C. Larroche, *Bioresource Technology*, 2017, **243**, 1194–1206.

[108] S. S. Merchant, S. E. Prochnik, O. Vallon, E. H. Harris, S. J. Karpowicz, G. B. Witman, A. Terry, A. Salamov, L. K. Fritz-Laylin and L. Marechal-Drouard, *Science*, 2007, **318**, 245–250.

[109] A. R. Grossman, C. Catalanotti, W. Yang, A. Dubini, L. Magneschi, V. Subramanian, M. C. Posewitz and M. Seibert, *New Phytologist*, 2011, **190**, 279–288.

[110] J. Li, J. Pan, J. Zhang and J. H. Xu, *Journal of Molecular Catalysis B: Enzymatic*, 2014, **105**, 11–17.

[111] E. Vázquez-Figueroa, J. Chapparro-Riggers and A. S. Bommarius, *ChemBioChem*, 2007, **8**, 2295–2301.

[112] M. Biermann, D. Bakonyi, W. Hummel and H. Gröger, *Green Chemistry*, 2017, **19**, 405–410.

[113] A. Sengupta, A. V. Sunder, S. V. Sohoni and P. P. Wangikar, *Journal of Biotechnology*, 2019, **289**, 1–6.

[114] L. Schmermund, V. Jurkaš, F. F. Özgen, G. D. Barone, H. C. Büchsenschütz, C. K. Winkler, S. Schmidt, R. Kourist and W. Kroutil, *ACS Catalysis*, 2019, **9**, 4115–4144.

[115] D. Leister, *Essays in Biochemistry*, 2018, **62**, 77–84.

[116] V. I. Tishkov and V. O. Popov, *Biochemistry*, 2004, **69**, 1252–1267.

[117] J. Löwe, *M. Sc. Thesis, Entwicklung eines chemoenzymatischen Verfahrens zur Herstellung enantiomerenreiner Amine mit Indanstruktur und moegliche Anwendungen*, 2016.

[118] S. Wang, X. Meng, H. Zhou, Y. Liu, F. Secundo and Y. Liu, *Catalysts*, 2016, **6**, 1–16.

[119] A. A. Ingram, *B. Sc. Thesis, Wege zur Synthese chiraler Verbindungen mittels immobilisierter Enzyme*, Universität Bielefeld, 2017.

[120] A. Plagens, *Namen- und Schlagwort-Reaktionen der Organischen Chemie*, 1st edn., 1994.

[121] L. L. Poulsen and D. M. Ziegler, *Chemico-Biological Interactions*, 1995, **96**, 57–73.

[122] V. Massey, *Journal of Biological Chemistry*, 1994, **269**, 22459–22462.

[123] T. Heine, W. van Berkel, G. Gassner, K.-H. van Pée and D. Tischler, *Biology*, 2018, **7**, 42.

[124] A. Riebel, M. J. Fink, M. D. Mihovilovic and M. W. Fraaije, *ChemCatChem*, 2014, **6**, 1112–1117.

[125] D. Sheng, D. P. Ballou and V. Massey, *Biochemistry*, 2001, **40**, 11156–11167.

[126] N. A. Donoghue and P. W. Trundill, *European Journal of Biochemistry*, 1975, **60**, 1–7.

[127] G. Grogan, S. Roberts, P. Wan and A. Willetts, *Biotechnology Letters*, 1993, **15**, 913–918.

[128] A. Reimer, S. Wedde, S. Staudt, S. Schmidt, D. Höffer, W. Hummel, U. Kragl, U. T. Bornscheuer and H. Gröger, *Journal of Heterocyclic Chemistry*, 2017, **54**, 391–396.

[129] S. Wedde, P. Rommelmann, C. Scherkus, S. Schmidt, U. T. Bornscheuer, A. Liese and H. Gröger, *Green Chemistry*, 2017, **19**, 1286–1290.

[130] C. Scherkus, S. Schmidt, U. T. Bornscheuer, H. Gröger, S. Kara and A. Liese, *Biotechnology and Bioengineering*, 2017, **114**, 1215–1221.

[131] K. Balke, M. Bäumgen and U. T. Bornscheuer, *ChemBioChem*, 2017, **18**, 1627–1638.

[132] C. N. Jensen, J. Cartwright, J. Ward, S. Hart, J. P. Turkenburg, S. T. Ali, M. J. Allen and G. Grogan, *ChemBioChem*, 2012, **13**, 872–878.

[133] O. Verho and J. E. Bäckvall, *J. Am. Chem. Soc.*, 2015, **137**, 3996–4009.

[134] Erdiwansyah, R. Mamat, M. S. Sani, K. Sudhakar, A. Kadarohman and R. E. Sardjono, *Energy Reports*, 2019, **5**, 467–479.

[135] T. Nakajima, S. Suga, T. Sugita and K. Ichikawa, *Tetrahedron*, 1969, **25**, 1807–1816.

[136] H. Gröger, *Angewandte Chemie - International Edition*, 2014, **53**, 3067–3069.

[137] V. Resch and U. Hanefeld, *Catalysis Science and Technology*, 2015, **5**, 1385–1399.

[138] V. Resch, C. Seidler, B. S. Chen, I. Degeling and U. Hanefeld, *European Journal of Organic Chemistry*, 2013, 7697–7704.

[139] X. Zhang and K. N. Houk, *Accounts of Chemical Research*, 2005, **38**, 379–385.

[140] T. Genda, S. Watabe and H. Ozaki, *Bioscience, Biotechnology and Biochemistry*, 2006, **70**, 1102–1109.

[141] A. G. Rocha and A. Dancis, *Molecular Microbiology*, 2016, **99**, 821–826.

[142] J. R. Mohrig, *Accounts of Chemical Research*, 2013, **46**, 1407–1416.

[143] C. S. Turbek, D. A. Smith and C. L. Schardl, *FEMS Microbiology Letters*, 1992, **94**, 187–190.

[144] D. Brodkorb, M. Gottschall, R. Marmulla, F. Lüddeke and J. Harder, *Journal of Biological Chemistry*, 2010, **285**, 30436–30442.

[145] A. Hiseni, I. W. Arends and L. G. Otten, *Applied Microbiology and Biotechnology*, 2011, **91**, 1029–1036.

[146] J. P. Bennett, L. Bertin, B. Moulton, I. J. Fairlamb, A. M. Brzozowski, N. J. Walton and G. Grogan, *Biochemical Journal*, 2008, **414**, 281–289.

[147] J. J. Jin, P. C. Oskam, S. K. Karmee, A. J. J. Straathof and U. Hanefeld, *Chemical Communications*, 2010, **46**, 8588–8590.

[148] C. Liu, F. Liu, J. Cai, U. W. Xie, T. E. Long, S. R. Turner, A. Lyons and R. A. Gross, *ACS Symposium Series*, 2012, **1105**, 131–150.

[149] A. Świzdor, A. Panek, N. Milecka-Tronina and T. Kołek, *International Journal of Molecular Sciences*, 2012, **13**, 16514–16543.

[150] S. Schneider, M. G. Wubbolts, D. Sanglard and B. Witholt, *Tetrahedron: Asymmetry*, 2002, **9**, 2832–2844.

[151] R. D. Ashby, D. K. Solaiman, C. K. Liu, G. Strahan and N. Latona, *Journal of the American Oil Chemists' Society*, 2016, **93**, 347–358.

[152] J. Hu, Z. Jin, T. Y. Chen, J. D. Polley, M. F. Cunningham and R. A. Gross, *Macromolecules*, 2014, **47**, 113–120.

[153] H. Mutlu and M. A. Meier, *European Journal of Lipid Science and Technology*, 2010, **112**, 10–30.

[154] C. T. Hou, *New Biotechnology*, 2009, **26**, 2–10.

[155] S. Soni and M. Agarwal, *Green Chemistry Letters and Reviews*, 2014, **7**, 359–382.

[156] O. G. Mountanea, D. Limnios, M. G. Kokotou, A. Bourboula and G. Kokotos, *European Journal of Organic Chemistry*, 2019, 2010–2019, doi: 10.1002/ejoc.201801881.

[157] K. R. Kim and D. K. Oh, *Biotechnology Advances*, 2013, **31**, 1473–1485.

[158] K. R. Kim, H. J. Oh, C. S. Park, S. H. Hong, J. Y. Park and D. K. Oh, *Biotechnology and Bioengineering*, 2015, **112**, 2206–2213.

[159] U. T. Bornscheuer, *Annual Review of Food Science and Technology*, 2018, **9**, 116–127.

[160] L. L. Wallen, R. G. Benedict and W. R. Jackson, *Archives of Biochemistry and Biophysics*, 1962, **99**, 249–253.

[161] M. Engleder, T. Pavkov-Keller, A. Emmerstorfer, A. Hromic, S. Schrempf, G. Steinkellner, T. Wriessnegger, E. Leitner, G. A. Strohmeier, I. Kaluzna, D. Mink, M. Schürmann, S. Wallner, P. Macheroux, K. Gruber and H. Pichler, *ChemBioChem*, 2015, **16**, 1730–1734.

[162] A. Volkov, S. Khoshnevis, P. Neumann, C. Herrfurth, D. Wohlwend, R. Ficner and I. Feussner, *Acta Crystallographica Section D*, 2013, **69**, 648–657.

[163] M. Engleder and H. Pichler, *Applied Microbiology and Biotechnology*, 2018, **102**, 5841–5858.

[164] J. Schmid, L. Steiner, S. Fademrecht, J. Pleiss, K. B. Otte and B. Hauer, *Journal of Molecular Catalysis B: Enzymatic*, 2016, **133**, 243–249.

[165] A. Hirata, S. Kishino, S.-B. Park, M. Takeuchi, N. Kitamura and J. Ogawa, *Journal of Lipid Research*, 2015, **56**, 1340–1350.

[166] A. Volkov, A. Liavonchanka, O. Kamneva, T. Fiedler, C. Goebel, B. Kreikemeyer and I. Feussner, *Journal of Biological Chemistry*, 2010, **285**, 10353–10361.

[167] S. Koritala, C. T. Hou, C. W. Hesseltine and M. O. Bagby, *Applied Microbiology and Biotechnology*, 1989, **32**, 299–304.

[168] S. H. El-Sharkawy, W. Yang, L. Dostal and J. P. N. Rosazza, *Applied and Environmental Microbiology*, 1992, **58**, 2116–2122.

[169] D. Fabritius, H. J. Schäfer and A. Steinbüchel, *Applied Microbiology and Biotechnology*, 1996, **45**, 342–348.

[170] T. Kaneshiro, T. Min Kuo and L. K. Nakamura, *Current Microbiology*, 1999, **38**, 250–255.

[171] L. E. Bevers, M. W. Pinkse, P. D. Verhaert and W. R. Hagen, *Journal of Bacteriology*, 2009, **191**, 5010–5012.

[172] E. Y. Jeon, J. H. Lee, K. M. Yang, Y. C. Joo, D. K. Oh and J. B. Park, *Process Biochemistry*, 2012, **47**, 941–947.

[173] B. N. Kim, Y. C. Joo, Y. S. Kim, K. R. Kim and D. K. Oh, *Applied Microbiology and Biotechnology*, 2012, **95**, 929–937.

[174] M. Takeuchi, S. Kishino, A. Hirata, S. B. Park, N. Kitamura and J. Ogawa, *Journal of Bioscience and Bioengineering*, 2015, **119**, 636–641.

[175] W. R. Kang, M. J. Seo, K. C. Shin, J. B. Park and D. K. Oh, *Biotechnology and Bioengineering*, 2017, **114**, 74–82.

[176] Y. C. Joo, E. S. Seo, Y. S. Kim, K. R. Kim, J. B. Park and D. K. Oh, *Journal of Biotechnology*, 2012, **158**, 17–23.

[177] J. Y. Park, S. H. Lee, K. R. Kim, J. B. Park and D. K. Oh, *Journal of Biotechnology*, 2015, **208**, 1–10.

[178] M. Takeuchi, S. Kishino, S. B. Park, A. Hirata, N. Kitamura, A. Saika and J. Ogawa, *Applied Microbiology and Biotechnology*, 2016, **120**, 1282–1288.

[179] KR2013126354, 2013.

[180] R. M. Demming, K. B. Otte, B. M. Nestl and B. Hauer, *ChemCatChem*, 2017, **9**, 758–766.

[181] M. Engleder, G. A. Strohmeier, H. Weber, G. Steinkellner, E. Leitner, M. Müller, D. Mink, M. Schürmann, K. Gruber and H. Pichler, *Angewandte Chemie - International Edition*, 2019, **58**, 7480–7484.

[182] R. M. Demming, *Ph.D. thesis*, *Enzymatische Hydratisierung kurzkettiger Fettsäuren und Alkene*, Universität Stuttgart, 2018.

[183] D. Brady and J. Jordaan, *Biotechnology Letters*, 2009, **31**, 1639–1650.

[184] T. Pietrowski, *B. Sc. Thesis, Prozessoptimierung und Immobilisierung ausgewählter Fettsäure-Hydratasen*, Universität Bielefeld, 2019.

[185] H. Bork, *M. Sc. Thesis, Herstellung von Monomeren für Polyurethane ausgehend von nachwachsenden Rohstoffen unter Einsatz von Biokatalysatoren*, Universität Bielefeld, 2020.

[186] Y. S. Jo, J. U. An and D. K. Oh, *Journal of Agricultural and Food Chemistry*, 2014, **62**, 6736–6745.

[187] http://www.spinchem.com, *last accessed*, 22. Mai 2020.

[188] A. Demirbas, *Energy Sources, Part a: Recovery, Utilization and Environmental Effects*, 2010, **32**, 628–636.

[189] J. H. Choi, M. J. Seo, K. T. Lee and D. K. Oh, *Biotechnology and Bioprocess Engineering*, 2017, **22**, 709–716.

[190] E. Y. Jeon, J. H. Seo, W. R. Kang, M. J. Kim, J. H. Lee, D. K. Oh and J. B. Park, *ACS Catalysis*, 2016, **6**, 7547–7553.

[191] S. H. Heo, C. T. Hou and B. S. Kim, *New Biotechnology*, 2009, **26**, 105–108.

[192] I. Tiryaki, *Turkish Journal of Agriculture and Forestry*, 2004, **28**, 291–299.

[193] R. Bari and J. D. Jones, *Plant Molecular Biology*, 2009, **69**, 473–488.

[194] M. Hasanuzzaman, M. A. Hossain, J. A. T. da Silva and M. Fujita, *Plant Response and Tolerance to Abiotic Oxidative Stress: Antioxidant Defense Is a Key Factor*, Springer, Dordrecht, 1st edn., 2011, pp. 261–315.

[195] R. A. Creelman and J. E. Mullet, *Annual Review of Plant Physiology*, 1997, **48**, 355–381.

[196] F. Schaller, A. Schaller and A. Stintzi, *Journal of Plant Growth Regulation*, 2004, **23**, 179–199.

[197] L. Guan, N. Denkert, A. Eisa, M. Lehmann, I. Sjuts, A. Weiberg, J. Soll, M. Meinecke and S. Schwenkert, *Proceedings of the National Academy of Sciences*, 2019, **116**, 10568–10575.

[198] C. Wasternack and B. Hause, *Nature Plants*, 2019, **5**, 776–777.

[199] I. Stenzel, B. Hause, O. Miersch, T. Kurz, H. Maucher, H. Weichert, J. Ziegler, I. Feussner and C. Wasternack, *Plant Molecular Biology*, 2003, **51**, 895–911.

[200] C. Chapuis, *Helvetica Chimica Acta*, 2012, **95**, 1479–1511.

[201] D. C. Zimmerman and P. Feng, *Lipids*, 1978, **13**, 313–316.

[202] B. A. Vick and D. C. Zimmerman, *Plant Physiology*, 1987, **85**, 1073–1078.

[203] D. Maynard, H. Gröger, T. Dierks and K. J. Dietz, *Journal of Experimental Botany*, 2018, **69**, 5341–5354.

[204] E. Ricciotti and A. G. Fitzgerald, *Arteriosclerosis, Thrombosis, and Vascular Biology*, 2011, **31**, 986–1000.

[205] N. Taki, Y. Sasaki-Sekimoto, T. Obayashi, A. Kikuta, K. Kobayashi, T. Ainai, K. Yagi, N. Sakurai, H. Suzuki, T. Masuda, K. I. Takamiya, D. Shibata, Y. Kobayashi and H. Ohta, *Plant Physiology*, 2005, **139**, 1268–1283.

[206] H. Cheong, I. Barbosa dos Santos, W. Liu, H. N. Gosse and S. W. Park, *Plant Signaling & Behavior*, 2017, **12**, e1362520.

[207] P. A. Grieco and N. Abood, *Journal of Organic Chemistry*, 1989, **54**, 6008–6010.

[208] T. Ainai, M. Matsuumi and Y. Kobayashi, *Journal of Organic Chemistry*, 2003, **68**, 7825–7832.

[209] H. Nonaka, N. Ogawa, N. Maeda, Y. G. Wang and Y. Kobayashi, *Organic & Biomolecular Chemistry*, 2010, **8**, 5212–5223.

[210] M. Ernst and G. Helmchen, *Angewandte Chemie - International Edition*, 2002, 4054–4056.

[211] D. Laudert, P. Hennig, B. A. Stelmach, A. Müller, L. Andert and E. W. Weiler, *Analytical Biochemistry*, 1997, **246**, 211–217.

[212] P. Zerbe, E. W. Weiler and F. Schaller, *Phytochemistry*, 2007, **68**, 229–236.

[213] A. Kajiwara, T. Abe, T. Hashimoto, H. Matusuura and K. Takahashi, *Bioscience, Biotechnology, and Biochemistry*, 2012, **76**, 2325–2328.

[214] T. B. Le, C. S. Han, K. Cho and O. Han, *Artificial Cells, Nanomedicine, and Biotechnology*, 2017, 1523–1529.

[215] D. Maynard, S. M. Müller, M. Hahmeier, J. Löwe, I. Feussner, H. Gröger, A. Viehhauser and K. J. Dietz, *Bioorganic and Medical Chemistry*, 2018, **26**, 1356–1364.

[216] I. Ivanov, D. Heydeck, K. Hofheinz, J. Roffeis, V. B. O'Donnell, H. Kuhn and M. Walther, *Archives of Biochemistry and Biophysics*, 2010, **503**, 161–174.

[217] I. Feussner and C. Wasternack, *Annual Review of Plant Physiology*, 2002, **53**, 275–297.

[218] R. K. Hughes, E. J. Belfield, R. Ashton, S. A. Fairhurst, C. Göbel, M. Stumpe, I. Feussner and R. Casey, *FEBS Letters*, 2006, **580**, 4188–4194.

[219] P. B. Danielson, *Current Drug Metabolism*, 2005, **3**, 561–597.

[220] W.-C. Song, C. D. Funk and A. R. Brash, *Proceedings of the National Academy of Sciences*, 1993, **90**, 8519–8523.

[221] D. S. Lee, P. Nioche, M. Hamberg and C. S. Raman, *Nature*, 2008, **455**, 363–368.

[222] J. Ziegler, I. Stenzel, B. Hause, H. Maucher, M. Hamberg, R. Grimm, M. Ganal and C. Wasternack, *Journal of Biological Chemistry*, 2000, **275**, 19132–19138.

[223] M. Otto, C. Naumann, W. Brandt, C. Wasternack and B. Hause, *Plants*, 2016, **5**, 3.

[224] E. Hofmann, P. Zerbe and F. Schaller, *Plant Cell Online*, 2006, **18**, 3201–3217.

[225] F. Schaller, P. Zerbe, S. Reinbothe, C. Reinbothe, E. Hofmann and S. Pollmann, *FEBS Journal*, 2008, **275**, 2428–2441.

[226] K. Ziegler and H.-G. Gellert, *Verfahren zur Herstellung von Aluminiumtrialkylen und Aluminiumalkylhydriden (Direktsynthese von Aluminiumalkylen)*, DBP961537, 1957.

[227] H. Sousa Eletterio, *Polymerization of cyclic olefins*, US3074918, 1963.

[228] N. Calderon, H. Y. Chen and K. W. Scott, *Tetrahedron Letters*, 1967, **34**, 3327–3329.

[229] Y. Chauvin, *Angewandte Chemie - International Edition*, 2006, **45**, 3741–3747.

[230] E. O. Fischer and A. Maasböl, *Angewandte Chemie - International Edition*, 1964, **76**, 645–645.

[231] R. Schrock, S. Rocklage, J. Wengrovius, G. Rupprecht and J. Fellmann, *Preprints*, 1980, **25**, 382–391.

[232] R. R. Schrock, *Tetrahedron*, 1999, **55**, 8141–8153.

[233] S. B. T. Nguyen, L. K. Johnson, R. H. Grubbs and J. W. Ziller, *Journal of the American Chemical Society*, 1992, **114**, 3974–3975.

[234] P. Schwab, R. H. Grubbs and J. W. Ziller, *Journal of the American Chemical Society*, 1996, **118**, 100–108.

[235] M. Scholl, T. M. Trnka, J. P. Morgan and R. H. Grubbs, *Tetrahedron Letters*, 1999, **40**, 2247–2250.

[236] M. Scholl, S. Ding, C. W. Lee and R. H. Grubbs, *Organic Letters*, 1999, **1**, 953–956.

[237] S. B. Garber, J. S. Kingsbury, B. L. Gray and A. H. Hoveyda, *Journal of the American Chemical Society*, 2000, **122**, 8168–8179.

[238] M. S. Sandford, J. A. Love and R. H. Grubbs, *Journal of the American Chemical Society*, 2001, **123**, 6543–6554.

[239] J. A. Love, J. P. Morgan, T. M. Trnka and R. H. Grubbs, *Angewandte Chemie - International Edition*, 2002, **41**, 4035–4037.

[240] T. L. Choi and R. H. Grubbs, *Angewandte Chemie - International Edition*, 2003, **42**, 1743–1746.

[241] S. H. Hong and R. H. Grubbs, *Journal of the American Chemical Society*, 2006, **128**, 3508–3509.

[242] P. Schwab, M. B. France, J. W. Ziller and R. H. Grubbs, *Angewandte Chemie - International Edition*, 1995, **18**, 1689–1699.

[243] K. M. Engle, G. Lu, S. X. Luo, L. M. Henling, M. K. Takase, P. Liu, K. N. Houk and R. H. Grubbs, *Journal of the American Chemical Society*, 2015, **137**, 5782–5792.

[244] R. H. Grubbs, A. G. Wenzel, D. J. O'Leary and E. Khosravi, *Handbook of Metathesis*, Wiley-VCH, Weinheim, 2nd edn., 2015.

[245] J. Li, T. S. Ahmed, C. Xu, B. M. Stoltz and R. H. Grubbs, *Journal of the American Chemical Society*, 2019, **141**, 154–158.

[246] T. P. Montgomery, A. M. Johns and R. H. Grubbs, *Catalysts*, 2017, **7**, 87.

[247] A. Nickel, T. Ung, G. Mkrtumyan, J. Uy, C. W. Lee, D. Stoianova, J. Papazian, W. H. Wei, A. Mallari, Y. Schrodi and R. L. Pederson, *Topics in Catalysis*, 2012, **55**, 518–523.

[248] J. Patel, J. Elaridi, W. R. Jackson, A. J. Robinson, A. K. Serelis and C. Such, *Chemical Communications*, 2005, 5546–5547.

[249] O. Brummer, A. Ruckert and S. Blechert, *Chemistry - A European Journal*, 1997, **3**, 1–4.

[250] J. Sekiya, S. Numa, T. Kajlwara and A. Hatanaka, *Agricultural and Biological Chemistry*, 1976, **40**, 185–190.

[251] D. Laudert, U. Pfannschmidt, F. Lottspeich, H. Holländer-Czytko and E. W. Weiler, *Plant Molecular Biology*, 1996, **31**, 323–335.

[252] L. Belval, A. Marquette, P. Mestre, M. C. Piron, G. Demangeat, D. Merdinoglu and J. F. Chich, *Protein Expression and Purification*, 2015, **109**, 29–34.

[253] E. Bligh and W. Dyer, *Canadian Journal of Biochemistry and Physiology*, 1959, **37**, year.

[254] J. Britton, C. L. Raston and G. A. Weiss, *Chemical Communications*, 2016, **52**, 10159–10162.

[255] R. Porta, M. Benaglia and A. Puglisi, *Organic Process Research and Development*, 2016, **20**, 2–25.

[256] M. Planchestainer, M. L. Contente, J. Cassidy, F. Molinari, L. Tamborini and F. Paradisi, *Green Chemistry*, 2017, **19**, 372–375.

[257] J. D. Tibhe, H. Fu, T. Noël, Q. Wang, J. Meuldijk and V. Hessel, *Journal of Organic Chemistry*, 2013, **9**, 2168–2179.

[258] A. Tušek, A. Šalić, Ž. Kurtanjek and B. Zelić, *Engineering in Life Sciences*, 2012, **12**, 49–56.

[259] X. Casadevall I Solvas and A. Demello, *Chemical Communications*, 2011, **47**, 1936–1942.

[260] N. Adebar, J. E. Choi, L. Schober, R. Miyake, T. Iura, H. Kawabata and H. Gröger, *ChemCatChem*, 2019, **11**, 5788–5793.

[261] M. Qiu, L. Zha, Y. Song, L. Xiang and Y. Su, *React. Chem. Eng.*, 2019, **4**, 351–361.

[262] V. Pflug, *B. Sc. Thesis, Herstellung von α-Linolensäure-Derivaten mittels Olefinmetathese & anschließender Umsetzung zu 12-OPDA-Derivaten*, Universität Bielefeld, 2018.

[263] X. Miao, P. H. Dixneuf, C. Fischmeister and C. Bruneau, *Green Chemistry*, 2011, **13**, 2258–2271.

[264] M. M. Bradford, *Anal. Biochem.*, 1976, **72**, 248–254.

[265] J. Löwe, O. Blifernez-Klassen, T. Baier, L. Wobbe, O. Kruse and H. Gröger, *Journal of Biotechnology*, 2019, **294**, 81–87.

[266] S. Kametani, A. Kojima-Yuasa, H. Kikuzaki, D. O. Kennedy, M. Honzawa and I. Matsui-Yuasa, *Bioscience, Biotechnology, and Biochemistry*, 2007, **71**, 1220–1229.

[267] S. W. Baertschi, C. D. Ingram, T. M. Harris and A. R. Brash, *Biochemistry*, 1988, **27**, 18–24.

[268] Y. Imada, H. Iida, S. I. Murahashi and T. Naota, *Angewandte Chemie - International Edition*, 2005, **44**, 1704–1706.

[269] I. Hermans, K. Janssen, B. Moens, A. Philippaerts, B. van Berlo, J. Peeters, P. A. Jacobs and B. F. Sels, *Advanced Synthesis & Catalysis*, 2007, **349**, 1604–1608.

[270] M. F. Díaz and J. A. Gavín, *Journal of the Brazilian Chemical Society*, 2007, **18**, 513–518.

[271] P. H. Cui, R. K. Duke and C. C. Duke, *Chemistry and Physics of Lipids*, 2008, **152**, 122–130.

[272] C. C. Uranga, J. Beld, A. Mrse, I. Córdova-Guerrero, M. D. Burkart and R. Hernández-Martínez, *Data in Brief*, 2016, **8**, 31–39.

[273] F. L. Scott, B. Clemons, J. Brooks, E. Brahmachary, R. Powell, H. Dedman, H. G. Desale, G. A. Timony, E. Martinborough, H. Rosen, E. Roberts, M. F. Boehm and R. J. Peach, *British Journal of Pharmacology*, 2016, **173**, 1778–1792.

[274] E. Martinborough, M. F. Boehm, A. R. Yeager, J. Tamiya, L. Huang, E. Brahmachary, M. Moorjani, G. A. Timony, J. L. Brooks, R. Peach, F. L. Scott and M. A. Hanson, *Selective Sphingosine 1 Phosphate Receptor Modulators and Combination Therapy therewith*, WO 2015066515, 2015.

[275] A. Ghanem and H. Aboul-Enein, *Chirality*, 2005, **17**, 59–77.

[276] L. A. Nelson, T. A. Foglia and W. N. Marmer, *Journal of the American Oil Chemists' Society*, 1996, **73**, 1191–1195.

[277] P. Strzelczyk, G. D. Bujacz, P. Kielbadinski and J. Blaszczyk, *Acta Biochimica Polonica*, 2016, **63**, 103–109.

[278] C.-E. Jäger, B. Dijkstra and M. T. Reetz, *Annual Reviews of Microbbiology*, 1999, **53**, 315–351.

[279] M. A. Veld, K. Hult, A. R. Palmans and E. W. Meijer, *European Journal of Organic Chemistry*, 2007, 5416–5421.

[280] E. Martinborough, M. F. Boehm, A. R. Yeager, J. Tamiya, L. Huang, E. Brahmachary, M. Moorjani, G. A. Timony, J. L. Brooks, R. Peach, F. L. Scott and M. A. Hanson, *Selective Sphingosine-1-Phosphate Receptormodulators and Methods of Chiral Synthesis*, US20110172202A1, 2011.